The Use of Stable Isotope Determinations from Brachiopod Shells in Environmental Reconstruction

David Parkinson B.Sc. (Hons)

Submitted in fulfilment of the requirements

for the

Degree of Doctor of Philosophy

Division of Earth Sciences, University of Glasgow

September 2004

Declaration

The material presented in this thesis summarises the results of three years of independent research carried out in the Division of Earth Sciences, University of Glasgow and the Scottish Universities Environmental Research Centre. The research was supervised by Dr G. B. Curry and Dr M. Cusack of the University of Glasgow and Prof. A. E. Fallick of the Scottish Universities Environmental Research Centre.

This thesis is entirely my own work and any published or unpublished results of other researchers has been given full acknowledgement in the text.

David Parkinson

Abstract

This study investigates $\delta^{13}C$ and $\delta^{18}O$ variations in the shells of modern brachiopods that represent all extant groups of calcite-precipitating brachiopods, and were collected live from 8 locations. Protocols and methods of sample preparation are presented that can produce good estimations of annual mean temperatures of ambient seawaters from some brachiopod groups.

SEM examinations determined the ultrastructural characteristics of each species prior to isotope analyses. $\delta^{13}C$ and $\delta^{18}O$ analyses of shell carbonate were carried out with samples representing different morphological features and ultrastructural shell layers of both ventral and dorsal valves.

Generally, $\delta^{18}O$ values from the fibrous secondary or prismatic tertiary shell layers of the articulated Terebratulida and Rhynchonellida species were in oxygen isotopic equilibrium with ambient seawater. Isotopic temperatures extrapolated from these values are close to measured annual mean seawater temperatures. $\delta^{18}O$ values were relatively unaffected by shell specialisation. The only exception was Antarctic species *Liothyrella uva*, which did not have a complete tertiary shell layer typical of this genus and had $\delta^{18}O$ values of the innermost layer strongly correlated with $\delta^{13}C$ and mostly not in oxygen isotopic equilibrium with ambient seawater. With the exception of the rhynchonellid *Notosaria nigricans*, the outer primary layer material was depleted in $\delta^{13}C$ and $\delta^{18}O$ and highly variable. Inclusion of this material even as part of a whole shell sample could lead to misinterpretation of seawater temperature, therefore only fossil secondary layer material should be used. The anomalous articulated thecideidine brachiopod *Thecidellina barretti* is composed of mainly primary shell material and was not in oxygen isotope equilibrium. $\delta^{18}O$ values from the laminar secondary layer material of the inarticulated Craniida are

highly variable. Therefore these species are not recommended for use as palaeoenvironmental proxies. This study suggests that caution should be taken when employing fossil brachiopod shells with similar ultrastructures to those seen in modern craniid and thecideidine brachiopods. If possible brachiopods of these types should be avoided should be avoided.

The carbon isotope composition is highly variable in all of the brachiopods studied. Analysis of samples from specialised regions of the secondary shell layer show a pattern of depletion in ^{13}C relative to non-specialised secondary material. The carbon isotope variability is independent of $\delta^{18}O$ and is repeated in most of the articulated species regardless of geographical location. This is possibly a vital effect produced by metabolic prioritisation.

At location 1, the Firth of Lorne, two subphyla of brachiopods live attached to the shells of a bivalve, *Modiolus modiolus*. Comparison was made between the brachiopods and the host mussel shell. $\delta^{18}O$ values in the craniid brachiopod *Novocrania anomala* and the bivalve *Modiolus modiolus* were highly variable and yielded ambiguous environmental information. However, the terebratulid brachiopod *Terebratulina retusa* proved to be a good proxy for ambient seawater temperature.

Contents

Acknowledgements

Acknowledgements

Foremost I would like to thank Andrea for her financial and moral support, without which this project would not have been possible.

General funding for the project was provided by a Neilson Research Scholarship for which I am very grateful. Further funding was provided by a Scottish International Educational Trust (SIET) travel grant. This grant allowed me to travel to New Zealand to study fossil brachiopods from Pleistocene sediments in the Wanganui Basin. Samples of fossil brachiopods and molluscs were also collected for future research.

The project was supervised by Doctor Gordon B. Curry and Doctor Maggie Cusack from the Division of Earth Sciences in the Centre for Geosciences at the University of Glasgow. Additional supervision was provided by Professor Anthony E. Fallick from the Scottish Universities Environmental Research Centre. All provided considerable support and advice for which I am extremely grateful. I would also like to thank the late Sir Alwyn Williams FRS, FRSE for his general encouragement and assistance with the interpretation of scanning electron micrographs.

I are very grateful to The Dunstaffnage Marine Laboratory, Oban Scotland, especially Jim Watson ship's husband and Captain Roddy MacNeil and the crew of *RV Calanus*, for their considerable assistance with collection samples in Firth of Lorne. Thanks are also due to John Gilleece, Eddie Speirs and Peter Chung for help with transport to Dunstaffnage.

I am grateful for considerable support was given by the technical staff in the Division of Earth Sciences at the University of Glasgow. Namely: Kenny Roberts (divisional facilities), Robert M^{c}Donald (scanning electron microscope and electron microprobe), Bill

Higgison (atomic absorption spectrometer), John Gilleece (polished sections) and Sandra Tierney (sample preparation).

I also thank the technical staff at Scottish Universities Environmental Research Centre for their dedication and considerable technical assistance with the stable isotope analysis. Particular thanks are due to Terry Donnelly's persistence and expertise with the often problematic Prism mass spectrometer used for carbonate analysis and Andrew Tait's help with the seawater analysis.

Acknowledgment is due to Doctor Keith Probert who provided seawater temperature measurements from the archives of the Portobello Marine Laboratory, New Zealand. Professor Lloyd Peck (British Antarctic Survey); Doctor Kazuyoshi Endo (Institute of Geosciences, University of Tsukuba, Japan); Doctor Bernard L. Cohen (Institute of Biological and Life Sciences, Division of Molecular Genetics, University of Glasgow) and the late Sir Alwyn Williams FRS, FRSE (Palaeobiology Unit, University of Glasgow) for the supply of modern brachiopod specimens.

I would like to thank those who helped to make my field visit to New Zealand successful. Doctor Alan Beu of The Institute of Geological and Nuclear Sciences at the Gracefield Research Centre, Lower Hutt, near Wellington, New Zealand provided access to facilities and the opportunity it study fossil collections, which are of international importance. I was also grateful for the opportunity to consult Doctor Robert M. Carter of James Cook University of North Queensland, Australia and Doctor Stephan T. Abbot of Southern Cross University, Australia, visiting academics with specialist stratigraphical knowledge of the Wanganui Basin sediments. I would also like to thank Alan Hoverd of The School of Biology, Victoria University, Wellington and Chris and Romy Anderson for their friendship and hospitality in New Zealand.

Finally, I would like to mention my fellow postgraduate students in the Division of Earth Sciences at University of Glasgow: Alison, Claire, Corinne, Cristina, Davie, Duncan, Graham, Jenny, JJ, Kate, Kathy, Laiq, Liam, Liz, Sally, Sarah, Simon and Stewart. I thank them for their support and making postgraduate life at Glasgow so enjoyable.

Chapter 1

Introduction

1 Introduction

1.1 Background

The theory that the ^{18}O composition of biogenic carbonates could be used as a record of the temperature of the seawater in which they were formed was first proposed by Urey (1947). The application of this suggestion became possible through a series of developments. First, a modification to the design of the Nier (1940; 1947) stable isotope abundance mass spectrometer by McKinney *et al.* (1950), significantly improved precision for measuring relative stable isotope abundances. Second was the development of a reproducible method for yielding carbon dioxide (CO_2) from carbonates by digestion in phosphoric acid (H_3PO_4) at a known temperature (M^{c}Crea 1950). The third development was the construction of a carbonate palaeotemperature scale, which was determined using the relationship between temperature and the fractionation of oxygen isotopes in carbonate-water systems (M^{c}Crea 1950; Epstein *et al.* 1951; 1953). Lastly, the correction factors were calculated that allow mass spectrometer data to be adjusted for the effects of ^{17}O isotope in the analysed CO_2 gas (Craig 1957).

Over the years analytical techniques have been up-dated and reference materials standardised, but the basic principles have remained the same and have become widely accepted for use with a variety of biogenic carbonates. Using these techniques, oxygen and carbon stable isotope ratios determined from the fossilised shells of calcareous marine organisms have been used extensively for over 50 years in palaeoenvironmental studies. In particular $^{18}O/^{16}O$ has been employed as a proxy indicator of fluctuations in the temperature of ancient oceans. One of the most popular materials used in this kind of palaeoenvironmental investigation has been the fossil brachiopod shell. Brachiopods are considered to be exceptionally suitable, because the phylum is diverse and both ubiquitous

and continuous throughout the fossil record with a range spanning from Cambrian to Recent. Stable isotope analyses of their shells therefore, have the potential to be good proxy indicators of secular changes in $^{18}O_{seawater}$ throughout the Phanerozoic. In addition, most brachiopod species have shells composed of low-magnesium calcite (LMC); that is shells with between 0.5 and 7.0mol % $MgCO_3$ (Brand 1989a). This is the most stable form of skeletal carbonate and therefore is considered more resistant to diagenetic alteration (e.g. Lowenstam 1961; Al-Assam & Veizer 1982; Brand 1989a).

1.2 Brachiopod isotope research

The first published research into the relative abundance of ^{18}O and ^{13}C in fossilised brachiopod shells was probably that of Urey *et al.*(1951) in an investigation of palaeotemperatures derived from fossil organisms extracted from Upper Cretaceous chalk. Urey *et al.* concluded that the temperature record within the shells of the brachiopods studied had been destroyed, possibly by diffusion of material into the open structure of the shell. A more detailed study using brachiopods and crinoids from Devonian and Permian coals by Compston (1960) also observed diagenetic alteration and only the Permian brachiopods retained the original oxygen isotope composition. As with Urey *et al.* (1951) it was concluded that alteration was due to impregnation of the shell structure by diagenetic calcite. This study also raised the possibility that brachiopods could exert some phylogenetic control over the carbon isotope fractionation, an issue that is commonly referred to as biological fractionation or vital effect.

Lowenstam (1961) carried out the first real testing of the oxygen isotope composition in brachiopod shells as a record of ambient seawater temperature. Lowenstam's influential study was based on the analyses of modern articulated brachiopod shells from a variety of different taxa collected from locations with different environmental conditions and latitudes around the world. Lowenstam's specimens came from the Marshall Islands in the

Pacific, Bermuda, Barbados, California, New Zealand, the Mediterranean, and Alaska. Bottom water samples were collected from the sea at the same locations as the specimens and were analysed to determine the local ^{18}O content of the seawater. Isotopic temperatures were derived following the work of Epstein *et al.* (1953). Lowenstam (1961) compared the calculated temperatures with the measured seawater temperature ranges at the same locations. Calculated temperatures fell within the measured ranges and it was concluded that brachiopods precipitate their shell material oxygen stable isotopic equilibrium with ambient seawater. Lowenstam (1961) went further and compared data from his modern brachiopod analyses with fossil samples from the Pliocene, Cretaceous, Permian and Carboniferous. Only samples that retained the original ultrastructure were used and comparisons were made between the $^{18}O/^{16}O$ ratios and $SrCO_3$ and $MgCO_3$ concentrations in modern species. Where the relationship was compatible, it was concluded that the isotope signal remained intact.

The conclusion of Lowenstam (1961) that brachiopods precipitate skeletal calcite in equilibrium with ambient seawater was widely accepted. Workers studying palaeoenvironments were confident that the oxygen isotope fractionation in fossilised brachiopod shells was an accurate record of the temperature of the seas in which they were formed, and any biological effects were minimal. However, it was also generally accepted that care had to be taken when selecting fossil specimens for analysis to make sure that the original calcite was unaltered by diagenetic processes. Trace element analysis and cathodoluminescence are commonly used to identify suitable samples. The theories and methods of these procedures have been discussed in detail by, for example, Veizer (1983a);Veizer (1983b); Popp *et al.* (1986a); Rush and Chafetz (1990); Wenzel & Joachimski (1996) and Samtleben *et al.* (2001).

Confidence in the analytical techniques, together with the abundance of brachiopod remains in the fossil record, has led to stable isotope analyses of fossil brachiopod shells

being employed over the last 40 years in many extensive and detailed palaeoenvironmental investigations covering periods ranging throughout the Phanerozoic. Veizer *et al.* (1986) used trace element and isotope determinations from 319 brachiopod fossils spanning the Ordovician through to the Permian in order to establish evidence for change in the chemical composition of Palaeozoic oceans. Similarly, Popp *et al.* (1986a; 1986b) produced work on brachiopods from Palaeozoic limestones. Examples of other notable palaeoenvironmental works involving isotopic analyses of brachiopods include: Brand (1989a), Devonian-Carboniferous; Brand (1989b), Carboniferous; Marshall and Middleton (1990), late Ordovician; Grossman *et al.* (1991; 1993), Carboniferous; Qing & Veizer (1994) Ordovician; Wenzel & Joachimski (1996), Silurian; Veizer *et al.* (1999), Phanerozoic; Wenzel *et al.* (2000), Silurian; Mii *et al.* (2001), Carboniferous and Stanton *et al.* (2002), Carboniferous.

1.3 The equilibrium debate

Underpinning the use of stable isotope determinations from brachiopod shells for environmental investigations is the widely accepted assumption that their shells are secreted in isotopic equilibrium with ambient seawater. Lepzelter *et al.* (1983) added some weight to the supposition with a small study of $^{18}O/^{16}O$ ratios in several recent species, which were considered representative of extant brachiopods. The specimens used by Lepzelter *et al.* (1983) came from different locations in both the Atlantic and Pacific Oceans. The study concurred with that of Lowenstam's (1961) in that covariance between $\delta^{18}O$ and $\delta^{13}C$ was not observed, and the study concluded that brachiopod shells are precipitated in equilibrium with the seawater in which they form. The only detraction from this position noted by Lepzelter *et al.* (1983) was in the case of specimens taken from cold-water habitats, where isotopic disequilibrium was reported.

The suggestion that variations in oxygen isotopic ratios observed in disparate, but contemporary brachiopod genera collected from the same location, could be due to biological rather than diagenetic effects, was first reported by Popp *et al.* (1986b). The inference of this is that brachiopods could have precipitated shell calcite out of isotopic equilibrium as a result of 'vital effects'. However, despite this possibility little was done to test the reliability of stable isotopes in brachiopod shells as recorders of seawater temperature until Carpenter & Lohmann (1995) decided to examine the isotopic equilibrium position of Lowenstam (1961) further.

Carpenter & Lohmann (1995) noted that isotopic disequilibria attributed to biological fractionation or 'vital effects', are frequently reported in biogenic carbonates precipitated by a variety of marine organisms, for example: Compston (1960); Keith & Weber (1965); Weber & Raup (1966); Weber & Woodhead (1970); Erez (1978); Swart (1983); Gonzalez & Lohmann (1985); Rosenberg *et al.* (1988) McConnaughey (1989a; 1989b); Oritz *et al.* (1996); Böhm *et al.* (2000). In a recent study Adkins *et al.* (2003) suggested an alternative mechanism to explain these observed variations. Adkins *et al.* (2003) proposed that 'vital effects' observed in deep sea corals were the result of "a thermodynamic response to a biologically induced pH gradient in the calcifying region", rather than biological effects. However, notwithstanding the mechanism, it is clear that stable isotope variation does occur in some biogenic carbonates. Carpenter & Lohmann (1995) argued that the assertion that brachiopods precipitate calcite in isotopic equilibrium was based on very little evidence. Carpenter & Lohmann (1995) also maintained that if other calcareous marine organisms display vital effects, then there are too little data to confidently claim that brachiopods exhibit a unique characteristic. Given the widespread use of brachiopod isotope data, Carpenter & Lohmann (1995) considered that further examination was required.

Carpenter & Lohmann (1995) determined $\delta^{18}O$ and $\delta^{13}C$ values in a range of modern brachiopods, using specimens originating from a variety of environments and latitudes. Carpenter & Lohmann (1995) obtained a total of 44 specimens from Antarctica, Washington, New Zealand, Japan and Palau in the Pacific; Norway, Canada, South Africa and Curacao (South America) in the Atlantic and Sicily in the Mediterranean. The term 'modern brachiopod' was defined by Carpenter & Lohmann (1995) as a brachiopod that had been alive in the last 100 years. The University of Michigan Invertebrate Paleontology Collection supplied most of their specimens. These specimens were reported as collected alive or 'recently dead', however details of the collection of individual specimens were not known, nor were accurate water depths available for every location.

The strategy of Carpenter & Lohmann (1995) was to look at variations in ^{18}O and ^{13}C content within individuals, both intra and inter-species, from a range of different environments. A total of 420 analyses were made from shell material extracted from a variety of areas differentiated on the basis of shell ultrastructure (i.e. disparate shell layers: outer primary and inner secondary layers), and also from different readily identifiable morphological features of the secondary shell layer (i.e. hinge foramen, brachidium and muscle scars). Unfortunately the ^{18}O content of ambient seawater was measured at only one locality. Therefore in order to assess whether the brachiopods had precipitated their shell calcite in equilibrium, it was necessary to calculate $\delta^{18}O_{water}$ from salinity information supplied by the National Oceanic and Atmospheric Administration (NOAA) and National Oceanographic Data Centre (NODC) databases using the $\delta^{18}O_{water}$ – salinity relationship described in Broecker (1989). Using the salinity-corrected $\delta^{18}O_{water}$ values and temperatures from the NOAA and NODC files Carpenter & Lohmann (1995) calculated parameters for low-magnesium calcite precipitated in equilibrium using the fractionation factors detailed in Friedman & O'Neil (1977).

Carpenter & Lohmann (1995) present their data in a series of crossplots ($\delta^{13}C$ ‰ PDB v. $\delta^{18}O$ ‰ PDB) with carbonate $\delta^{18}O$ and $\delta^{13}C$ values expected under equilibrium conditions overlaid. The results show that material from the primary layer, and some areas of the secondary layer that form specialised morphological structures show a positive correlation between $\delta^{13}C$ and $\delta^{18}O$. The reasons suggested are metabolic ('vital effects') or kinetic isotope effects either during the hydroxylation of CO_2, or as a result of rapid calcite precipitation, or possibly a combination of some or all of these factors. Carpenter & Lohmann (1995) advised against the use of these parts of the shell during investigations employing ancient brachiopods. However, the non-specialised areas of the secondary layer close to the anterior margin were less fractionated and therefore closer to equilibrium. Generally Carpenter & Lohmann's (1995) data show the non-specialised secondary shell material to be in or close to oxygen isotopic equilibrium. However, the data frequently had very wide-ranging $\delta^{18}O$ and $\delta^{13}C$ values, many of which fall outside the equilibrium parameters. There were two exceptions to this trend: (i) *Thecidellina* sp. and (ii) *Stethothyris* sp. from Antarctica. *Thecidellina* sp have no clearly defined shell structure, and are mainly comprised of prismatic primary layer calcite (Williams 1973). Measurements from this yielded results that were frequently isotopically heavier than oxygen equilibrium. The Antarctic brachiopods, as in Lepzelter *et al.*'s (1983) study, were considerably depleted relative to expected oxygen isotope equilibrium values.

Carpenter & Lohmann's (1995) data shows little evidence of carbon isotopic equilibrium in respect of their calculated equilibrium parameters. Values of $\delta^{13}C$ were nearly always lower than the expected range.

Marshall *et al.* (1996) also worked with modern brachiopods from Antarctica. This study highlighted the uncertainties in obtaining meaningful oxygen isotopic values from very low temperature habitats with regard to their use as proxy indicators of seawater temperatures. The conventional palaeotemperature equations for biogenic carbonates are

derived from the work of Epstein *et al.* (1953) and are only based on carbonates precipitated from 7 to 30°C. The inorganic calcite – water fractionation curve (O'Neil *et al.* 1969; Friedman & O'Neil 1977), employed by Carpenter & Lohmann (1995), is more wide-ranging, and was determined from experimental data produced at temperatures from 0 to 700°C. However, the bulk of this work was done at temperatures above 200°C and true equilibrium was never really achieved at low temperatures. Marshall *et al.* (1996) further point out that at very low temperatures the lines for the two equations diverge leaving no adequate method for the determination of oxygen isotope equilibrium. Notwithstanding these difficulties, Marshall *et al.* (1996) argued that the ~2‰ range of $\delta^{18}O$ values, which signifies a range of temperatures of around 8°C, is very difficult to justify given the very narrow seasonal fluctuation in the region. This level of variation cannot be explained solely by problems with the palaeotemperature scales.

Since Carpenter & Lohmann (1995) opened the equilibrium debate, four small-scale studies from temperate waters have considered the issue. Buening & Spero (1996) analysed four specimens of the modern brachiopod *Laqueus californianus* (Koch) collected near the Californian coast. The study did not determine whether ^{13}C was in equilibrium with ambient seawater, but used the ^{18}O content from individual growth bands within the shell. Buening & Spero (1996) were able to identify El Niño warming events. The study concluded that the ^{18}O content of the brachiopod shell is a useful recorder of environmental change in temperate waters.

Two other investigations were conducted with modern brachiopods collected from the Lacepede Shelf, southern Australia. Rahimpour-Bonab *et al.* (1997) investigated stable isotopes in the shells of modern gastropods, bivalves and brachiopods. Ten brachiopod specimens were used but the species was unspecified. The results suggested that the gastropods and bivalves had $\delta^{18}O$ values in equilibrium with ambient seawater whereas brachiopods were isotopically heavier and not in equilibrium. Rahimpour-Bonab *et al.*

(1997) also observed a high degree of isotopic covariance, which they suggest was indicative of vital effects, resulting in disequilibrium precipitation. James *et al.* (1997), working at the same location analysed 48 modern brachiopods from 4 terebratulid species. The brachiopods were grab sampled, allowing differentiation between specimens from discrete parts of the shelf. Disregarding the advice of Carpenter & Lohmann (1995) on the grounds that primary layer calcite accounted for less than 6% of the bulk, James *et al.* (1997) analysed samples of crushed whole shells. Their results distinguished between specimens collected in areas of the Lacepede Shelf influenced by seasonal upwelling of colder water and those not. The conclusion of the study was that the $\delta^{18}O$ content of the brachiopod shell did reflect variations in ambient seawater temperature.

Curry & Fallick (2002) added to the controversy when they reported different $\delta^{18}O$ values from the dorsal and ventral valves of the articulated brachiopod *Calloria inconspicua* (Sowerby) from the Otago Shelf in New Zealand. This observation was corroborated in the same study using well preserved fossil specimens of *Calloria inconspicua* extracted from upper Pleistocene deposits from the Wanganui Basin, North Island, New Zealand (Curry 1999).

Much of the published data on modern brachiopod isotope analysis is brought together along with a large amount of new data in a recent study by Brand *et al.* (2003). The work assesses whether a variety of modern brachiopods are in oxygen isotopic equilibrium with ambient seawater. Brand *et al.* (2003) devised an "oxygen isotope equilibrium incorporation test". However, their criteria for equilibrium were quite liberal, requiring only 75% of isotopic temperatures calculated from brachiopod shell carbonate to fall within the measured seawater temperature range. Given this and the fact that in many cases measured seawater temperatures are wide-ranging, there are still many analyses that fail their test and have ambiguous or disequilibrium results.

Clearly, there is still much controversy surrounding brachiopods and their ability to precipitate their shells in isotopic equilibrium with ambient seawater. It could be that the diversity of modern brachiopods with a variety of ecologies, environments, shell structures and biomineralisation regimes leads to many of the conflicting data. The understanding of stable isotope distribution within living brachiopods is vital to decipher the signal from fossil specimens and improve the resolution of palaeoenvironmental investigations.

1.4 The aims and approach of this study

1.4.1 Aims

This study aims: (1) to thoroughly investigate the variability of oxygen and carbon stable isotopes in modern brachiopod shells. This will be structured so as to provide an insight into the viability of using oxygen and carbon stable isotope determinations from brachiopod shells in both environmental and palaeoenvironmental studies.

(2) To produce standardised protocols for sample preparation and analysis that can produce consistently reproducible results from brachiopod shell carbonate in respect to oxygen and carbon isotope ratio mass spectrometry.

(3) To assess the diversity of modern brachiopods in respect of taxonomic grouping; shell fabric; ecology; environmental conditions and geographical location, and consider any palpable variations in oxygen and carbon stable isotopic composition vis-à-vis these factors.

(4) To make comparisons between the use of stable oxygen isotope determinations from brachiopod shells as recorders of ambient seawater temperature and a co-existing molluscan species in the Firth of Lorne.

1.4.2 Approach

This study systematically examines the structure and isotopic composition of the shells of representatives of each group of extant calcitic brachiopods as classified by Williams *et al.* (1996).

The specimens were taken from a wide range of locations, from low to high latitudes, with a variety of environmental settings. The ultrastructures of each were examined by scanning electron microscopy (SEM), and stable isotope analyses were carried out on material from different ultrastructural layers as well as from different morphological components of the shell. These analyses enable identification of intra-specimen as well as taxonomic and geographical trends and patterns of isotopic distribution. The trends and patterns observed provide a valuable guide for avoiding potential problems.

Comparisons are also made between oxygen and carbon stable isotope determinations from two contrasting groups of calcitic brachiopods and a co-existing bivalve with a mixed calcite/aragonite composition, in a modern marine epibenthic community.

Chapter 2

Specimens and locations

2 Specimens and locations

2.1 Brachiopod specimens and classification

The Brachiopoda is a widespread and diverse phylum that was at its most prolific during the Cambrian and Ordovician periods. Although 95% of all genera are now extinct, the Brachiopoda have survived to the present day and are represented by over 100 genera from varied groups that are globally distributed and representative of former diversity. This study has utilised 122 individuals from 12 modern species collected live from 8 different environments with a global distribution (see section 2.2). The species selected represent each extant group of calcareous shelled brachiopods identified in the most recently adopted classification (Williams *et al.* 1996) (Fig2.1). A simplified form of those elements that relate to modern brachiopods is given below (Williams *et al.* 1996; Williams & Brunton 1997; Clarkson 1998).

PHYLUM BRACHIOPODA (Cambrian to Recent): Sessile marine invertebrates with two unequal but bilaterally symmetrical valves. Valves can be either organophosphatic or calcitic. Brachiopods are bathyal to intertidal in distribution. They may be free lying or attached to a substrate either by a stalk-like pedicle protruding from ventral (pedicle) valve or cementing of ventral valve. The shell is secreted by mantle which is an extension of the body wall.

The Brachiopoda are divided into 3 subphyla:

SUBPHYLUM LINGULIFORMEA (Lower Cambrian to Recent): Inarticulated valves, in which teeth or sockets are absent. All Linguliformea have organophosphatic shells and are therefore excluded from this investigation.

SUBPHYLUM CRANIIFORMEA (Lower Cambrian to Recent): Calcareous shelled inarticulated brachiopods, without teeth or sockets. The pedicle is either diminished or absent. The ventral valve is normally cemented to substrate and the intestine has an anus.

CLASS CRANIATA (Lower Cambrian to Recent)

ORDER CRANIIDA (Middle Cambrian to Recent): Calcareous rounded punctate shell. The ventral valve is normally cemented to the substrate, while the dorsal (brachial) valve is usually conical. Muscle scars are prominent, for example *Novocrania anomala* (Müller) and *Neoancistrocrania norfolki* (Laurin).

SUBPHYLUM RHYNCHONELLIFORMEA (Lower Cambrian to Recent): Calcareous shelled articulated brachiopods with teeth and sockets. Shells are endopunctate, impunctate or pseudopunctate. Crura (singular crus) are normally present which can be elongated to form a loop. Valves are opened by diductor and closed by adductor muscles. The intestine has no anus.

CLASS RHYNCHONELLATA (Lower Cambrian to Recent): Biconvex calcite shells. May be impunctate or endopunctate. A calcified loop may be present.

ORDER RHYNCHONELLIDA (Middle Ordovician to Recent) Astrophic shell usually with a beak. Normally attached to substrate by pedicle. Delthyrium partially closed visible in crura in ventral valve. Coarse ribs usually meeting along a zigzag commissure. Fold and sulcus usually well defined. Internally has a spirolophous loop, for example *Notosaria nigricans* (Sowerby).

ORDER TEREBRATULIDA (Lower Devonian to Recent): Articulated brachiopods with a biconvex punctate shell and short astrophic hinge. Functional pedicle emerging from umbonal foramen. Brachidium loop-like. Usually plectolophous.

SUBORDER TEREBRATULIDINA (Lower Devonian to Recent): Short loop with median septum normally absent; spicules developed internally, for example *Liothyrella neozelanica* (Thomson), *Liothyrella uva* (Broderip) and *Terebratulina retusa* (Linnaeus).

SUBORDER TEREBRATELLIDINA (Triassic to Recent): Long loop with cardinalia and median septum, for example *Calloria inconspicua* (Sowerby), *Laqueus rubellus* (Sowerby), *Neothyris lenticularis* (Deshayes), *Terebratalia transversa* (Sowerby) and *Terebratella sanguiea* (Leach).

ORDER THECIDEIDINA (Triassic to Recent): Small thick shelled articulated brachiopods. The shell can open very wide because the pedicle is absent and ventral valve is usually cemented to a substrate. Ptycholophe recessed deep within granular interior, for example *Thecidellina barretti* (Davidson).

Table 2.1

Figure 2.1

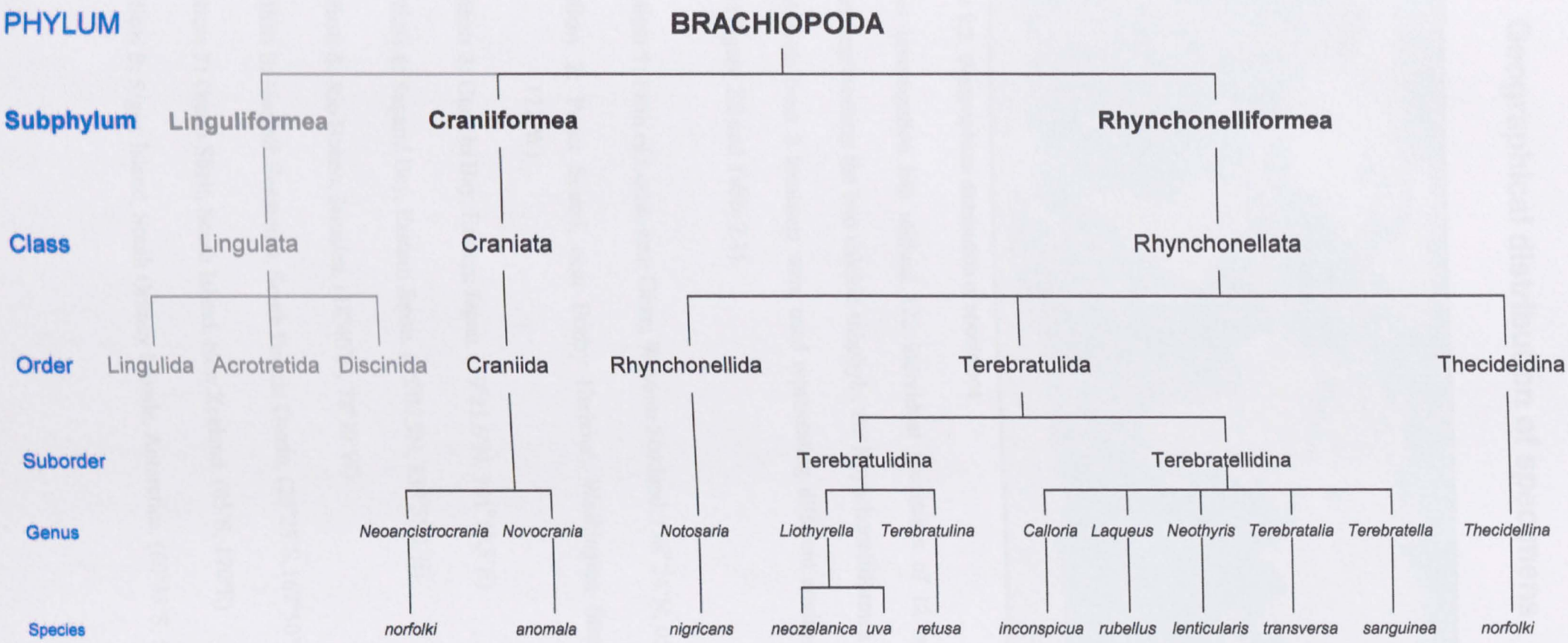

Figure 2.1: Cladogram detailing family structure of the extant brachiopods studied.

2.2 Geographical distribution of specimens

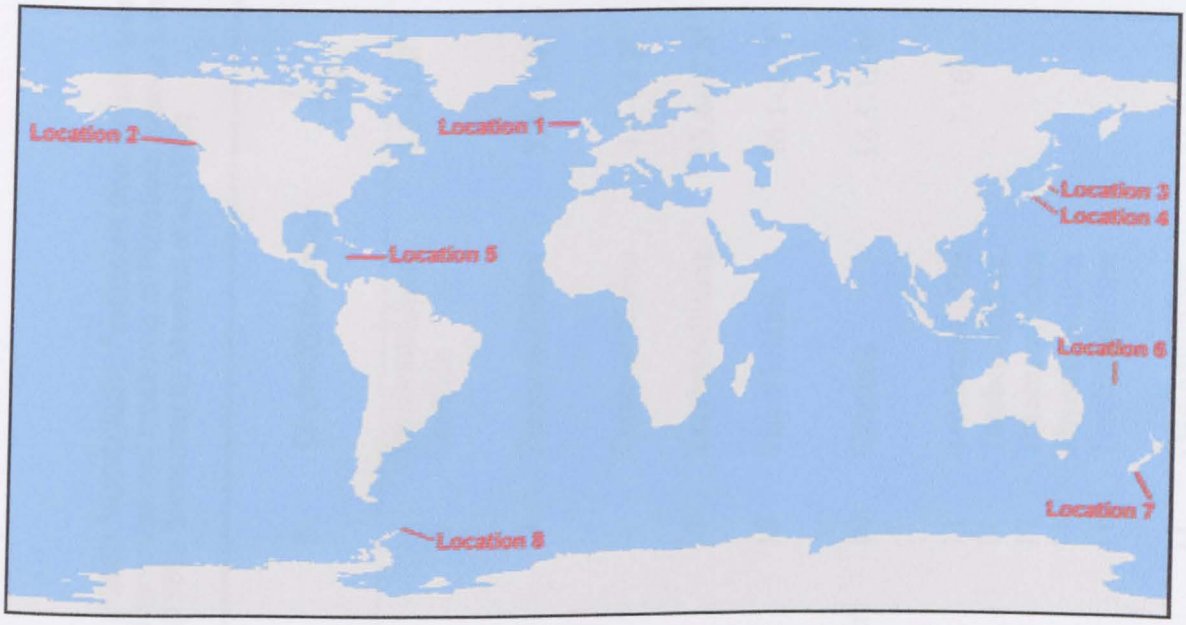

Figure 2.2: Geographical distribution of specimens.

This investigation has utilised 122 individual specimens of 12 modern brachiopod species, representing the two calcitic subphyla, the Rhynchonelliformea and Craniiformea. Brachiopods from 8 locations were used representing different environments around the world (Figure 2.2 and Table 2.1).

Location 1: Firth of Lorne, near Oban, Western Scotland. (56° 24'N, 05°38.4W)

Location 2: Puget Sound, near Friday Harbour, Washington State, USA. (48.5°N, 122°W)

Location 3: Otsuchi Bay, Eastern Japan. (39°23.6'N, 141°59.5'E)

Location 4: Sagami Bay, Eastern Japan. (35°07.9N, 139°35.1'E)

Location 5: Rio Bueno, Jamaica. (18°40'N, 78°30'W)

Location 6: Norfolk Seamount, South Pacific Ocean. (23°27'S,167°50'E)

Location 7: Otago Shelf, South Island, New Zealand. (45°S, 170°E)

Location 8: Signy Island, South Orkney Islands, Antarctica. (60°43'S, 5°36'W)

Table 2.1: Location species and status of the ambient seawater [a](BODC, 2003); [b]Carpenter & Lohmann (1995); [c]JODC(2001); [d]estimated from salinity data supplied by JODC (2001); [e]Rao (1996); [f]estimated from salinity data (Rao, 1996); [g]daily seawater surface temperatures measured at Portobello Marine Laboratory from 1953–1997, supplied by Dr Keith Probert; [h]Measured by Crowley & Taylor (2000); [i]Clarke *et al.* (1988); [j]Measured by Marshall *et al.*(1996).

Location	Position	Depth (m)	Species	n	Order/Suborder	T (°C)	$\delta^{18}O$ water (‰ VSMOW
Firth of Lorne, Scotland	56°26'N, 5°38'W	150-200	*Terebratulina retusa*	11	Terebratulidina	6.2-12.3[a]	0.06
			Novocrania anomala	11	Craniida		
Puget Sound, Nr. Friday Harbor, Washington, USA	48.5°N, 122°W	~45	*Terebratalia transversa*	11	Terebratellidina	7.4-11.4[b]	0.50[b]
Otsuchi Bay, Japan	39°24'N, 141°60'E	~70	*Laqueus rubellus*	2	Terebratellidina	4.4-16.8[c]	-0.05[d]
Sagami Bay, Japan	35°08'N, 139°35'E	85-90	*Laqueus rubellus*	11	Terebratellidina	13.4-17.6[c]	0.29[d]
Rio Buneo, Jamaica	18°40'N, 78°30'W	~20	*Thecidellina barretti*	10	Thecideidina	26.1-28.7[e]	0.78[f]
Norfolk Seamount, Southern Pacific Ocean	23°27'S, 167°50'E	276-350	*Neoancistrocrania norfolki*	10	Craniida	16.5-18.9[c]	0.75[d]
Otago Shelf, SI New Zealand	45°S, 170°E	80-85	*Calloria inconspicua*	11	Terebratellidina	7-16[g]	0.29[h]
			Liothyrella neozelanica	11	Terebratulidina		
			Neothyris lenticularis	11	Terebratellidina		
			Notosaria nigricans	11	Rhynchonellida		
			Terebratella sanguinea	11	Terebratellidina		
Signy Island, Antarctica	60°43'S45°36'W	~12	*Liothyrella uva*	11	Terebratulidina	-1.8-0.4[i]	-1.21[j]

2.3 Study locations, species and environmental data

2.3.1 *Location 1: Firth of Lorne, near Oban, Western Scotland*

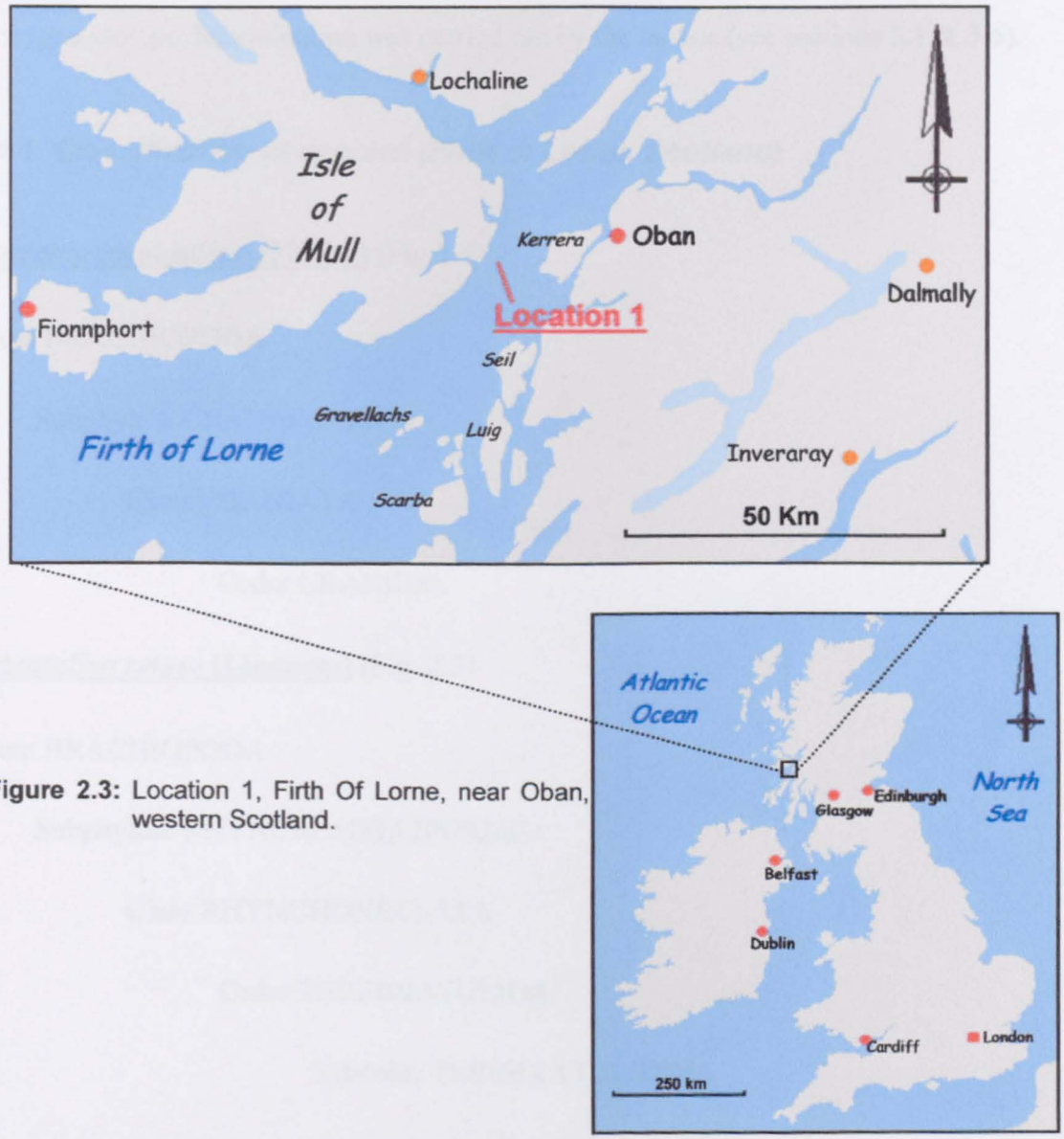

Figure 2.3: Location 1, Firth Of Lorne, near Oban, western Scotland.

Location 1 is situated in the Firth of Lorne on the west coast of Scotland, UK (56° 24'N, 5°38,4'W) (Fig. 2.3). At this location, two brachiopods *Novocrania anomala* (Fig 2.4) and *Terebratulina retusa* (Fig 2.5) were collected together with a bivalve, the horse mussel *Modiolus modiolus* (Linnaeus) (Fig 2.6) to which the brachiopods were attached (see Chapter 7). Specimens were collected by dredging the mussel bed during cruises of *RV Calanus*, a research vessel based at Dunstaffnage Marine Laboratory, Oban, Scotland in 2002. The bed is located on the gently sloping margins of a depression in the seafloor, at depths of 150 to 200 metres. The local seawater has a monthly mean temperature range of

6.2°C to 12.3°C and an annual mean of 9.1°C. The oxygen isotope composition of seawater in the area has been determined from actual measurements: $\delta^{18}O = 0.06‰$. Temperature data was provided by the British Oceanographic Data Centre (2003). Sampling of seawater and oxygen isotope determination was carried out by the author (see sections 3.1 & 3.6).

2.3.1.1 Classification of species (Firth of Lorne, Scotland)

***Novocrania inconspicua* (Müller)** (Fig.2.4)

Phylum BRACHIOPODA

Subphylum CRANIIFORMEA

Class CRANIATA

Order CRANIIDA

***Terebratulina retusa* (Linnaeus)** (Fig. 2.5)

Phylum BRACHIOPODA

Subphylum RHYNCHONELLIFORMEA

Class RHYNCHONELLATA

Order TEREBRATULIDA

Suborder TEREBRATULIDINA

***Modiolus modiolus* (Linnaeus)** – horse mussel (Fig. 2.6)

Phylum MOLLUSCA

Class BIVALVIA

Order MYTILOIDA

Superfamily MYTILACEA

Family MYTILIDAE

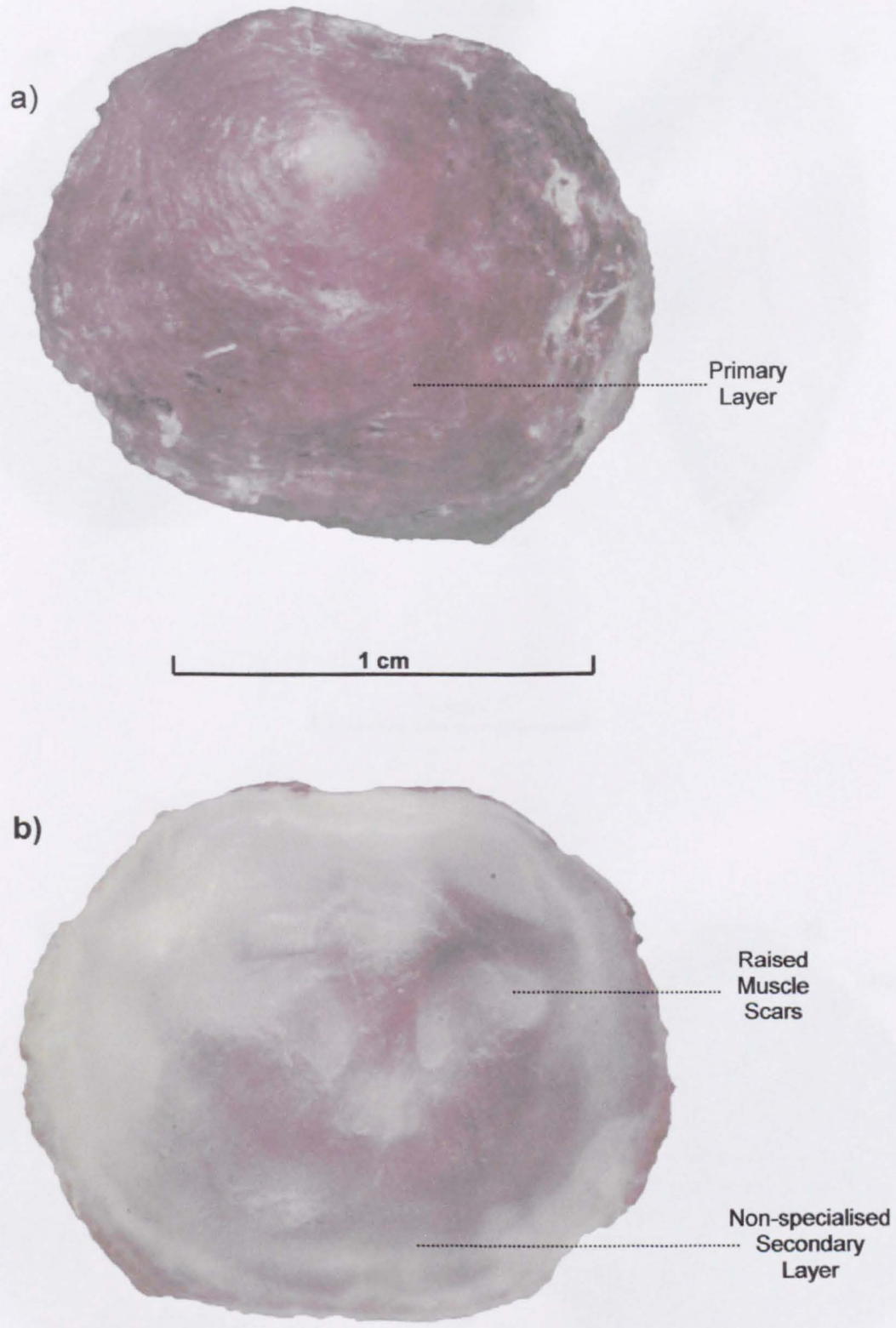

Figure 2.2.2: *Novocrania anomala* (Müller).

a) dorsal valve exterior view; **b)** dorsal valve interior view.

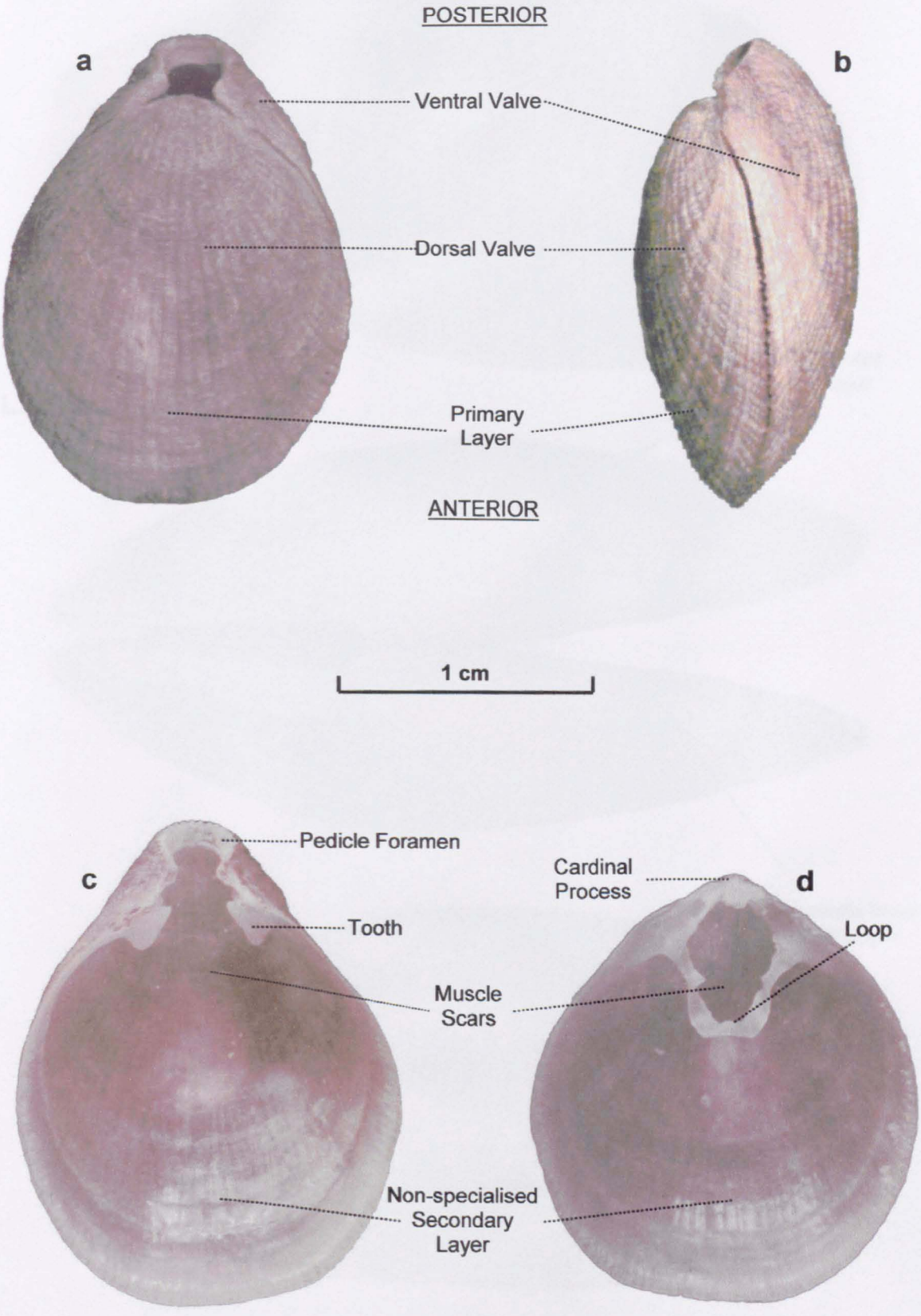

Figure 2.5: *Terebratulina retusa* (Linnaeus).

a) exterior dorsal view; **b)** exterior lateral view; **c)** interior view of ventral valve; **d)** interior view of dorsal valve.

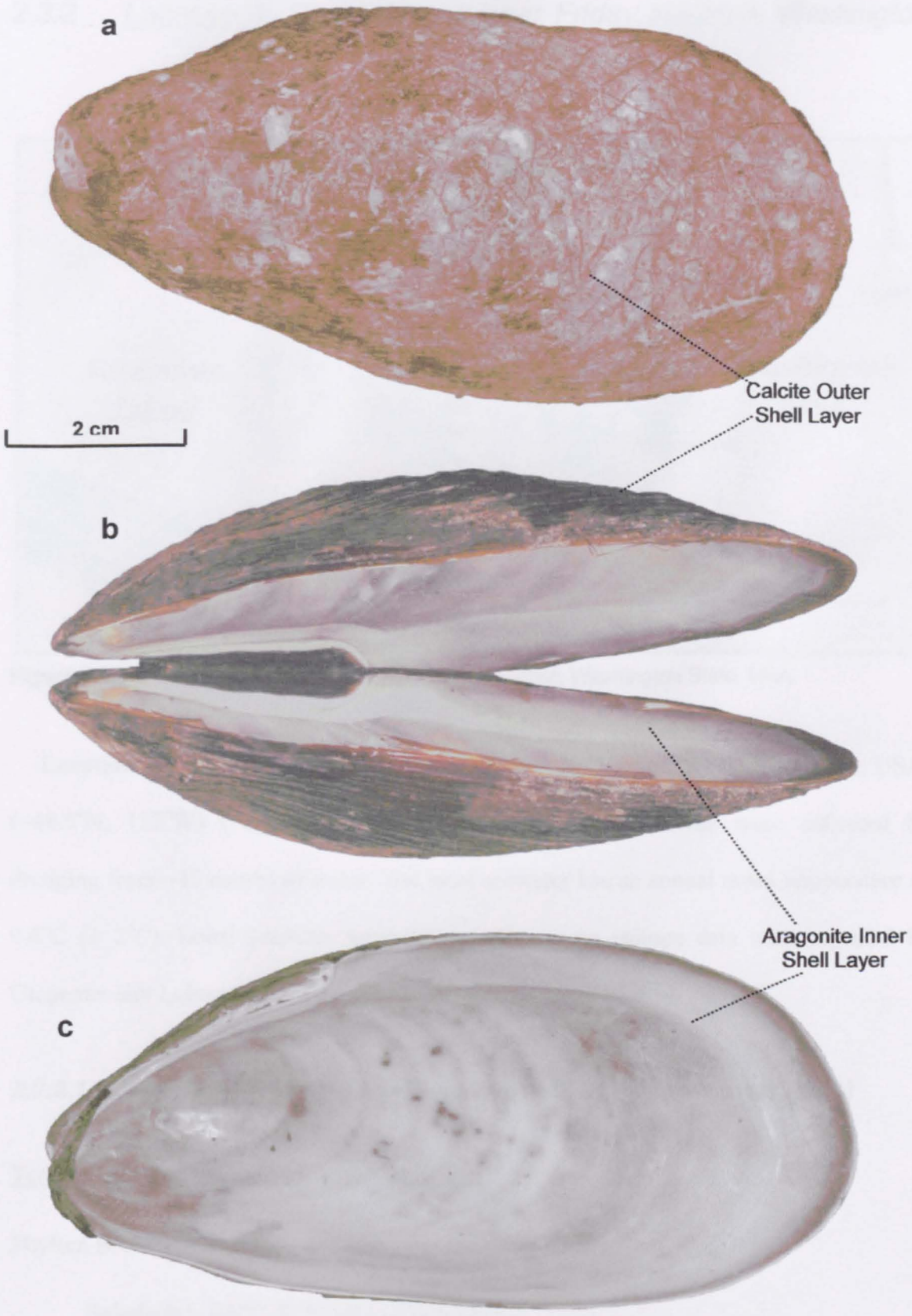

Figure 2.6: *Modiolus modiolus* (Linnaeus) – horse mussel.

a) exterior view; **b)** exterior view showing the two mirror image valves attached at the dorsal side by a horny ligament; **c)** interior of right valve.

2.3.2 Location 2: Puget Sound, near Friday Harbour, Washington State, USA.

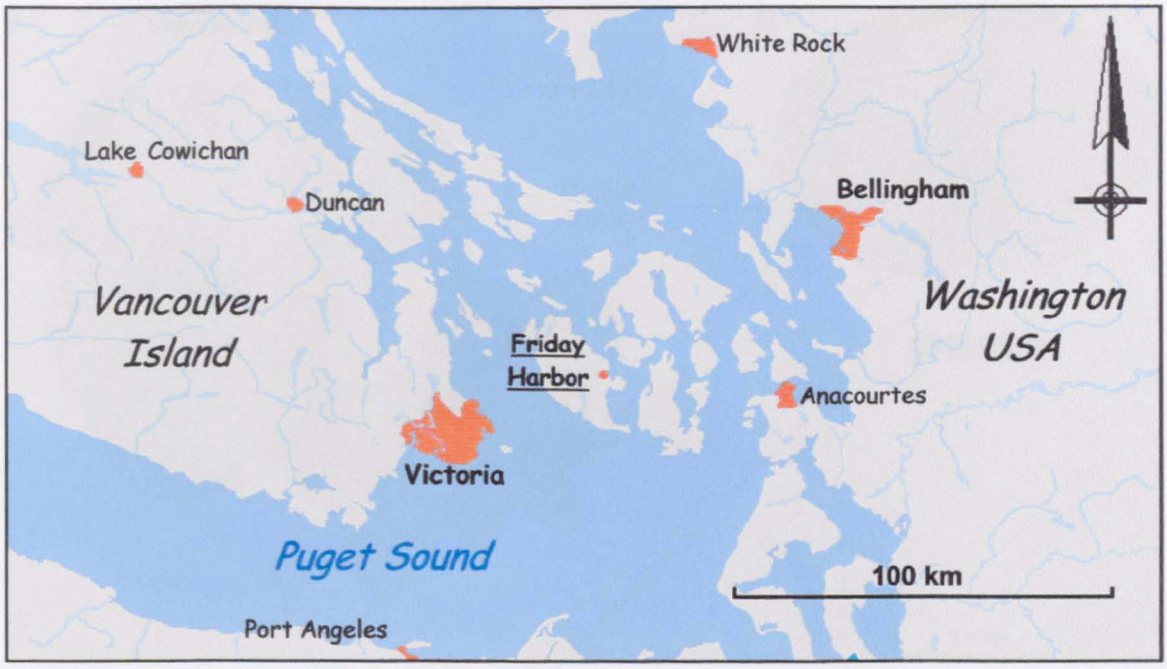

Figure 2.2.3: Location 2, Puget Sound, near Friday Harbor, Washington State, USA.

Location 2 is situated in the Puget Sound near Friday Harbor, Washington State, USA. (~48.5°N, 122°W) (Fig. 2.7), *Terebratalia transversa* specimens were collected by dredging from ~45 metres of water. The local seawater has an annual mean temperature of 9.4°C (± 2°C). Local seawater temperature and oxygen isotope data were reported by Carpenter and Lohmann (1995).

2.3.2.1 Classification of species (Puget Sound, Nr Friday Harbor, USA)

***Terebratalia transversa* (Sowerby)** (Fig.2.8)

Phylum BRACHIOPODA

Subphylum RHYNCHONELLIFORMEA

Class RHYNCHONELLATA

Order TEREBRATULIDA

Suborder TEREBRATELLIDINA

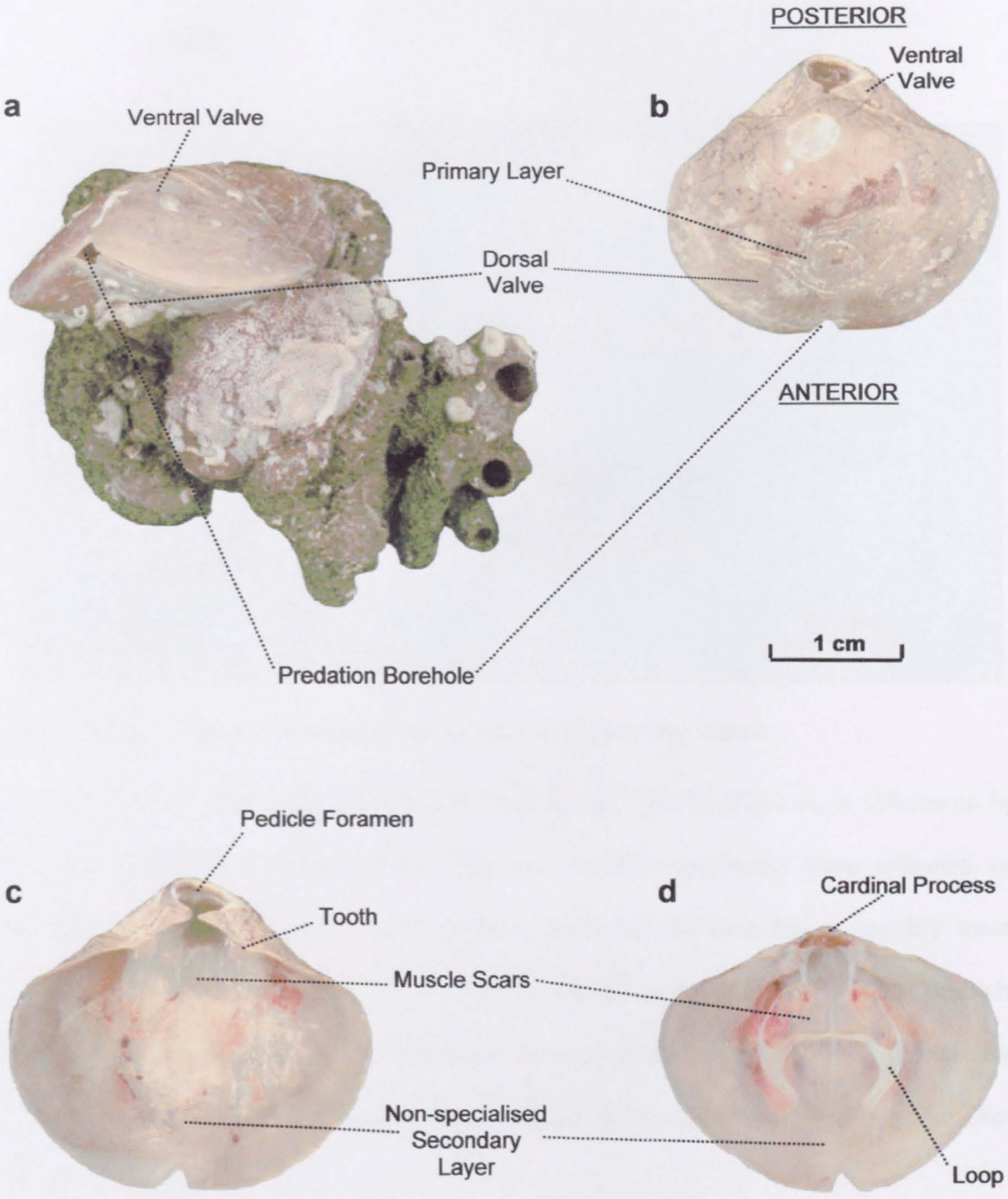

Figure 2.2.4: *Terebratulina transversa* (Sowerby).

a) shown attached to substrate, anterior view with ventral valve uppermost; **b)** exterior dorsal view; **c)** interior view of ventral valve; **d)** interior view of dorsal valve. NB: The hole at the anterior of the shell is the result of boring.

2.3.3 Location 3: Otsuchi Bay, and Location 4 Sagami Bay, Eastern Japan

Figure 2.2.5: Location 3, Otsuchi bay and Location 4, Sagami Bay, Japan.

Location 3 Otsuchi Bay, position 39° 23.6'N, 141° 59.5'E (Fig.2.9), is influenced by the relatively cool Oyashio current. *Laqueus rubellus* specimens were collected by dredging from 70 metres of water. Bottom water for the area has a monthly mean temperature range of 4.4°C to 16.8°C, with an annual mean of 11.0°C. $\delta^{18}O$ of ambient seawater was estimated to be –0.05‰ using the mean salinity value of 33.9‰ (see section 3.7). Temperature and salinity data were provided by the Japanese Oceanographic Data Centre (JODC 2001).

Location 4 Sagami Bay lies about 2km west of the western end of Jogashima Inlet at position 35° 07.9'N, 139° 35.1'E (Fig. 2.10), and is influenced by the relatively warm Kuroshio current. *Laqueus rubellus* specimens were collected by dredging from 85 to 90 metres of water. Bottom water for the area has a monthly mean temperature range of 13.4°C to 17.6°C, with an annual mean of 14.8°C. $\delta^{18}O$ of ambient seawater was estimated

to be 0.30‰ using the mean salinity value of 34.6% (see section 3.7). Temperature and salinity data were provided by the Japanese Oceanographic Data Centre (JODC 2001).

2.3.3.1 Classification of species (Otsuchi and Sagami bays, Japan)

***Laqueus rubellus* (Sowerby)** (Fig. 2.10)

Phylum BRACHIOPODA

Subphylum RHYNCHONELLIFORMEA

Class RHYNCHONELLATA

Order TEREBRATULIDA

Suborder TEREBRATELLIDINA

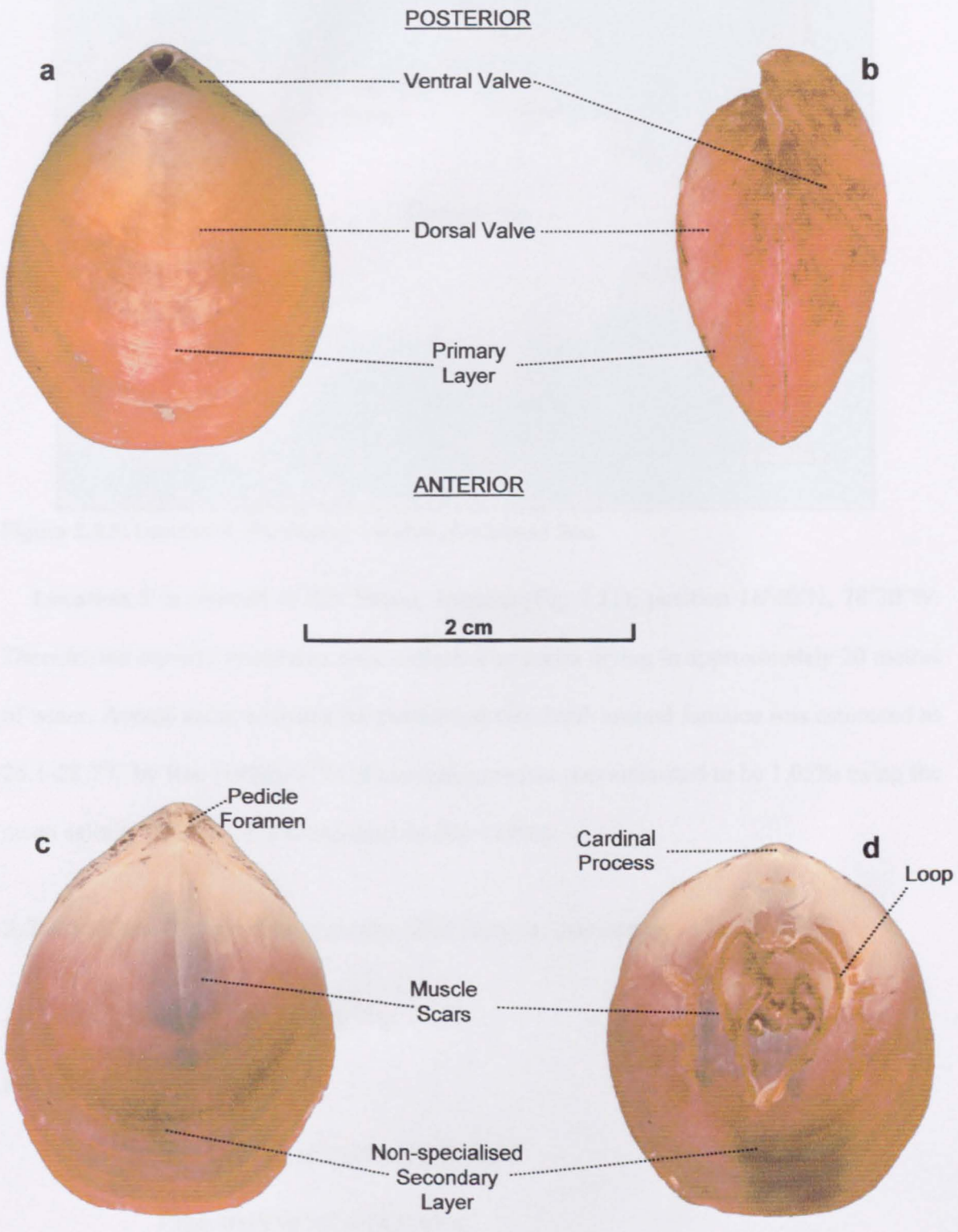

Figure 2.2.6: *Laqueus rubellus* (Sowerby).

a) exterior dorsal view; **b)** exterior lateral view; **c)** interior view of ventral valve; **d)** interior view of dorsal valve.

2.3.4 Location 5: Rio Bueno, Jamaica

Figure 2.2.7: Location 5, Rio Bueno, Jamaica, Caribbean Sea.

Location 5 is situated at Rio Bueno, Jamaica (Fig 2.11); position 18°40'N, 78°30'W. *Thecidellina barretti* specimens were collected by scuba diving in approximately 20 metres of water. Annual mean seawater temperature at this depth around Jamaica was estimated as 26.1-28.7°C by Rao (1996). $\delta^{18}O$ of ambient seawater was estimated to be 1.05‰ using the mean salinity value of 36.1‰ reported by Rao (1996).

2.3.4.1 Classification of species (Rio Bueno, Jamaica)

***Thecidellina barretti* (Davidson)** (Fig. 2.12)

Phylum BRACHIOPODA

Subphylum RHYNCHONELLIFORMEA

Class RHYNCHONELLATA

Order THECIDEIDINA

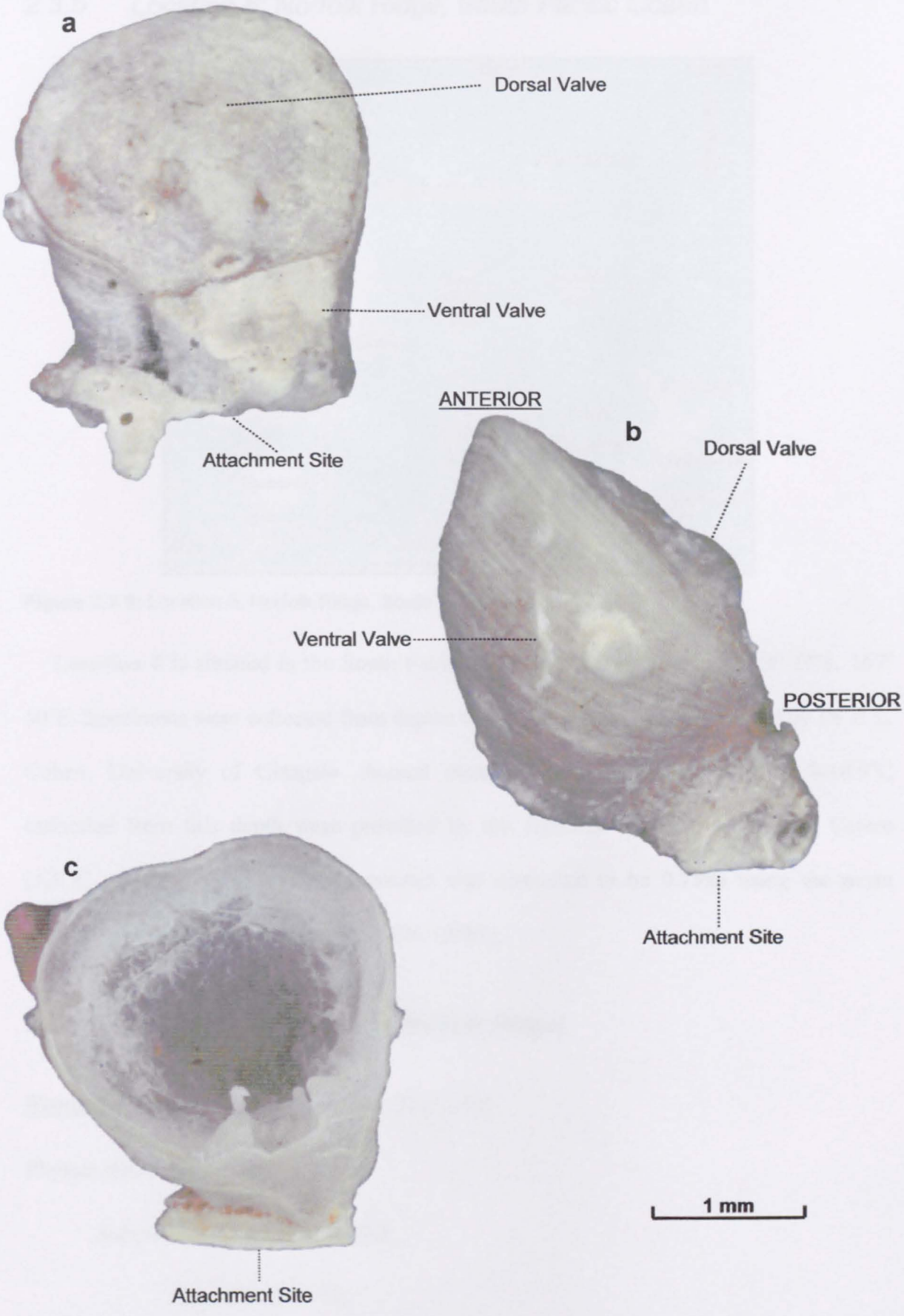

Figure 2.2.8: *Thecidellina barretti* (Davidson).

a) dorsal view of whole shell; **b)** lateral view of whole shell; **c)** interior view of ventral valve.

2.3.5 Location 6: Norfolk Ridge, South Pacific Ocean

Figure 2.2.9: Location 6, Norfolk Ridge, South Pacific Ocean.

Location 6 is situated in the South Pacific Ocean (Fig 2.13); position: 23° 27'S, 167° 50'E. Specimens were collected from depths of 276 - 350 metres and supplied by Dr B.L. Cohen, University of Glasgow. Annual mean seawater temperatures of 16.5-18.9°C estimated from this depth were provided by the Japanese Oceanographic Data Centre (JODC 2001). $\delta^{18}O$ of ambient seawater was estimated to be 0.75‰ using the mean salinity value of 35.5‰ supplied by JODC (2001).

2.3.5.1 Classification of species (Norfolk Ridge)

Neoancistrocrania norfolki **(Laurin)** (Fig. 2.14)

Phylum BRACHIOPODA

Subphylum CRANIIFORMEA

Class CRANIATA

Order CRANIIDA

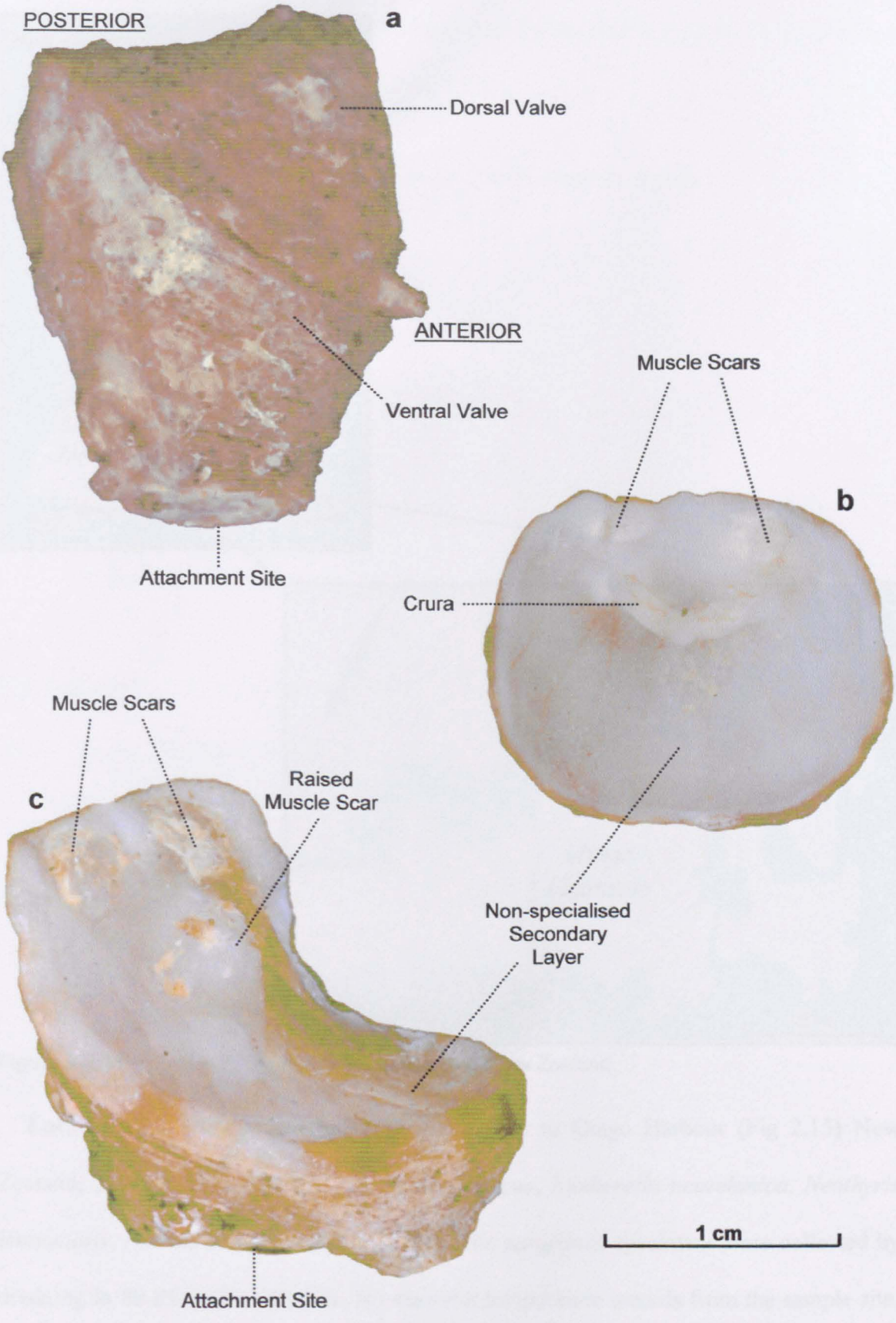

Figure 2.2.10: *Neoancistrocrania norfolki* (Laurin).

a) exterior lateral view of whole shell; **b)** interior view of dorsal valve; **c)** interior view of ventral valve.

2.3.6 Location 7: Otago Shelf, South Island, New Zealand

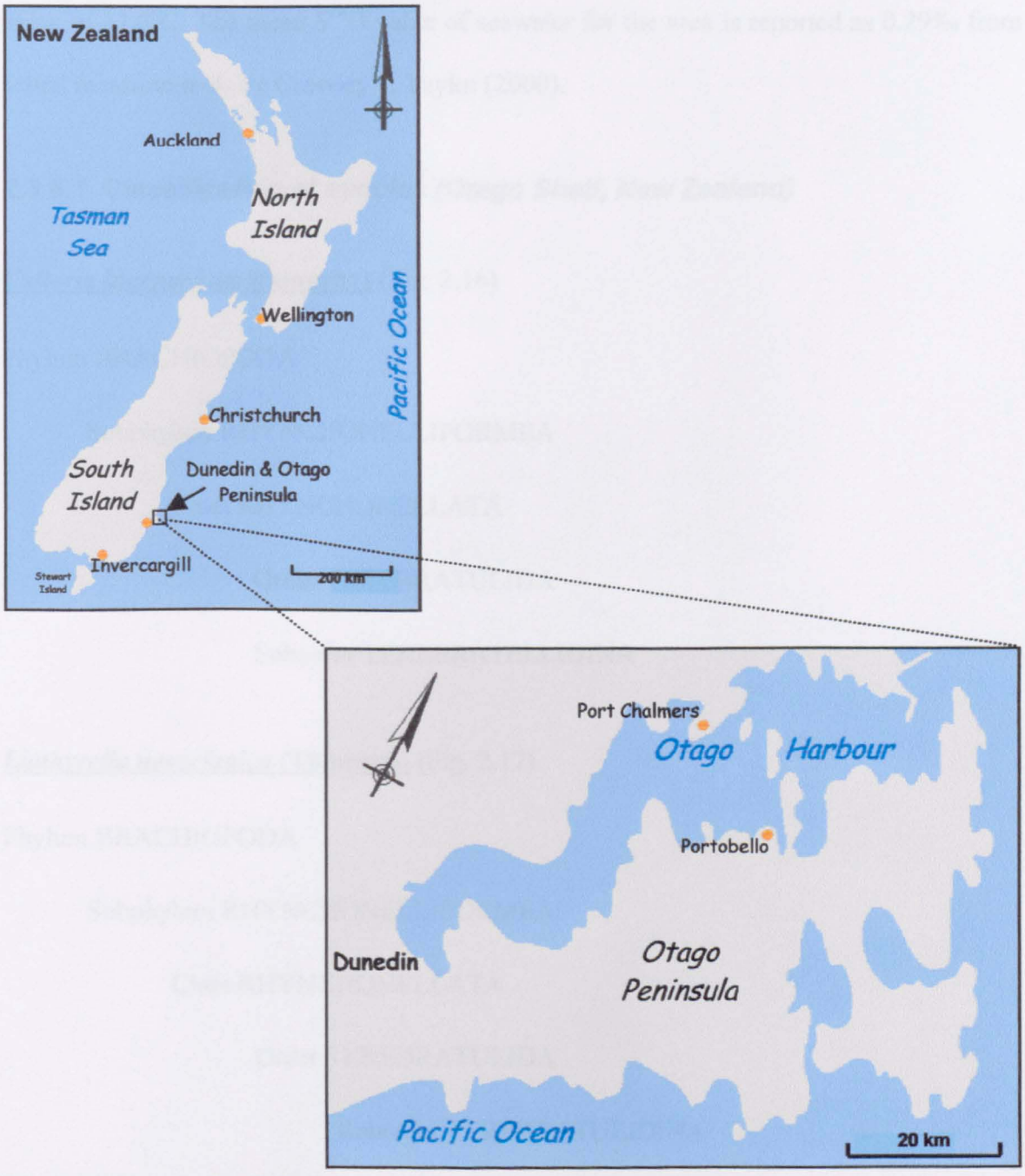

Figure 2.2.11: Location 7, Otago Shelf, South Island, New Zealand.

Location 7 is situated on the Otago Shelf near to Otago Harbour (Fig 2.15) New Zealand; position 45°S, 170°E. *Calloria inconspicua*, *Liothyrella neozelanica*, *Neothyris lenticularis*, *Notosaria nigricans* and *Terebratella sanguinea* specimens were collected by dredging in 80-85 metres of water. No seawater temperature records from the sample site, however daily surface seawater temperatures in the area have been measured at the Portobello Marine Laboratory since 1953 and were supplied by Dr Keith Probert. The

measured daily means give an annual seawater temperature range of 7-16°C with an annual mean of 11.6°C. The mean $\delta^{18}O$ value of seawater for the area is reported as 0.29‰ from actual measurements by Crowley & Taylor (2000).

2.3.6.1 Classification of species (Otago Shelf, New Zealand)

***Calloria inconspicua* (Sowerby)** (Fig. 2.16)

Phylum BRACHIOPODA

Subphylum RHYNCHONELLIFORMEA

Class RHYNCHONELLATA

Order TEREBRATULIDA

Suborder TEREBRATELLIDINA

***Liothyrella neozelanica* (Thomson)** (Fig. 2.17)

Phylum BRACHIOPODA

Subphylum RHYNCHONELLIFORMEA

Class RHYNCHONELLATA

Order TEREBRATULIDA

Suborder TEREBRATULIDINA

***Neothyris lenticularis* (Deshayes, 1839)** (Fig. 2.18)

Phylum BRACHIOPODA

Subphylum RHYNCHONELLIFORMEA

Class RHYNCHONELLATA

Order TEREBRATULIDA

Suborder TEREBRATELLIDINA

***Notosaria nigricans* (Sowerby)** (Fig. 2.19)

Phylum BRACHIOPODA

Subphylum RHYNCHONELLIFORMEA

Class RHYNCHONELLATA

Order RHYNCHONELLIDA

***Terebratella sanguinea* (Leach)** (Fig. 2.20)

Phylum BRACHIOPODA

Subphylum RHYNCHONELLIFORMEA

Class RHYNCHONELLATA

Order TEREBRATULIDA

Suborder TEREBRATELLIDINA

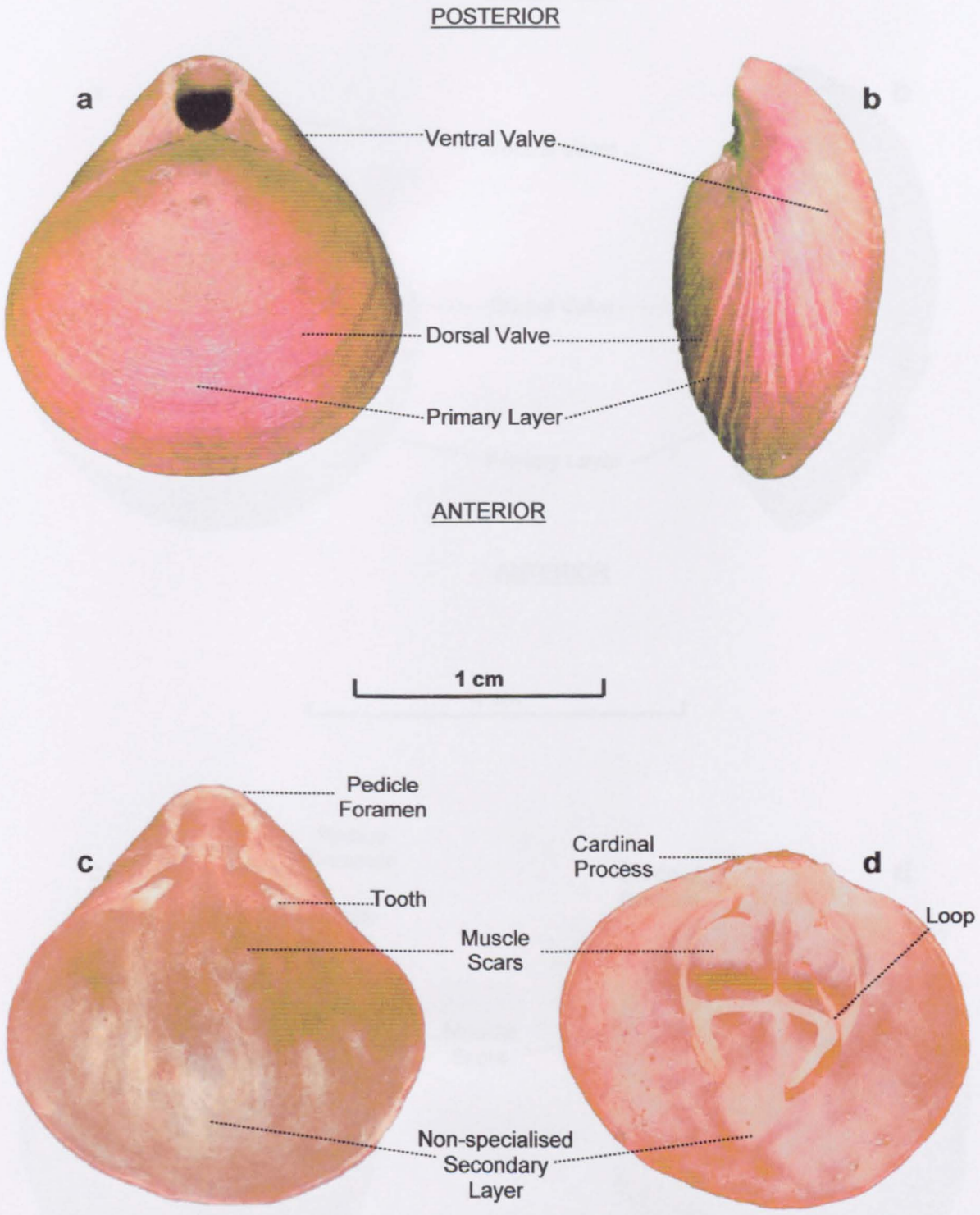

Figure 2.2.12: *Calloria inconspicua* (Sowerby).

a) exterior dorsal view; **b)** exterior lateral view; **c)** interior view of ventral valve; **d)** interior view of dorsal valve.

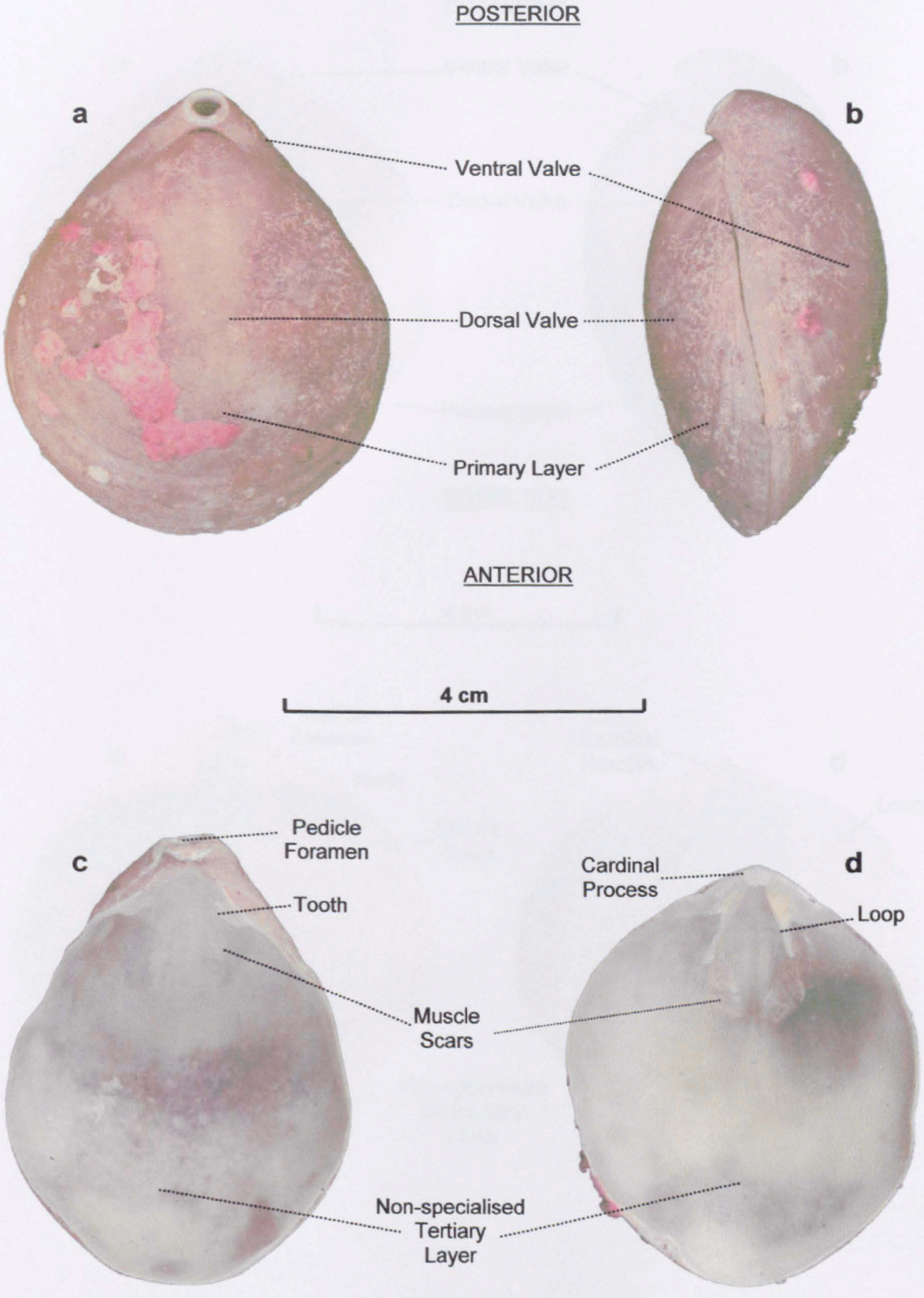

Figure 2.2.13: *Liothyrella neozelanica* (Thomson).

a) exterior dorsal view; **b)** exterior lateral view; **c)** interior view of ventral valve; **d)** interior view of dorsal valve.

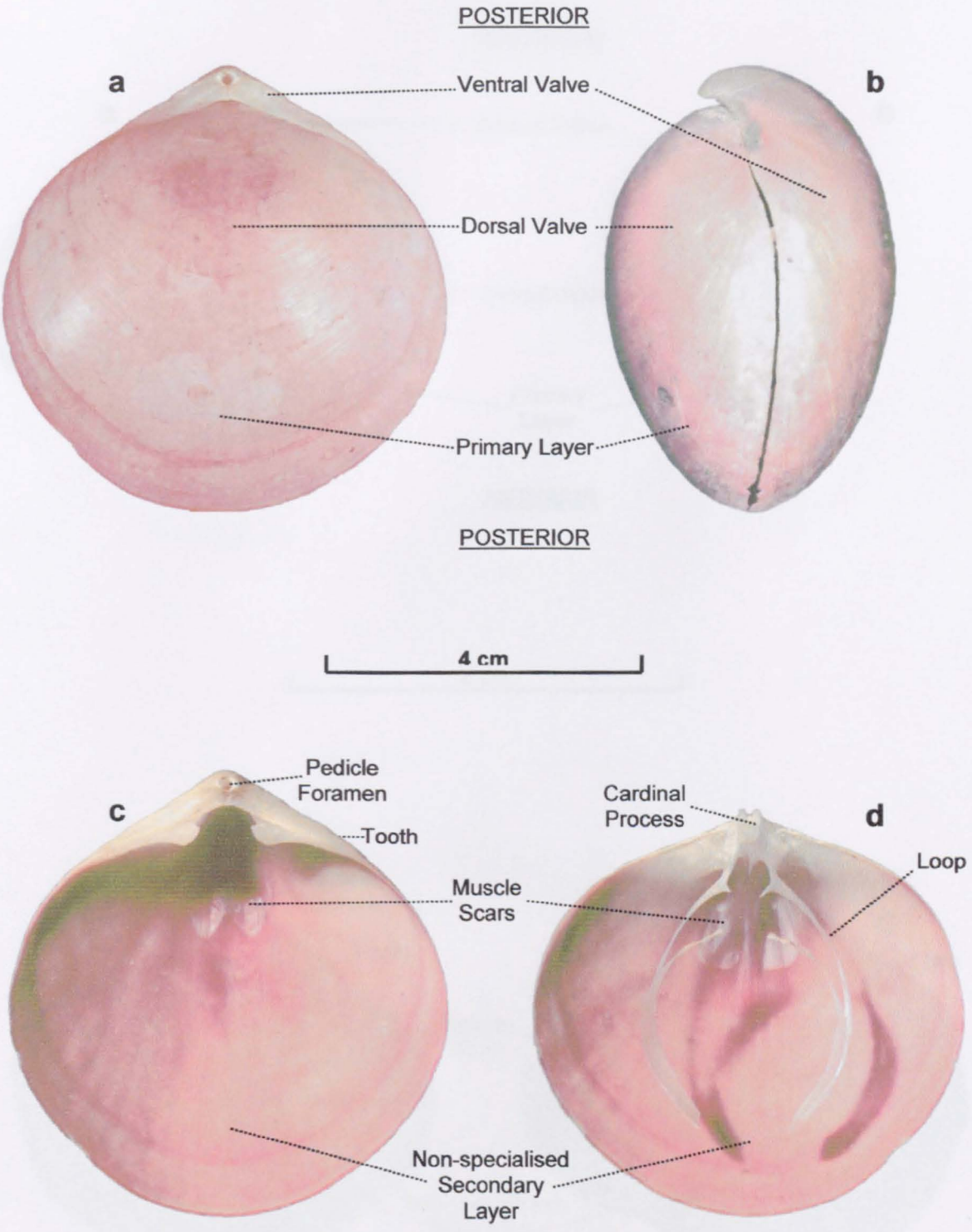
POSTERIOR
a
Ventral Valve
b
Dorsal Valve
Primary Layer
POSTERIOR
4 cm
Pedicle
Foramen
c
Tooth
Muscle
Scars
Cardinal
Process
d
Loop
Non-specialised
Secondary
Layer

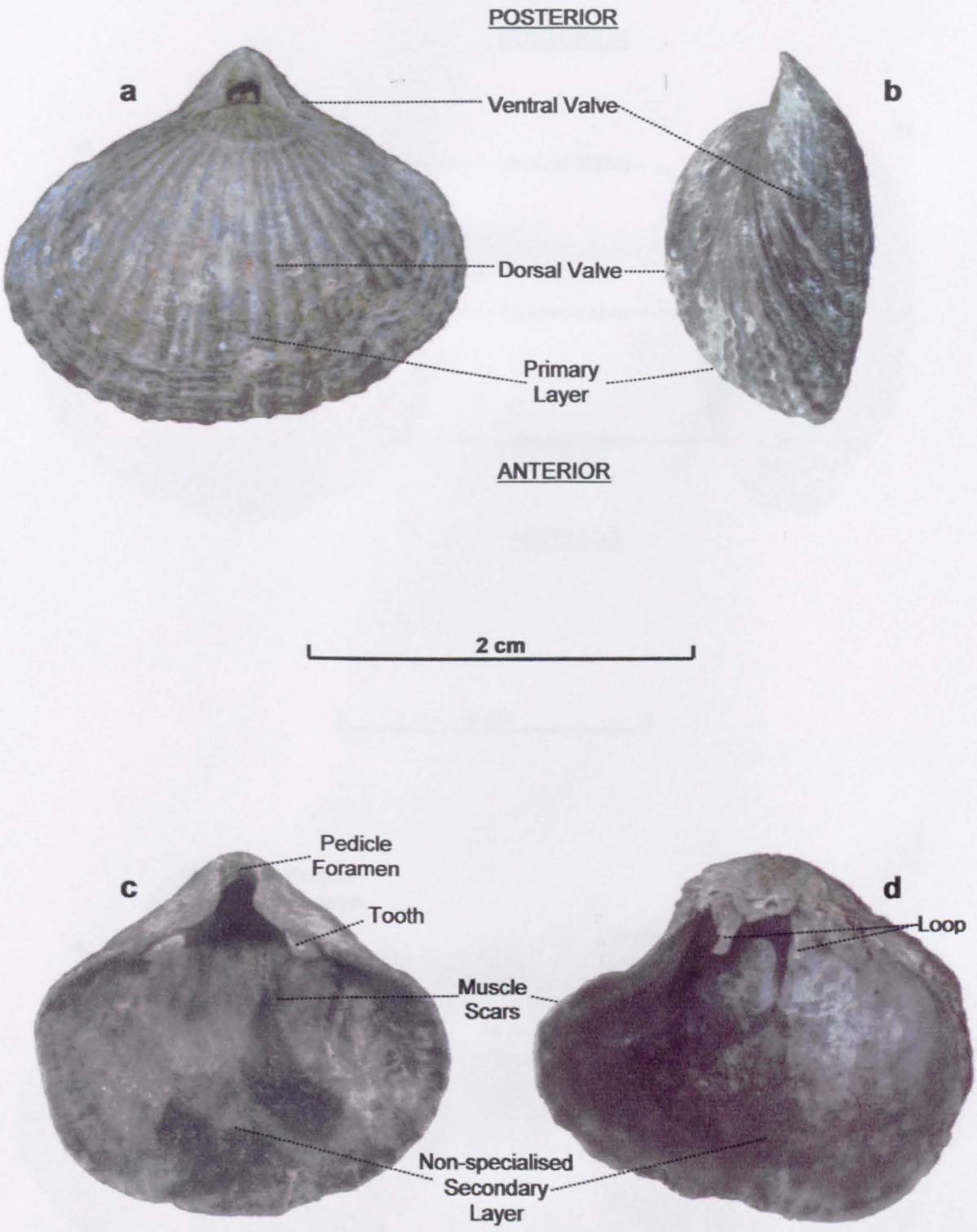

Figure 2.2.15: *Notosaria nigricans* (Sowerby).

a) exterior dorsal view; **b)** exterior lateral view; **c)** interior view of ventral valve; **d)** interior view of dorsal valve.

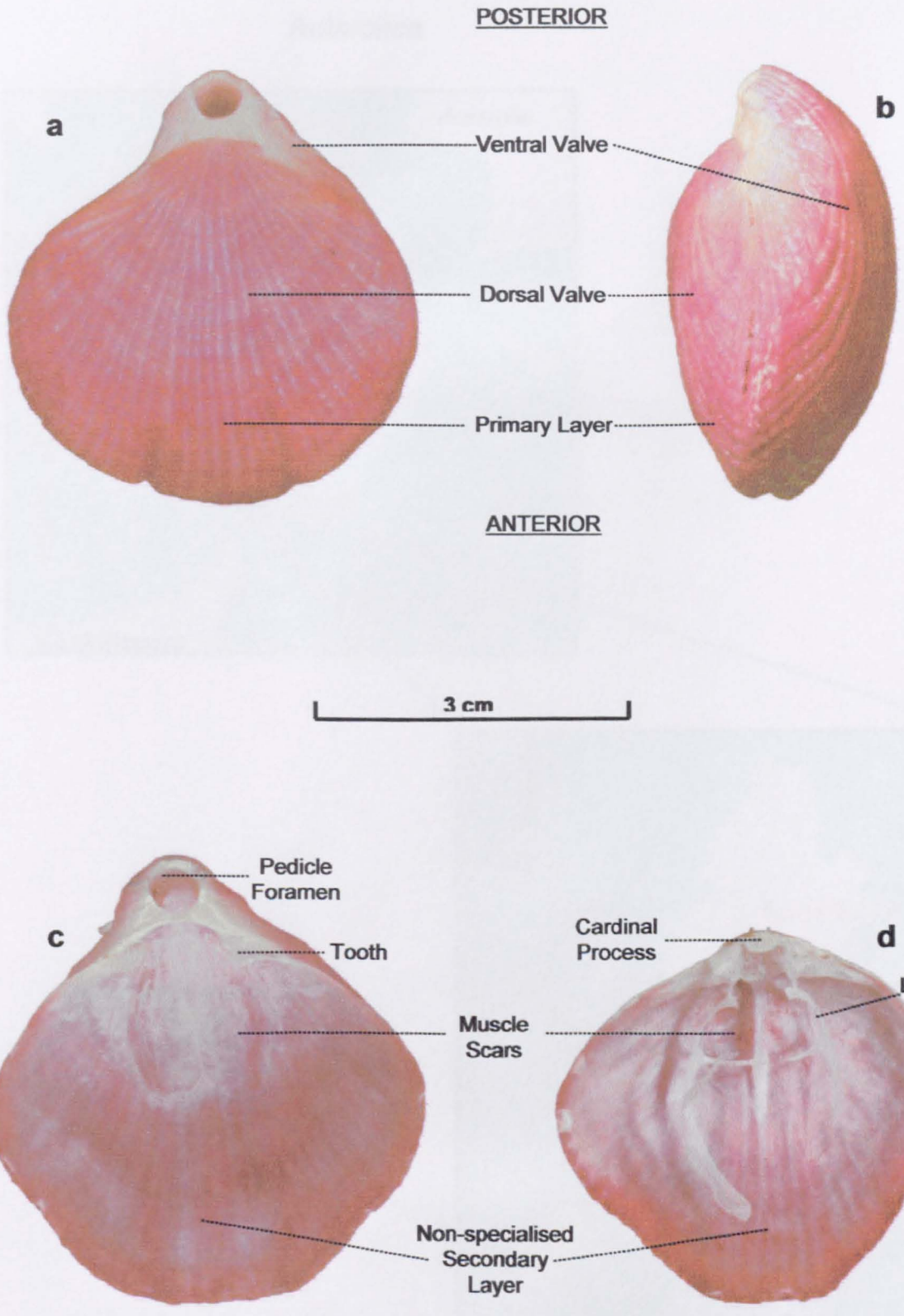

Figure 2.2.16: *Terebratella sanguinea* (Leach).

a) exterior dorsal view; **b)** exterior lateral view; **c)** interior view of ventral valve; **d)** interior view of dorsal valve.

2.3.7 Location 8: Borge Bay, Signy Island, South Orkney Islands, Antarctica

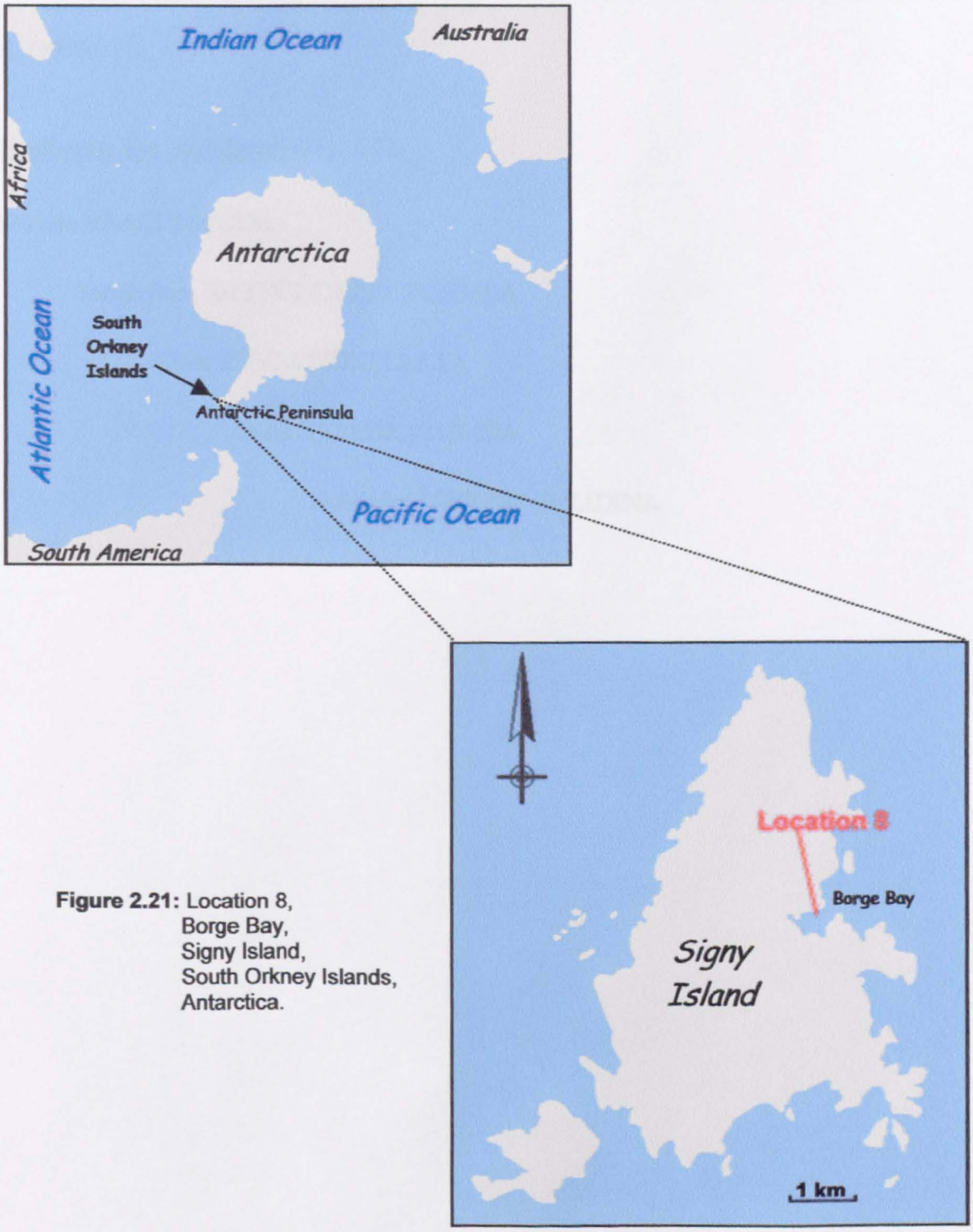

Figure 2.21: Location 8, Borge Bay, Signy Island, South Orkney Islands, Antarctica.

Location 8 is situated at Borge Bay, Signy Island in the South Orkney Islands, Antarctica (60°43'S, 45° 36'W) (Fig. 2.21). *Liothyrella uva* specimens (Fig. 2.22) were collected by scuba diving from a cave at 12 metres depth. The brachiopods were living

several deep, attached to the upper cave surface. The ambient seawater temperature range in Borge Bay has been measured as –1.8°C to 0.4°C by Clarke *et al.* (1988). $\delta^{18}O$ of seawater in Borge Bay is reported to be –1.21‰ from actual measurements by Marshall et al. (1996).

***Liothyrella uva* (Broderip)** (Fig. 2.22)

Phylum BRACHIOPODA

Subphylum RHYNCHONELLIFORMEA

Class RHYNCHONELLATA

Order TEREBRATULIDA

Suborder TEREBRATULIDINA

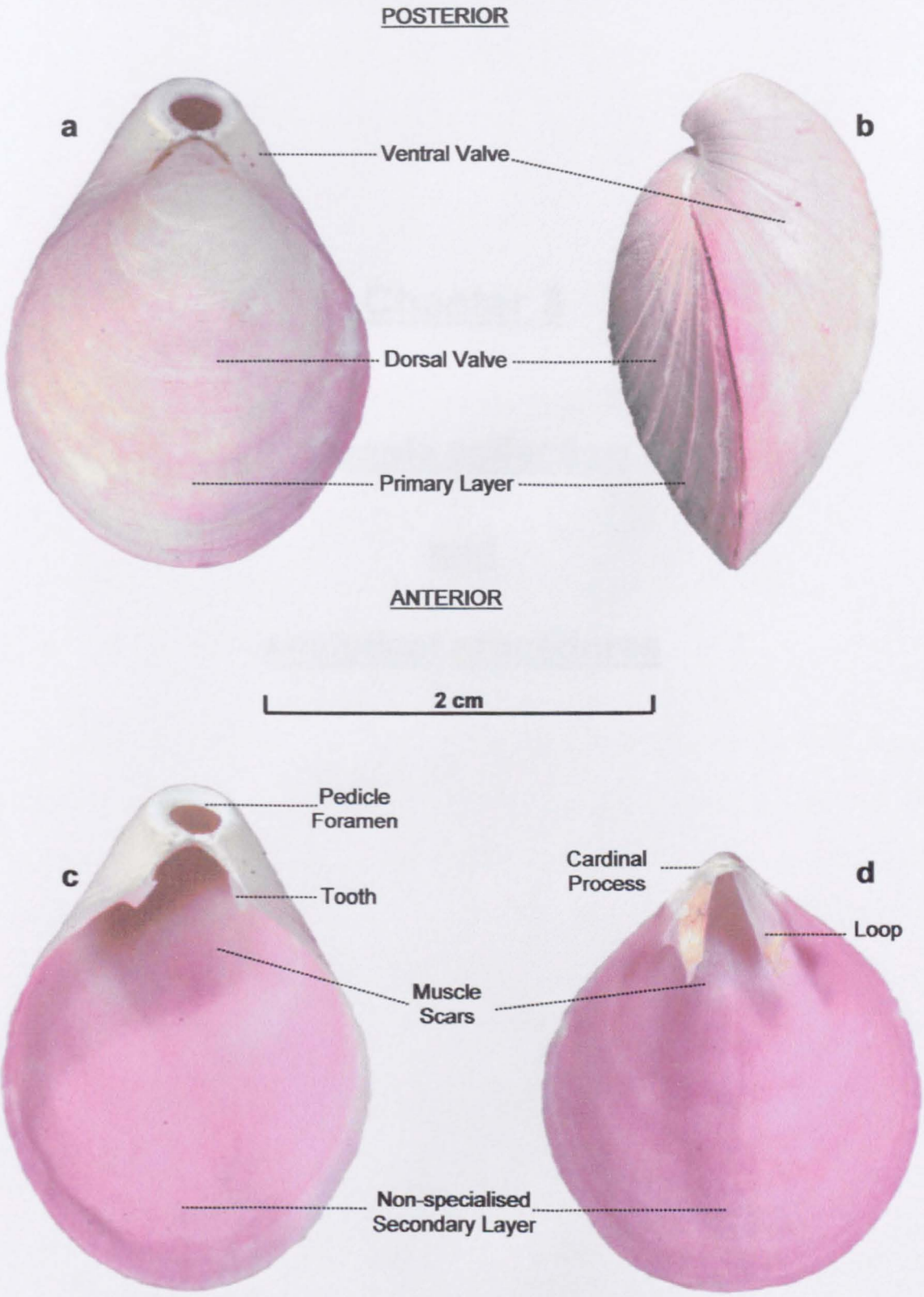

Figure 2.2.17: *Liothyrella uva* (Broderip).

a) exterior dorsal view; **b)** exterior lateral view; **c)** interior view of ventral valve; **d)** interior view of dorsal valve.

Chapter 3

Sample collection

and

analytical procedures

3 Sample collection and analytical procedures

3.1 Collection of samples

3.1.1 Firth of Lorne

Specimens from Location 1, Firth of Lorne, off the west coast of Scotland (56°26'N, 5°38'W) were collected personally. The brachiopods *Novocrania anomala* (Müller) and *Terebratulina retusa* (Linnaeus), together with the bivalve *Modiolus modiolus* (Linnaeus) coexist in an epibenthic community at a depth of 150-200 metres. The samples were collected alive in 2002 by trawling the sea bed using a modified clam dredger (Fig. 3.1) during cruises of the *RV Calanus*, a research vessel based at the Dunstaffnage Marine Laboratory, Oban, Scotland.

During the same cruises, samples of seawater were collected for oxygen stable isotope analysis. These were collected from the seafloor in the sample area using a reversing bottle attached to a Lebus Hydrographic probe (Figure 3.2). This device is lowered to the seabed with both ends open to permit free flow of water through the bottle. After allowing time for the water to thoroughly flush, the sealing mechanism is triggered allowing a sample of seawater from the vicinity of the seafloor to be returned to the surface. A winter collection of ten samples of seawater was made on the 17th January 2002. A further collection of ten samples of seawater was made during the summer on the 27th June 2002.

3.1.2 Other brachiopod specimens

All other samples were collected and supplied by a variety of institutions. Details are listed in chapter 2.

Figure 3.1: Dredging for brachiopods and bivalves from *RV Calanus*.

Figure 3.2: Collecting bottom water with a reversing bottle attached to a Lebus Hydrographic Probe from *RV Calanus*.

3.2 Scanning electron microscopy (SEM)

The ultrastructure of the shell of each brachiopod species was observed in two different ways: (i) Some shells were fractured laterally, then coated with gold/palladium; (ii) Other shells were cut both laterally and transversely using a diamond saw, set in an epoxy resin and polished. The exposed sections were etched using an aqueous solution of hydrochloric acid (0.1M) for 30 seconds, then rinsed and dried prior to coating with gold/palladium. These samples were studied using a Cambridge Instruments S360 scanning electron microscope equipped with an Oxford Instruments ISIS microanalysis system.

3.3 Cathodoluminescence (CL)

Samples of each brachiopod species were checked using cathodoluminescence to ensure that no recrystallisation was evident. These analyses were carried out using a CITL Technosyn 8200 Mk 4 mounted on a Zeiss Axioplan petrological microscope.

3.4 Sample preparation for stable isotope analysis

The valves of each specimen were separated and any soft tissues removed. The shells were then treated in an ultrasonic bath with dilute commercial bleach to assist in the removal of remaining organic material and foreign particles. After 30 minutes, the valves were brushed and rinsed several times with deionised water and then air dried. This is a variation of the method used by Rahimpour-Bonab *et al.* (1997) and recommended by Love & Woronow (1991) and Gaffey & Bronnimann (1993). Small samples of shell material from specific areas of each specimen were extracted under a binocular microscope using a low-speed drill with a 1.5mm tapered dental burr. Alternatively, a dental scraper was used for particularly delicate specimens.

Modern terebratulid and rhynchonellid brachiopod shells have two or three calcitic layers. The outer primary layer is a thin prismatic structure. In most genera this is underlain by a thicker fibrous secondary shell layer (Fig. 3.3a). However, in some genera the secondary shell deposition is discontinued in favour of a tertiary succession, which forms the innermost shell layer (Fig. 3.3b). Shell carbonate was extracted from the anterior portion of the external primary layer (Fig. 3.4) and the non-specialised area, which lies to the anterior of the innermost (secondary/tertiary) layer of both valves. In addition, specialised regions of the internal secondary/tertiary shell layers that form identifiable morphological features were also sampled. The specialised areas of the dorsal valve sampled were: a) loop; b) the cardinal process and c) the muscle scars (Fig. 3.4). The specialised areas of the ventral valve sampled were: a) the pedicle foramen, b) the teeth and, c) the muscle scars (Fig 3.4). See appendix A for a full list of samples.

The craniids are inarticulated brachiopods and are structurally and morphologically different from the terebratulids and rhynchonellids. The general shell structure is composed of two calcite layers as shown in Figure 3.3a. However, the secondary layer is composed

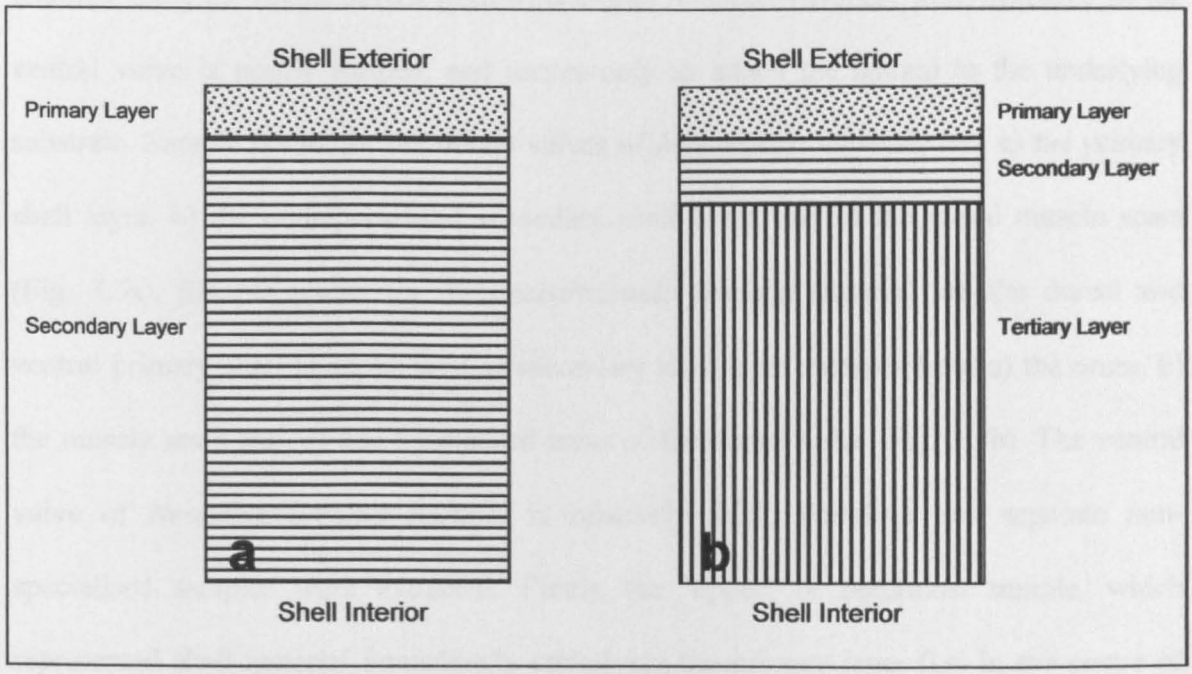

Figure 3.3: Schematic diagram showing shell succession in terebratulid and rhynchonellid brachiopods.

a) Common ultrastructure with prismatic external primary layer and fibrous internal secondary layer. **b)** Ultrastructure with three calcitic layers. Secondary shell precipitation discontinues and succeeds into a prismatic tertiary layer, e.g.

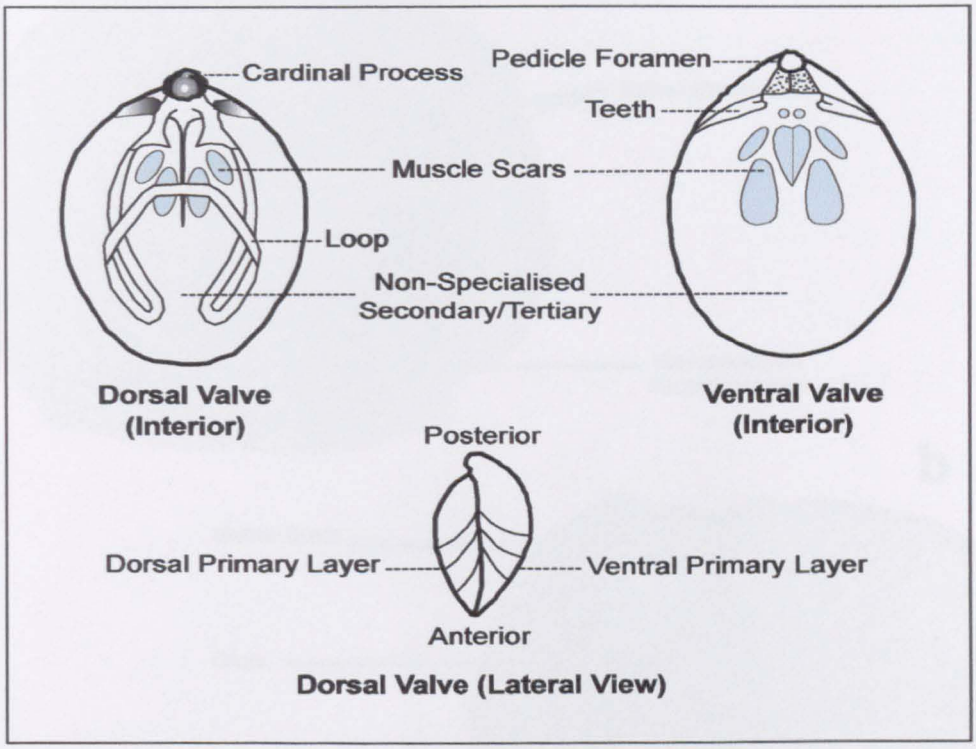

Figure 3.4: Generalised sketch detailing the sampling areas of articulated brachiopod shells. (Based on Black 1970)

of laminae (see chapter 4). The internal morphology is less complex with few specialised features. Only the dorsal valves from *Novocrania anomala* (Müller) were available as the ventral valve is poorly formed, and serves only to attach the animal to the underlying substrate. Sample points for the dorsal valves of *Novocrania anomala* are: a) the primary shell layer, b) the non-specialised secondary shell layer, and c) the raised muscle scars (Fig. 3.5a). Sample points for *Neoancistrocrania norfolki* (Laurin) are the dorsal and ventral primary shell layer, as well as secondary shell layer samples from a) the crura, b) the muscle scars and, c) non-specialised areas of the dorsal valve (Fig. 3.5b). The ventral valve of *Neoancistrocrania norfolki* is relatively thick, therefore two separate non-specialised samples were extracted. Firstly the 'upper' or outermost sample, which represented shell material immediately underlying the primary layer (i.e. in the centre of the succession). This material was collected after sectioning the valves with a diamond saw. Second the 'lower' or innermost sample represented non-specialised secondary shell

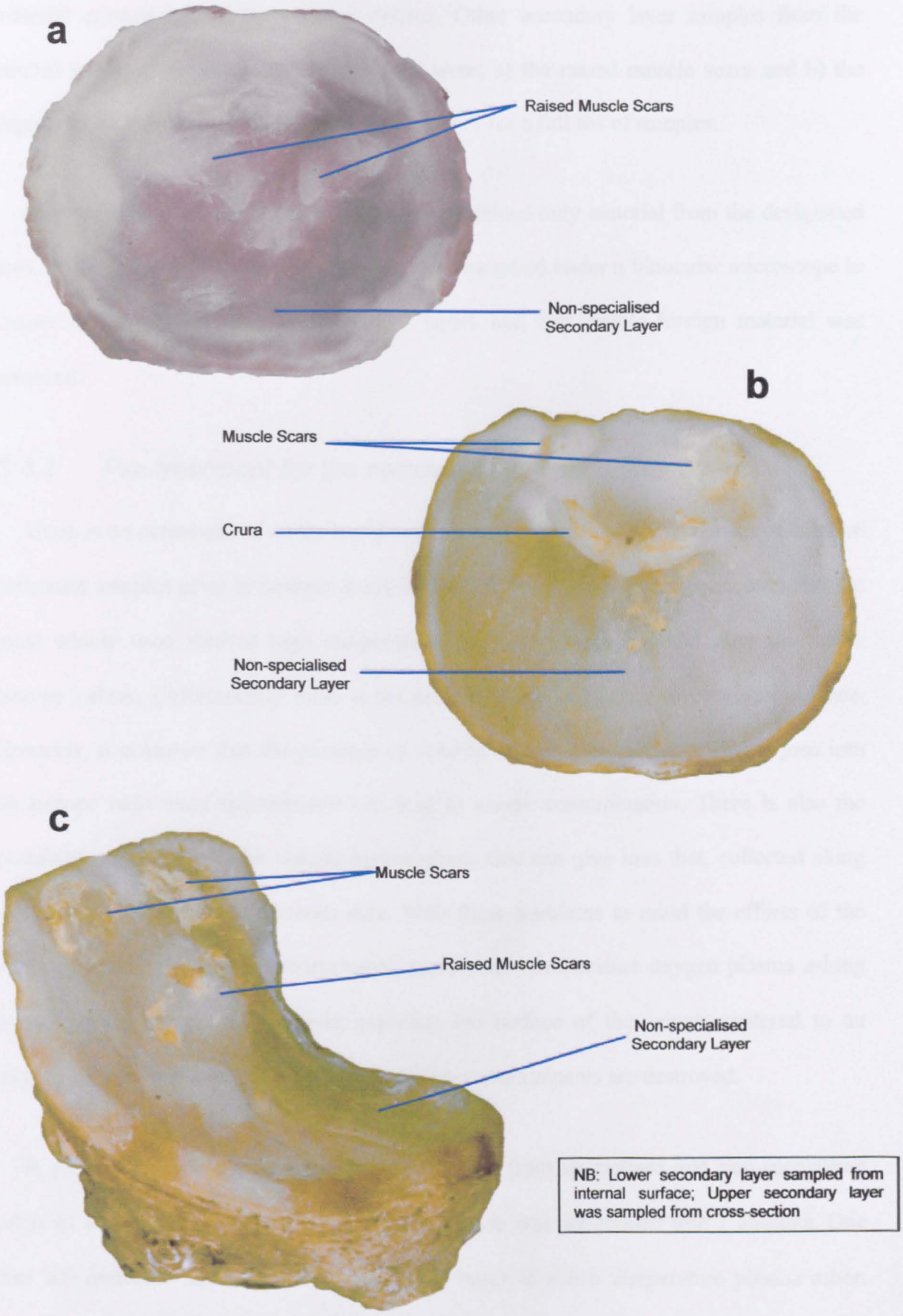

Figure 3.5: Secondary shell carbonate sample points on craniid brachiopod shells

a) *Novocrania anomala* (Müller) dorsal valve, internal view; **b)** *Neoancistrocrania norfolki* (Laurin) dorsal valve, internal view; **c)** *Neoancistrocrania norfolki* (Laurin) ventral valve.

material extracted from the internal surface. Other secondary layer samples from the ventral valve of *Neoancistrocrania norfolki* were; a) the raised muscle scars and b) the depressed muscle scars (Fig. 3.5c). See appendix A for a full list of samples.

Care was taken to ensure that each sample contained only material from the designated area. After extraction each sample powder was examined under a binocular microscope to ensure that there had been no mixing of layers and any visible foreign material was removed.

3.4.1 *Pre-treatment for the removal of volatile contaminants*

There is no consensus of on the benefits of various methods of pre-treatment of calcium carbonate samples prior to isotopic analysis. Indeed, some analysts are concerned that the most widely used method high temperature 'in-vacuo roasting' could alter the stable isotope values. Unfortunately there is no dedicated published data to provide guidance. However, it is known that the presence of volatile organic contaminants, which pass into an isotope ratio mass spectrometer can lead to severe contamination. There is also the possibility of low molecular weight hydrocarbons that can give ions that, collected along with CO_2 ions, can give erroneous data. With these problems in mind the effects of the least aggressive method of pre-treatment, namely low-temperature oxygen plasma ashing were tested. This method involves exposing the surface of the sample material to an oxygen plasma in a vacuum chamber, any organic contaminants are destroyed.

A pilot study was carried out using 68 samples from specialised and non-specialised areas of 4 modern brachiopod species. Each sample was subdivided into 2 aliquots. One was left untreated and the other treated for 4 hours in a low temperature plasma asher. Oxygen and carbon stable isotope ratios were determined by mass spectrometry (see section 3.5) (For results see appendix B). The paired results were tested statistically using the Wilcoxon signed rank test. Table 3.1 shows the p-values for the two-tailed statistical

tests at 0.05 significance for both $\delta^{18}O$ and $\delta^{13}C$. The null hypothesis is that the medians of treated and untreated samples are the same, and the alternative hypothesis is that the medians of treated and untreated samples are different. The p-values for $\delta^{18}O$ are all greater than 0.05, therefore there is no statistical evidence that plasma ashing has an effect on $\delta^{18}O$ values. *Calloria inconspicua* and *Neothyris lenticularis* have significantly different $\delta^{13}C$ values (i.e. p-values < 0.05). The reasons for this are unclear, but it may be due to the removal of organic contaminants from the treated samples. However, the results indicate that overall any effects are likely to be minimal. Therefore, to reduce the risk of contamination of the mass spectrometer in this study all samples were plasma ashed for 4 hours prior to analysis.

Table 3.1: Results of Wilcoxon signed rank test @ 0.05 significance - no pre-treatment versus plasma ashing

Brachiopod Species	Number of Paired Samples	P-Value @ 0.05	
		$\delta^{18}O$	$\delta^{13}C$
Calloria inconspicua	12	0.351	0.018
Neothyris lenticularis	35	0.124	0.004
Notosaria nigricans	10	0.086	0.554
Terebratulina retusa	11	0.541	0.610

3.5 Stable isotope analysis (carbonate)

The $^{18}O/^{16}O$ and $^{13}C/^{12}C$ values were determined from carbon dioxide produced by reacting 0.2-1.5 mg of sample material in a sealed vessel with 103% phosphoric acid (H_3PO_4) at 90°C, a method similar that described by M^{c}Crea (1950). These analyses were performed using a VG ISOCARB automated preparation system attached to a VG ISOGAS PRISM II isotope ratio mass-spectrometer at the Scottish Universities Environmental Research Centre (SUERC). The mass-spectrometer results are corrected for isotopic fractionation between calcite and CO_2 using a fractionation factor ($10^3 \ln\alpha$) of

7.904 for the reaction with 103% H_3PO_4 at 90°C. Corrections were also made for isobaric molecular ions and ^{17}O using the methods described by Craig (1957). All the isotope ratios are reported using the accepted delta (δ) notation in permil (‰) relative to the Vienna Pee Dee Belemnite (VPDB) international standard (Coplen 1995; Gonfiantini *et al.* 1995). The δ value is defined as:

$$\delta(‰) = \frac{R_{(sample)} - R_{(standard)}}{R_{(standard)}} \times 1000 \qquad [3.1]$$

where R represents the measured isotope ratio of $^{18}O/^{16}O$ or $^{13}C/^{12}C$ (Hoefs 1997 p.22)

Incorporating internal laboratory marble standards within each batch of analyses allowed precision to be monitored. Standard material was calibrated to the International Atomic Energy Agency's (IAEA) intercomparison material IAEA-CO-1 Carrara marble (Gonfiantini *et al.* 1995). Reproducibility of the standard material was better than 0.1 ‰ at 1σ. Each sample was replicated up to 3 times on different runs. The precise number of replicates depended on the quantity of sample material extracted. Replication was usually < 0.2 ‰ at 1σ. Occasional samples with outlying values were probably due to either lack of homogeneity, slight contamination between shell layers or the traces of foreign material infiltrating the shell structure.

3.6 Oxygen stable isotope analysis of seawater

The oxygen isotopic compositions of the seawater samples from the Firth of Lorne (location 1) were determined at the SUERC laboratories. Samples of seawater (1 ml) were added to 12 ml exetainer tubes. Air in the head space was flushed using helium prior to injecting 300 µl of CO_2. Samples were allowed to equilibrate for twenty four hours. Stable oxygen isotope analysis of the CO_2 in the head space was carried out using an AP2003 mass spectrometer, coupled to a fully-automated 'Gas Preparation Interface Module' (APGP) with integral water trap, GC and reference gas injector. Incorporating two internal

laboratory water standards within the batch analyses allowed precision to be monitored. Standard waters were calibrated to the International Atomic Energy Agency's (IAEA) intercomparison material. SMOW (Standard Mean Ocean Water), SLAP (Standard Light Antarctic Precipitation) and GISP (Greenland Ice Sheet Precipitation) (Gonfiantini *et al.* 1995). Precision and accuracy were < 0.2‰ and the results are reported as $\delta^{18}O$ in relation to Vienna Standard Mean Ocean Water (VSMOW) (Coplen 1995; Gonfiantini *et al.* 1995).

3.7 Calculations and statistical analysis

3.7.1 Use of 'palaeotemperature' equations

Epstein *et al.* (1951) established the first isotopic temperature scale based on the relationship between seawater temperature and the isotopic composition of biogenic carbonate. In a revision Epstein *et al.* (1953) proposed the equation [3.2]:

$$T\ (^{\circ}C) = 16.5 - 4.3\ (\delta^{18}O_{calcite} - \delta^{18}O_{seawater}) + 0.14\ (\delta^{18}O_{calcite} - \delta^{18}O_{seawater})^2 \qquad [3.2]$$

An updated version of this equation, which takes into account modifications in analytical procedures is recommended by Anderson & Arthur (1983) [Equation 3.3] and was used in this study:

$$T\ (^{\circ}C) = 16.0 - 4.14\ (\delta^{18}O_{calcite} - \delta^{18}O_{seawater}) + 0.13\ (\delta^{18}O_{calcite} - \delta^{18}O_{seawater})^2 \qquad [3.3]$$

The formulae for determining seawater temperatures from $\delta^{18}O_{carbonate}$ values are frequently referred to as palaeotemperature equations. However, their application requires the knowledge of local $\delta^{18}O_{seawater}$ values, therefore they are only practical in investigations of contemporary environments. It is more appropriate to refer to them as isotopic temperature equations (Rye & Sommer II 1980; Donner & Nord 1986). Therefore, all temperatures extrapolated from $\delta^{18}O_{carbonate}$ values in this study are referred to as isotopic temperatures.

Research has produced compelling evidence that oxygen isotope fractionation between aragonite and water differs from that between calcite and water. Epstein *et al.* (1953) suggest that aragonite was depleted in ^{18}O relative to calcite. This was supported by Horibe & Oba (1972). Others have reported that aragonite is enriched in ^{18}O relative to calcite (Tarutani *et al.* 1969; Grossman & Ku 1986; Barrera *et al.* 1994; Kim & O'Neil 1997). The work by Grossman & Ku (1986) established the commonly used equation [3.4] for the oxygen isotope fractionation between biogenic aragonite in mollusc shells and water:

$$T\,(^{\circ}C) = 21.8 - 4.69 * (\delta^{18}O_{aragonite} - \delta^{18}O_{seawater}) \quad [3.4]$$

Grossman & Ku's (1986) relationship has a slope similar to the inorganic curve of O'Neil *et al.* (1969). Grossman & Ku's (1986) equation has been used in studies of modern bivalves, for example Marshall *et al.* (1996) from Antarctic waters, and Lécuyer *et al.* (in press) from tropical waters. Böhm *et al.* (2000) using new and published data (Tarutani *et al.* 1969; Grossman & Ku 1986; Rahimpour-Bonab *et al.* 1997) reduced the error of the original Grossman and Ku (1986) equation proposing:

$$T\,(^{\circ}C) = (19.7 \pm 0.6) - (4.34 \pm 0.24) * (\delta^{18}O_{aragonite} - \delta^{18}O_{seawater}) \quad [3.5]$$

The original Grossman and Ku (1986) equation and the revision by Böhm *et al.* (2000) were compared in chapter 7 of this study when used to calculate isotopic temperatures from the $\delta^{18}O$ values of the aragonite samples from the bivalve *Modiolus modiolus* collected from the temperate waters of the Firth of Lorne. The resulting isotopic temperatures extrapolated using the version of Böhm *et al.* (2000) proved to be more compatible with the measured seawater temperature range.

Using actual measured seawater temperatures, these equations also were used to calculate the carbonate $\delta^{18}O$ parameters expected under equilibrium conditions (Fig. 8.8).

3.7.2 *Estimation of $\delta^{18}O_{seawater}$ from salinity*

Calculations of isotopic temperatures using the palaeotemperature equation of Anderson & Arthur (1983) [3.3], require a knowledge of the oxygen isotopic composition of the ambient seawater. Where actual or published water $\delta^{18}O$ data were unavailable estimations of $\delta^{18}O_{seawater}$ were made using the relationship between salinity and the oxygen isotopic composition of seawater. This linear relationship was first proposed by Epstein & Mayeda (1953), and later modified by Craig & Gordon (1965), in Faure (2001) who published the equation:

$$\delta^{18}O_{seawater} = -21.2 + 0.61S \quad [3.6]$$

where S is the salinity of the seawater per mil (‰)

Recent studies of modern brachiopods have utilised similar relationships. Carpenter & Lohmann (1995) adopted the relationship suggested by Broecker (1989), which was based on previously unpublished data by H. Craig:

$$\Delta^{18}O_{water}\ (‰) / \Delta \text{ salinity } (‰) = 0.50. \quad [3.7]$$

Where average values for the Atlantic and Pacific oceans are $\delta^{18}O = 1.0‰$, S = 36‰ and $\delta^{18}O = 0.5‰$, S = 35‰ respectively.

The study of Buening & Spero (1996) used the formula:

$$\delta^{18}O_{seawater}\ (‰) = 0.39 * \text{salinity } (‰) - 13.46 \quad [3.8]$$

This equation [3.8] was produced from California water data and later adopted by Brand *et al.* (2003) who considered it suitable for use in modern environmental applications.

This study has tested the above relationships in the light of the known $\delta^{18}O_{seawater}$ (mean 0.29‰) and salinity (mean 34.7‰) reported by Crowley & Taylor (2000) from the vicinity of location 7, Otago Shelf, New Zealand (see Table 3.2)

Table 3.2: Comparisons of estimated $\delta^{18}O_{seawater}$ – salinity using different relationships, with the mean measured $\delta^{18}O_{seawater}$ (Crowley & Taylor 2000) from the Otago Shelf, New Zealand.

Relationship	Mean measured $\delta^{18}O_{seawater}$ for the Otago area (Crowley & Taylor 2000)	Estimated $\delta^{18}O_{seawater}$	Δ mean measured $\delta^{18}O_{seawater}$ and estimated $\delta^{18}O_{seawater}$
Craig & Gordon (1965)	0.29‰	-0.033‰	0.32‰
Broecker (1989)	0.29‰	0.35‰	0.06‰
Buening & Spero (1996)	0.29‰	0.073‰	0.22‰

The $\delta^{18}O_{seawater}$ – salinity relationship of Broecker (1989) [3.7] produced the estimated $\delta^{18}O_{seawater}$ for the Otago Shelf closest to the mean of the actual measurements made by Crowley & Taylor (2000). Therefore the Broecker (1989) [3.7] is used in all subsequent estimations of $\delta^{18}O_{seawater}$ from salinity values in this study.

3.7.3 Statistical analysis

Where statistical analysis was required, appropriate tests were employed using Minitab v.13:

3.7.3.1 Wilcoxon signed rank test

Wilcoxon signed rank test is a non-parametric test, which compares the medians two non-independent paired-samples. In this study it was used to compare the affect of pre – treatment versus no pre-treatment for carbonates analysed by mass spectrometry.

Hypotheses

Null hypothesis (H_0): the medians of the two samples is the same, i.e. The difference in the medians is zero.

Alternative hypothesis (H_1): the medians of the two samples is not the same, i.e. The difference in the medians is not zero.

3.7.3.2 Two-way analysis of variance (ANOVA)

Two-way analysis of variance (ANOVA), is used to compare the variability of more than two sample groups. This method compares variability within groups to variability between groups. In this study the method was used to compare statistically the delta values obtained from different components of the secondary/tertiary layers.

Hypotheses

(H_0): the mean oxygen or carbon isotopic values for all the secondary/tertiary layer components are equal, i.e. There is no statistical difference in oxygen or carbon isotopic composition between different components of the secondary/tertiary layer.

(H_1): the mean oxygen or carbon isotopic values for all the secondary/tertiary layer components are not equal, i.e. There is a statistical difference in oxygen or carbon isotopic composition between different components of the secondary/tertiary layer.

3.7.3.3 Mann-Whitney Two-sample test

Mann-Whitney Two-sample test is a non-parametric test, which compares the medians two -independent paired-samples. In this study it was used to compare oxygen or carbon isotopic values between two secondary/tertiary layer components

Hypotheses

(H_0): the medians of the two samples is the same, i.e. The difference in the medians is zero.

(H_1): the medians of the two samples is not the same, i.e. The difference in the medians is not zero.

3.7.3.4 Spearman rank correlation coefficient (r_s)

Spearman rank correlation coefficient (r_s) is a non-parametric correlation test, and makes no assumption about the distribution of data. In this study it is used to ascertain whether $\delta^{18}O$ and $\delta^{13}C$ values are correlated.

Hypotheses

(H_0): there is no significant correlation between $\delta^{18}O$ and $\delta^{13}C$.

(H_1): a significant correlation exists between $\delta^{18}O$ and $\delta^{13}C$.

3.7.3.5 Boxplots

Boxplots, also commonly referred to as box and whisker plots are particularly useful for demonstrating the distributional characteristics of data, see Figure 3.6 for explanation.

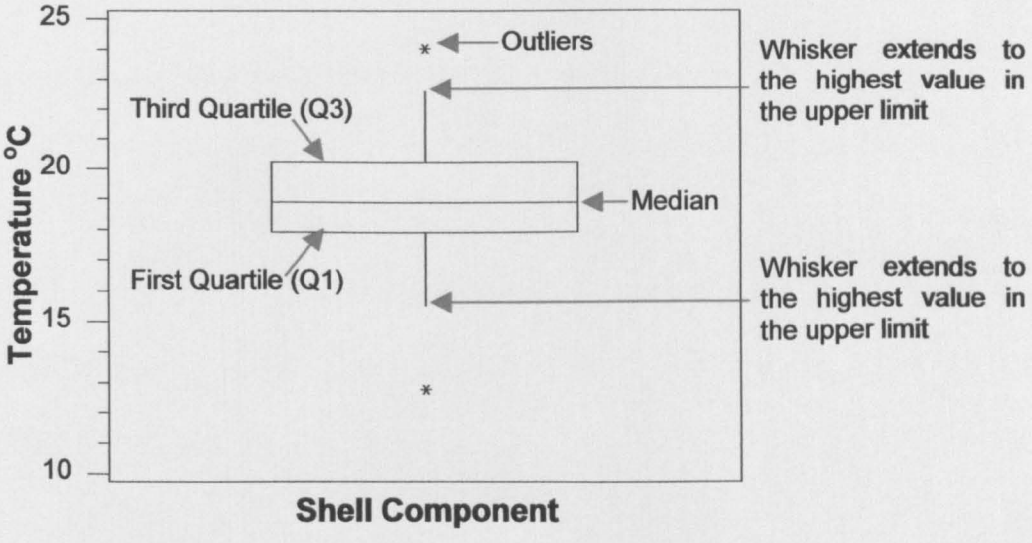

Figure 3.6: Explanation of boxpot components. A line is drawn across the box at the median. The box represents the interquartile range. The whiskers are lines that extend from the top and bottom of the box to the highest and lowest values within the region defined by the following limits:

Upper limit = Q1 + 1.5 (Q3 – Q1)
Lower limit = Q1 – 1.5 (Q3 – Q1)

Chapter 4

Disparate ultrastructures

in

modern brachiopod shells

4 Disparate ultrastructures in modern brachiopod shells

4.1 Introduction

The extant species of the Brachiopoda that precipitate calcite shells are divided into a number of taxonomic groups. Williams *et al.* (1996) classified modern calcitic brachiopods in two subphyla (See section 2.1): (i) the inarticulated Craniiformea with only one surviving order (the Craniida), represented in this study by the species *Novocrania anomala* (Müller) (Firth of Lorne, Scotland) and *Neoancistrocrania norfolki* (Laurin) (South Pacific Ocean); (ii) the articulated Rhynchonelliformea. The Rhynchonelliformea have three surviving orders, including the order Rhynchonellida represented in this study by *Notosaria nigricans* (Sowerby) (Otago Shelf, New Zealand). The order Terebratulida, is further divided into two suborders: (i) the suborder Terebratulidina represented in this study by *Liothyrella neozelanica* (Thomson) (Otago Shelf, New Zealand), *Liothyrella uva* (Broderip) (Signy Island, Antarctica) and Terebratulina retusa (Firth of Lorne, Scotland); (ii) the suborder Terebratellidina represented in this study by *Calloria inconspicua* (Sowerby) (Otago Shelf, New Zealand), *Laqueus rubellus* (Sowerby) (Otsuchi Bay and Sagami Bay, Japan), *Neothyris lenticularis* (Deshayes) (Otago Shelf, New Zealand), *Terebratalia transversa* (Sowerby) (Puget Sound, Washington, USA) and *Terebratella Sanguinea* (Leach) (Otago Shelf, New Zealand). The third order of the Rhynchonelliformea is the Thecideidina, which is represented by *Thecidellina barretti* (Davidson) (Rio Bueno, Jamaica) in this study.

Within these two subphyla are a variety of shell ultrastructures and successions, which can differ both within and between taxonomic groups. To determine whether disparate

biomineralisation systems may have an effect on oxygen and carbon stable isotope compositions, samples of each representative species were examined using scanning electron microscopy (SEM) (see section 3.2) to determine shell ultrastructure. Isotopic compositions were then interpreted in this context (see Chapters 5 and 6).

4.2 'Standard model', two-layered structure

The dominant ultrastructural succession in the shells of both the Terebratulida and Rhynchonellida, regarded as a 'standard model' for articulated brachiopods (Williams 1968b), is shown in Figure 4.1 and applies to both dorsal and ventral valves. There are two well-defined layers. The outer primary layer is formed of granular or acicular calcite (Williams 1968a; 1997) and viewed with the SEM shows little obvious structure (see Fig. 4.2). Calcite shell material is precipitated by epithelial cells in the mantle, which is the membrane lining the internal surface of each valve. The primary shell fabric is only secreted by cells at the outer edge of the mantle as the shell enlarges (Rudwick 1970). Therefore, the primary layer maintains a reasonably constant thickness and grows relatively quickly compared to the rest of the shell. The primary/secondary layer boundary is abrupt and well defined (Fig. 4.2). The secondary layer is composed of individual inclined calcite fibres stacked at a shallow angle to the primary shell and aligned in the direction of growth (Fig. 4.3). However, the secondary layer continues to thicken throughout the life of the organism, with each fibre continuing to develop as long as its secretory cell remains active (Williams 1968b; Rudwick 1970). SEM examination of the internal surface reveals the rounded terminal faces of individual fibres (Fig. 4.4). This common type of two-layered structure may be either endopunctate i.e. containing well defined perforations (Fig. 4.4) penetrating the shell (as in *Calloria inconspicua*, *Laqueus rubellus*, *Neothyris lenticularis*, *Terebratalia transversa*, *Terebratella sanguinea*, and *Terebratulina retusa*), or impunctate i.e. with no perforations (as in *Notosaria nigricans*).

4.3 Additional Tertiary Layer

In some terebratulid and rhynchonellid genera, for example the terebratulid *Liothyrella*, an additional tertiary layer underlies the secondary succession (MacKinnon & Williams 1974; Williams 1997). This is a readily identified continuous prismatic layer (Fig. 4.5, Fig. 4.6) forming the inner surface of each valve. The abrupt change from the fibrous secondary layer is indicative of a physiological change in the secretory regime of the outer epithelial cells at a later ontogenetic stage (Williams 1997). Although the present study has observed this type of succession in the New Zealand species *Liothyrella neozelanica* (Fig. 4.5, Fig. 4.6), SEM investigation of eight valves from a different species of the same genus, the Antarctic brachiopod *Liothyrella uva* has found the expected tertiary layer to be incompletely developed in both the dorsal and the ventral valves of even mature specimens.

In *Liothyrella uva*, while the fibrous secondary succession remains dominant (e.g. Fig 4.7), fibres frequently change orientation, whereas in most terebratulid shells the fibres are predominantly aligned radially in the direction of growth. In some *Liothyrella uva* individuals, only fibrous material is present below the primary shell layer (Fig. 4.8). The scanning electron micrographs shown in Figures 4.8 and 4.9 illustrate the comparison between the internal surfaces of such a specimen of *Liothyrella uva* that has secondary fibres but lacks a tertiary succession, and the terminal faces of tertiary shell prisms seen in *Liothyrella neozelanica*. In the eight specimens examined, only one valve of *Liothyrella uva* showed the possible development of tertiary succession (Fig. 4.10). However, this shell layer is in its early stages and it is unclear from this observation whether the prismatic growth would have continued or if it would have been interspersed with fibrous growth.

4.4 Thecideidine ultrastructure

The Thecideidina are an anomalous extant group of articulated brachiopods (Williams 1968a). This order is represented in this study by *Thecidellina barretti* (Fig. 4.11). Thecideidine brachiopods have small but relatively thick calcite shells with no obvious layering, and with shell fabric composed almost entirely of primary layer material (Williams 1968a; 1973). SEM examination of *Thecidellina barretti* samples used in this study revealed no ultrastructural features that differ from the simple structure previously reported.

4.5 Inarticulated Craniida

The inarticulated Craniida have a secretory regime distinct from the articulated species and showing differences between the separate valves of an individual. Craniids have two calcitic layers. In the dorsal valve, a thin outer primary layer of acicular crystallites is succeeded by calcitic sheets, which form laminae (Williams & Wright 1970) rather than the fibres seen in the Rhynchonelliformea. This kind of structure can be seen in the dorsal valves of both *Novocrania anomala* (Fig. 4.12, Fig. 4.13) and *Neoancistrocrania norfolki* (Fig. 4.14). The secondary shell layer laminae grow spirally by screw dislocation, which can be seen in SEM images of the internal surface of the dorsal valve of *Novocrania anomala* (Fig. 4.15).

However, there is no ultrastructural similarity between the dorsal and ventral valves of either of the species. The ventral valve of *Novocrania anomala* is no more than a fine calcitic sheet, cementing the animal to an anchoring substrate such as a pebble or a larger shell. These valves were too difficult to remove from the substrate and were therefore excluded from this study. However, the ventral valve of *Neoancistrocrania norfolki* has a

thick and complex structure. The valve is attached to a substrate by a thick cement. A thin primary shell layer overlies a relatively thick secondary shell with an open structure showing two discernable growth phases (Fig. 4.16). In general the secondary shell layer is composed of a series of laminar chambers with a hooped construction. In the upper (oldest) part of the secondary layer these chambers is well formed and rounded, and is terminated by an aperture with a wall of calcite rhombohedra (Fig. 4.17 and Fig. 4.18). At approximately mid-way through the secondary succession, a transition occurs and the chambers change orientation, become flattened and are infilled by calcite. The most likely interpretation of this change within the lower secondary layer is a reduction in growth rate in the later ontogenetic stage of the organism, causing the chambers to become collapsed and infilled (A. Williams, personal communication, 18th November 2002).

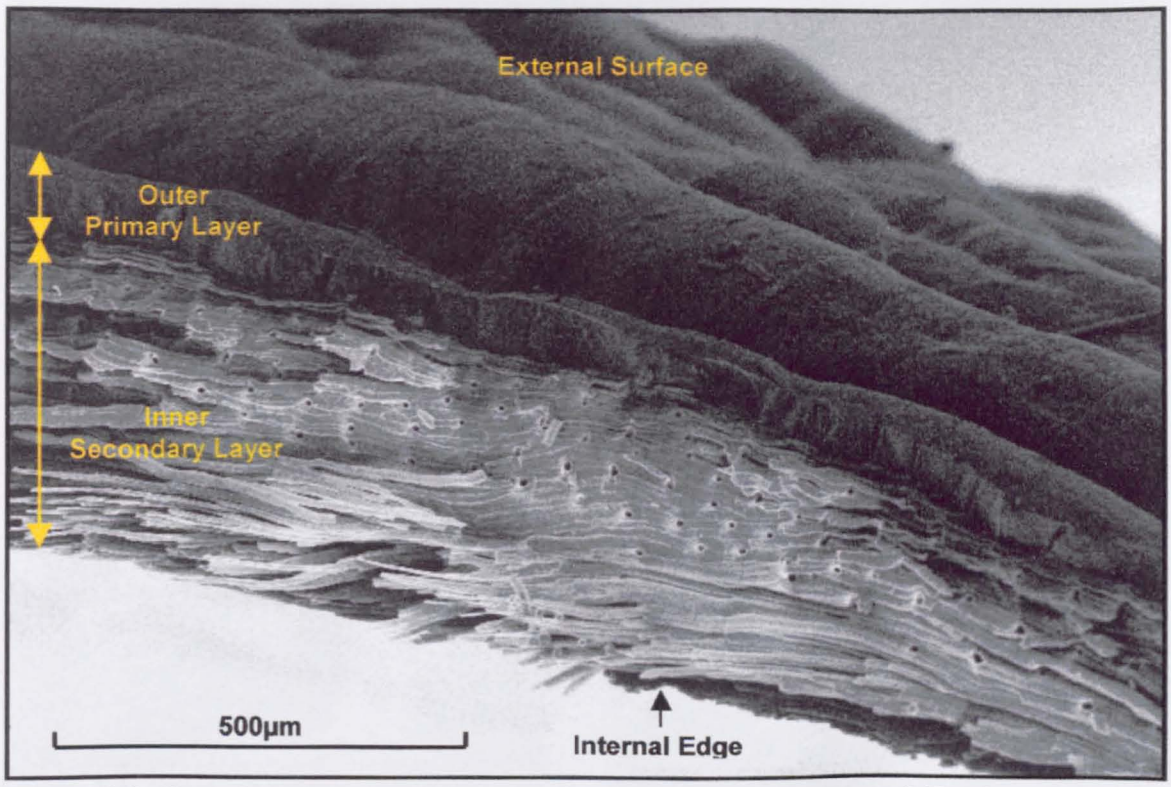

Figure 4.1: Scanning electron micrograph of a lateral dorsal fracture of *Terebratulina retusa* (Linnaeus).

The micrograph shows the two-layered calcitic structure with an outer primary shell layer underlain by an inner fibrous secondary shell layer.

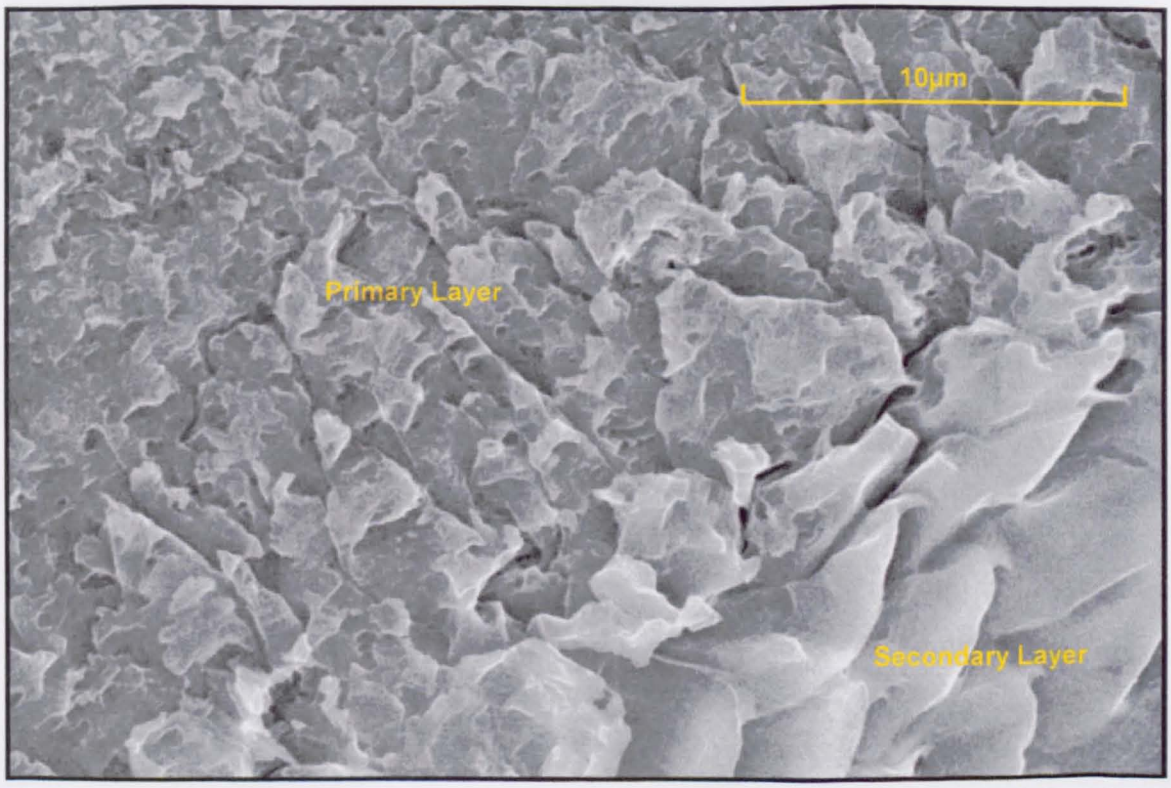

Figure 4.2: Scanning electron micrograph of the primary and secondary shell interface in an etched transverse section of *Notosaria nigricans* (Sowerby).

The primary shell shows little structure; secondary shell has a fibrous structure (transverse view).

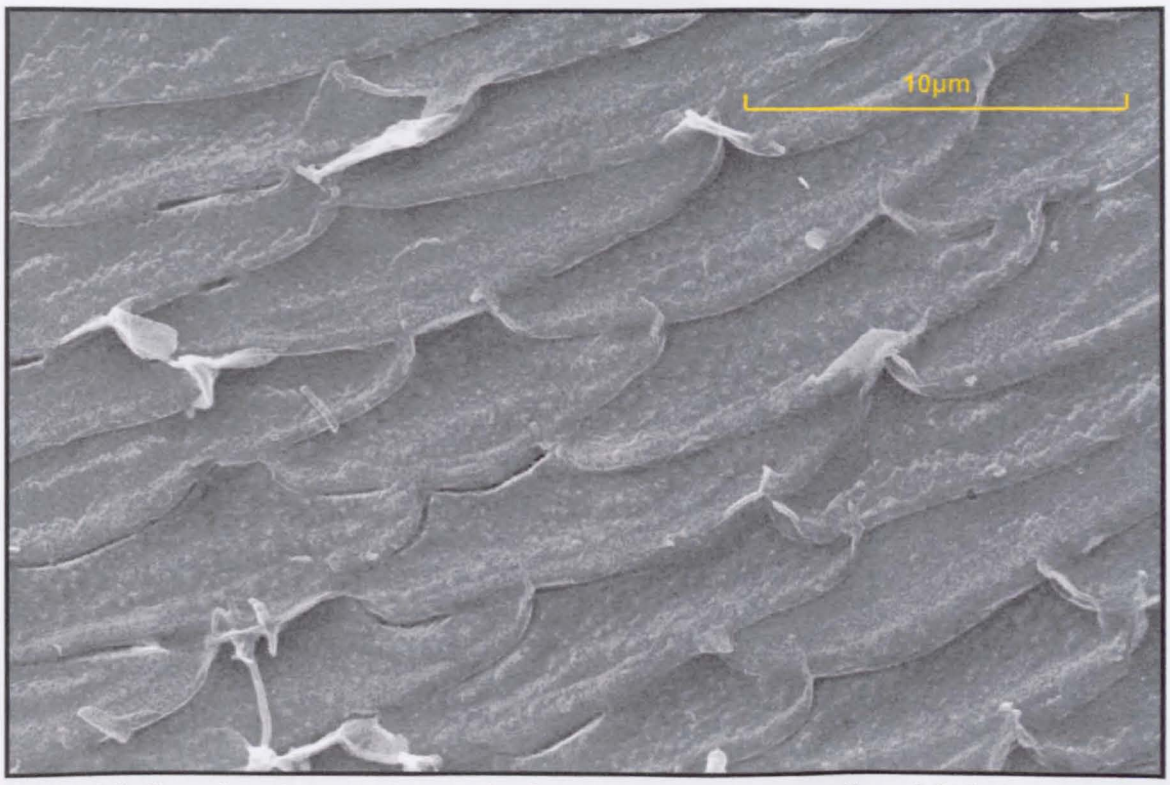

Figure 4.3: Scanning electron micrograph of an etched transverse section of *Calloria inconspicua* (Sowerby).

The micrograph shows a transverse section through the stacked secondary shell fibres

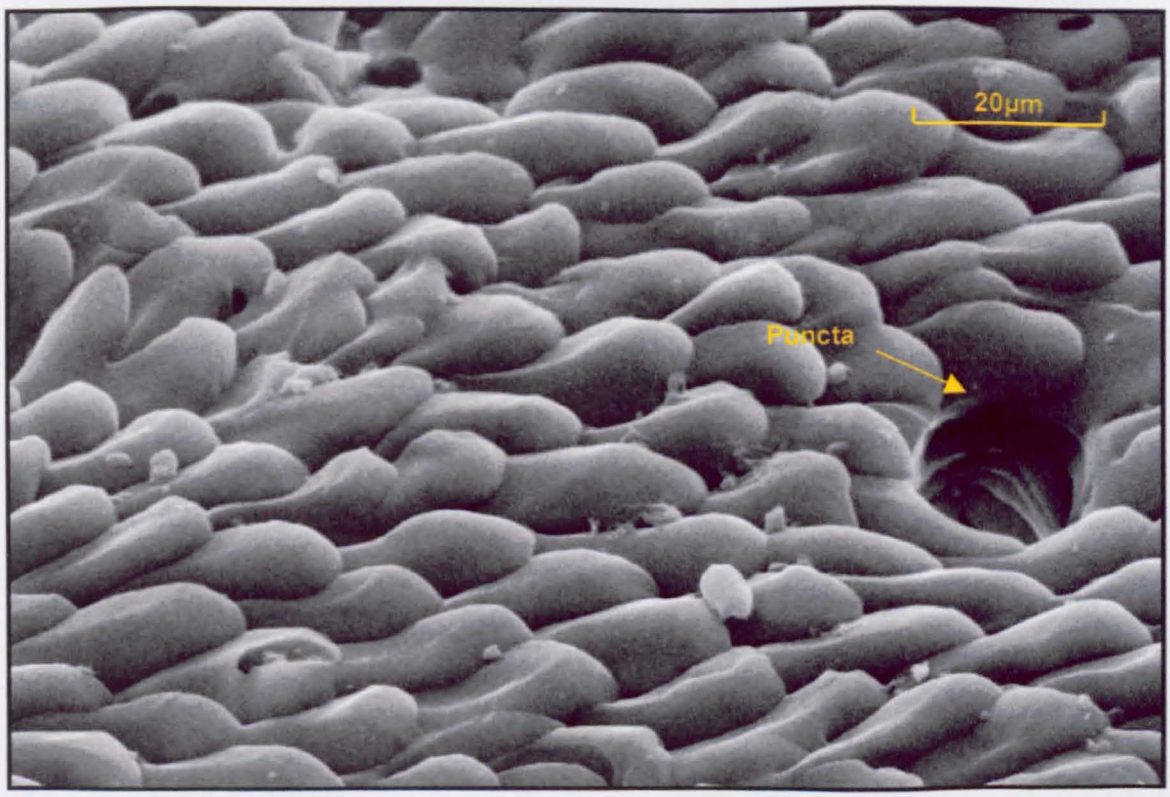

Figure 4.4: Scanning electron micrograph *Calloria inconspicua* (Sowerby).

The internal surface of a dorsal valve showing the terminations of secondary layer fibres with rounded ends.

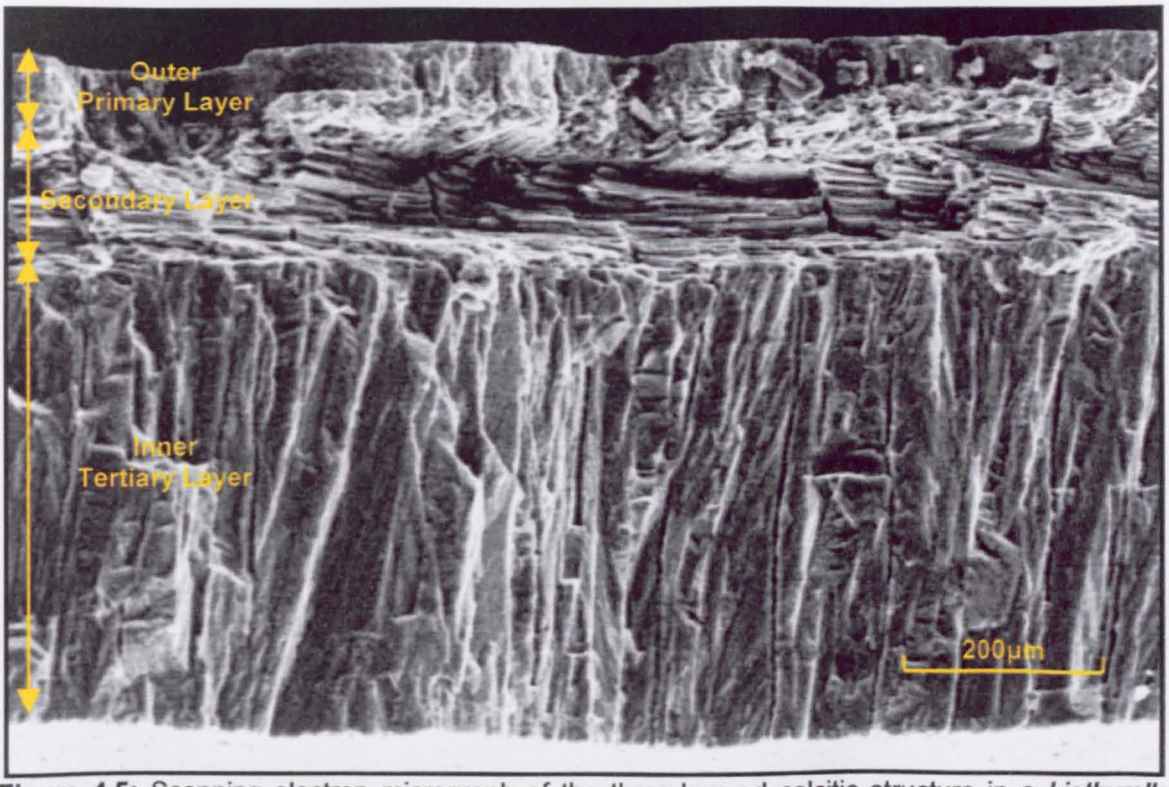

Figure 4.5: Scanning electron micrograph of the three-layered calcitic structure in a *Liothyrella neozelanica* (Thomson).

This lateral dorsal fracture shows the outer prismatic primary shell layer with underlying fibrous secondary shell layer, which succeeds to a relatively thick prismatic internal tertiary layer.

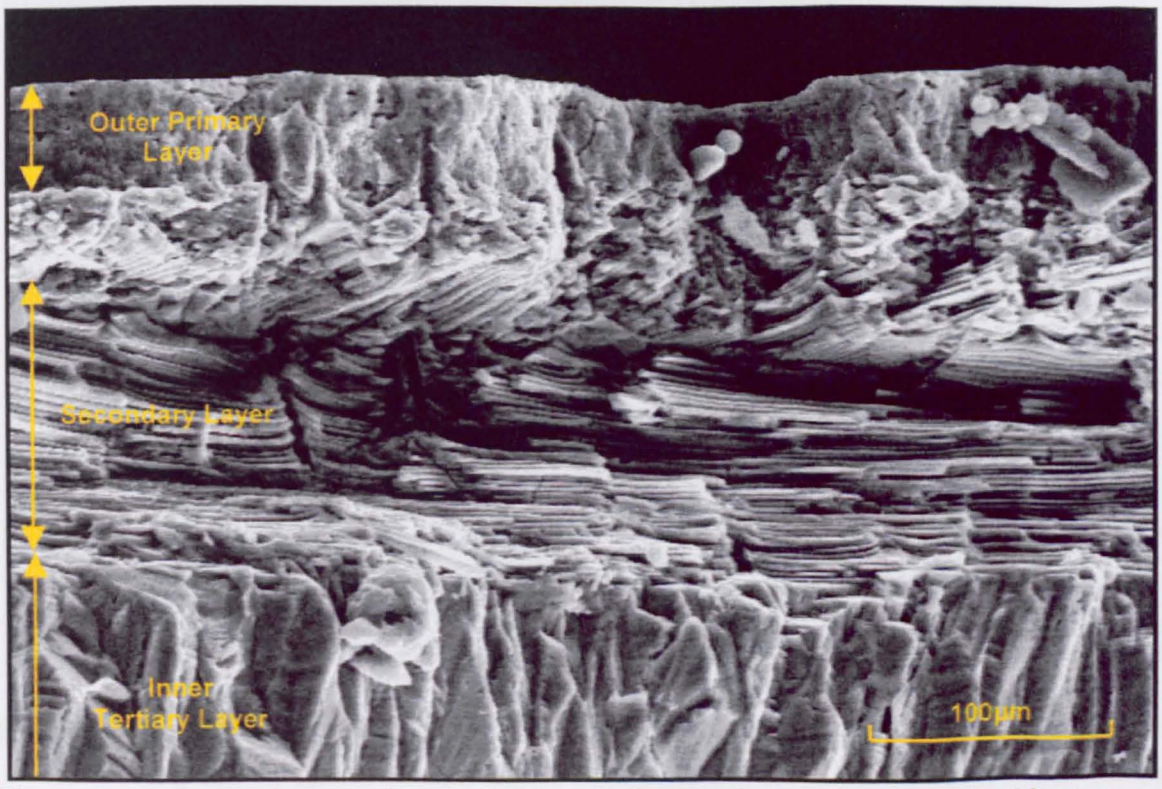

Figure 4.6: Scanning electron micrograph of *Liothyrella neozelanica* (Thomson) lateral fracture.

A closer view of the succession in the shell from the outer primary through secondary tertiary shell layers.

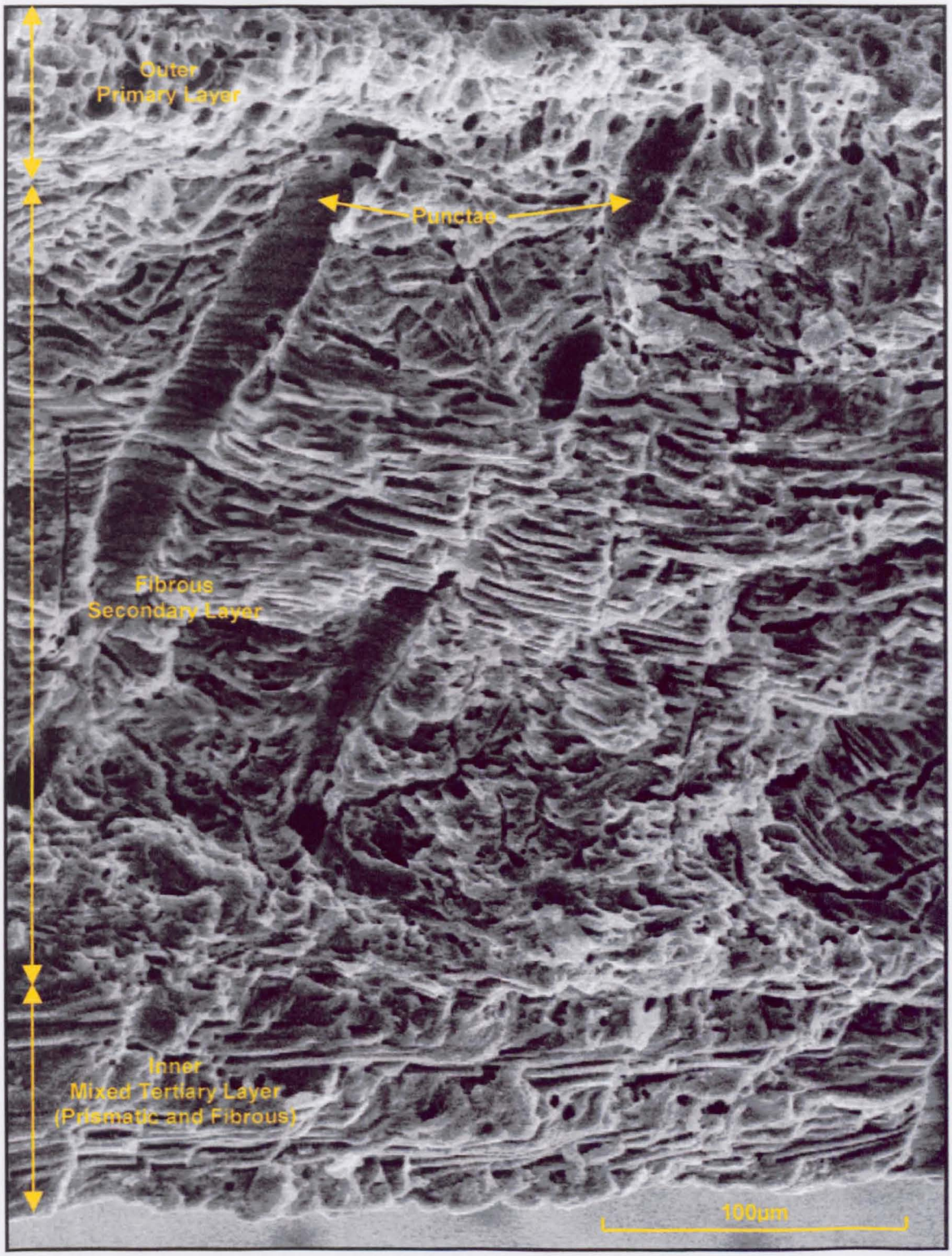

Figure 4.7: Scanning electron micrograph of the *Liothyrella uva* (Broderip) structure.

The etched ventral fracture shows incomplete tertiary succession with mixed fibrous and prismatic material.

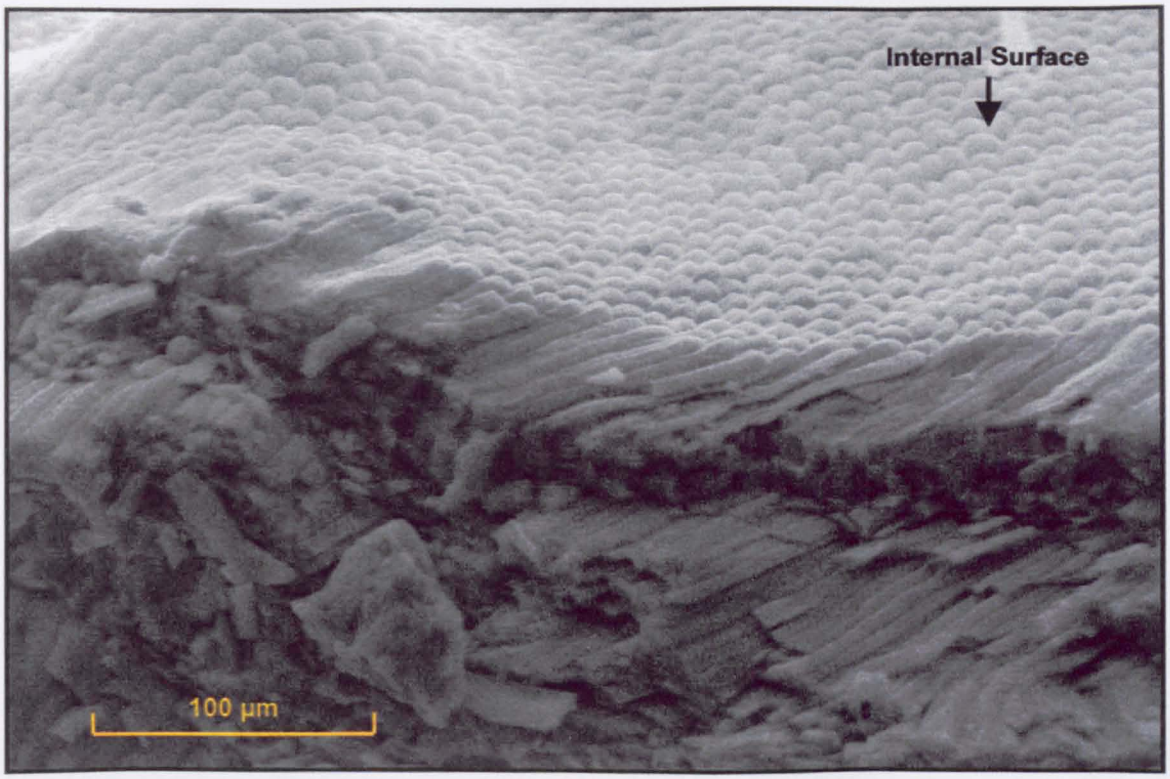

Figure 4.8: Scanning electron micrograph of the internal surface of a *Liothyrella uva* (Broderip).

Fractured dorsal valve showing the terminal facies of fibres normally associated with secondary succession.

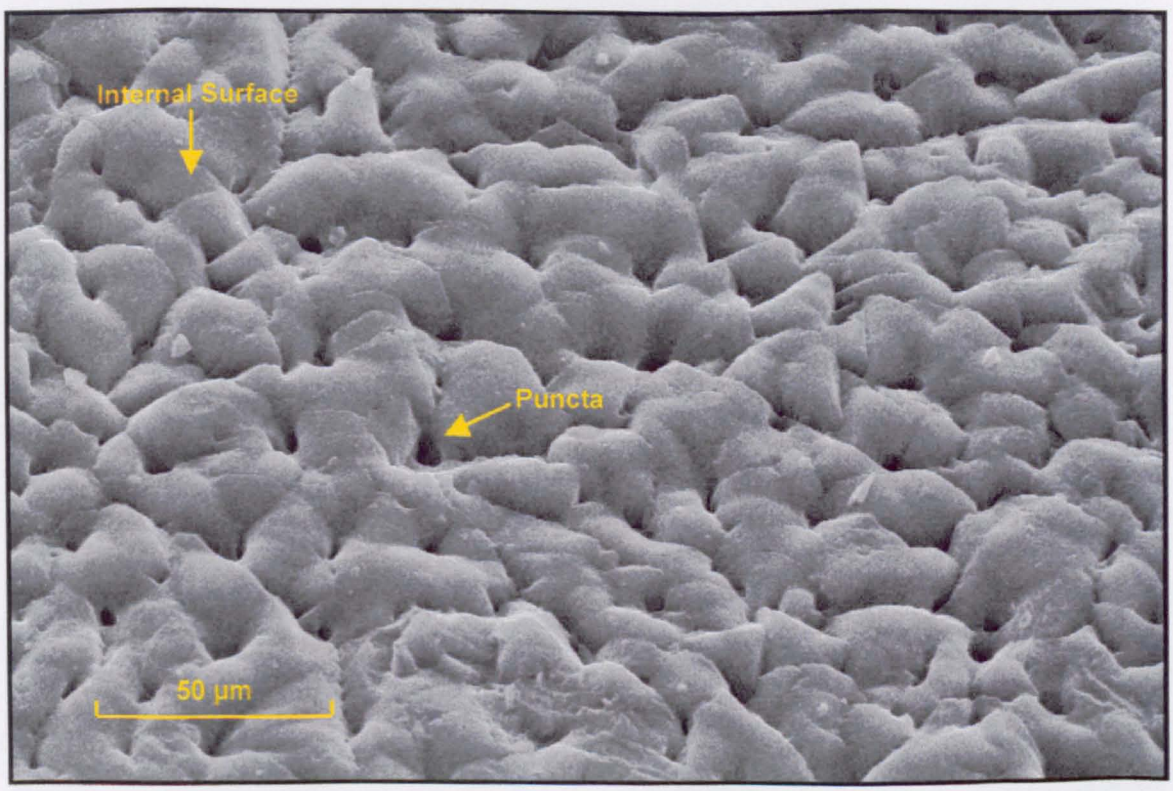

Figure 4.9: Scanning electron micrograph of the internal surface of a *Liothyrella neozelanica* (Thomson).

Dorsal valve showing the terminal facies of tertiary layer prisms.

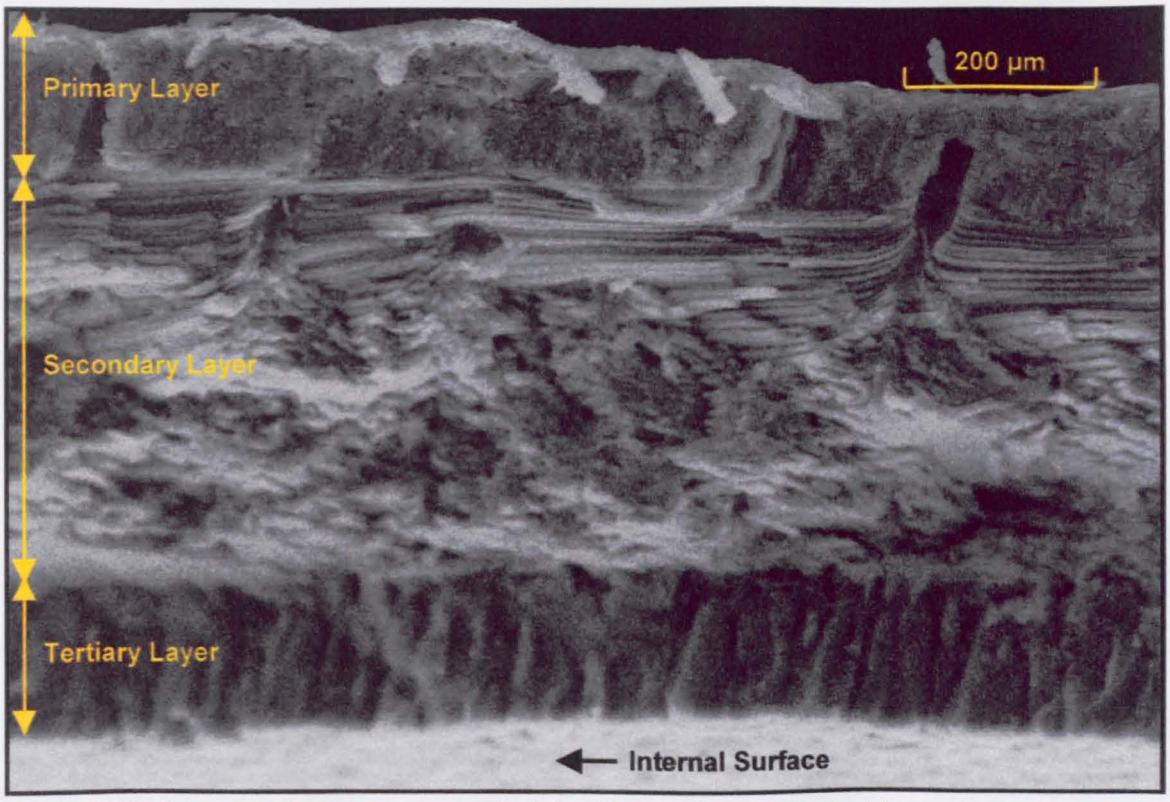

Figure 4.10: Scanning electron micrograph of the *Liothyrella uva* (Broderip) structure.

The ventral fracture shows primary layer, fibrous secondary and the possible beginnings of tertiary succession.

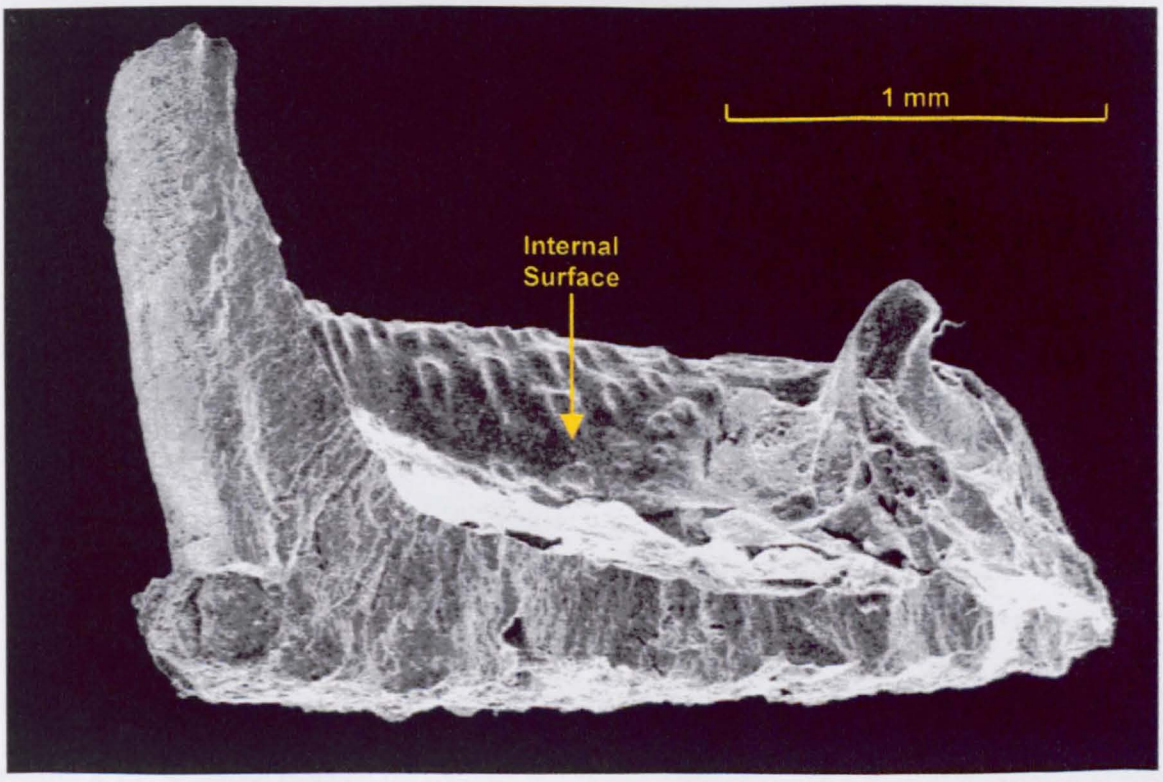

Figure 4.11: Scanning electron micrograph of a ventral fracture of *Thecidellina barretti* (Davidson).

Typical of the Thecideidina, small articulated brachiopods, composed of primary shell material.

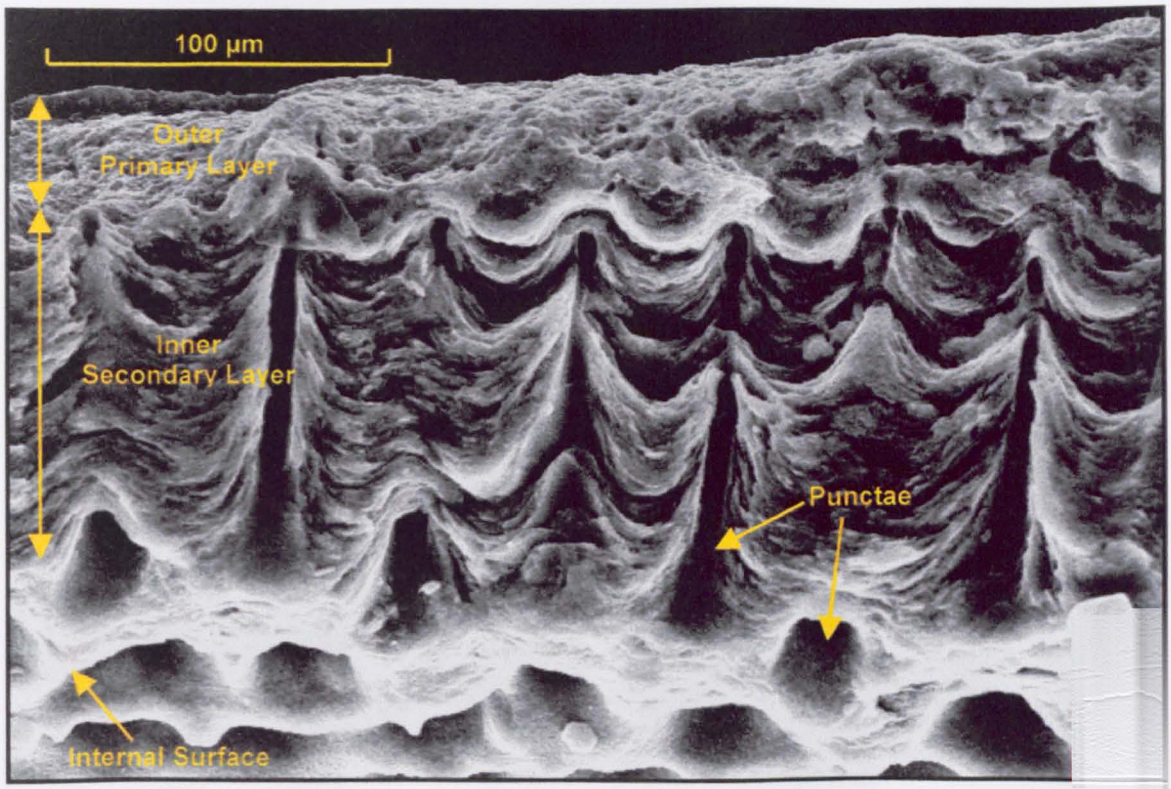

Figure 4.12: Scanning electron micrograph of a dorsal fracture of the craniid *Novocrania anomala* (Müller).

The micrograph shows the endopunctate laminar structure.

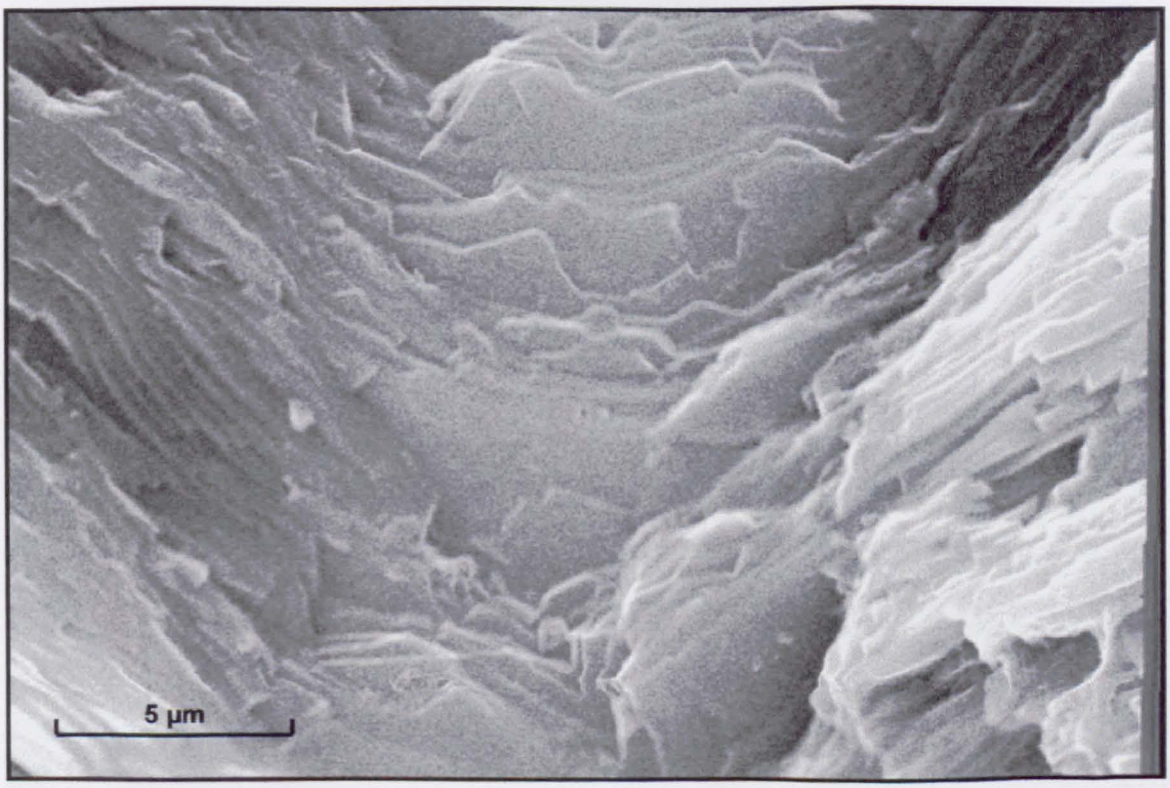

Figure 4.13: Scanning electron micrograph of a dorsal fracture of the craniid *Novocrania anomala* (Müller).

The micrograph shows laminae of the secondary shell layer. The central depression is the result of its endopunctate structure.

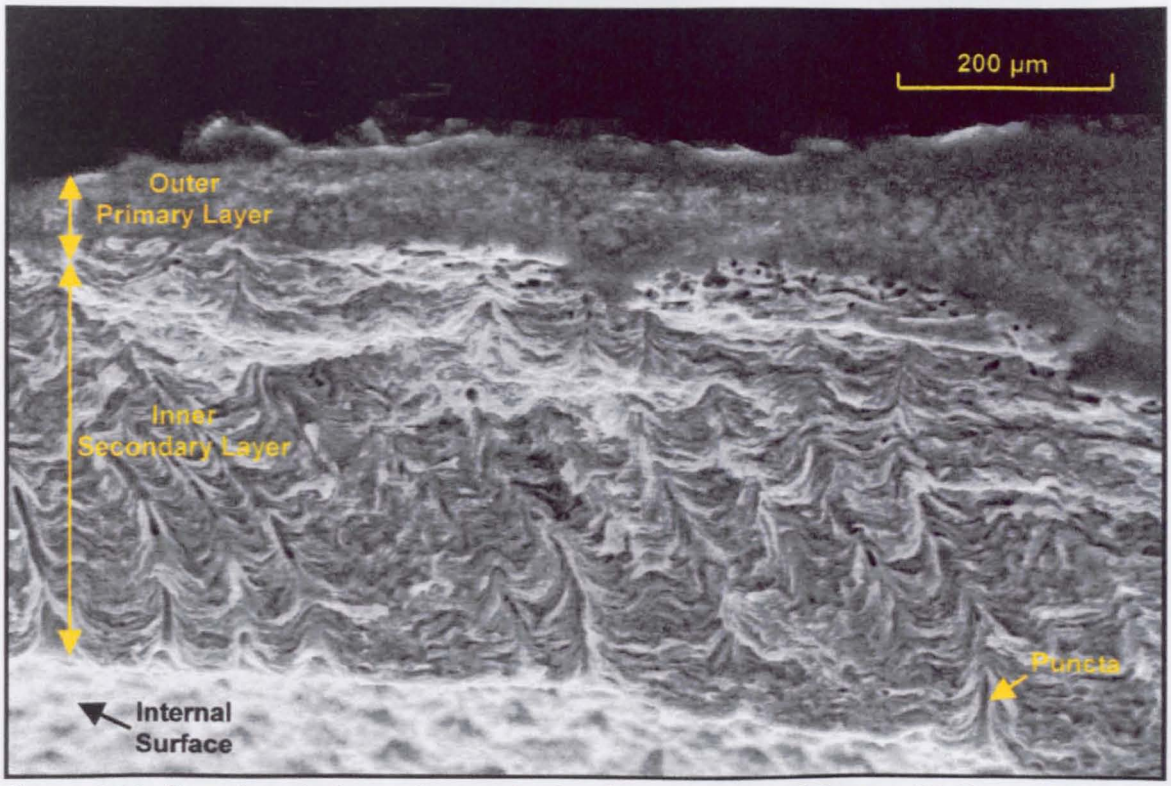

Figure 4.14: Scanning electron micrograph of a dorsal fracture of the craniid *Neoancistrocrania norfolki* (Laurin).

The micrograph shows a endopunctate laminar structure. (Courtesy of Sir Alwyn Williams FRS)

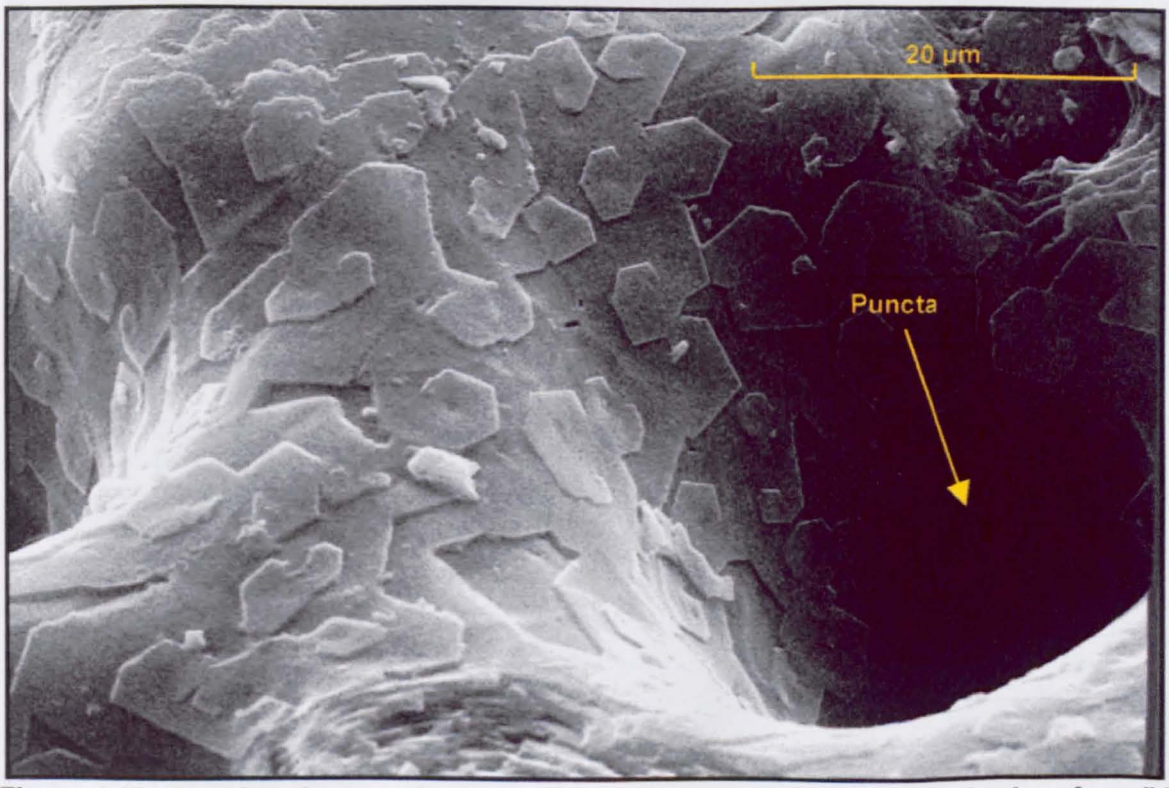

Figure 4.15: Scanning electron micrograph of the internal surface of the dorsal valve of craniid *Novocrania anomala* (Müller).

The micrograph shows the spiral growth of secondary laminae in the secondary shell layer.

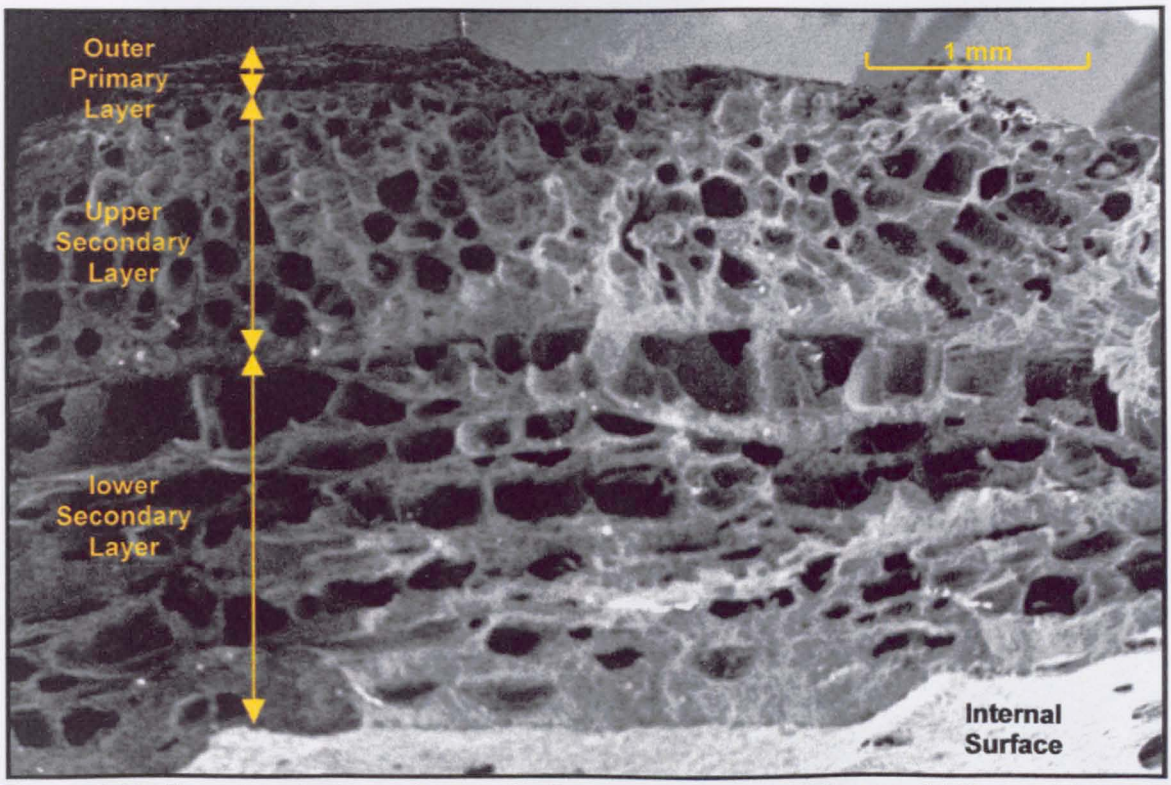

Figure 4.16: Scanning electron micrograph of a ventral fracture of the craniid *Neoancistrocrania norfolki* (Laurin).

The micrograph shows the chambered structure of the upper secondary layer and the collapsed chambers of the lower secondary layer.

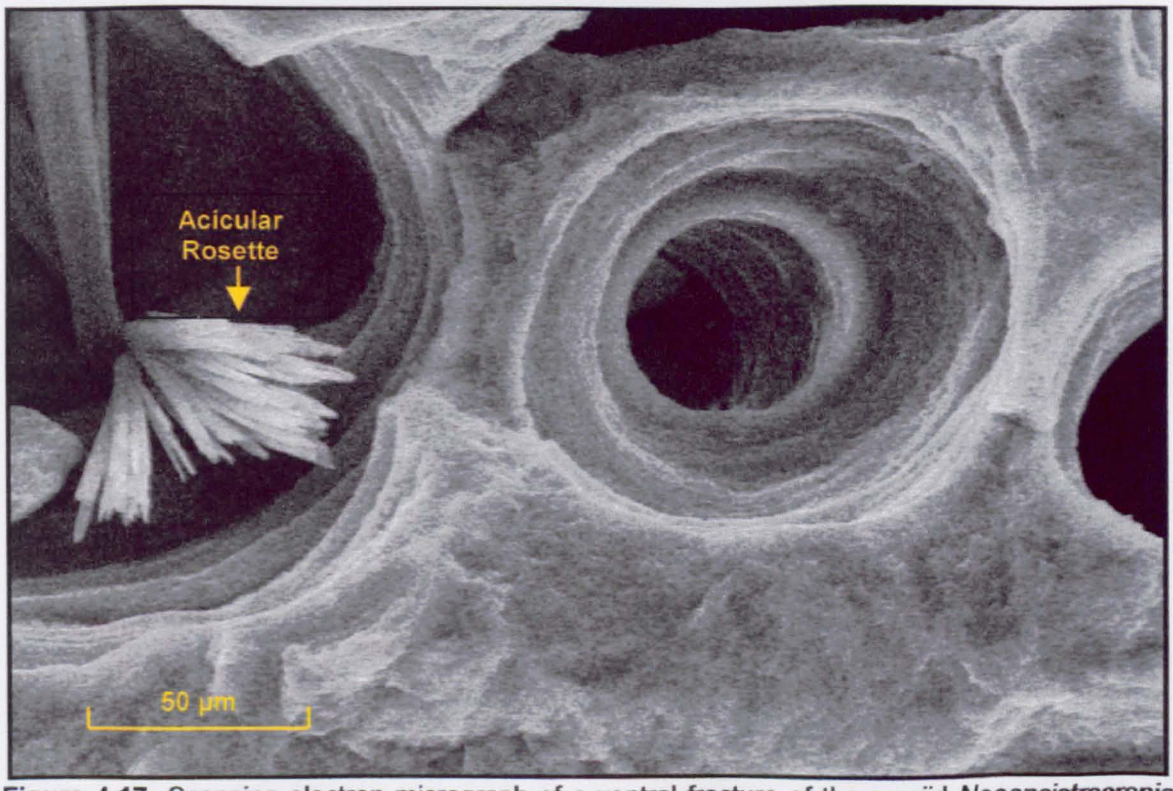

Figure 4.17: Scanning electron micrograph of a ventral fracture of the craniid *Neoancistrocrania norfolki* (Laurin).

The micrograph shows the chambered structure of the younger upper secondary layer. Acicular rosette is secondary calcite growing in a chamber enlarged by overlapping. (Courtesy of Sir Alwyn Williams FRS)

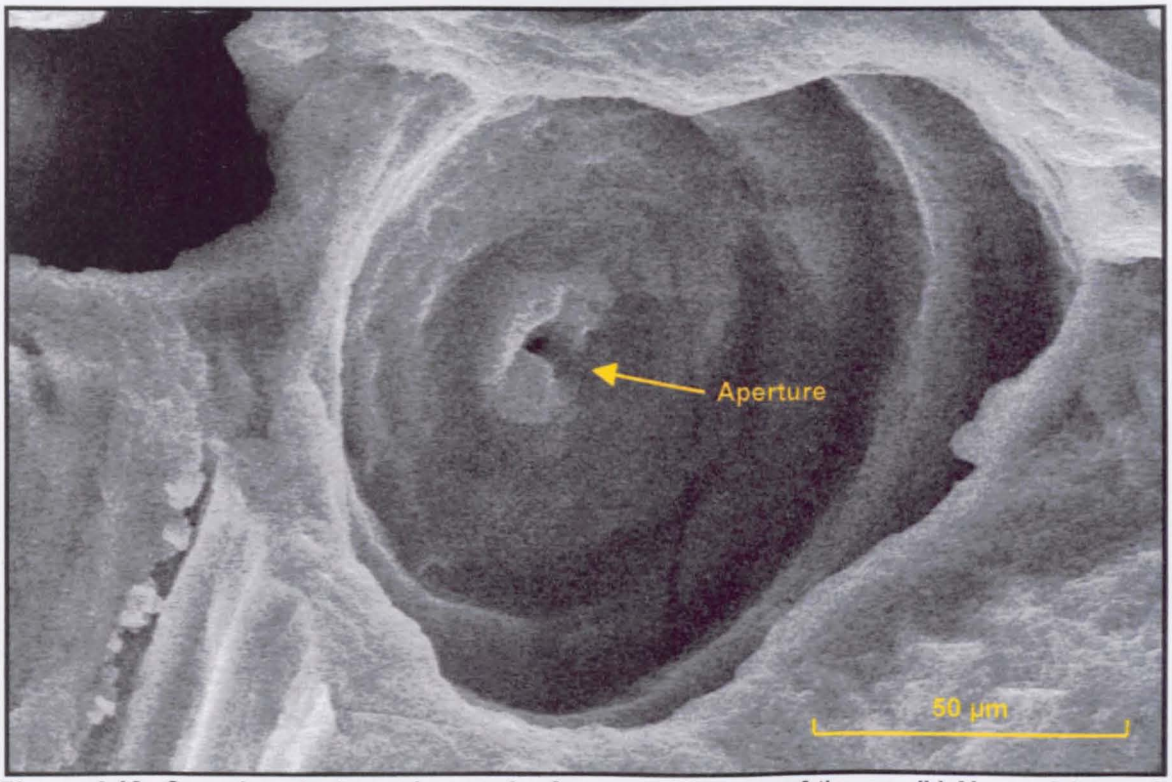

Figure 4.18: Scanning electron micrograph of a ventral fracture of the craniid *Neoancistrocrania norfolki* (Laurin).

The micrograph shows the hooped chambered structure of the upper secondary layer with the terminal aperture. (Courtesy of Sir Alwyn Williams FRS)

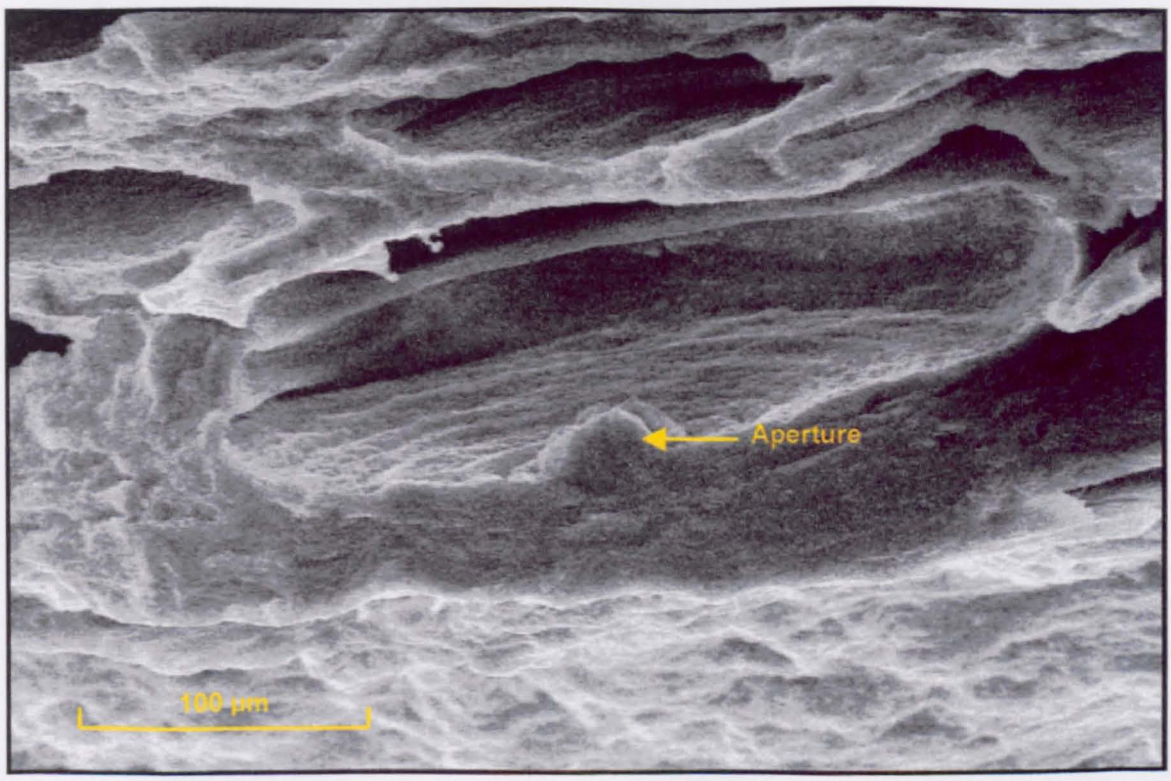

Figure 4.19: Scanning electron micrograph of a ventral fracture of the craniid *Neoancistrocrania norfolki* (Laurin).

The micrograph shows the collapsed and in filled chambers of the lower secondary layer and change in orientation of the aperture. (Courtesy of Sir Alwyn Williams FRS)

Chapter 5

Oxygen stable isotopic composition

of

modern brachiopod shells

5 Oxygen stable isotopic composition of modern brachiopod shells

5.1 Introduction

The principle of using the stable oxygen isotope composition of fossil brachiopod shells and other biogenic carbonates as a palaeothermometer for ancient seas is based on two premises. Firstly, the carbonate is precipitated in oxygen isotopic equilibrium with ambient seawater, and secondly, the equilibrium isotope fractionation factor for partitioning of oxygen isotopes between carbonate and seawater is temperature dependent. As previously discussed (see section 1.2), brachiopods are considered particularly suitable and are widely used in palaeoenvironmental studies. The possibility that brachiopods could precipitate shell calcite out of oxygen isotopic equilibrium had received little attention even though many workers have reported the possibility of biological fractionations, which are often referred to as vital effects. However, some studies using modern brachiopod shells (see section 1.3) have reported problems with oxygen isotopic variability between species, within individual specimens, and in cool environments (e.g. Lepzelter *et al.* 1983; Carpenter & Lohmann 1992; Marshall *et al.* 1996; Curry & Fallick 2002). Such observations have given rise to increased debate over the extent to which brachiopods precipitate calcite in oxygen isotopic equilibrium with the seawater in which they live. One aim of this study is to help resolve these uncertainties by undertaking a thorough and systematic study of variability of $\delta^{18}O$ values from modern brachiopod shells collected from locations with known environmental parameters.

In order to conduct a rigorous investigation of the oxygen stable isotopic composition of modern calcitic brachiopods, 1115 samples of shell calcite were extracted from 132 individual specimens from 8 locations around the world, with varying environmental

conditions, which are detailed in Table 5.1. Twelve species were used representing all the extant taxonomic groups of calcite shelled brachiopods as defined by Williams *et al.* (1996).

Table 5.1: Brachiopod shell material samples analysed in this study.

Species	Location	Valves	Specimens	Number of Samples		Number of Analyses	
				Shell Components	Bulk	Shell Components	Bulk
Terebratulida							
Terebratulina retusa	Firth of Lorne, Scotland	Complete Shells	11	100	1	34	10
Laqueus rubellus	Otsuchi Bay, Japan	Complete Shells	2	20	0	27	0
Laqueus rubellus	Sagami Bay, Japan	Complete Shells	11	100	1	192	10
Calloria inconspicua	Otago Shelf, New Zealand	Complete Shells	11	100	1	236	10
Liothyrella neozelanica	Otago Shelf, New Zealand	Complete Shells	11	100	1	251	10
Neothyris lenticularis	Otago Shelf, New Zealand	Complete Shells	11	100	1	289	10
Terebratella sanguinea	Otago Shelf, New Zealand	Complete Shells	11	100	1	270	10
Liothyrella uva	Signy Island, Antarctica	Complete Shells	11	100	1	165	10
Rhynchonellida							
Notosaria nigricans	Otago Shelf, New Zealand	Complete Shells	11	100	1	223	10
Thecideidina							
Thecidellina barretti	Rio Bueno, Jamaica	Complete Shells	10	0	10	0	26
Craniida							
Novocrania anomala	Firth of Lorne, Scotland	Dorsal Valves	11	30	1	34	10
Neoancistrocrania norfolki	South Pacific Ocean	5 Dorsal 5 Ventral	10	45	0	89	0
Overall Totals			**132**	**1115**		**2286**	

Brachiopod shells were prepared and sample material was extracted from different regions of each shell on the basis of ultrastructural and morphological components. Samples were then pre-treated by plasma-ashing prior to analysis (see section 3.4). Oxygen and carbon stable isotope ratios were determined by mass spectrometry (see section 3.5), with each sample being replicated up to three times depending on the quantity of material. Where available, one specimen of each species was crushed whole and ten aliquots of the bulk material analysed for comparison. In total, 2286 individual analyses were made. The resulting isotope data are presented as permil (‰) relative to the international standard VPDB using the standard $\delta^{18}O$ and $\delta^{13}C$ notation (Coplen 1995; Gonfiantini *et al.* 1995), and are recorded in appendix C.

5.2 The Terebratulida

The articulated Terebratulida include suborders Terebratulidina and Terebratellidina. Although there are some morphological differences between these groups, the stable oxygen isotope compositions are similar and they will therefore be considered together. A useful and conventional method of plotting isotope data is on a cross-plot of $\delta^{18}O$ versus $\delta^{13}C$. Figure 5.1, shows the isotopic results obtained from the shells of a typical modern terebratulid, *Calloria inconspicua* (Sowerby) collected from the South Island of New Zealand. The individual data points in this and subsequent crossplots represent the mean value of all the replicates for one sample from one individual brachiopod. This is a typical example of the general pattern when the values for all samples of one terebratulid species are plotted and is consistent with patterns observed in other studies of modern brachiopods (e.g. Carpenter & Lohmann 1995; Marshall *et al.* 1996; Crowley & Taylor 2000; Auclair *et al.* 2003). There is a significant positive correlation (Spearman's rank correlation coefficient = r_s) in the overall distribution of oxygen and carbon isotopic data in this cross-plot (Spearman's rank: $n = 100$, $r_s = 0.582$, $p = 0.000$). However, there is a distinct differentiation in the results obtained from the primary and secondary layers of the shell of

Calloria inconspicua. Indeed isotopic analyses carried out on the primary and secondary layers yield results that are so different that there is no overlap, $\delta^{18}O$ and $\delta^{13}C$ values are consistently lower in the primary layer than those in the secondary layer (Fig. 5.1), thus they can be discussed separately.

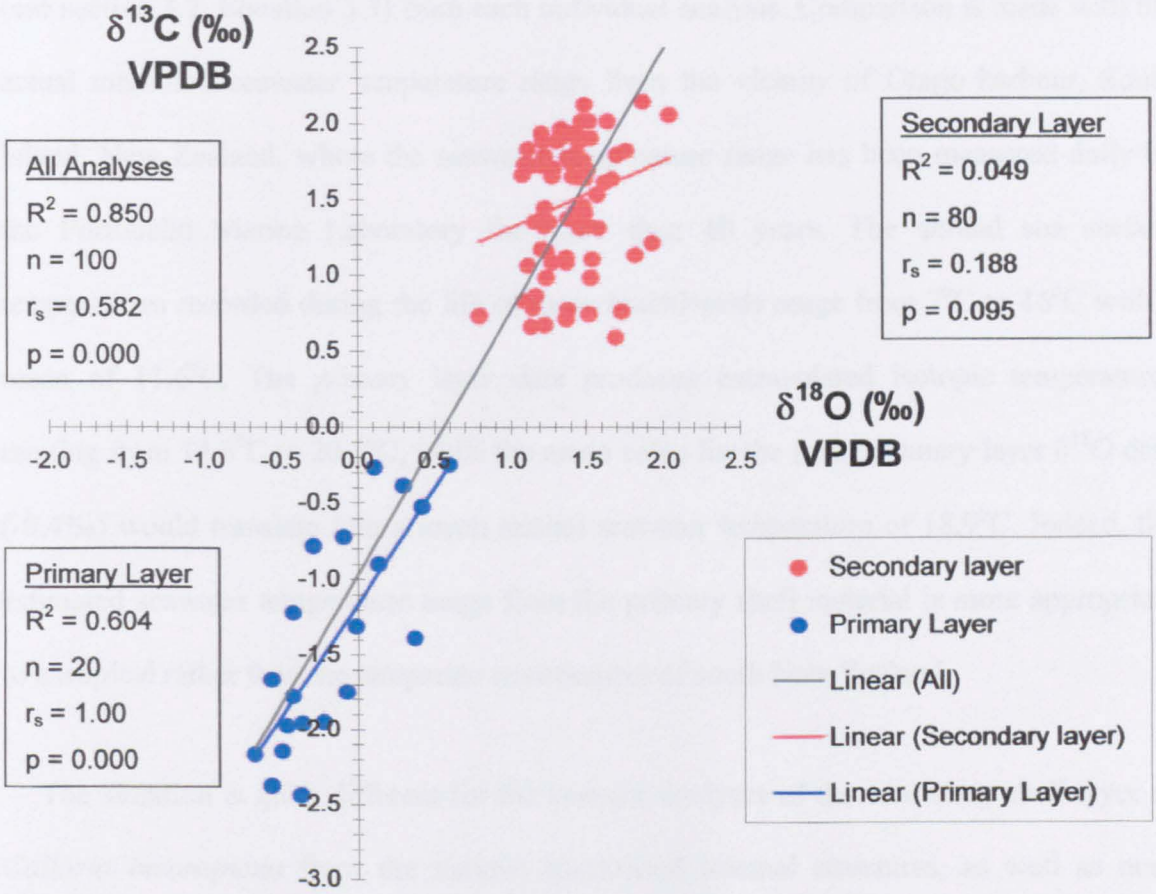

Figure 5.1: $\delta^{18}O$ – $\delta^{13}C$ crossplot for terebratulid brachiopod *Calloria inconspicua* (Sowerby) from the Otago Shelf, New Zealand.

Individual data points represent the mean value of analyses from one individual specimen. r_s value = Spearman's rank correlation coefficient. p value is for Spearman's rank correlation test @ 0.05 significance.

$\delta^{18}O$ and $\delta^{13}C$ values from the primary layer of *Calloria inconspicua* are positively correlated (Spearman's rank: n = 20, r_s = 1.000; p = <0.001) and produces $\delta^{18}O$ values ranging from –0.67‰ to 0.62‰ VPDB, a range depleted in ^{18}O relative to expected equilibrium values of 0.3‰ to 2.6‰ (Fig. 5.2, see section 3.7 for explanation of expected equilibrium range calculation). Although it is not possible to calculate meaningful isotopic temperatures in palaeoenvironmental investigations due to the lack of precise local

seawater data, it is useful to do so with modern brachiopod data in order to visualise the implications of fluctuations in $\delta^{18}O$ values on environmental interpretation.

The boxplot (Fig. 5.3) shows the distribution around the median of isotopic temperatures calculated using Anderson & Arthur's (1983) isotopic temperature equation (see section 3.7, Equation 3.3) from each individual analysis. Comparison is made with the actual measured seawater temperature range from the vicinity of Otago harbour, South Island, New Zealand, where the seawater temperature range has been measured daily by the Portobello Marine Laboratory for more than 40 years. The annual sea surface temperatures recorded during the life of these brachiopods range from 7°C to 16°C with a mean of 11.6°C. The primary layer data produces extrapolated isotopic temperatures ranging from 14.6°C to 20.1°C, while the mean value for the entire primary layer $\delta^{18}O$ data (-0.4‰) would translate into a mean annual seawater temperature of 18.9°C. Indeed, the estimated seawater temperature range from the primary shell material is more appropriate to a tropical rather than the temperate environment of south New Zealand.

The situation is quite different for the isotopic analyses of the secondary shell layer of *Calloria inconspicua* from the various specialised internal structures, as well as non-specialised areas of the secondary shell layer. No significant relationship between $\delta^{18}O$ and $\delta^{13}C$ exists (Spearman's rank: $n = 80$, $r_s = 0.188$ $p = 0.095$) and $\delta^{18}O$ values have a much smaller range than $\delta^{13}C$. Plotting the values from each of the secondary layer elements (Fig. 5.2) shows that, in each case, the measured mean oxygen isotopic value from the carbonate falls within the expected seawater oxygen isotope equilibrium range. The minimum and maximum $\delta^{18}O$ values from all of the secondary layer elements, regardless of specialisation, are 0.8‰ to 2.1‰, which represents an isotopic temperature range of 8.9°C to 13.9°C, falling within the range of temperatures actually measured (Fig. 5.3). Analyses of bulk material from a whole *Calloria inconspicua* shell produced wide ranging $\delta^{18}O$ values (0.19‰ to 1.92‰), which are strongly correlated with $\delta^{13}C$ values

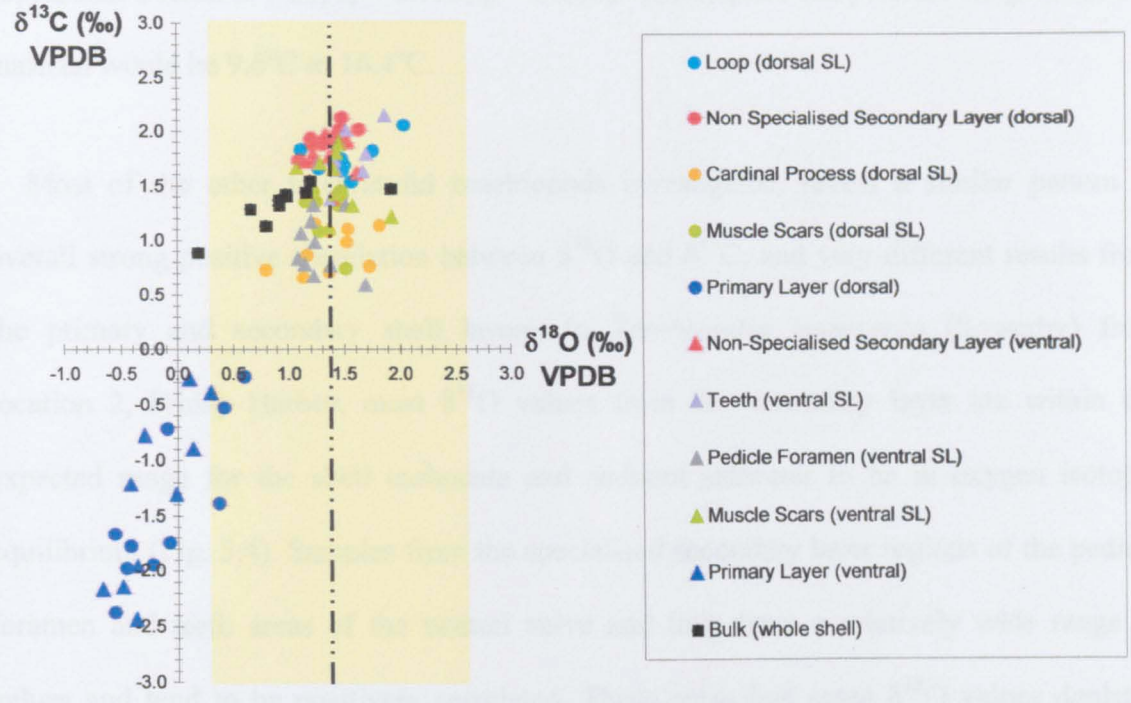

Figure 5.2: $\delta^{18}O - \delta^{13}C$ crossplot for terebratulid brachiopod *Calloria inconspicua* (Sowerby) from the Otago Shelf, New Zealand.

The shaded area represents the calculated range of expected equilibrium from $\delta^{18}O_{seawater}$ values, dashed line represents the mean $\delta^{18}O_{seawater}$ value. Individual data points represent the mean value of replicate analyses from one individual specimen.

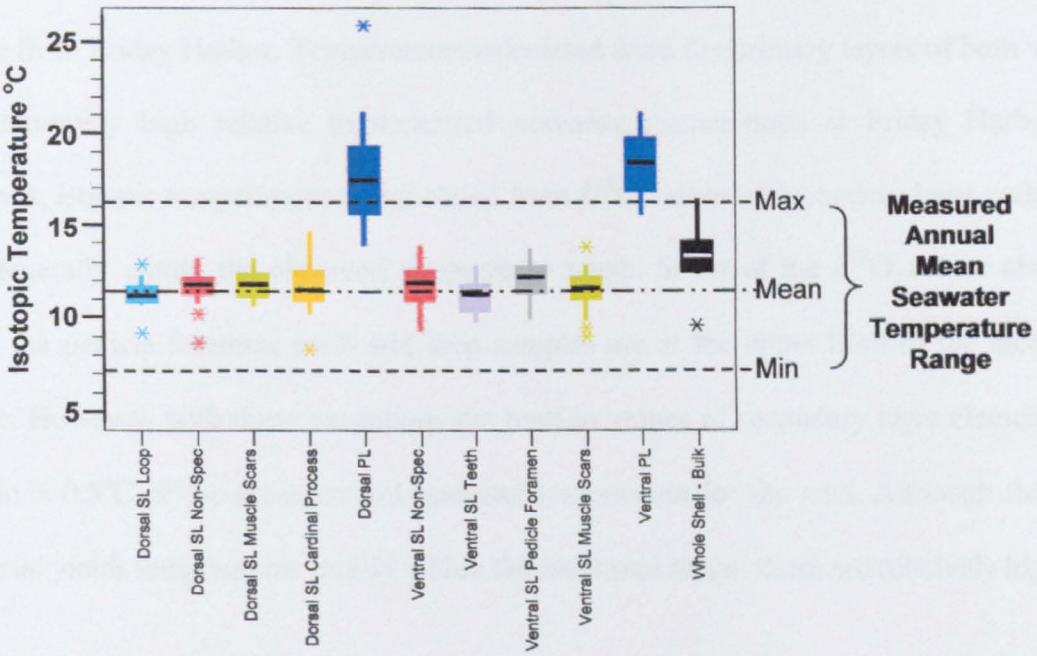

Figure 5.3: Boxplot showing the range of isotopic temperatures extrapolated from $\delta^{18}O$ values of all analyses determined from different regions of the shell of the terebratulid brachiopod *Calloria inconspicua* (Sowerby).

Comparison is made with the measured seawater temperature range from the Otago Shelf (Courtesy of Portobello Marine Laboratory).

(Spearman's rank: $n = 10$, $r_s = 0.793$, $p = 0.006$). The implied temperature range from this material would be 9.6°C to 16.4°C.

Most of the other terebratulid brachiopods investigated, reveal a similar pattern of overall strong positive correlation between $\delta^{18}O$ and $\delta^{13}C$, and very different results from the primary and secondary shell layers. In *Terebratalia transversa* (Sowerby) from location 2, Friday Harbor, most $\delta^{18}O$ values from the secondary layer are within the expected range for the shell carbonate and ambient seawater to be in oxygen isotopic equilibrium (Fig. 5.4). Samples from the specialised secondary layer regions of the pedicle foramen and teeth areas of the ventral valve and loop have a relatively wide range of values and tend to be positively correlated. These areas had some $\delta^{18}O$ values depleted relative to other secondary layer samples. The boxplot (Fig. 5.5) shows the distribution around the median of isotopic temperatures extrapolated from $\delta^{18}O$ values using Anderson & Arthur's (1983) palaeotemperature equation (see section 3.7, Equation 3.2) from each individual analysis. Comparison is made with the actual measured seawater temperature range from Friday Harbor. Temperatures calculated from the primary layers of both valves are extremely high relative to measured seawater temperatures at Friday Harbor. In contrast, isotopic temperatures extrapolated from $\delta^{18}O$ values of secondary layer carbonate are generally within the observed temperature range. Some of the $\delta^{18}O$ values obtained from the pedicle foramen, teeth and loop samples are at the upper limit of the measured range. However, with these exceptions the median values of secondary layer elements are within ± 0.5°C of the mean annual seawater temperature for the area. Although the bulk material yields temperatures mostly within the measured range, these are relatively high.

Laqueus rubellus (Sowerby) specimens were collected from two locations in Eastern Japan: location 3, Otsuchi Bay (Figs. 5.6 & 5.7) is influenced by the relatively cool Oyashio Current and location 4, Sagami Bay is influenced by the warmer Kuroshio Current

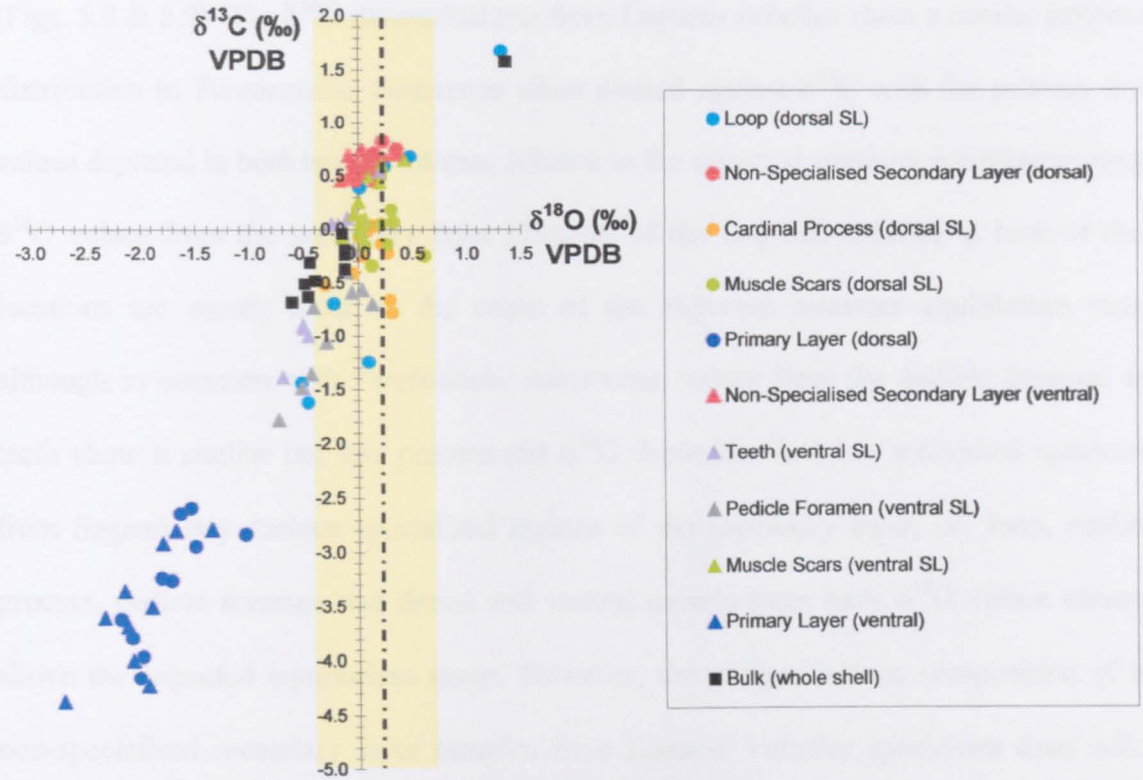

Figure 5.4: $\delta^{18}O$ – $\delta^{13}C$ crossplot for terebratulid brachiopod *Terebratalia transversa* (Sowerby) from the Puget Sound, near Friday Harbor, Washington, USA.

The shaded area represents the calculated range of expected equilibrium from $\delta^{18}O_{seawater}$ values, dashed line represents the mean $\delta^{18}O_{seawater}$ value. Individual data points represent the mean value of replicate analyses from one individual specimen.

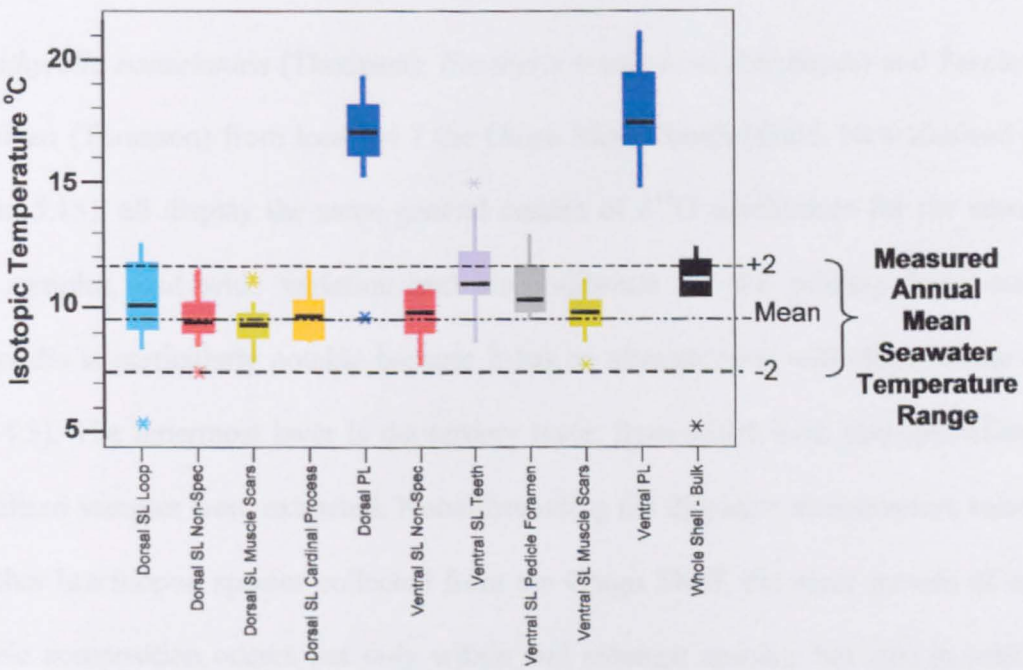

Figure 5.5: Boxplot showing the range of isotopic temperatures extrapolated from $\delta^{18}O$ values of all analyses from different regions of the shell of terebratulid brachiopod *Terebratalia transversa* (Sowerby).

Comparison is made with the measured seawater temperature range from Friday Harbor (Carpenter & Lohmann 1995).

(Figs. 5.8 & 5.9). The $\delta^{18}O$ determinations from *Laqueus rubellus* show a similar pattern of distribution to *Terebratalia transversa* when plotted against $\delta^{13}C$ with the primary layer values depleted in both heavy isotopes, relative to the expected seawater equilibrium range. $\delta^{18}O$ values from the secondary layer elements of the *Laqueus rubellus* at both of these locations are mostly close to the mean of the expected seawater equilibrium range, although in common with *Terebratalia transversa*, values from the pedicle foramen and teeth show a similar but less pronounced $\delta^{18}O$ depletion. In some individual specimens from Sagami Bay various specialised regions of the secondary layer, i.e. loop, cardinal process, pedicle foramen and dorsal and ventral muscle scars have $\delta^{18}O$ values elevated above the expected equilibrium range. However, the oxygen isotope composition of the non-specialised secondary layer samples from *Laqueus rubellus* specimens does reflect accurately differences in water temperature between the two sample locations. Mean isotopic temperatures calculated are 11.0°C for Otsuchi Bay compared with the measured annual mean seawater temperature of 11.3°C (JODC 2001), and 14.4°C for Sagami Bay compared with the measured annual mean seawater temperature of 14.8°C (JODC 2001).

Liothyrella neozelanica (Thomson), *Neothyris lenticularis* (Deshayes) and *Terebratella sanguinea* (Thomson) from location 7 the Otago Shelf, South Island, New Zealand (Figs. 5.10 to 5.15), all display the same general pattern of $\delta^{18}O$ equilibrium for the secondary layer samples, and wide variation and disequilibrium for the primary layer material. *Liothyrella* is particularly notable because it has an ultrastructure with three calcite layers (Fig. 4.5). The innermost layer is the tertiary layer, from which both non-specialised and specialised samples were extracted. Notwithstanding the disparate ultrastructure relative to the other brachiopod species collected from the Otago Shelf, the same pattern of oxygen isotopic composition occurs not only within and amongst species, but also in relation to expected parameters for isotopic equilibrium with ambient seawater. Figure 5.16 illustrates the comparison between mean isotopic temperatures extrapolated from $\delta^{18}O$

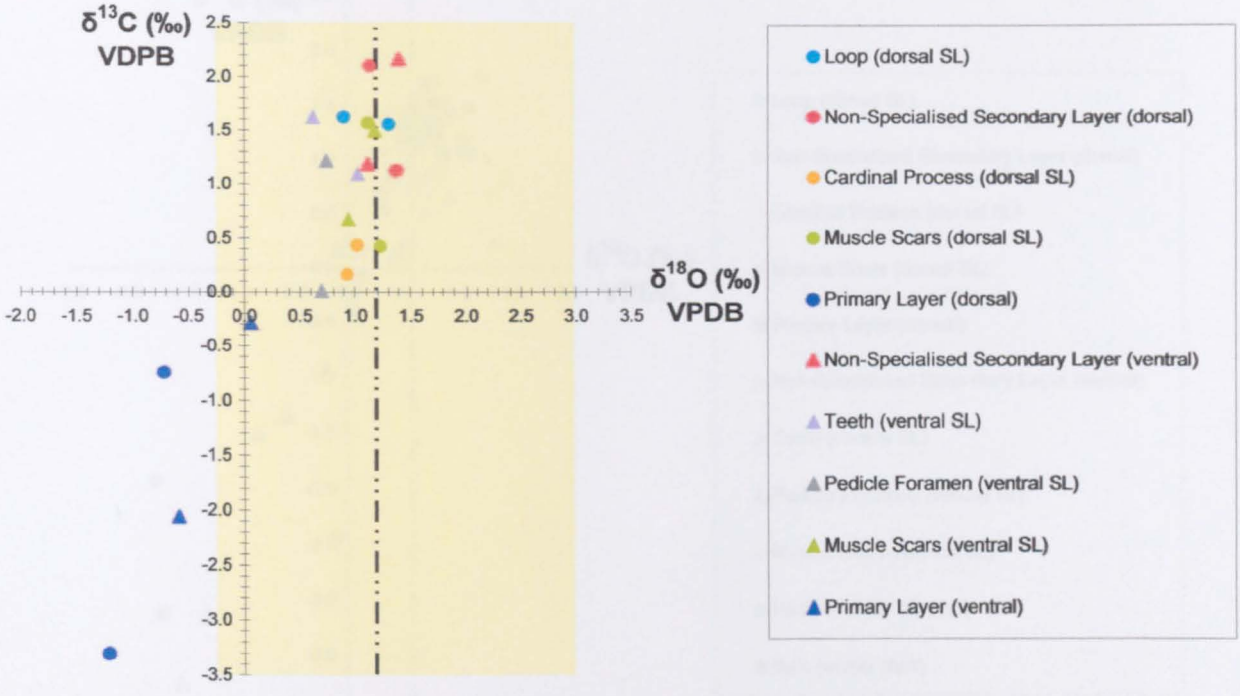

Figure 5.6: $\delta^{18}O$ – $\delta^{13}C$ crossplot for terebratulid brachiopod *Laqueus rubellus* (Sowerby) from Otsuchi Bay, Japan.

The shaded area represents the calculated range of expected equilibrium from $\delta^{18}O_{seawater}$ values, dashed line represents the mean $\delta^{18}O_{seawater}$ value. Individual data points represent the mean value of replicate analyses from one individual specimen.

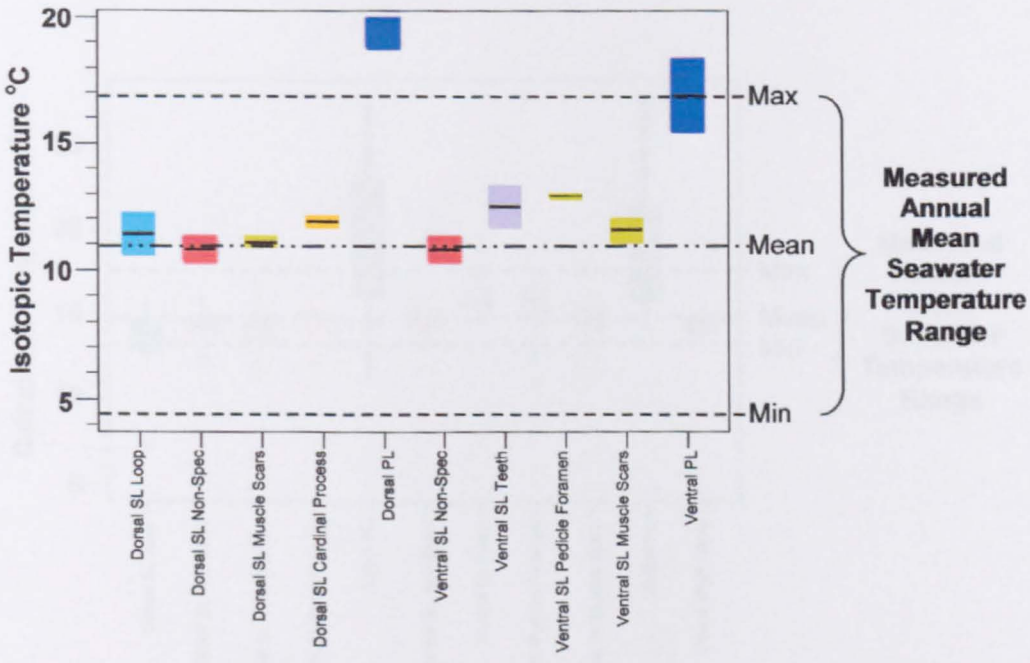

Figure 5.7: Boxplot showing the range of isotopic temperatures extrapolated from $\delta^{18}O$ values of all analyses determined from different regions of the shell of terebratulid brachiopod *Laqueus rubellus* (Sowerby) from Otsuchi Bay, Japan.

Comparison is made with the measured seawater temperature range from the Otsuchi Bay area (JODC 2001).

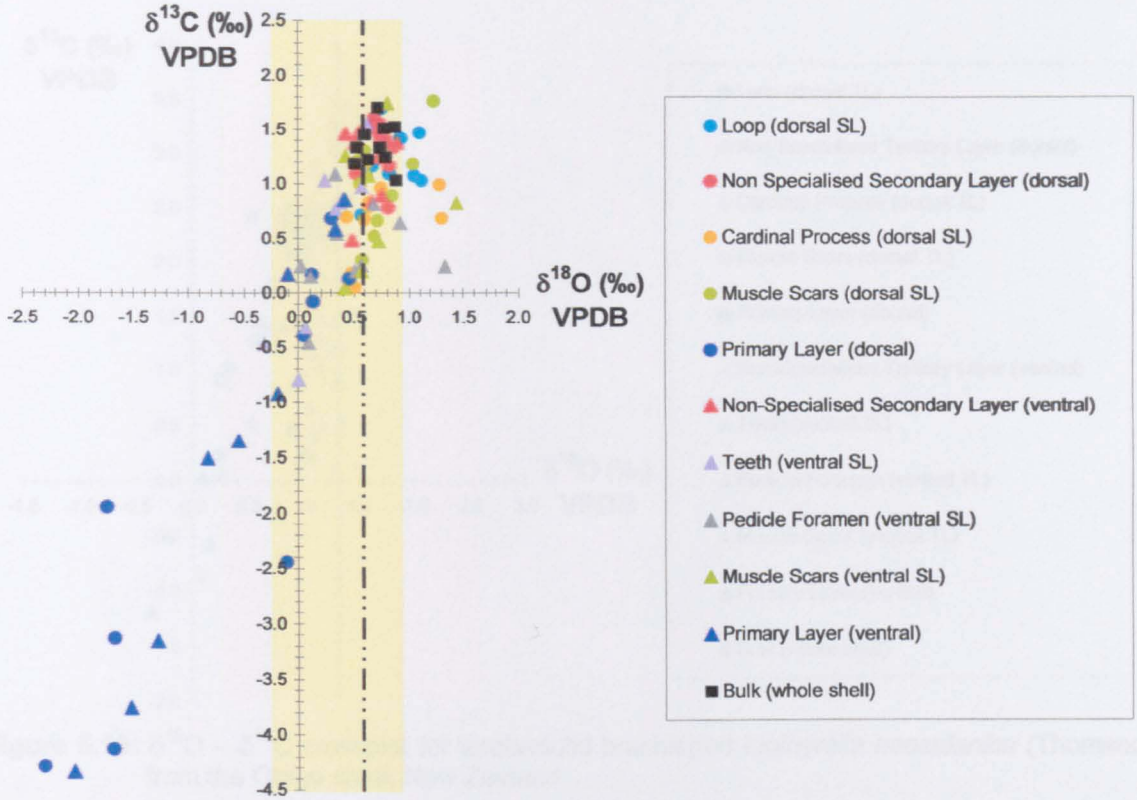

Figure 5.8: $\delta^{18}O$ – $\delta^{13}C$ crossplot for terebratulid brachiopod *Laqueus rubellus* (Sowerby) from Sagami Bay, Japan.

The shaded area represents the calculated range of expected equilibrium from $\delta^{18}O_{seawater}$ values, dashed line represents the mean $\delta^{18}O_{seawater}$ value. Individual data points represent the mean value of replicate analyses from one individual specimen.

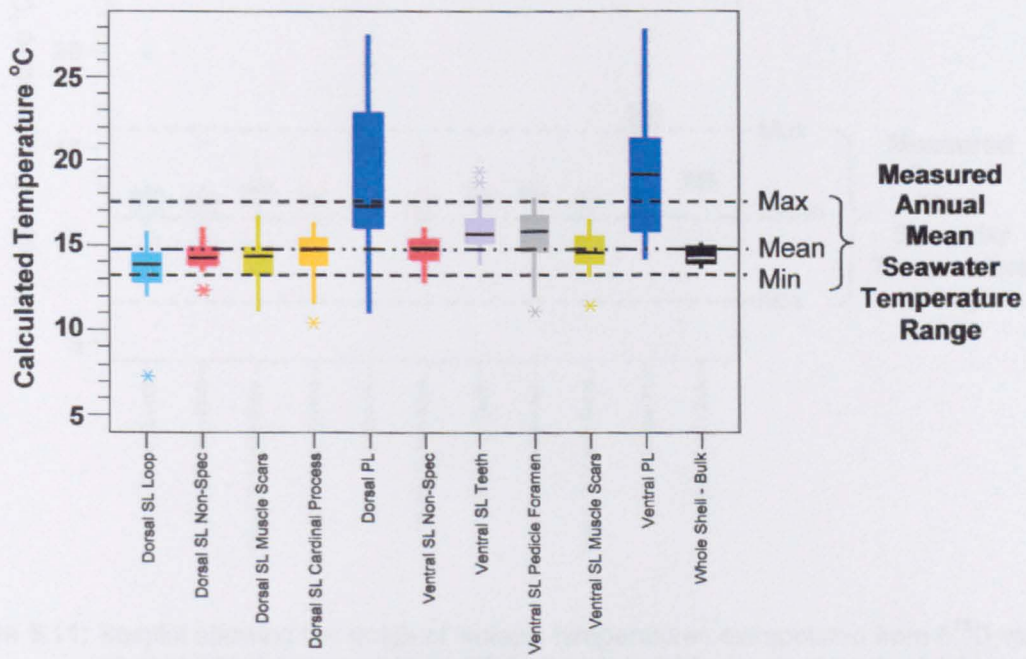

Figure 5.9: Boxplot showing the range of isotopic temperatures extrapolated from $\delta^{18}O$ values of all analyses determined from different regions of the shell of terebratulid brachiopod *Laqueus rubellus* (Sowerby) from Sagami Bay, Japan.

Comparison is made with the measured seawater temperature range from the Sagami Bay area (JODC 2001).

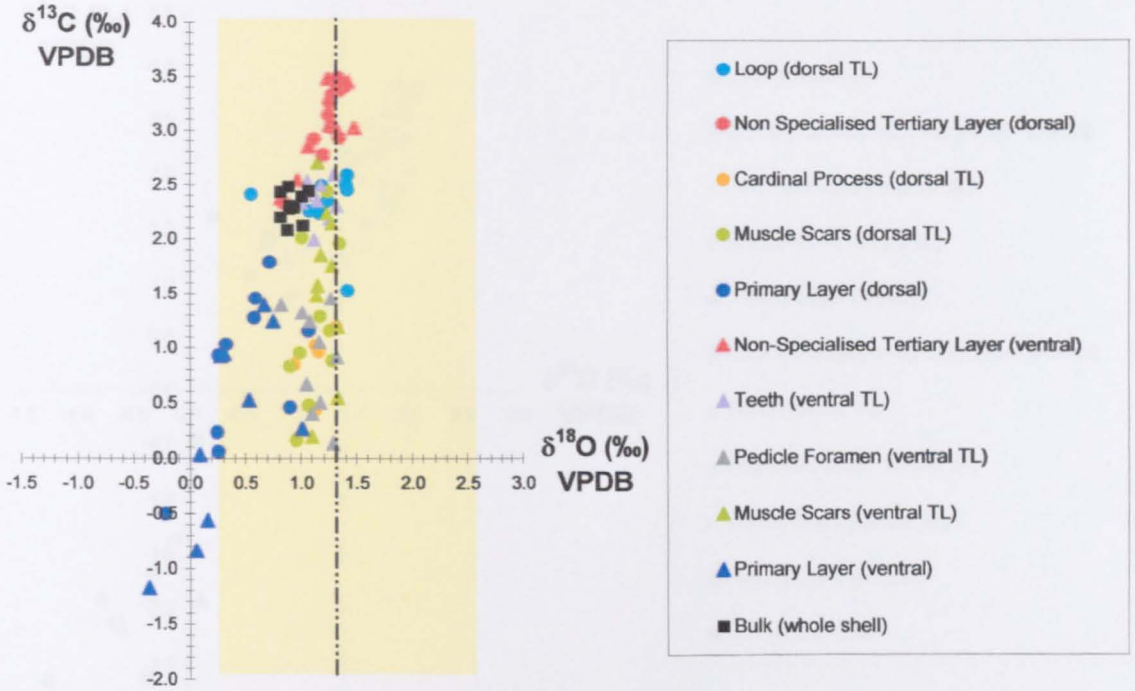

Figure 5.10: $\delta^{18}O$ – $\delta^{13}C$ crossplot for terebratulid brachiopod *Liothyrella neozelanica* (Thomson) from the Otago shelf, New Zealand.

The shaded area represents the calculated range of expected equilibrium from $\delta^{18}O_{seawater}$ values, dashed line represents the mean $\delta^{18}O_{seawater}$ value. Individual data points represent the mean value of replicate analyses from one individual specimen.

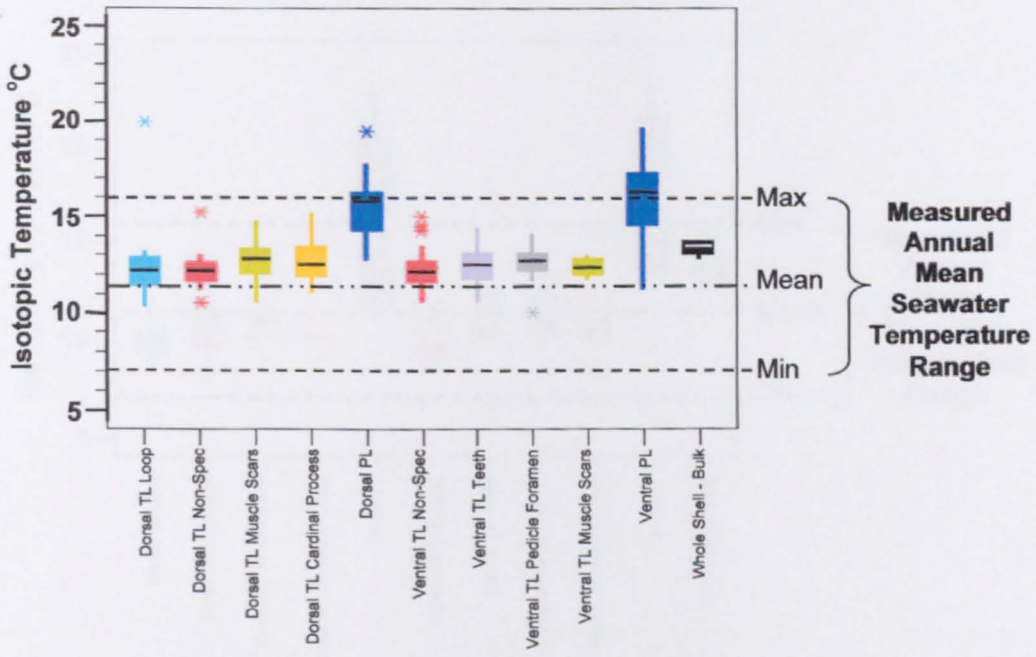

Figure 5.11: Boxplot showing the range of isotopic temperatures extrapolated from $\delta^{18}O$ values of all analyses determined from different regions of the shell of terebratulid brachiopod *Liothyrella neozelanica* (Thomson).

Comparison is made with the measured seawater temperature range from the Otago Shelf (Courtesy of Portobello Marine Laboratory).

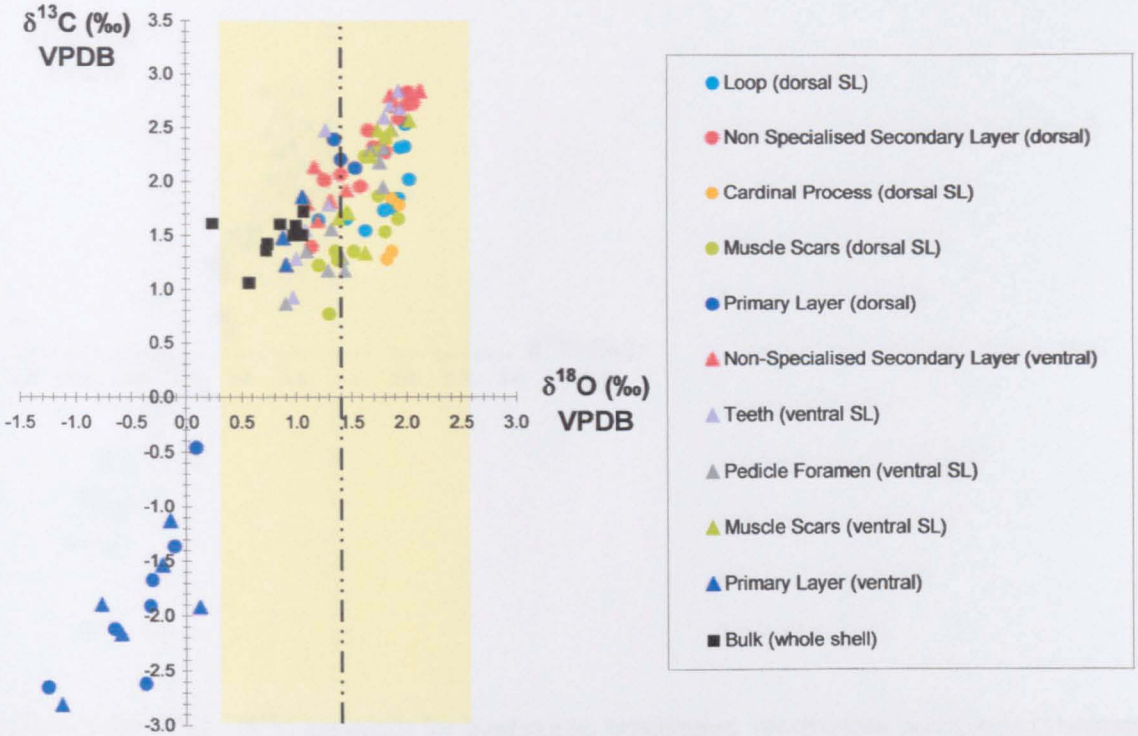

Figure 5.12: $\delta^{18}O$ – $\delta^{13}C$ crossplot for terebratulid brachiopod *Neothyris lenticularis* (Deshayes) from the Otago shelf, New Zealand.

The shaded area represents the calculated range of expected equilibrium from $\delta^{18}O_{seawater}$ values, dashed line represents the mean $\delta^{18}O_{seawater}$ value. Individual data points represent the mean value of replicate analyses from one individual specimen.

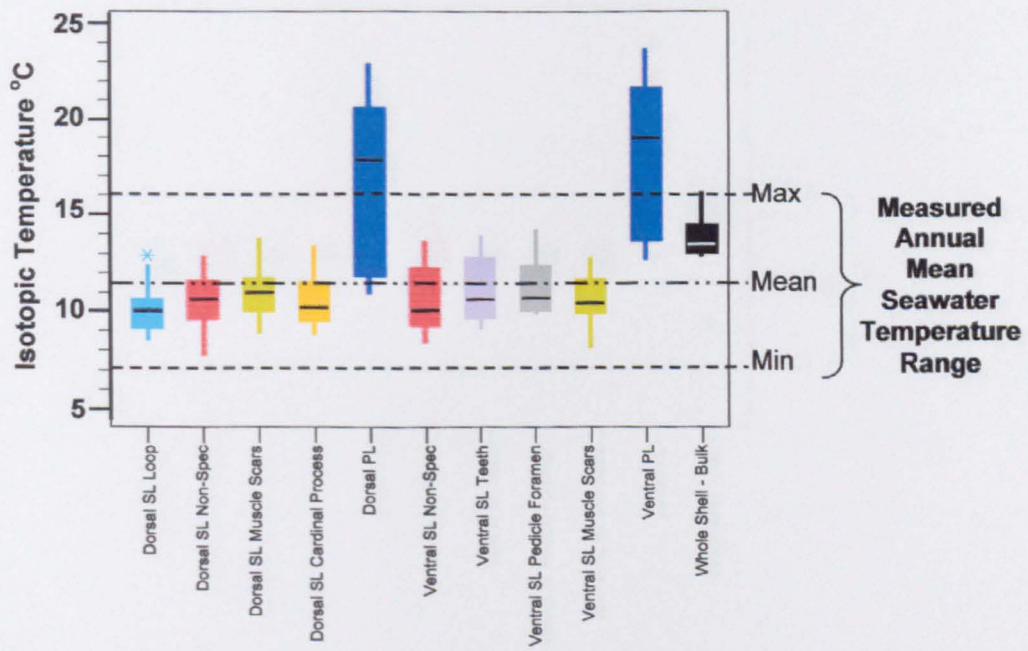

Figure 5.13: Boxplot showing the range of isotopic temperatures extrapolated from $\delta^{18}O$ values of all analyses determined from different regions of the shell of terebratulid brachiopod *Neothyris lenticularis* (Deshayes).

Comparison is made with the measured seawater temperature range from the Otago Shelf (Courtesy of Portobello Marine Laboratory).

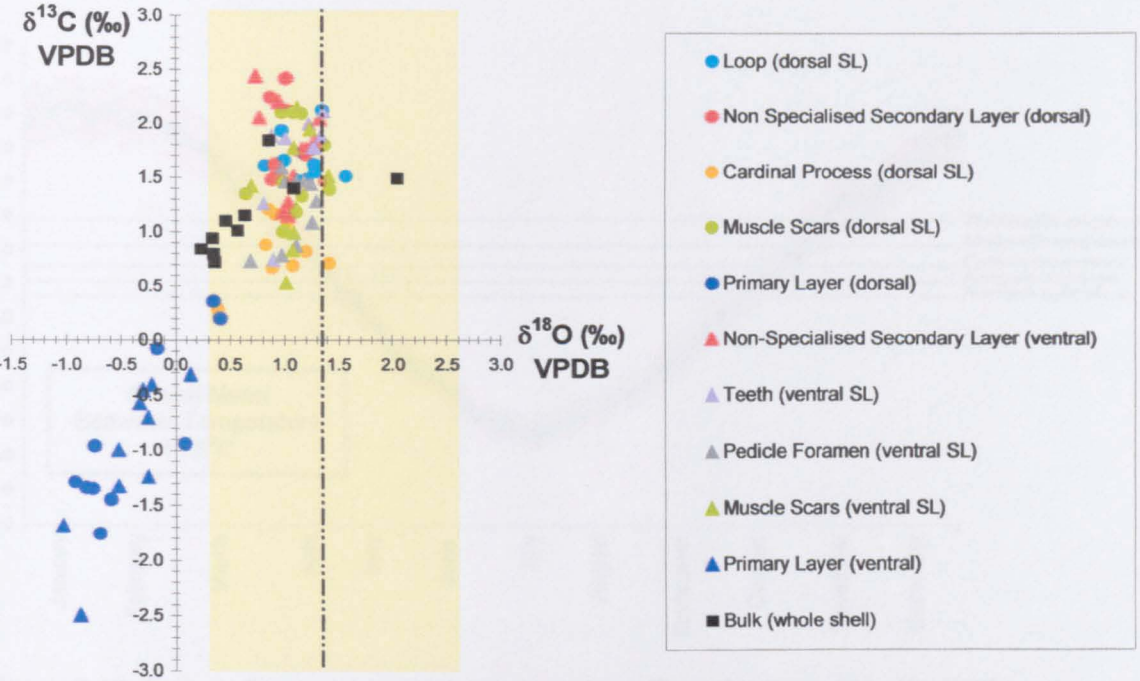

Figure 5.14: $\delta^{18}O$ – $\delta^{13}C$ crossplot for terebratulid brachiopod *Terebratella sanguinea* (Thomson) from the Otago shelf, New Zealand.

The shaded area represents the calculated range of expected equilibrium from $\delta^{18}O_{seawater}$ values, dashed line represents the mean $\delta^{18}O_{seawater}$ value. Individual data points represent the mean value of replicate analyses from one individual specimen.

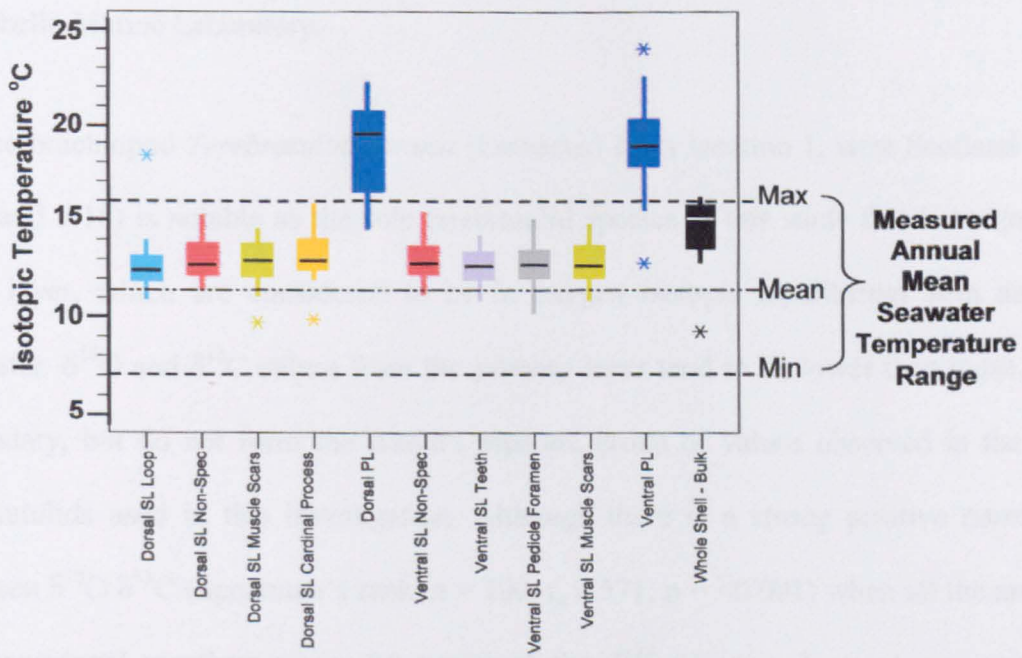

Figure 5.15: Boxplot showing the range of isotopic temperatures extrapolated from $\delta^{18}O$ values of all analyses determined from different regions of the shell of terebratulid brachiopod *Terebratella sanguinea* (Thomson).

Comparison is made with the measured seawater temperature range from the Otago Shelf (Courtesy of Portobello Marine Laboratory).

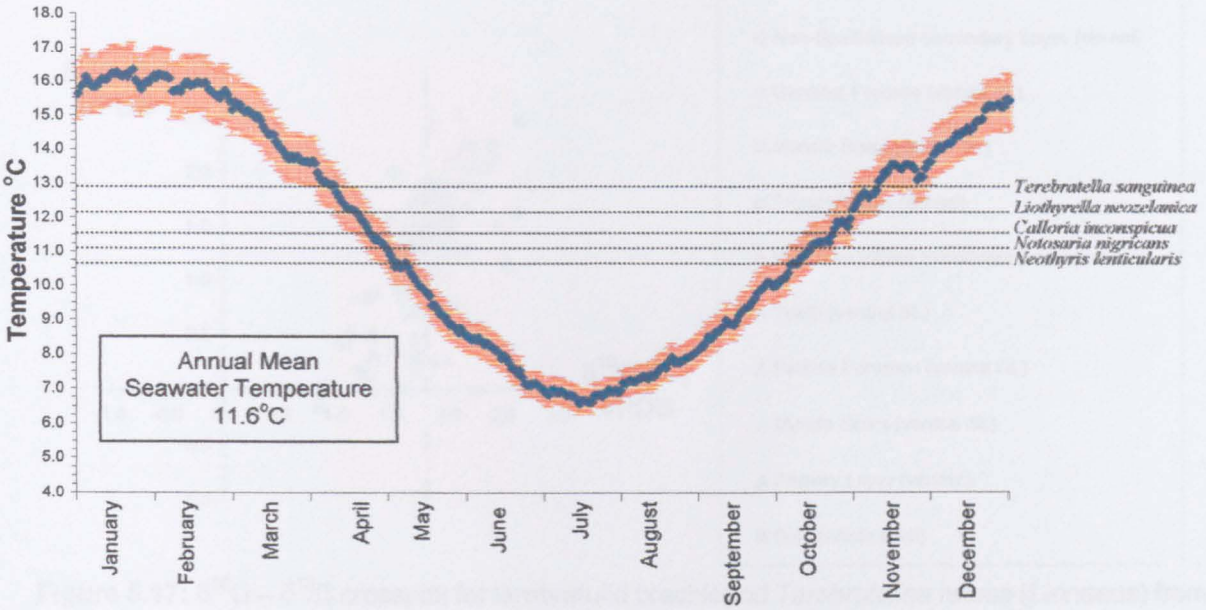

Figure 5.16: Daily surface seawater temperatures from Otago Harbour, New Zealand.

Data was supplied by Dr K Probert, Portobello Marine Laboratory. Comparison is made with temperatures calculated from $\delta^{18}O$ values determined from non-specialised secondary layer material extracted from five species at location 7. Mean daily temperatures are blue. The red error bars are ± 5%.

values determined from the non-specialised secondary layer or tertiary layer samples from the Otago shelf brachiopods and the daily surface seawater temperature measured by the Portobello Marine Laboratory.

The brachiopod *Terebratulina retusa* (Linnaeus) from location 1, west Scotland (Figs. 5.17 and 5.18) is notable as the sole terebratulid species in this study that has a primary shell layer, which are considered to be in oxygen isotopic equilibrium with ambient seawater. $\delta^{18}O$ and $\delta^{13}C$ values from the primary layer tend to be lower than those in the secondary, but do not form the distinct separate group of values observed in the other terebratulids used in this investigation. Although there is a strong positive correlation between $\delta^{18}O$ $\delta^{13}C$ (Spearman's rank: n = 100, r_s 0.571, p = <0.001) when all the analyses are considered together; when the means of the different sample areas are compared statistically (ANOVA see section 3.7) they are not significantly different (p = 0.498). Therefore, any variation in $\delta^{18}O$ values are minor and all areas of the shell are good indicators of the mean ambient seawater temperature.

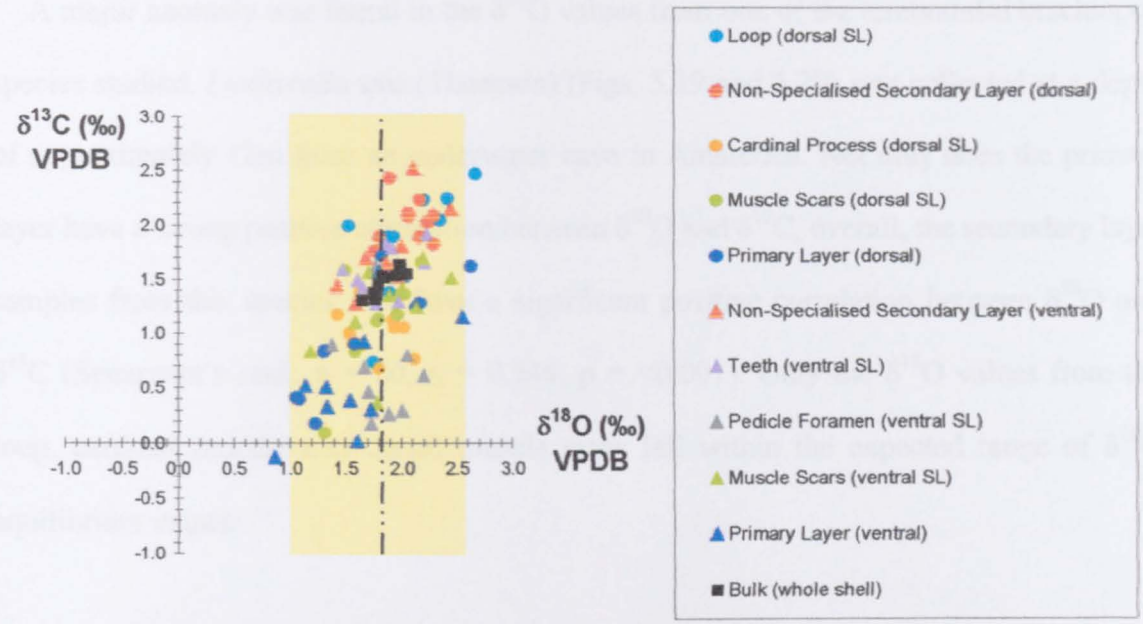

Figure 5.17: $\delta^{18}O - \delta^{13}C$ crossplot for terebratulid brachiopod *Terebratulina retusa* (Linnaeus) from the Firth of Lorne, Scotland.

The shaded area represents the calculated range of expected equilibrium from $\delta^{18}O_{seawater}$ values, dashed line represents the mean $\delta^{18}O_{seawater}$ value. Individual data points represent the mean value of replicate analyses from one individual specimen.

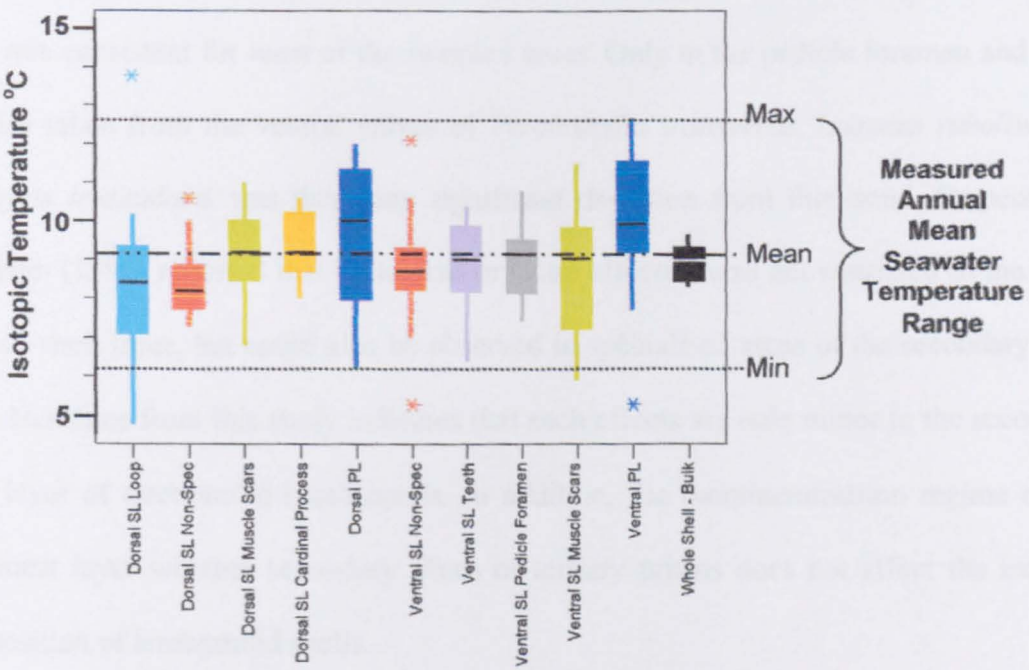

Figure 5.18: Boxplot showing the range of isotopic temperatures extrapolated from $\delta^{18}O$ values of all analyses determined from difference regions of the shell of terebratulid brachiopod *Terebratulina retusa* (Linnaeus).

Comparison is made with the measured seawater temperature range from the Firth of Lorne (BODC 2003).

A major anomaly was found in the $\delta^{18}O$ values from one of the terebratulid brachiopod species studied. *Liothyrella uva* (Thomson) (Figs. 5.19 and 5.20) was collected at a depth of approximately 12m from an underwater cave in Antarctica. Not only does the primary layer have a strong positive correlation between $\delta^{18}O$ and $\delta^{13}C$, overall, the secondary layer samples from this species also have a significant positive correlation between $\delta^{18}O$ and $\delta^{13}C$ (Spearman's rank: $n = 80$, $r_s = 0.544$, $p = <0.001$). Only the $\delta^{18}O$ values from the loop, cardinal process and dorsal muscle scars fall within the expected range of $\delta^{18}O$ equilibrium values.

5.2.1 *Terebratulida discussion*

With the exception of *Liothyrella uva*, the innermost calcareous layer of the terebratulids, whether secondary or tertiary, yielded mean $\delta^{18}O$ values almost always in equilibrium with ambient seawater. Mean isotopic temperatures calculated using these values are close to the means of measured values. The oxygen isotopic composition of this layer was consistent for most of the sampled areas. Only in the pedicle foramen and teeth samples taken from the ventral valves of *Terebratella transversa*, *Laqueus rubellus* and *Neothyris lenticularis* was there any significant deviation from this trend. Carpenter & Lohmann (1995) reported that biological or 'vital effects' were not restricted to the outer primary shell layer, but could also be observed in specialised areas of the secondary shell layer. Evidence from this study indicates that such effects are only minor in the secondary shell layer of terebratulid brachiopods. In addition, the biomineralisation regime of the innermost layer whether secondary fibres or tertiary prisms does not affect the isotopic composition of terebratulid shells.

Samtleben *et al.* (2001) found that prismatic tertiary layer calcite from fossilised Silurian brachiopods had $\delta^{18}O$ values that were not in equilibrium with assumed values for ambient seawater. However, analyses of tertiary shell material in his study are

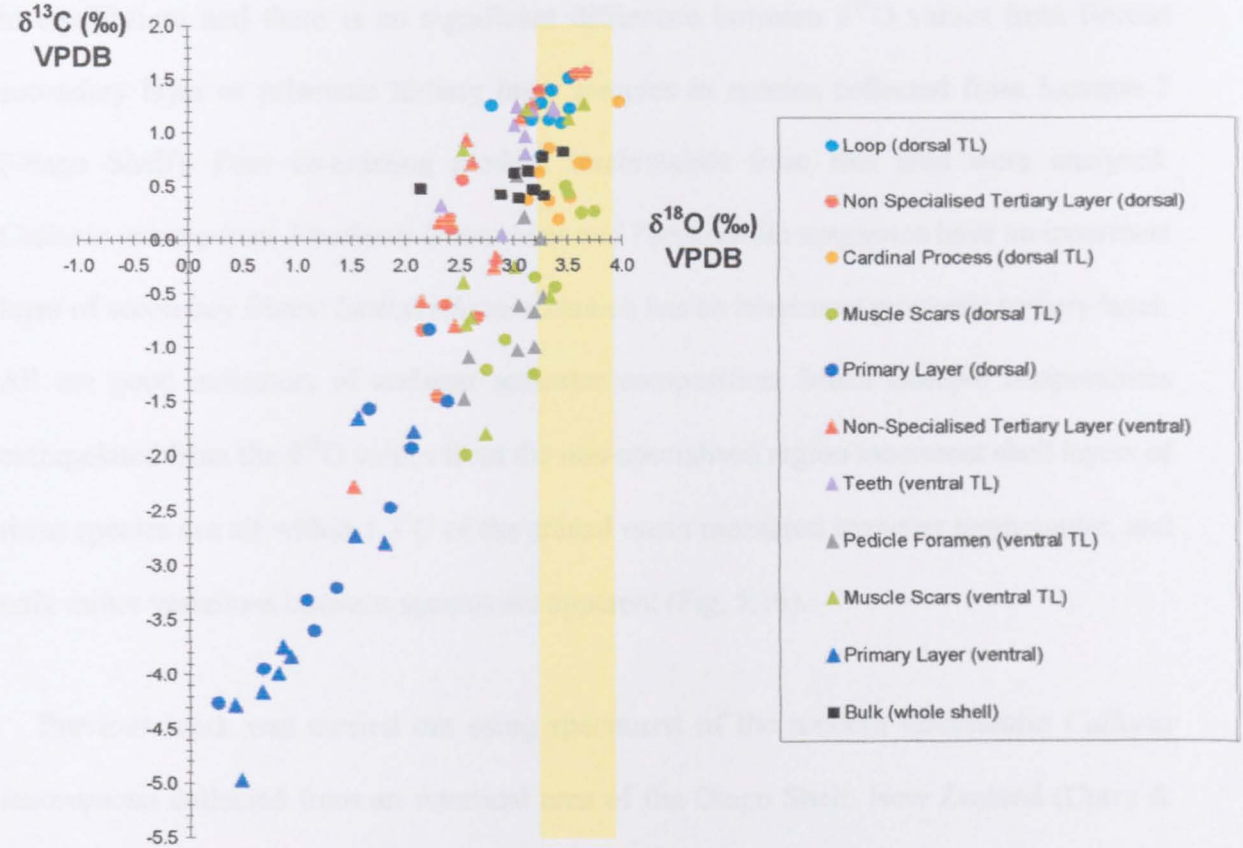

Figure 5.19: $\delta^{18}O$ – $\delta^{13}C$ crossplot for terebratulid brachiopod *Liothyrella uva* (Thomson) from Borge Bay Signy Island, South Orkney Island, Antarctica.

The shaded area represents the calculated range of expected equilibrium from $\delta^{18}O_{seawater}$ values. Individual data points represent the mean value of replicate analyses from one individual specimen.

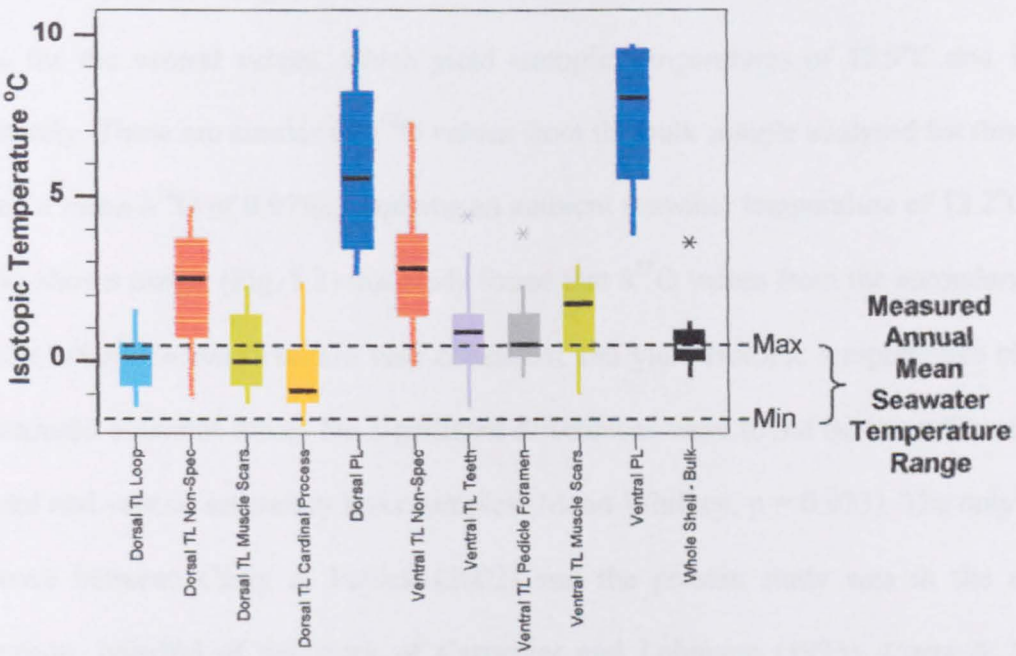

Figure 5.20: Boxplot showing the range of isotopic temperatures extrapolated from $\delta^{18}O$ values of all analyses determined from different regions of the shell of terebratulid brachiopod *Liothyrella uva* (Thomson).

Comparison is made with the measured seawater temperature range from the Borge Bay, Signy Island (Clarke *et al.* 1988)

in equilibrium and there is no significant difference between $\delta^{18}O$ values from fibrous secondary layer or prismatic tertiary layer samples in species collected from location 7 (Otago Shelf). Four co-existing modern terebratulids from this area were analysed: *Calloria inconspicua, Neothyris lenticularis and Terebratella sanguinea* have an innermost layer of secondary fibres; *Liothyrella neozelanica* has an innermost prismatic tertiary layer. All are good indicators of ambient seawater composition. Mean isotopic temperatures extrapolated from the $\delta^{18}O$ values from the non-specialised region innermost shell layers of these species are all within 1.3°C of the annual mean measured seawater temperature, and only minor variations between species are apparent (Fig. 5.16).

Previous work was carried out using specimens of the modern terebratulid *Calloria inconspicua* collected from an intertidal area of the Otago Shelf, New Zealand (Curry & Fallick 2002). They reported a systematic difference in oxygen isotopic composition between the dorsal and ventral valves of individual specimens. Curry and Fallick (2002) report $\delta^{18}O$ values which produce isotopic temperatures at the high end of the measured seawater temperature range. Mean $\delta^{18}O$ values were 1.06‰ for the dorsal valves and 0.58‰ for the ventral valves, which yield isotopic temperatures of 12.9°C and 14.8°C respectively. These are similar to $\delta^{18}O$ values from the bulk sample analysed for this study that had a mean $\delta^{18}O$ of 0.97‰, implying an ambient seawater temperature of 13.2°C (Fig. 5.3). As shown earlier (Fig. 5.2) this study found that $\delta^{18}O$ values from the secondary layer only of *Calloria inconspicua* are very consistent and yield isotopic temperatures close to the measured seawater mean. No significant differences were found between the medians of dorsal and ventral secondary layer samples (Mann-Whitney, $p = 0.933$). The only major difference between Curry & Fallick (2002) and the present study was in the sample preparation. Mindful of the work of Carpenter and Lohmann (1995), Curry & Fallick (2002) avoided specialised areas of the shell and analysed the non-specialised anterior portion, which included the primary layer. James *et al.* (1997) adopted a similar approach

studying modern terebratulids from the Lacepede Shelf, southern Australia. James *et al.* (1997) estimated that the weight of primary layer material was proportionally insignificant, therefore sampled whole shells. Their investigation found a higher degree of variability for $\delta^{18}O$ than $\delta^{13}C$. This study has shown the opposite to James *et al.* (1997), with greater variability in $\delta^{13}C$ than $\delta^{18}O$ in all species at all locations. The $\delta^{18}O$ results for Curry & Fallick (2002) and James *et al.* (1997) are considered to be due to the inclusion of ^{18}O depleted primary material. The primary shell layer of brachiopods grows faster than the secondary or tertiary layers (Rudwick 1970), therefore it is possible that $\delta^{18}O$ is depleted due to kinetic fractionation. However, the effect of including primary material from terebratulids in isotopic investigations would not always be detrimental, as some species show little ^{18}O depletion in this area, e.g. *Terebratulina retusa*. Because there is an element of species dependence in the $\delta^{18}O$ value of primary layer and secondary layers, it is advisable to avoid using primary layer material. The differential in $\delta^{18}O$ between dorsal and ventral valves observed by Curry and Fallick (2002) is probably due to the proportion of primary shell in each sample. The anterior of the brachiopod is formed from the youngest material, and therefore contains the thinnest layer of secondary shell. The ventral valve is a much larger and heavier construction than the dorsal valve and therefore will produce proportionally more primary shell during the enlargement phase of growth. Bulk analysis of only the anterior proportion of each valve of a species such as *Calloria inconspicua*, which has a significant differential in $\delta^{18}O$ values between primary and secondary layers, will inevitably produce disparate results. The ventral valve samples with proportionally more primary material will be more depleted in ^{18}O, hence producing higher isotopic temperatures.

It is hard to reconcile the *Liothyrella uva* data with any factor other than survival in the extreme environment of Antarctic waters. The annual seawater temperature range at location 8 at Signy Island, Antarctica –1.8 to 0.4°C (Clarke *et al.* 1988) is very narrow. In

normal circumstances, the *Liothyrella* genus secretes a prismatic tertiary succession that forms the innermost calcareous shell layer (MacKinnon & Williams 1974; Williams 1997; Williams *et al.* 1997). Although this was the case for *Liothyrella neozelanica* (Fig. 4.5), in *Liothyrella uva* the layer was poorly formed and fibrous secondary material dominated (Fig. 4.7). In addition, this was the only terebratulid species to produce secondary/tertiary shell mostly in disequilibrium with ambient seawater. The strong positive correlation between $\delta^{18}O$ and $\delta^{13}C$ found throughout the secondary/tertiary shell layer is generally accepted as evidence of a biological fractionation or 'vital effect'. This is the only articulated species to demonstrate a strong metabolic influence over the oxygen isotopic composition of the shell. The reasons for such an effect may be due to its survival strategy. Peck *et al.* (1997) studied growth and metabolism of the species at the same location. It was observed that *Liothyrella uva* exhibited very slow but highly seasonal growth rates with the shell size increasing 5-13% faster during the winter months. Earlier work (Peck & Holmes 1989) found that the feeding cycle and the accompanied increase in soft tissue mass were synchronised with the phytoplankton bloom during the southern summer (Clarke *et al.* 1988). The conclusion was that *Liothyrella uva* had the ability to separate shell growth and increase in soft tissue mass. Such a strategy of metabolic control is beneficial for a creature living in a nutrient-poor environment because it allows for prioritisation of resources. It is reasonable to assume that such a highly regulated metabolic and biomineralisation regime is reflected in the isotopic composition. The implications are that brachiopods living in extreme environments may be poor recorders of ambient seawater.

5.3 The Rhynchonellida

One Rhynchonellid species, *Notosaria nigricans* (Sowerby) collected at location 7, Otago Shelf, south New Zealand, was available to this study. The pattern of stable isotope composition is akin to the Terebratulida (Fig. 5.21). $\delta^{18}O$ values from the secondary layer

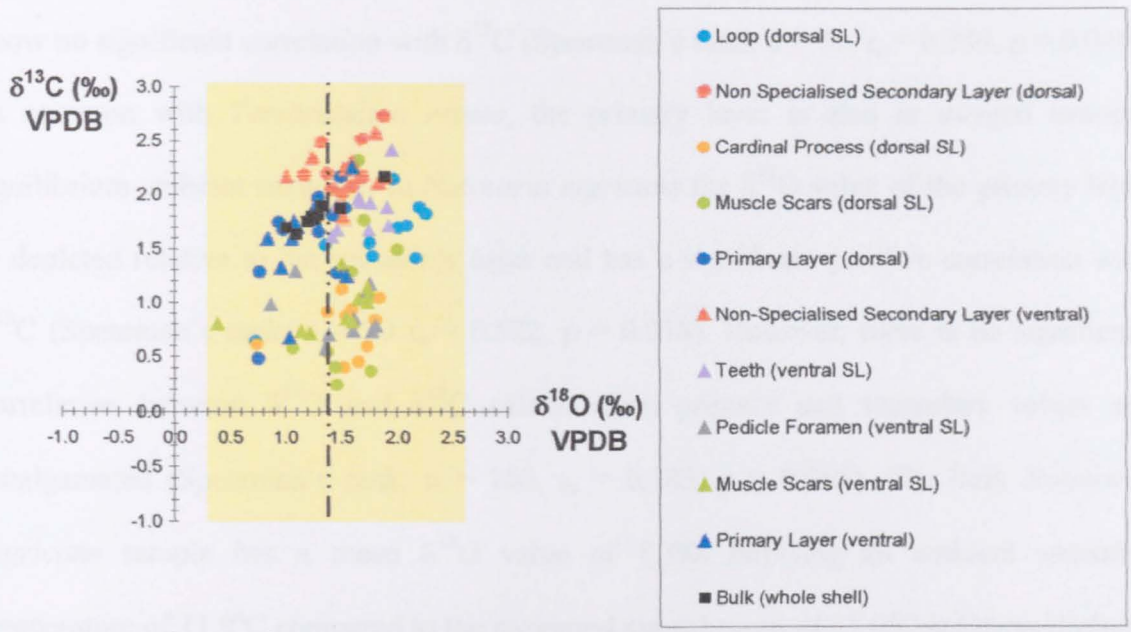

Figure 5.21: $\delta^{18}O$ – $\delta^{13}C$ crossplot for rhynchonellid brachiopod *Notosaria nigricans* (Sowerby) from the Otago shelf, New Zealand.

The shaded area represents the calculated range of expected equilibrium from $\delta^{18}O_{seawater}$ values, dashed line represents the mean $\delta^{18}O_{seawater}$ value. Individual data points represent the mean value of replicate analyses from one individual specimen.

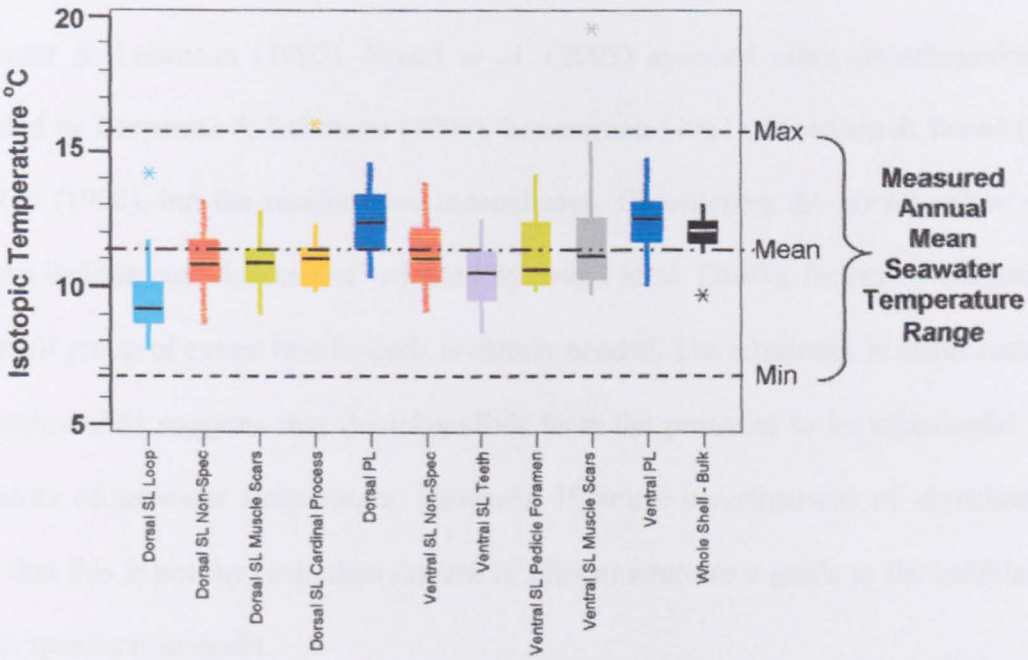

Figure 5.22: Boxplot showing the range of isotopic temperatures extrapolated from $\delta^{18}O$ values of all analyses determined from different regions of the shell of Rhynchonellid brachiopod *Notosaria nigricans* (Sowerby).

Comparison is made with the measured seawater temperature range from the Otago Shelf (Courtesy of Portobello Marine Laboratory).

elements are all in isotopic equilibrium with measured ambient seawater conditions and show no significant correlation with $\delta^{13}C$ (Spearman's rank: $n = 80$, $r_s = 0.230$, $p = 0.040$). In common with *Terebratulina retusa*, the primary layer is also in oxygen isotopic equilibrium ambient seawater. In *Notosaria nigricans* the $\delta^{18}O$ value of the primary layer is depleted relative to the secondary layer and has a significant positive correlation with $\delta^{13}C$ (Spearman's rank: $n = 20$ $r_s = 0.522$, $p = 0.018$). However, there is no significant correlation between $\delta^{18}O$ and $\delta^{13}C$ values when primary and secondary values are amalgamated (Spearman's rank: $n = 100$, $r_s = 0.185$, $p = 0.066$). The bulk *Notosaria nigricans* sample has a mean $\delta^{18}O$ value of 1.3‰ implying an ambient seawater temperature of 11.9°C compared to the measured annual mean of 11.6°C at Otago Harbour (Figs. 5.16 and 5.22).

The evidence presented here is favourable for the use of the Rhynchonellida as proxies for ambient seawater conditions, although only one species was studied. The findings are consistent with those of Brand *et al.* (2003) for the same species but contrary to those of Carpenter & Lohmann (1995). Brand *et al.* (2003) assessed other rhynchonellid data provided by Carpenter & Lohmann (1995), Lowenstam (1961), Morrison & Brand (1986) and Rao (1996), but the results were inconclusive. Considering the liberal nature of the 'oxygen isotope equilibrium test' adopted by Brand *et al.* (2003), further investigation of this small group of extant brachiopods is clearly needed. The similarity in ultrastructure to the terebratulids suggests that rhynchonellids have the potential to be meaningful proxy indicators of seawater temperature. However, if future investigations of rhynchonellids show that this is not the case, then the use of ultrastructure as a guide to the usefulness of extinct species is in doubt.

5.4 The Thecideidina

Modern thecideidine brachiopods are structurally different to other articulated groups. The shell is mostly composed of primary layer acicular crystallites inclined perpendicular to the secretory surface (see Chapter 4, Fig. 4.11). There is no well-defined secondary layer and only traces of fibrous material are present (Williams 1973). Due to this and the small size of the creatures (~3mm), the shells of *Thecidellina barretti* (Davidson) were sampled whole, i.e. ten complete shells were crushed and ten aliquots of the homogenised powder of each individual were analysed.

The bulk data, based on ten individual specimens of *Thecidellina barretti* from Jamaica show very little variation in $\delta^{18}O$, with a range of –1.29‰ to –0.93‰, a difference of only 0.36‰ (Fig. 5.23). Neither are they significantly correlated with $\delta^{13}C$ (Spearman's rank, n = 10, r_s = -0.517; p = 0.126). This is not considered to be due to the different sampling method, as bulk sampling of the other articulated species usually produced highly variable delta values for analyses from one individual specimen. For example, 1 bulk sampled specimen of *Calloria inconspicua* produced $\delta^{18}O$ values of 0.19‰ to 1.92‰ (Fig. 5.2), which were significantly correlated with $\delta^{13}C$ (Spearman's rank: n = 10 r_s = 0.960; p = 0.<001), and the $\delta^{18}O$ range corresponds an isotopic temperature variation of 6.8°C in just one *Calloria inconspicua* shell (Fig. 5.3).

Although the $\delta^{18}O$ values of *Thecidellina barretti* in this study are consistent throughout the individuals sampled, they are greater than the expected seawater equilibrium range (Fig. 5.23). Using these brachiopods in a palaeoenvironmental investigation may lead to an underestimation of the ancient seawater temperature (Fig. 5.24). Similar results to this study were recorded by Carpenter & Lohmann (1995) and Rao (1996), which are reviewed together with new data in Brand *et al.* (2003). The data from these studies, together with data from the present investigation suggest that the trend of $\delta^{18}O$ values is

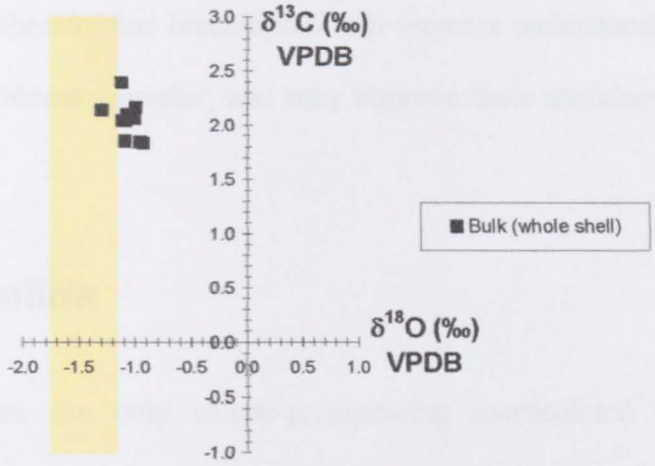

Figure 5.23: $\delta^{18}O - \delta^{13}C$ crossplot for the thecideidine brachiopod *Thecidellina barretti* (Davidson) from Rio Bueno, Jamaica.

The shaded area represents the calculated range of expected equilibrium from $\delta^{18}O_{seawater}$ values. Individual data points represent the mean value of replicate analyses from one individual specimen.

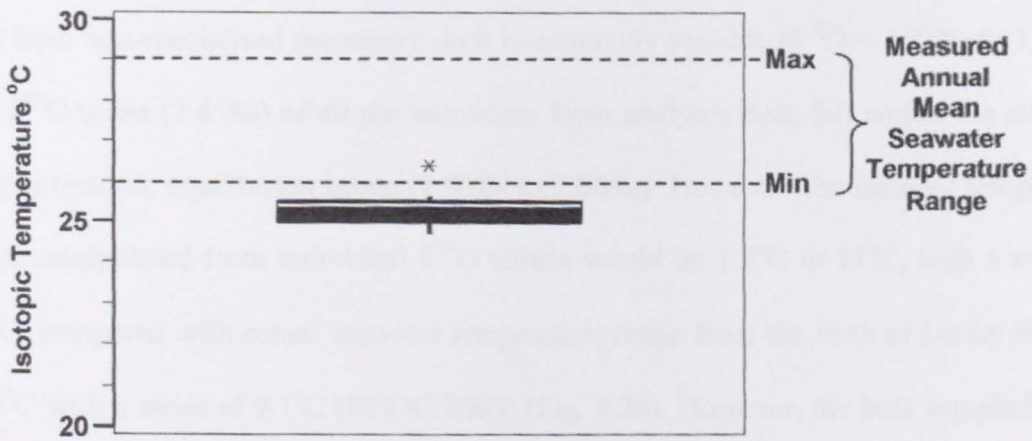

Figure 5.24: Boxplot showing the range of isotopic temperatures extrapolated from $\delta^{18}O$ values of all analyses determined bulk samples of the thecideidine brachiopod *Thecidellina barretti* (Davidson).

Comparison is made with the measured seawater temperature range around Jamaica (JODC 2001).

towards the higher end or above the expected seawater equilibrium range. Dedicated future study of the thecideidine brachiopods will increase understanding of their isotopic relationship with ambient seawater, and may improve their usefulness as environmental indicators.

5.5 The Craniida

The Craniida are the only calcite-precipitating inarticulated brachiopods. Their ultrastructures differ from the Terebratulida in that the secondary shell layer is composed of laminar sheets rather than fibres (Figs. 4.11, 4.12, 4.13 and 4.14). *Novocrania anomala* (Müller) from Scotland shows the same depletion of the primary layer $\delta^{18}O$ and $\delta^{13}C$ relative to the secondary layer as seen in the terebratulids (Fig. 5.25). The majority of the primary layer data lies within the expected seawater equilibrium range, although close to the lower limit. $\delta^{18}O$ values from the raised muscle scars of the secondary layer lie closest to the mean equilibrium value with a wide range of 1.44‰ to 2.48‰. The oxygen isotope data from non-specialised secondary shell is extremely variable ($\delta^{18}O$ = 1.33‰ to 3.99‰). The $\delta^{18}O$ mean (2.45‰) of all the secondary layer analyses does fall within the expected oxygen isotopic equilibrium range (1.00‰ to 2.60‰). However, the isotopic temperature range extrapolated from individual $\delta^{18}O$ values would be 1.7°C to 11°C, with a mean of 6.8°C, compared with actual seawater temperature range from the Firth of Lorne: 6.2°C to 12.3°C with a mean of 9.1°C (BODC 2003) (Fig. 5.26). However, the bulk sampled dorsal valve of a *Novocrania anomala* specimen has a $\delta^{18}O$ range of 1.60‰ to 2.79‰, which produces an isotopic temperature range of 5.7°C to 9.9°C with a mean of 8.7°C; this compares favourably to the measured mean seawater temperature of 9.1°C in the Firth of Lorne. It is therefore possible that bulk sampling of this particular craniid will provide meaningful data. However, the erratic nature of the $\delta^{18}O$ values presented here suggest that the bulk sample results could be coincidental, and it is recommended that this species should be used in environmental studies with caution.

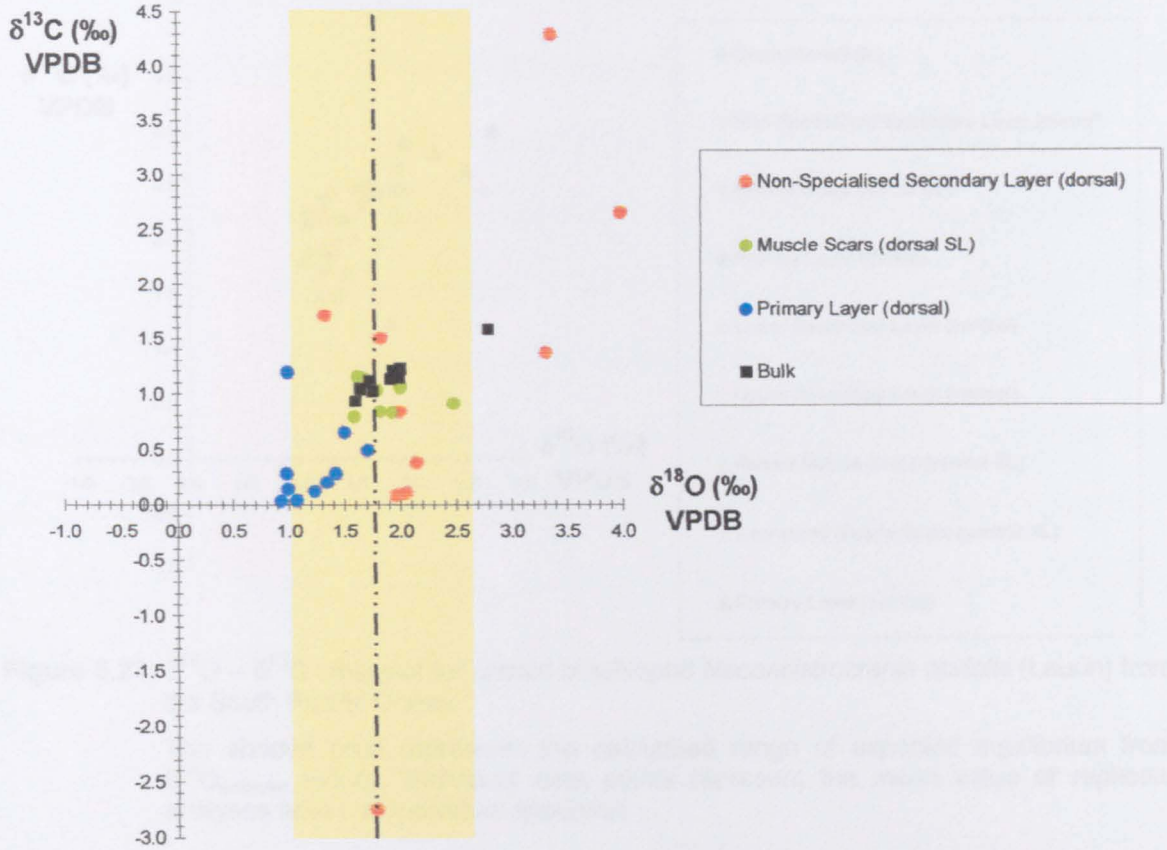

Figure 5.25: $\delta^{18}O$ – $\delta^{13}C$ crossplot for craniid brachiopod *Novocrania anomala* (Müller) from the Firth of Lorne, Scotland.

The shaded area represents the calculated range of expected equilibrium from $\delta^{18}O_{seawater}$ values, dashed line represents the mean $\delta^{18}O_{seawater}$ value. Individual data points represent the mean value of replicate analyses from one individual specimen.

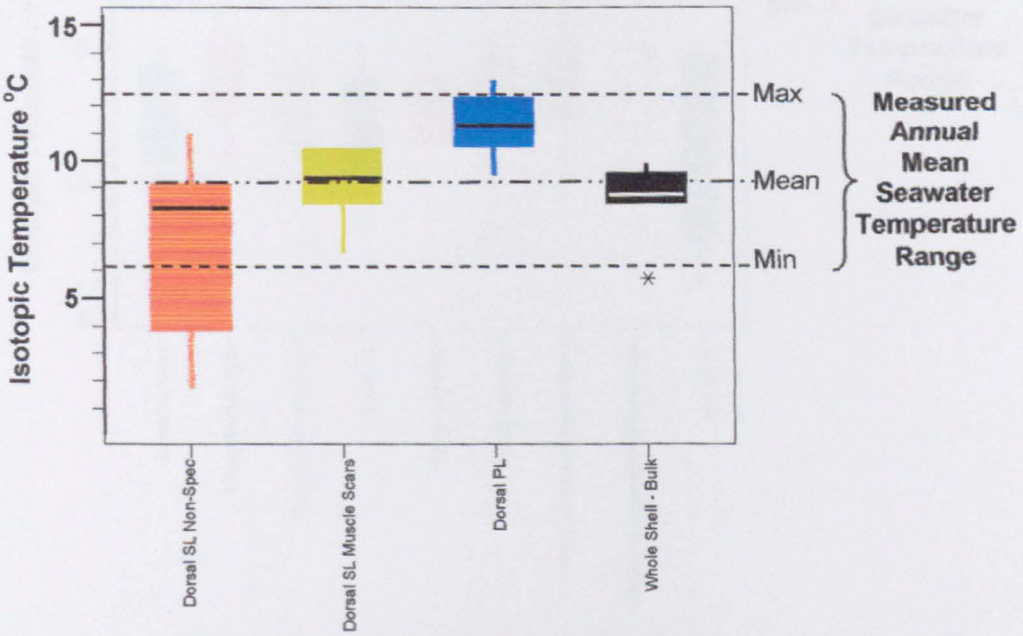

Figure 5.26: Boxplot showing the range of isotopic temperatures extrapolated from $\delta^{18}O$ values of all analyses determined from different regions of the shell of craniid brachiopod *Novocrania anomala* (Müller).

Comparison is made with the measured seawater temperature range from the Firth of Lorne (BODC 2003).

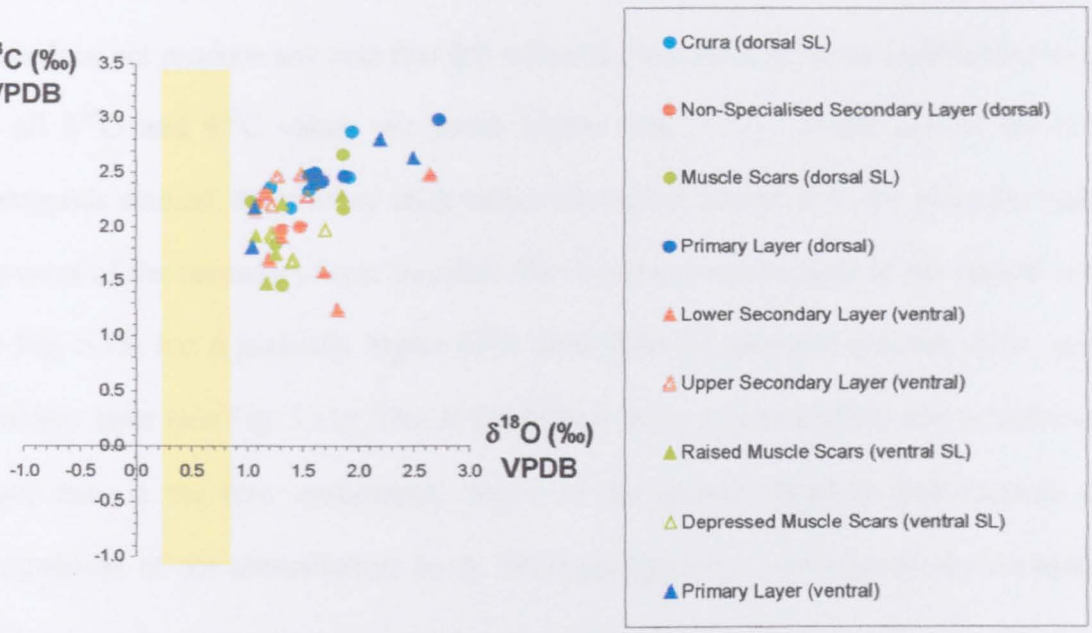

Figure 5.27: $\delta^{18}O$ – $\delta^{13}C$ crossplot for craniid brachiopod *Neoancistrocrania norfolki* (Laurin) from the South Pacific Ocean.

The shaded area represents the calculated range of expected equilibrium from $\delta^{18}O_{seawater}$ values. Individual data points represent the mean value of replicate analyses from one individual specimen.

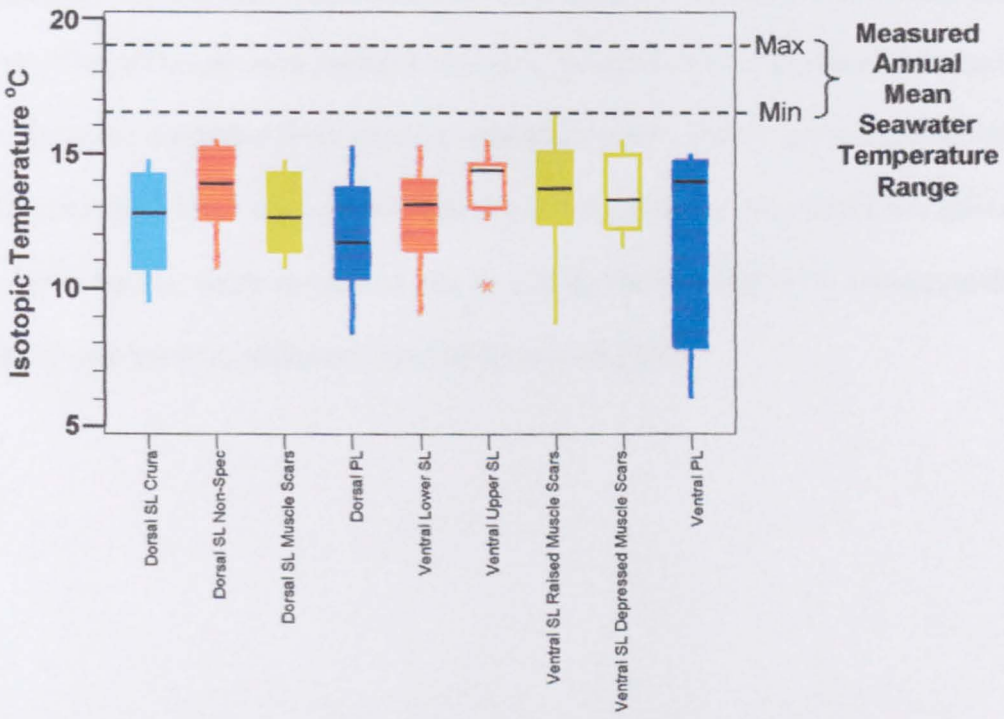

Figure 5.28: Boxplot showing the range of isotopic temperatures extrapolated from $\delta^{18}O$ values of all analyses determined from different regions of the shell of Craniid brachiopod *Neoancistrocrania norfolki* (Laurin).

Comparison is made with the measured seawater temperature range from this area of the South Pacific Ocean (JODC 2001).

A rare brachiopod, *Neoancistrocrania norfolki* (Laurin) from 23°S in the South Pacific Ocean does not produce any data that fall within the expected seawater equilibrium range; and all $\delta^{18}O$ and $\delta^{13}C$ values are much higher (Fig. 5.27). Unlike any of the other brachiopods studied, the primary layer values for both $\delta^{18}O$ and $\delta^{13}C$ are generally higher than most of the secondary layer samples. The lower secondary layer of the ventral valve (see Fig. 5.15) has a generally higher $\delta^{18}O$ value than the younger material of the upper secondary layer (see Fig. 5.15). This is considered to be a kinetic effect due to decreased growth rate in the later ontogenetic stages of the mature organism and supports the interpretation of the ultrastructure by A. Williams (personal communication, see section 4.5).

The oxygen isotope compositions of the Craniida are very variable. Even though *Novocrania anomala* appears to precipitate its shell in isotopic equilibrium, the lack of consistency could confuse any interpretation of data in a palaeoenvironmental investigation. The evidence from this study, that *Neoancistrocrania norfolki* precipitates its shell out of equilibrium with ambient seawater, is compelling. However, the equilibrium parameters were estimated from database material (JODC 2001), so it cannot be ruled out that there may be a local temperature anomaly at the collection site, which has affected this study. Until further work is carried out to clarify the position it is recommended that craniids are not used for palaeoenvironmental reconstruction.

Chapter 6

Carbon stable isotopic composition

of

modern brachiopod shells

6 Carbon stable isotopic composition of modern brachiopod shells

6.1 Introduction

The main inorganic component of the shell material of modern calcitic brachiopods is calcium carbonate ($CaCO_3$). Calcium carbonate amounts to between 94.6 to 98.6 percent in the articulated species (i.e. Terebratulida, Rhynchonellida and Thecideidina), and 87.8 to 88.6 percent in the inarticulated Craniida (Jope 1965). The inorganic carbon component of the shell is derived from bicarbonate ions (HCO_3^-), dissolved in ambient seawater (Hoefs 1997; Buening 2001). Global secular changes in the $^{13}C/^{12}C$ ratio of dissolved HCO_3^- are influenced by the level of volcanic degassing and the relative burial rates of organic carbon and carbonate carbon (Berner 1989; Hoefs 1997; Kump & Arthur 1999; Kump *et al.* 1999; Buening 2001). The effect of periods of high organic carbon burial is illustrated by for example, the positive ^{13}C excursion associated with the lower Hirnantian glaciation and falling sea levels at the end of the Ordovician. The lighter ^{12}C isotope was preferentially stored in ice and sediments, therefore the ^{13}C content of dissolved HCO_3^- is enriched causing the oceans to become isotopically heavier (Long 1993; Brenchley *et al.* 1995). Further evidence to show the true global nature of this event was provided by Marshall *et al.* (1997). A more recent factor influencing the carbon isotopic composition of the oceans is the addition of ^{12}C-rich CO_2, as a result of industrial anthropogenic activity. Observations imply that since pre-industrial times the total dissolved inorganic carbon (ΣCO_2) in the world's oceans has increased causing a 0.5‰ depletion in the $\delta^{13}C$ value of ΣCO_2(Kroopnick 1985).

In addition to long term fluctuations, the $\delta^{13}C$ values of HCO_3^- can be affected by seasonal or even daily cycles at a local level (Buening 2001). Effects are due to the

influence of the marine biota inhabiting an environment. Such communities can alter the local $^{13}C/^{12}C$ ratio through photosynthesis and respiration. High rates of photosynthesis will utilise dissolved ^{12}C preferentially thereby increasing the relative proportion of ^{13}C in the common carbon pool available for carbonate precipitating organisms (Swart 1983; M^{c}Connaughey 1989a; 1989b; Stanley & Swart 1995; M^{c}Connaughey *et al.* 1997; Reynaud-Vaganay *et al.* 2001). Respiration rates, due to metabolic activity may produce similar kinetic isotope effect, or vital effects in biogenic carbonates. Higher levels of respiration would return relatively more ^{12}C to the common carbon pool (Swart 1983; M^{c}Connaughey 1989a; 1989b; Wefer & Berger 1991; Hoefs 1997; M^{c}Connaughey *et al.* 1997; Buening 2001).

The factors affecting the composition of carbon isotopes in the dissolved HCO_3^- reservoir in marine habitats are very complex. It is clear that there are not only long term global influences but also short-term localised effects, which are determined both by the environment and by the population dynamics of individual marine communities. Such short term fluctuations could confuse environmental interpretations of $^{13}C/^{12}C$ values from biological carbonates. The situation is further complicated if carbon is not incorporated in such material uniformly and in isotopic equilibrium with ambient seawater. Very little research into $^{13}C/^{12}C$ ratios in brachiopod shells has been carried out to address this problem. Bates and Brand (1991) reported carbon isotope determinations from some fossil brachiopod shells were in isotopic equilibrium with ambient seawater. Variable $\delta^{13}C$ values, possibly due to metabolic 'vital' effects or ontogenetic changes, have been observed in modern brachiopods (Carpenter & Lohmann 1995; Buening & Spero 1996) and fossil brachiopods (Buening *et al.* 1998). The issue of uniform precipitation of shell material in carbon isotopic equilibrium with seawater remains unclear.

To investigate the carbon stable isotope composition of modern brachiopod shells a variety of different species were collected and prepared for $^{13}C/^{12}C$ analysis. Full details of

species and locations are given in Chapter 2, and the analytical procedures are provided in chapter 3 and summarised in Section 5.1.

6.2 Patterns of carbon isotopic distribution in modern brachiopod shells

6.2.1 The Terebratulida and Rhynchonellida

The results for $\delta^{18}O$ presented in chapter 5 show that the $\delta^{13}C$ and $\delta^{18}O$ values from the primary shell layer of all the brachiopods are positively correlated. With the exception of the rhynchonellid *Notosaria nigricans* (Sowerby) (Fig. 5.21) both $\delta^{13}C$ and $\delta^{18}O$ values are significantly depleted relative to secondary layer values. However, the $\delta^{13}C$ values from the secondary layer vary over a wider range than $\delta^{18}O$ and the two isotope ratios show little correlation. The stable carbon isotope composition is far more variable between different regions of the secondary layer than oxygen isotope composition.

The pattern of $\delta^{13}C$ in the secondary shell layer of *Calloria inconspicua* (Sowerby) from New Zealand (Fig. 6.1 & 6.2), displays a distinct groups of values for the different areas sampled in each valve. In the dorsal valve (Fig. 6.1) secondary layer $\delta^{13}C$ values range from a high in the non-specialised secondary layer of 2.18‰ to a low of 0.48‰ from cardinal process material. Although this is a wide range (1.70‰) the non-specialised secondary layer (mean $\delta^{13}C$ = 1.92‰) and cardinal process (mean $\delta^{13}C$ =0.92‰), these values form well defined groups (Fig. 6.1). Between the clusters of values from these two areas lie two further well defined groups of values, the loop material (mean $\delta^{13}C$ = 1.73‰) and muscle scar material with a mean $\delta^{13}C$ value of 1.29‰. The pattern of $\delta^{13}C$ values from the dorsal valve of *Calloria inconspicua* suggests that specialised areas of the secondary layer are depleted relative to the non-specialised material. The distinct grouping of values indicates that the level of ^{13}C depletion fluctuates in different areas, with the posterior-most samples (i.e. from the cardinal process) producing the lowest values.

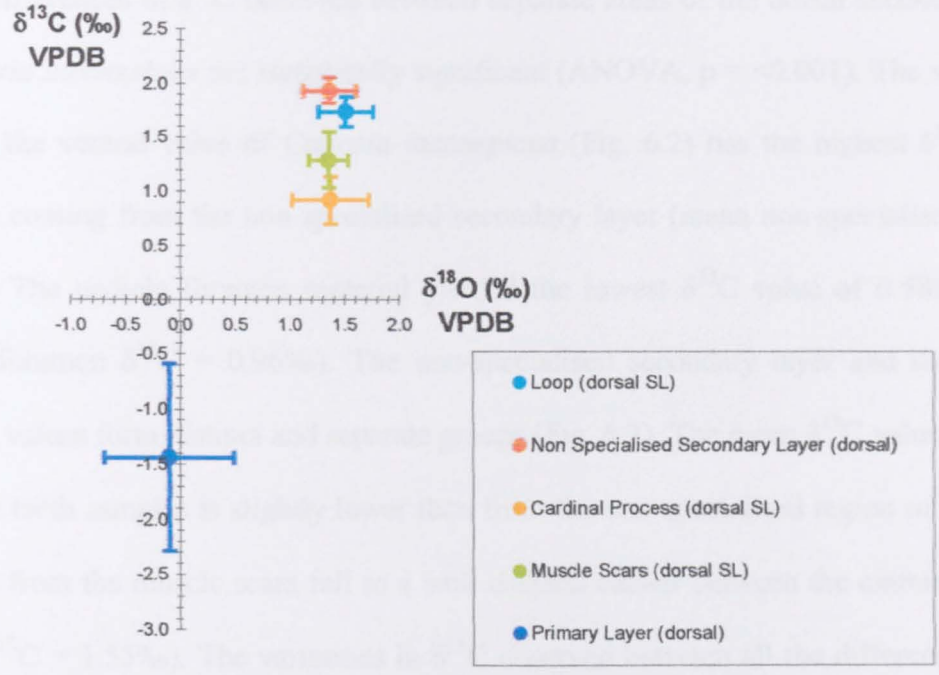

Figure 6.1: $\delta^{18}O$ – $\delta^{13}C$ crossplot for the dorsal valve of *Calloria inconspicua* (Sowerby) from Otago Shelf, New Zealand.

Data points represent mean values, error bars indicate 1σ.

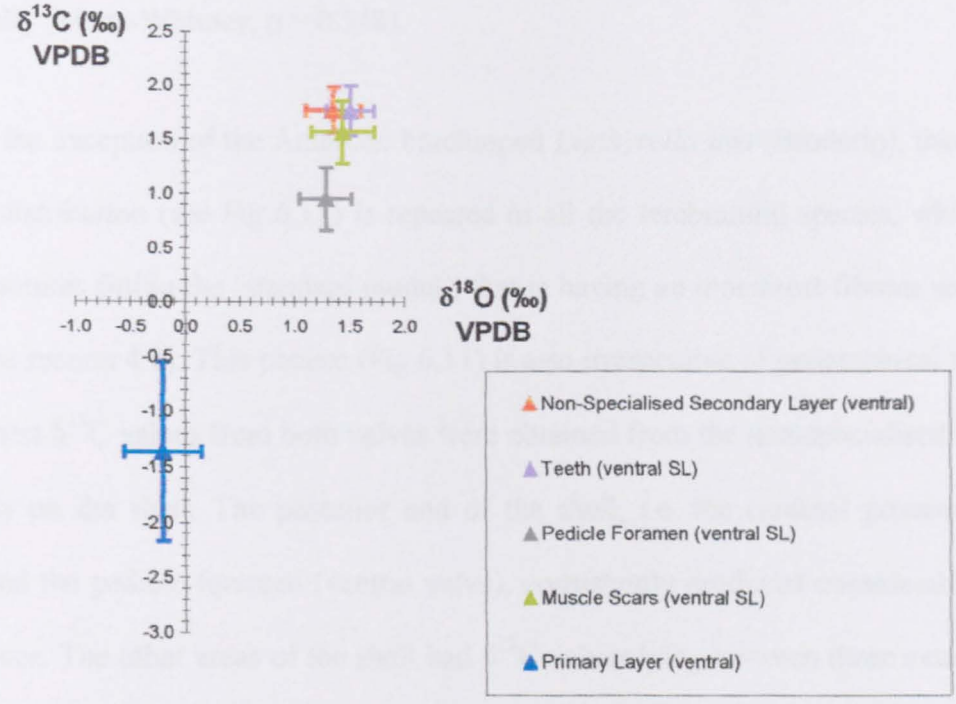

Figure 6.2: $\delta^{18}O$ – $\delta^{13}C$ crossplot for the ventral valve of *Calloria inconspicua* (Sowerby) from Otago Shelf, New Zealand.

Data points represent mean values, error bars indicate 1σ.

The differences in $\delta^{13}C$ observed between separate areas of the dorsal secondary layer in *Calloria inconspicua* are statistically significant (ANOVA, p = <0.001). The secondary layer of the ventral valve of *Calloria inconspicua* (Fig. 6.2) has the highest $\delta^{13}C$ value (2.25‰) coming from the non-specialised secondary layer (mean non-specialised $\delta^{13}C$ = 1.77‰). The pedicle foramen material yielded the lowest $\delta^{13}C$ value of 0.58‰ (mean pedicle foramen $\delta^{13}C$ = 0.96‰). The non-specialised secondary layer and the pedicle foramen values form distinct and separate groups (Fig. 6.2). The mean $\delta^{13}C$ value (1.74‰) from the teeth samples is slightly lower than from the non-specialised region of the shell. Samples from the muscle scars fall in a well defined cluster between the extreme groups (mean $\delta^{13}C$ = 1.55‰). The variations in $\delta^{13}C$ observed between all the different areas of the ventral secondary layer in *Calloria inconspicua* are statistically significant (ANOVA, p = <0.001). However, because the $\delta^{13}C$ values of the non-specialised and teeth groups are in close proximity, a further statistical test was calculated that did not separate them statistically (Mann-Whitney, p = 0.548).

With the exception of the Antarctic brachiopod *Liothyrella uva* (Broderip), this pattern of $\delta^{13}C$ distribution (see Fig 6.11) is repeated in all the terebratulid species, which have shell structures fitting the 'standard model', that is having an innermost fibrous secondary layer (see section 4.2). This pattern (Fig 6.11) is also irrespective of geographical location. The highest $\delta^{13}C$ values from both valves were obtained from the non-specialised material anteriorly on the shell. The posterior end of the shell, i.e. the cardinal process (dorsal valve) and the pedicle foramen (ventral valve), consistently produced considerably lower $\delta^{13}C$ values. The other areas of the shell had $\delta^{13}C$ values lying between these extremes. In *Terebratulina retusa* (Linnaeus) from Scotland (Figs 6.3 & 6.4), *Laqueus rubellus* (Sowerby) from Otsuchi Bay, Japan (Figs 6.5 & 6.6), *Neothyris lenticularis* (Deshayes) from New Zealand (Figs 6.7 & 6.8) and *Terebratella sanguinea* (Leach) from New Zealand (Figs 6.9 & 6.10), the order of $\delta^{13}C$ depletion in different areas of the secondary

shell is the same as described above for *Calloria inconspicua*. Dorsal valve $\delta^{13}C$ values decrease from the non-specialised material at the anterior through the loop, muscle scars to the cardinal process. In the ventral valve the decreasing order of $\delta^{13}C$ values is: non-specialised, teeth, muscle scars, pedicle foramen.

A minor variation to this trend was observed in the dorsal valve of terebratulid *Terebratalia transversa* (Sowerby) from Friday Harbor, USA (Fig. 6.12). In this species the loop material was highly variable producing $\delta^{13}C$ values from –2.11‰ to 1.70‰, a range of 3.81‰. The mean $\delta^{13}C$ value from the loop material of –0.34‰ was isotopically lighter than the muscle scar samples (mean $\delta^{13}C$ = 0.01‰). Variations from the pattern in Figure 6.11 were also noted in the ventral valves of terebratulids *Terebratalia transversa* from Friday Harbor, USA (Fig. 6.13) and *Laqueus rubellus* from Sagami Bay, Japan (Fig.6.15). In both these species secondary shell material from the teeth yielded higher $\delta^{13}C$ than the ventral muscle scars. However, the dorsal valve of *Laqueus rubellus* from Sagami Bay (Fig. 6.14) follows the general trend (Fig. 6.11).

The terebratulid *Liothyrella neozelanica* (Thomson) (Figs 6.16 & 6.17) and rhynchonellid *Notosaria nigricans* (Fig. 6.18 & 6.19) have different characteristics, but follow the $\delta^{13}C$ general trend (Fig. 6.11). *Liothyrella neozelanica* is from the same order (Terebratulida) as the species previously discussed. However, the shell differs in structure. The innermost shell layer is a prismatic tertiary succession (see section 4.3). The samples for *Liothyrella neozelanica* were extracted from this material as opposed to the fibrous secondary material (see section 4.2) extracted from the other species. *Notosaria nigricans* is notable because it is from a different order, Rhynchonellida, although its shell structure is similar to most terebratulids (see 4.2).

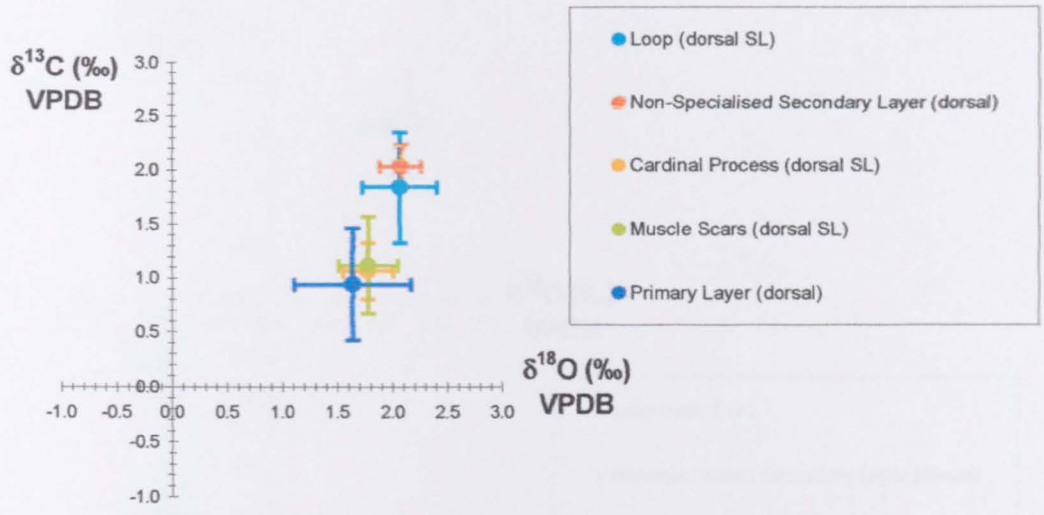

Figure 6.3: $\delta^{18}O$ – $\delta^{13}C$ crossplot for the dorsal valve of the terebratulid *Terebratulina retusa* (Linnaeus) from the Firth of Lorne, Scotland.

Data points represent mean values, error bars indicate 1σ.

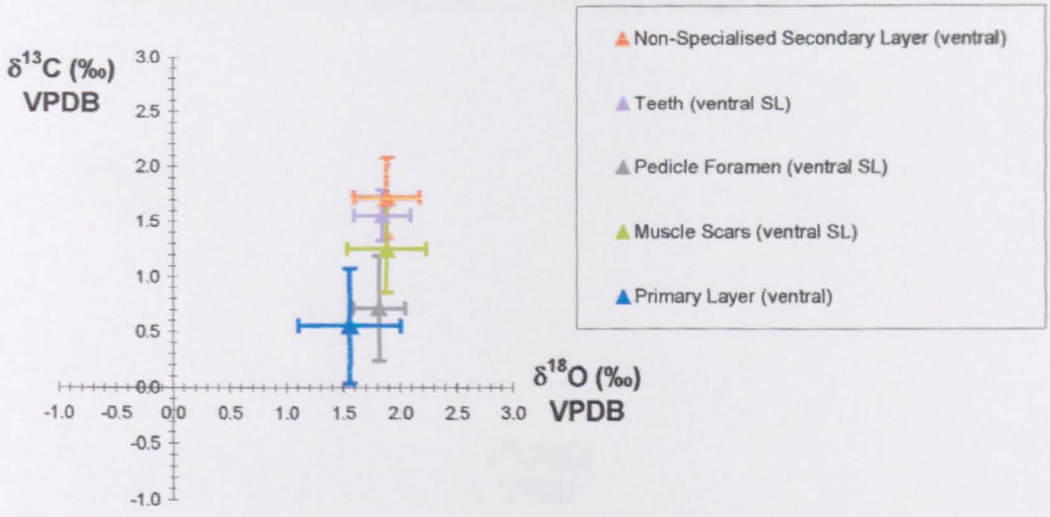

Figure 6.4: $\delta^{18}O$ – $\delta^{13}C$ crossplot for the ventral valve of the terebratulid *Terebratulina retusa* (Linnaeus) from the Firth of Lorne, Scotland.

Data points represent mean values, error bars indicate 1σ.

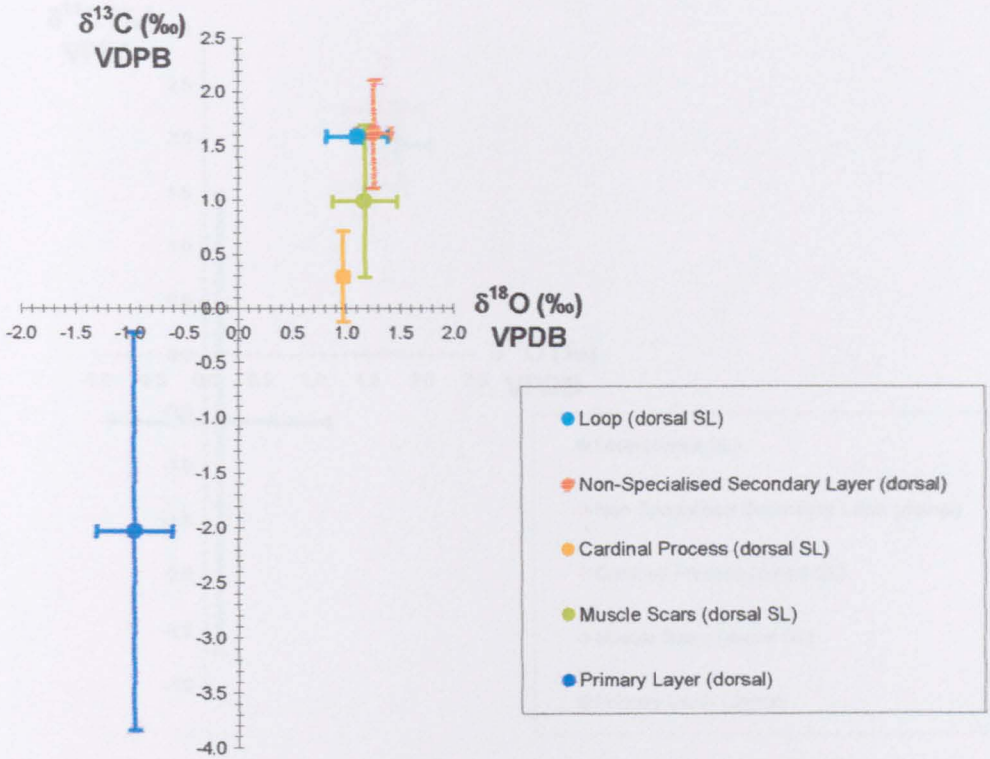

Figure 6.5: $\delta^{18}O$ – $\delta^{13}C$ crossplot for the dorsal valve of the terebratulid *Laqueus rubellus* (Sowerby) from Otsuchi Bay, Japan.

Data points represent mean values, error bars indicate 1σ.

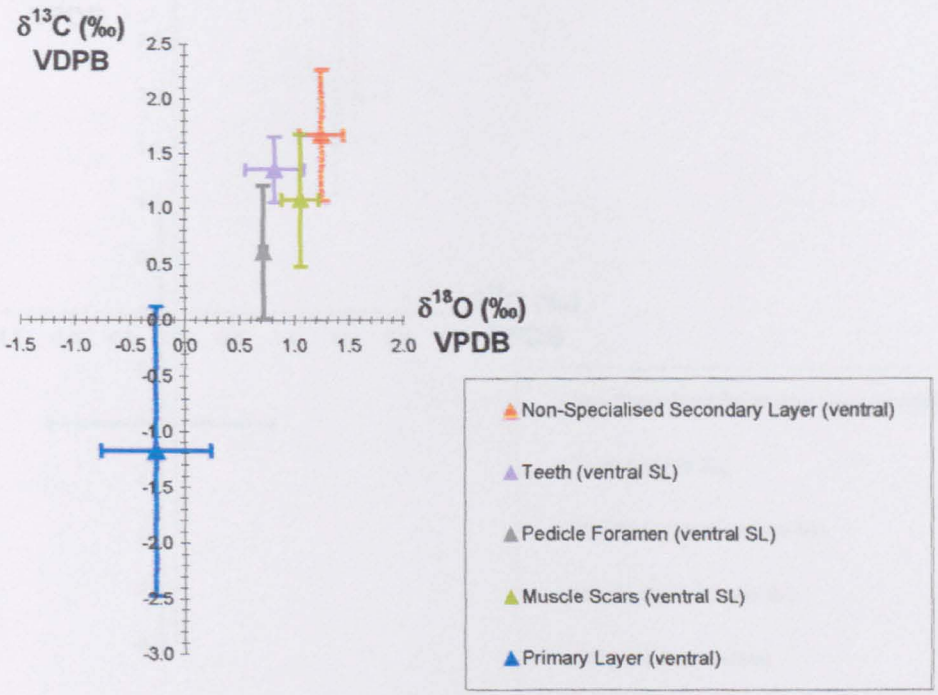

Figure 6.6: $\delta^{18}O$ – $\delta^{13}C$ crossplot for the ventral valve of the terebratulid *Laqueus rubellus* (Sowerby) from Otsuchi Bay, Japan.

Data points represent mean values, error bars indicate 1σ.

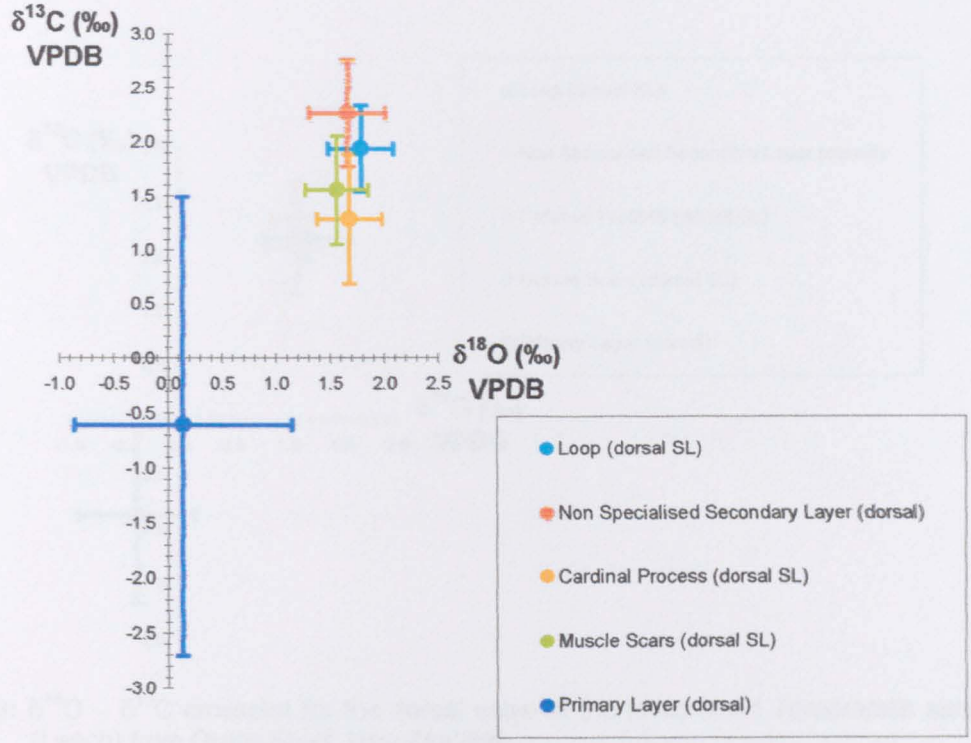

Figure 6.7: $\delta^{18}O$ – $\delta^{13}C$ crossplot for the dorsal valve of the terebratulid *Neothyris lenticularis* (Deshayes) from Otago Shelf, New Zealand.

Data points represent mean values, error bars indicate 1σ.

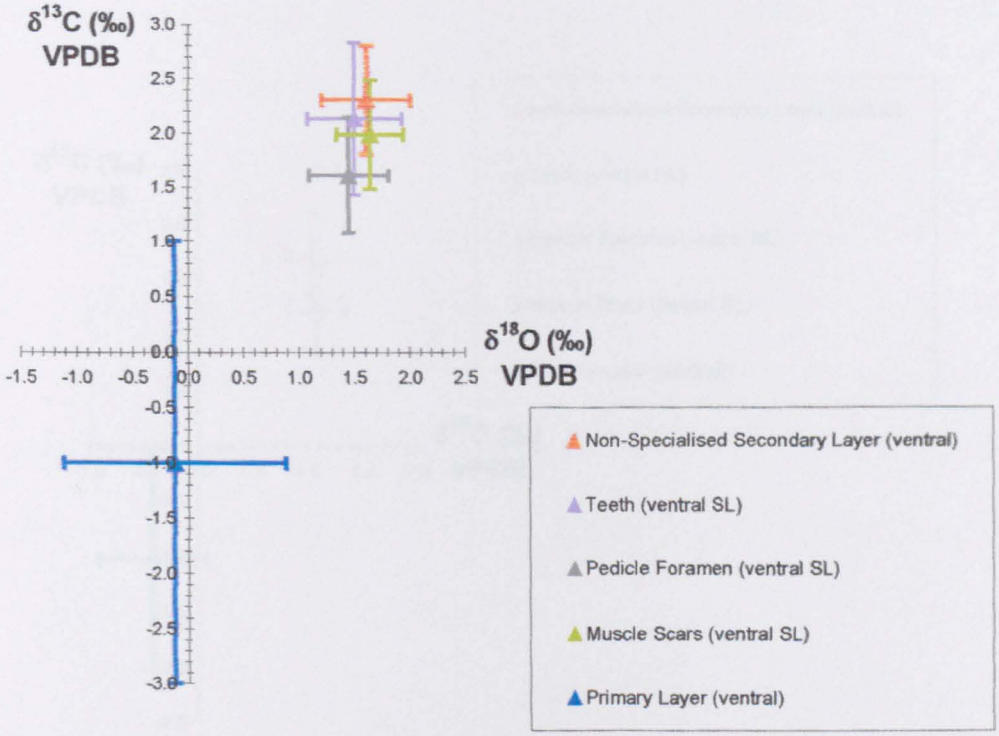

Figure 6.8: $\delta^{18}O$ – $\delta^{13}C$ crossplot for the ventral valve of the terebratulid *Neothyris lenticularis* (Deshayes) from Otago Shelf, New Zealand.

Data points represent mean values, error bars indicate 1σ.

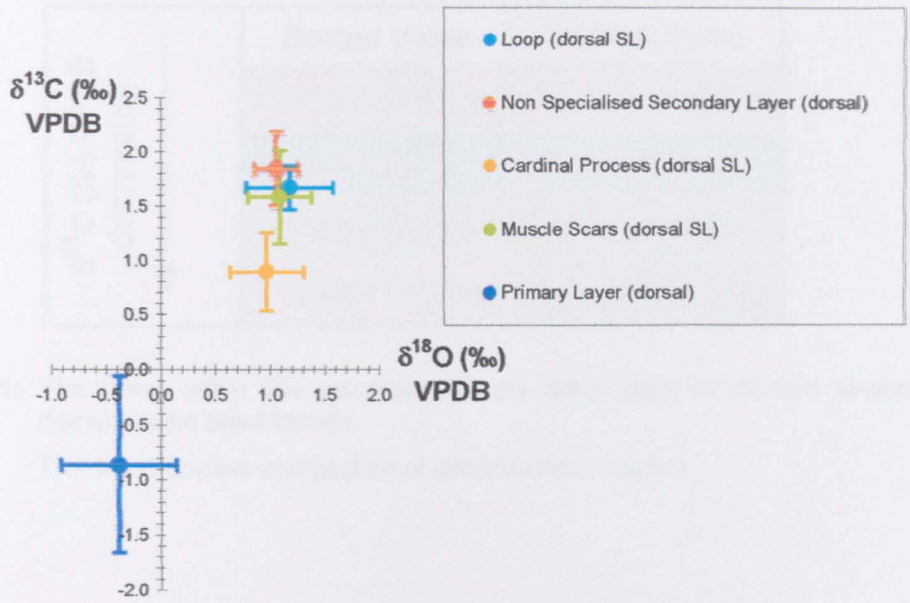

Figure 6.9: $\delta^{18}O$ – $\delta^{13}C$ crossplot for the dorsal valve of the terebratulid *Terebratella sanguinea* (Leach) from Otago Shelf, New Zealand.

Data points represent mean values, error bars indicate 1σ.

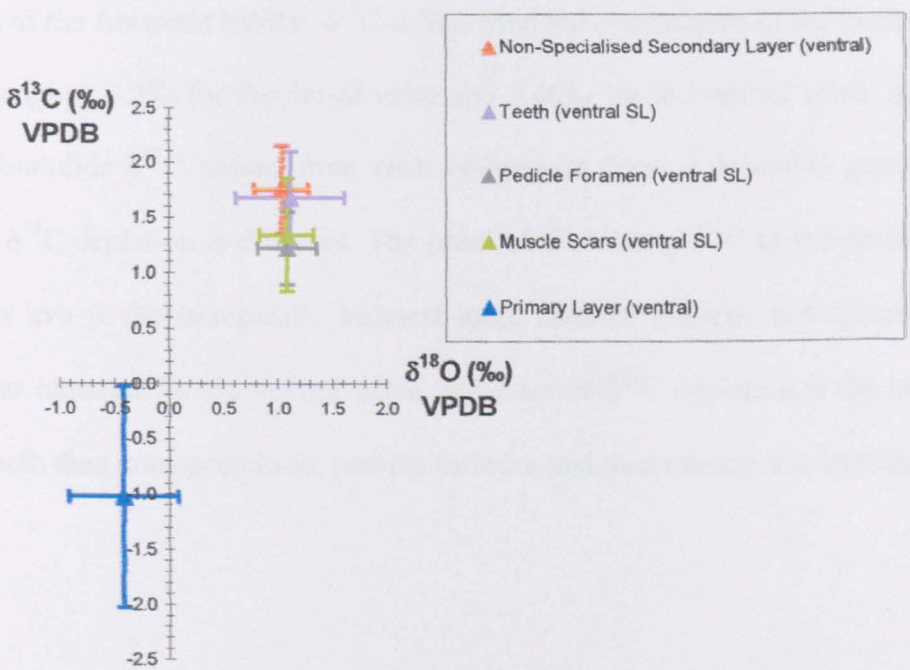

Figure 6.10: $\delta^{18}O$ – $\delta^{13}C$ crossplot for the ventral valve of the terebratulid *Terebratella sanguinea* (Leach) from Otago Shelf, New Zealand.

Data points represent mean values, error bars indicate 1σ.

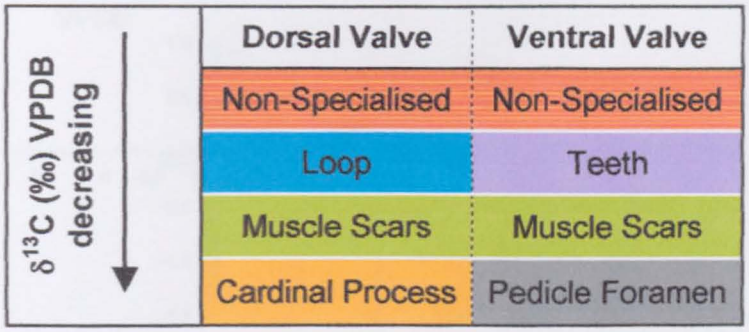

Figure 6.11: The trend within the secondary/tertiary shell layer of modern terebratulid and rhynchonellid brachiopods.

This trend applies irrespective of geographical location.

For *Liothyrella uva* from Signy Island, Antarctica (Figs 6.20 & 6.21), as with $\delta^{18}O$ (see 5.2), $\delta^{13}C$ values do not conform to the trends seen in the other terebratulids. The expected shell structure for *Liothyrella uva* would be similar to *Liothyrella neozelanica* (see 4.3). However, SEM examination of the *Liothyrella uva* specimens employed in this study show that the tertiary succession is incomplete. This could be a response to the extreme conditions of the Antarctic habitat. $\delta^{13}C$ values from the components of the innermost layer are wide ranging, 3.5‰ for the dorsal valve and 3.46‰ for the ventral valve. As with the other terebratulids $\delta^{13}C$ values from each component form a definable group, but the pattern of $\delta^{13}C$ depletion is different. The order of decreasing $\delta^{13}C$ in the dorsal valve of *Liothyrella uva* is the isotopically heaviest loop, cardinal process, non-specialised then muscle scar material. In the ventral valve the order of $\delta^{13}C$ depletion is the isotopically heaviest teeth then non-specialised, pedicle foramen and then muscle scar material.

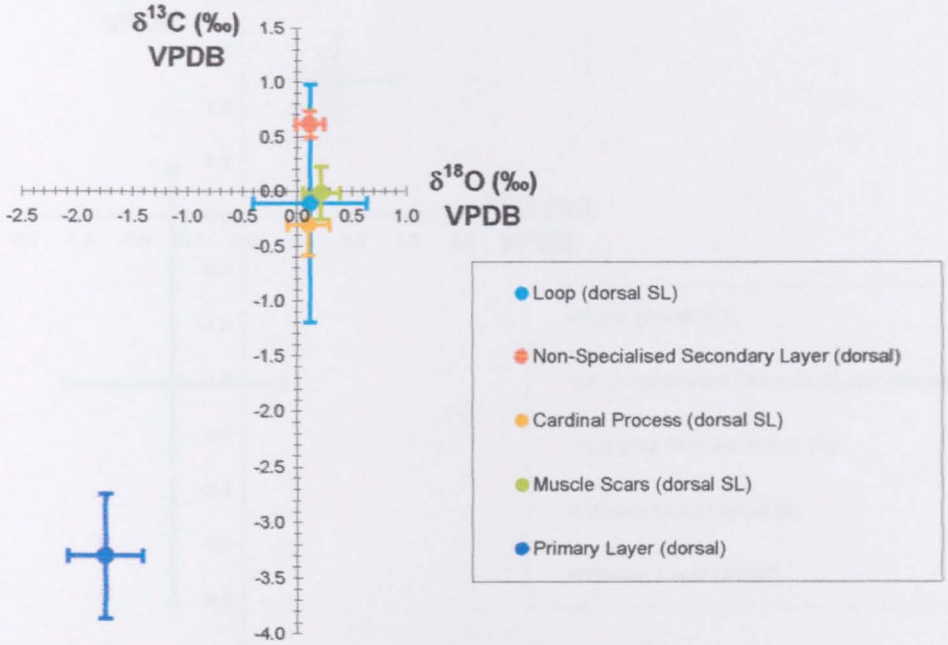

Figure 6.12: $\delta^{18}O$ – $\delta^{13}C$ crossplot for the dorsal valve of the terebratulid *Terebratalia transversa* (Sowerby) from near Friday Harbor, Washington, USA.

Data points represent mean values, error bars indicate 1σ.

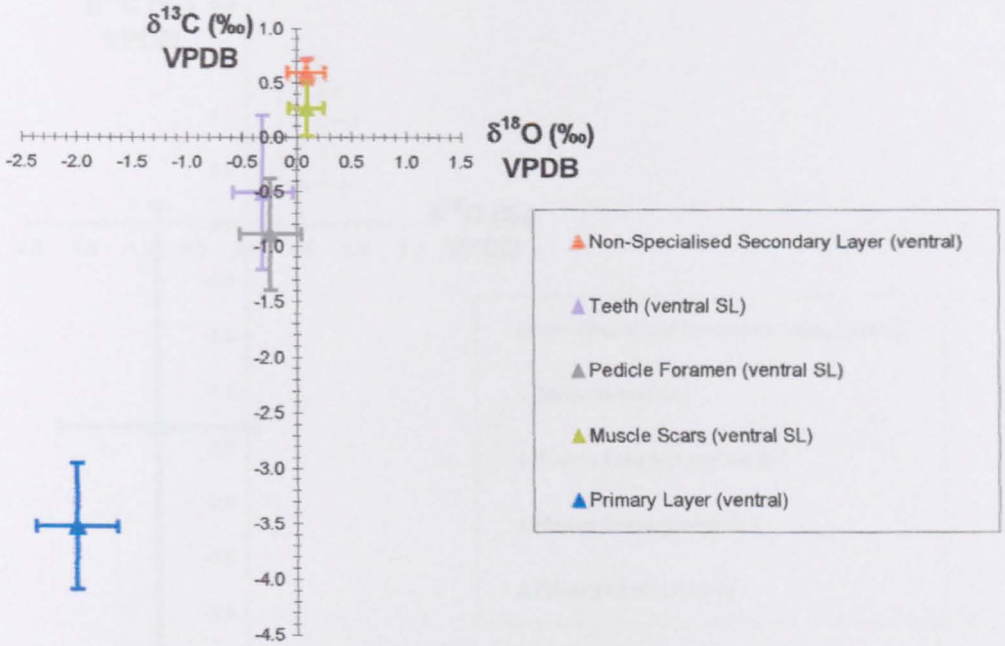

Figure 6.13: $\delta^{18}O$ – $\delta^{13}C$ crossplot for the ventral valve of the terebratulid *Terebratalia transversa* (Sowerby) from near Friday Harbor, Washington, USA.

Data points represent mean values, error bars indicate 1σ.

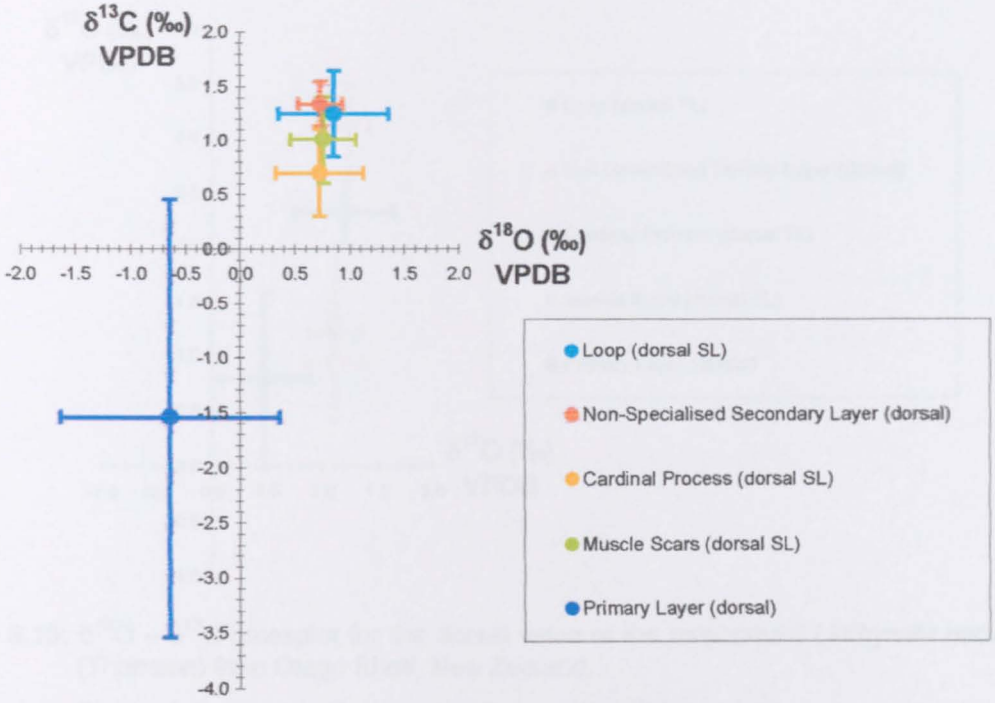

Figure 6.14: $\delta^{18}O$ – $\delta^{13}C$ crossplot for the dorsal valve of terebratulid *Laqueus rubellus* (Sowerby) from Sagami Bay, Japan.

Data points represent mean values, error bars indicate 1σ.

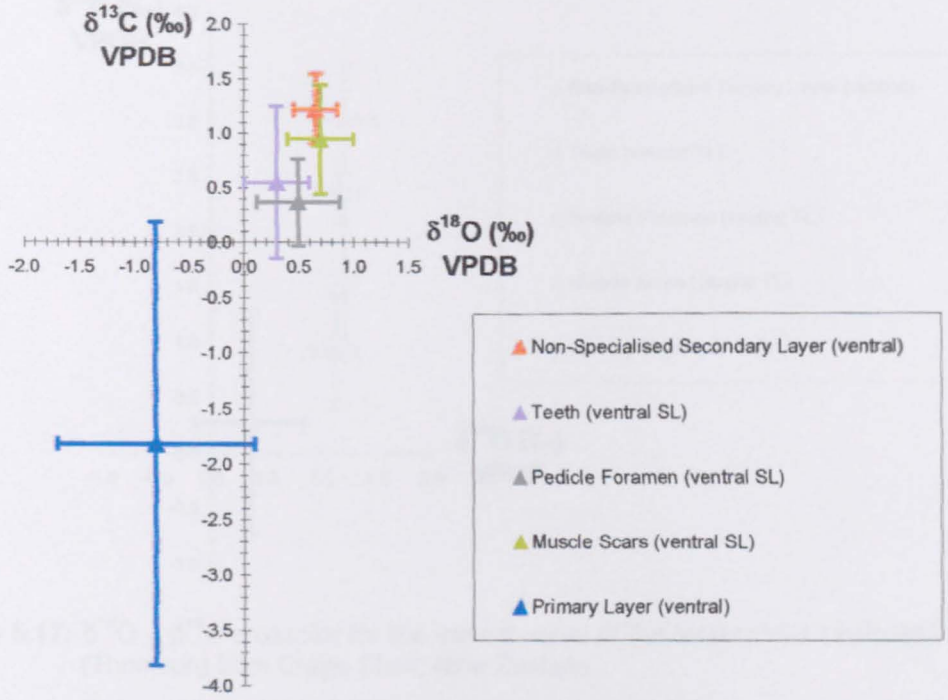

Figure 6.15: $\delta^{18}O$ – $\delta^{13}C$ crossplot for the ventral valve of the terebratulid *Laqueus rubellus* (Sowerby) from Sagami Bay, Japan.

Data points represent mean values, error bars indicate 1σ.

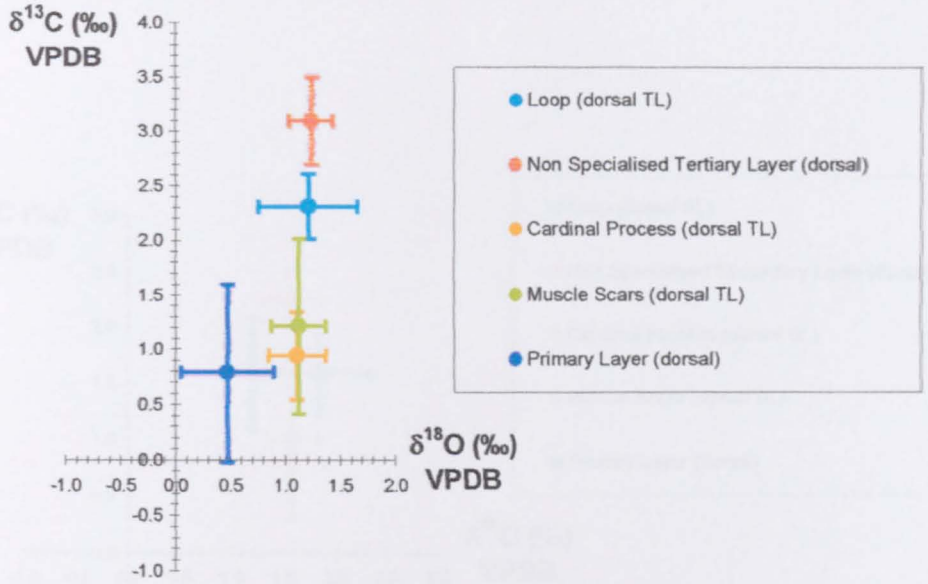

Figure 6.16: $\delta^{18}O$ – $\delta^{13}C$ crossplot for the dorsal valve of the terebratulid *Liothyrella neozelanica* (Thomson) from Otago Shelf, New Zealand.

Data points represent mean values, error bars indicate 1σ.

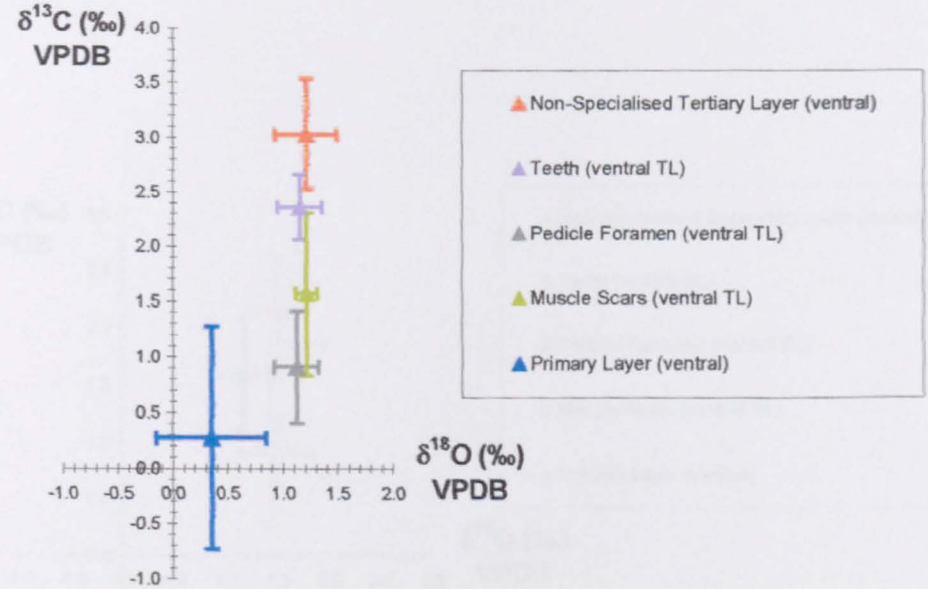

Figure 6.17: $\delta^{18}O$ – $\delta^{13}C$ crossplot for the ventral valve of the terebratulid *Liothyrella neozelanica* (Thomson) from Otago Shelf, New Zealand.

Data points represent mean values, error bars indicate 1σ.

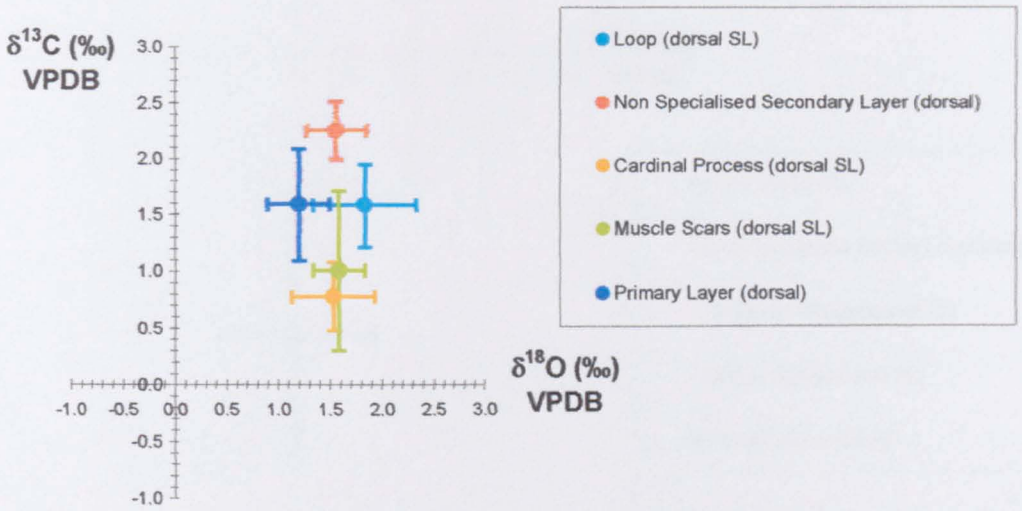

Figure 6.18: $\delta^{18}O$ – $\delta^{13}C$ crossplot for the dorsal valve of the rhynchonellid *Notosaria nigricans* (Sowerby) from Otago Shelf, New Zealand.

Data points represent mean values, error bars indicate 1σ.

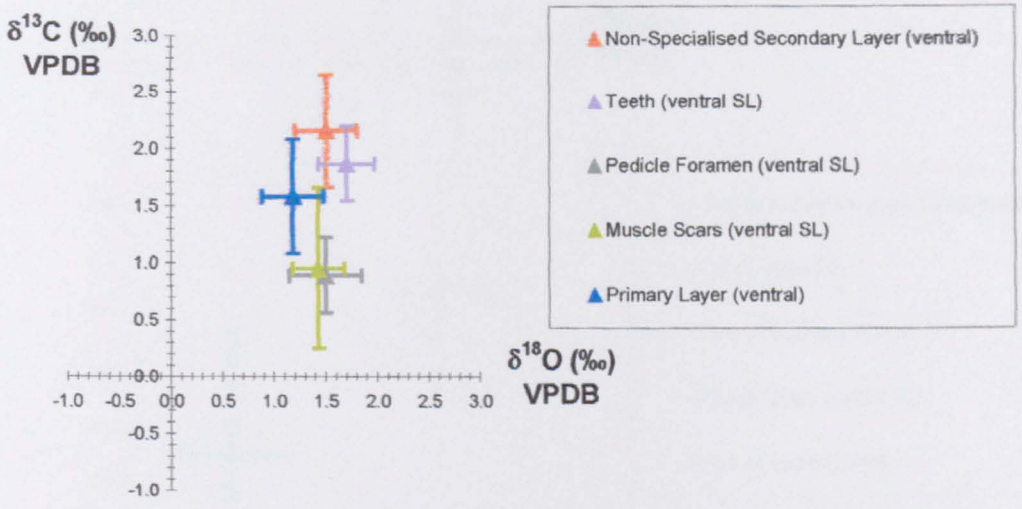

Figure 6.19: $\delta^{18}O$ – $\delta^{13}C$ crossplot for the dorsal valve of the rhynchonellid *Notosaria nigricans* (Sowerby) from Otago Shelf, New Zealand.

Data points represent mean values, error bars indicate 1σ.

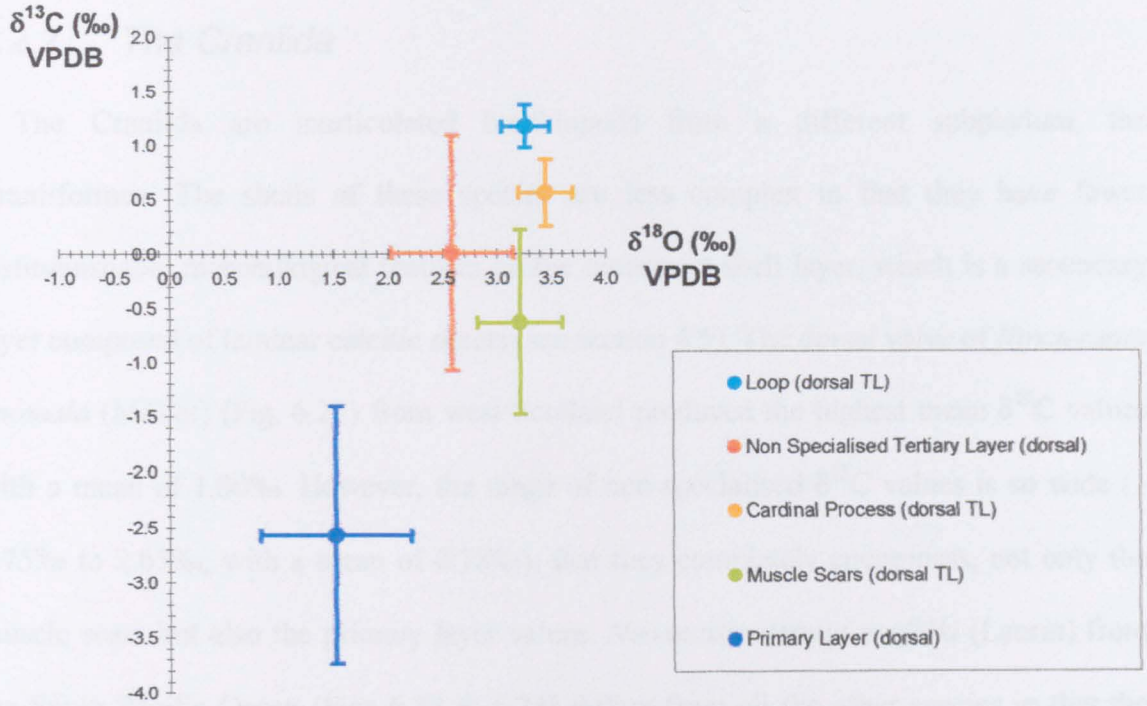

Figure 6.20: $\delta^{18}O - \delta^{13}C$ crossplot for the dorsal valve of the terebratulid *Liothyrella uva* (Broderip) from Signy Island, Antarctica.

Data points represent mean values, error bars indicate 1σ.

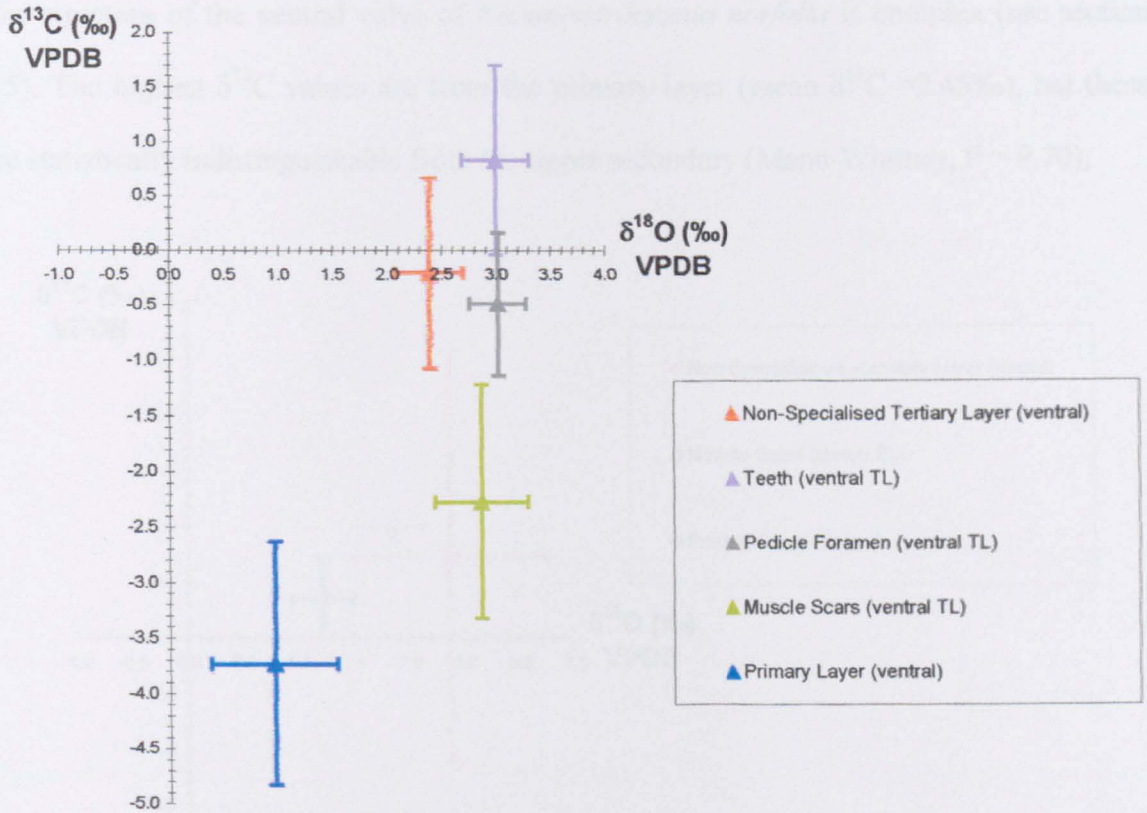

Figure 6.21: $\delta^{18}O - \delta^{13}C$ crossplot for the ventral valve of the terebratulid *Liothyrella uva* (Broderip) from Signy Island, Antarctica.

Data points represent mean values, error bars indicate 1σ.

6.2.2 *The Craniida*

The Craniida are inarticulated brachiopods from a different subphylum, the Craniiformea. The shells of these species are less complex in that they have fewer distinguishable morphological features on the innermost shell layer, which is a secondary layer composed of laminar calcitic sheets (see section 4.5). The dorsal valve of *Novocrania anomala* (Müller) (Fig. 6.22) from west Scotland produced the highest mean $\delta^{13}C$ values with a mean of 1.00‰. However, the range of non-specialised $\delta^{13}C$ values is so wide (–2.75‰ to 2.65‰, with a mean of 0.78‰), that they completely encompass, not only the muscle scars but also the primary layer values. *Neoancistrocrania norfolki* (Laurin) from the South Pacific Ocean (Figs 6.23 & 6.24) differs from all the other species in that the highest $\delta^{13}C$ values are found in the primary layer of both dorsal and ventral valves. In the secondary layer of the dorsal valve the crura, a simple form of loop, yielded the highest mean $\delta^{13}C$ value with the non-specialised material and muscle scars depleted respectively. The structure of the ventral valve of *Neoancistrocrania norfolki* is complex (see section 4.5). The highest $\delta^{13}C$ values are from the primary layer (mean $\delta^{13}C$ =2.45‰), but these are statistically indistinguishable from the upper secondary (Mann-Whitney, P = 9.70),

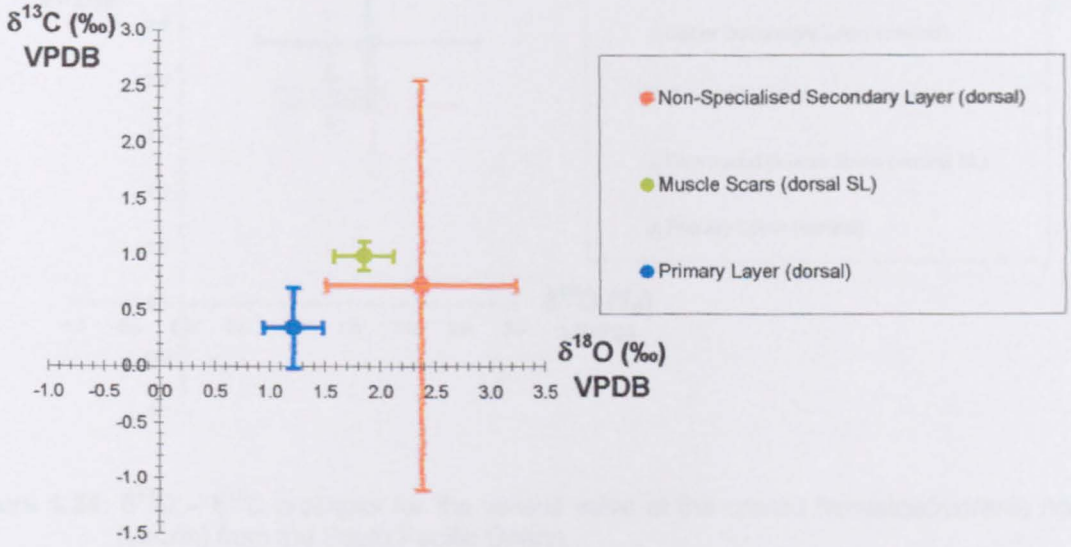

Figure 6.22: $\delta^{18}O - \delta^{13}C$ crossplot for the dorsal valve of the craniid *Novocrania anomala* (Müller) from the South Pacific Ocean.

Data points represent mean values, error bars indicate 1σ.

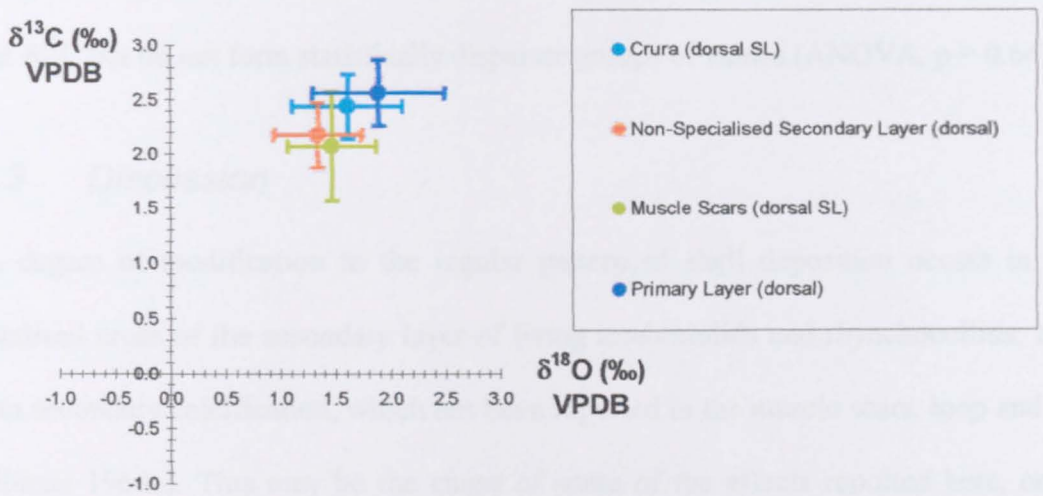

Figure 6.23: $\delta^{18}O - \delta^{13}C$ crossplot for the dorsal valve of the craniid *Neoancistrocrania norfolki* (Laurin) from the South Pacific Ocean.

Data points represent mean values, error bars indicate 1σ.

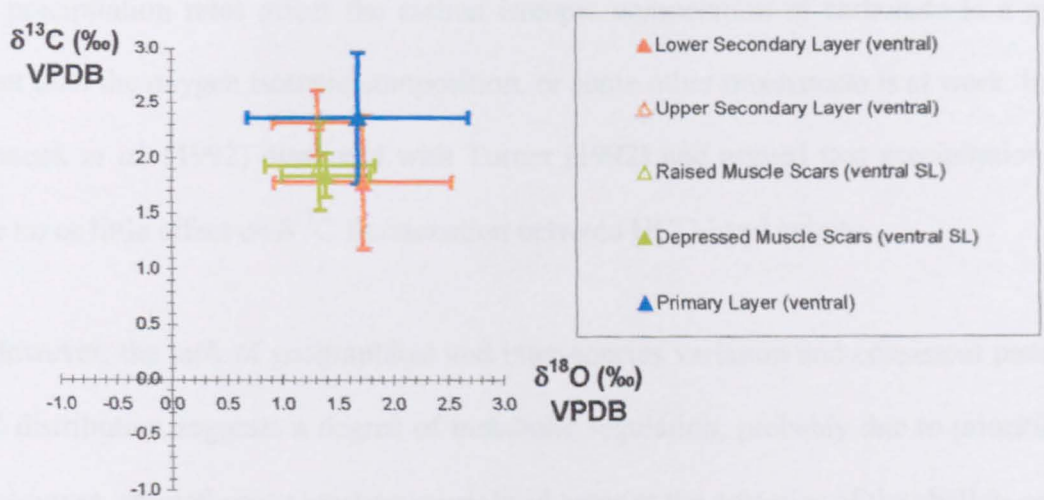

Figure 6.24: $\delta^{18}O - \delta^{13}C$ crossplot for the ventral valve of the craniid *Neoancistrocrania norfolki* (Laurin) from the South Pacific Ocean.

Data points represent mean values, error bars indicate 1σ.

which lies immediately below the primary layer (mean = 2.30‰). Isotopically lighter are the lower secondary layer, (mean $\delta^{13}C$ = 1.73‰), raised muscle scars (mean $\delta^{13}C$ = 1.89‰) and depressed muscle scars (mean = $\delta^{13}C$ 1.73‰), each of these categories have lower $\delta^{13}C$ but do not form statistically disparate groups of values (ANOVA, $p = 0.64$).

6.2.3 *Discussion*

A degree of modification to the regular pattern of shell deposition occurs in some specialised areas of the secondary layer of living terebratulids and rhynchonellids; this is due to secondary calcification, which has been reported in the muscle scars, loop and teeth (Williams 1968a). This may be the cause of some of the effects reported here, or they could be the result of a kinetic isotope effect linked to higher precipitation rates in the specialised areas. Turner (1992), in an experimental study observed that the $\delta^{13}C$ isotopic fractionation factor between HCO_3^- and $CaCO_3$ is dependent on the rate of carbonate precipitation and relatively high precipitation rates resulted in $\delta^{13}C$ depletion. However, with the exception of *Liothyrella uva*, little correlation exists between $\delta^{13}C$ and $\delta^{18}O$ in the secondary layer components of the articulated brachiopods studied. The implications are that precipitation rates affect the carbon isotopic composition of carbonate to a greater extent than the oxygen isotopic composition, or some other mechanism is at work. Indeed, Romanek *et al.* (1992) disagreed with Turner (1992) and argued that precipitation rates have no or little effect on $\delta^{13}C$ fractionation between HCO_3^- and calcite.

However, the lack of geographical and inter-species variation and consistent pattern in $\delta^{13}C$ distribution suggests a degree of metabolic regulation, probably due to prioritisation of resources, strengthening existing specialised areas at the posterior of the shell in order to facilitate an increase in shell size. If this is the case ^{12}C could be preferentially incorporated into the more specialised areas of the brachiopod shell, leading to 'vital effects'. Alternatively, from recent work using deep-sea corals, Adkins *et al.* (2003) suggest a new

mechanism to explain 'vital effects'. Their model predicts that any biogenic carbonate precipitated from an extra cellular fluid (ECF) between an impermeable membrane and the calcifying region, may be subject to a biologically induced pH gradient. A thermodynamic response to these conditions, breaks the linear trend between $\delta^{13}C$ and $\delta^{18}O$. However, in the Atkins *et al.* (2003) model, $\delta^{13}C$ remains relatively constant and $\delta^{18}O$ becomes depleted. However, the non-linear $\delta^{13}C$ v. $\delta^{18}O$ trend in the brachiopods used in this study does not conform with this suggestion, indeed the relationship is the direct opposite as it is the $\delta^{13}C$ that declines.

Further speculation is beyond the scope of the present study. However, the absence of a palpable local signal is problematic for the use of carbon stable isotopes in brachiopod shells as recorders of environmental information. Despite research into the incorporation of carbon isotopes in corals, the controlling mechanisms in biogenic carbonates are still a matter of scientific debate.

This study has shown that carbon isotope partitioning does occur in the shells of modern brachiopods. However, the mechanism for this effect remains unknown. Due to lack of local information on dissolved inorganic carbonate (DIC) in the seawater surrounding these samples, no conclusion regarding carbon isotopic equilibrium with ambient seawater can be made. Before meaningful environmental interpretation of $\delta^{13}C$ determinations from brachiopod shells can be made, a dedicated and robust study of the mechanisms controlling the carbon stable isotope composition of living brachiopods is required.

Chapter 7

A comparison of oxygen and carbon stable isotope ratios in brachiopods and bivalves from a modern marine epibenthic community in the Firth of Lorne, Scotland

7 A comparison of oxygen and carbon stable isotope ratios in brachiopods and bivalves from a marine epibenthic community in the Firth of Lorne, Scotland

7.1 Introduction

Oxygen and carbon stable isotope ratios determined from fossilised shells of calcareous marine organisms are frequently used to reconstruct the palaeoenvironmental conditions of ancient seas (Donner & Nord 1986; Qing & Veizer 1994; Hong *et al.* 1995; Azmy 1998; Kim *et al.* 1999; Steuber 1999; Veizer *et al.* 1999; Buchardt & Simonarson 2003). Particularly useful are oxygen stable isotope ratios since it has been shown that $^{18}O/^{16}O$ in biogenic carbonates is related to the temperature of the seawater in which they were formed (Epstein *et al.* 1951; 1953). The explanation for this is that these organisms precipitate their shells in temperature dependent isotopic equilibrium with ambient seawater. However, fossil shell samples recovered from sedimentary horizons may not only be from a variety of species, but also represent different phyla or subphyla. Such samples may also have shells that are a mixture of calcite and aragonite. Therefore, if this type of palaeo-investigative work is to be meaningful, it is important to understand the extent of possible differences in the isotopic signal from disparate creatures living contemporaneously in the same environment. Using modern shells, this study investigates the extent of variation in carbon and oxygen stable isotope ratios of different but contemporary calcareous marine organisms coexisting in a epibenthic community.

7.2 Study area

The study area is situated in the coastal waters of the inner Hebridean shelf, in the Firth of Lorne off the west coast of Scotland. The position is 56°24'N, 5°38'W close to the south east coast of the Isle of Mull (Fig. 7.1) The area is close to the Great Glen Fault, which diverges into numerous splay faults characterising the area. (Barber *et al.* 1979). The sample site is in the proximity of the divergence of two splays, the Firth of Lorne Fault (Holgate 1969) and the Bonnahaven Fault of Islay (Durrance 1976), in a zone of glacial over-deepening off shore between the sea lochs (fjords) Spelve and Buie (Barber *et al.* 1979) (Fig. 7.1). The study community thrives in a horse mussel (*Modiolus modiolus* (Linnaeus)) bed, located on soft mud at depths between 141 and 207 metres on the gently

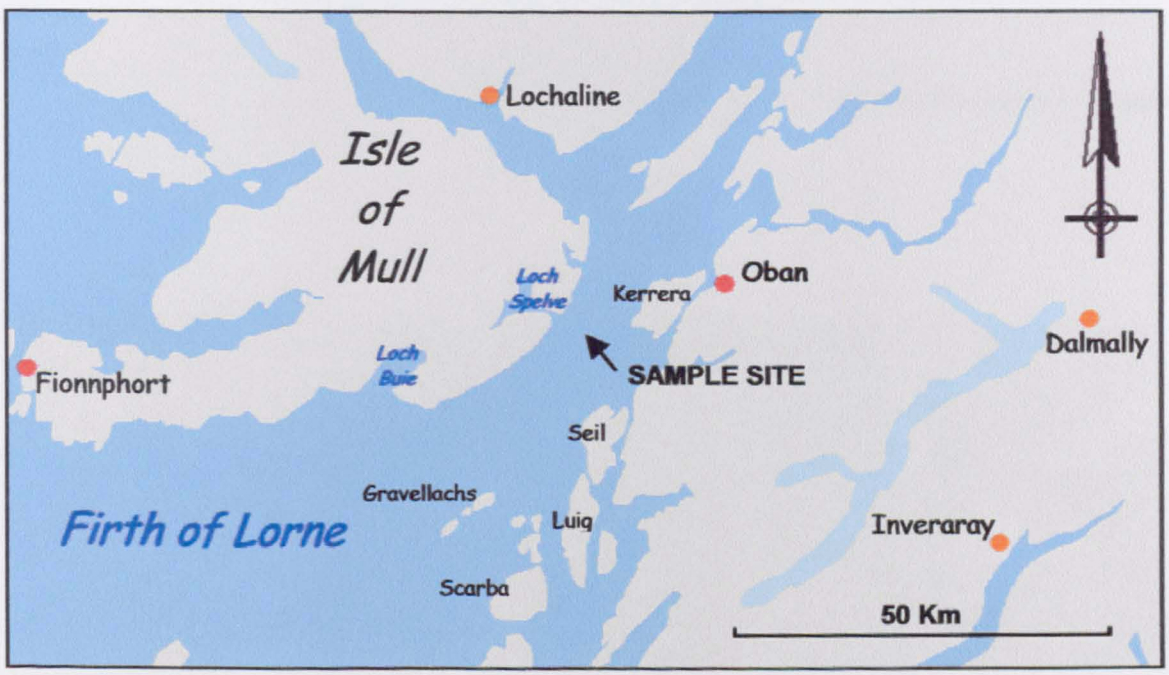

Figure 7.1: Sample location in the Firth of Lorne, near Oban, Western Scotland.

shelving slopes of a depression in the seafloor. The dominant carbonate shelled species of the community is *Modiolus modiolus* (Figs 7.2 & 7.3) a bivalve of the order Mytiloida, from the phylum Mollusca. *Modiolus modiolus* plays host to two species from the phylum Brachiopoda; these are sessile fauna, which predominately use the mussel shells directly as a substratum. However, the brachiopods belong to different subphyla. The articulated brachiopod *Terebratulina retusa* (Linnaeus), from the subphylum Rhynchonelliformea

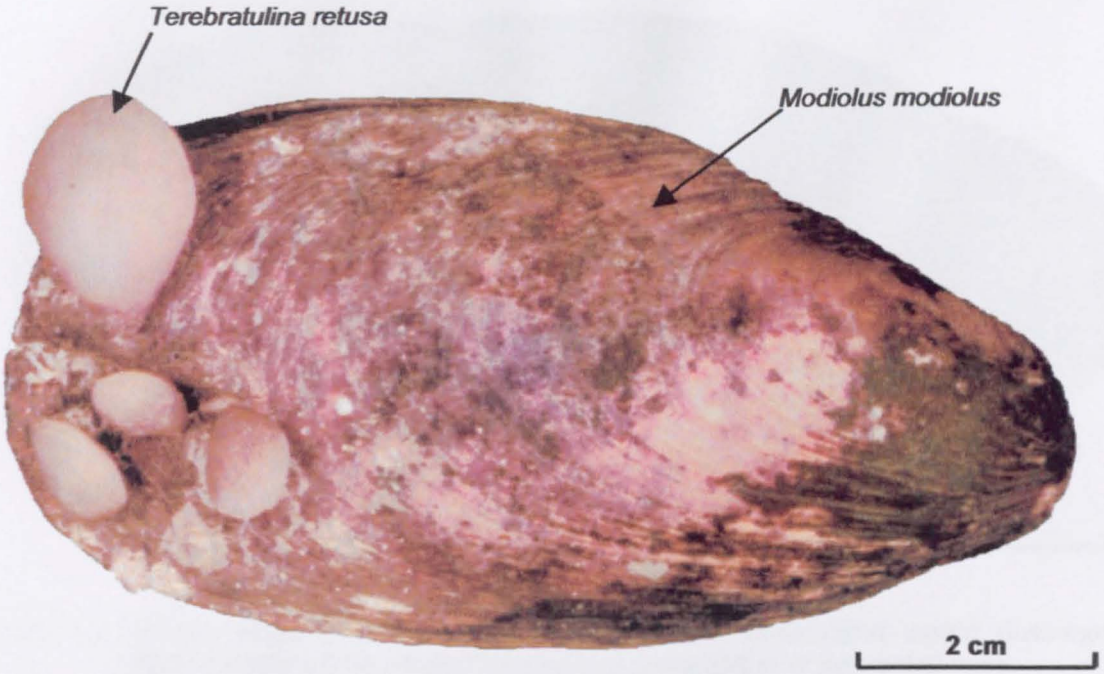

Figure 7.2: Bivalve *Modiolus modiolus* (Linnaeus).

The articulated terebratulid brachiopods *Terebratulina retusa* (Linnaeus) are attached via their pedicles.

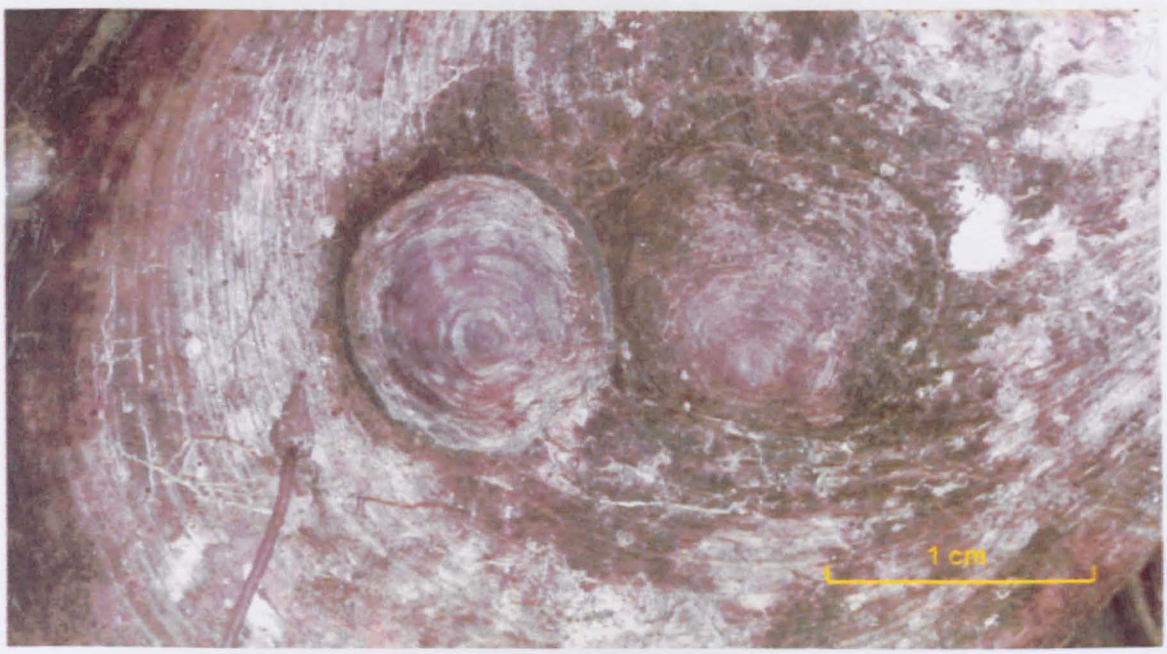

Figure 7.3: Dorsal view of *Novocrania anomala* (Müller)

The craniids are cemented to a *Modiolus modiolus* (Linnaeus) shell via the lower ventral valve.

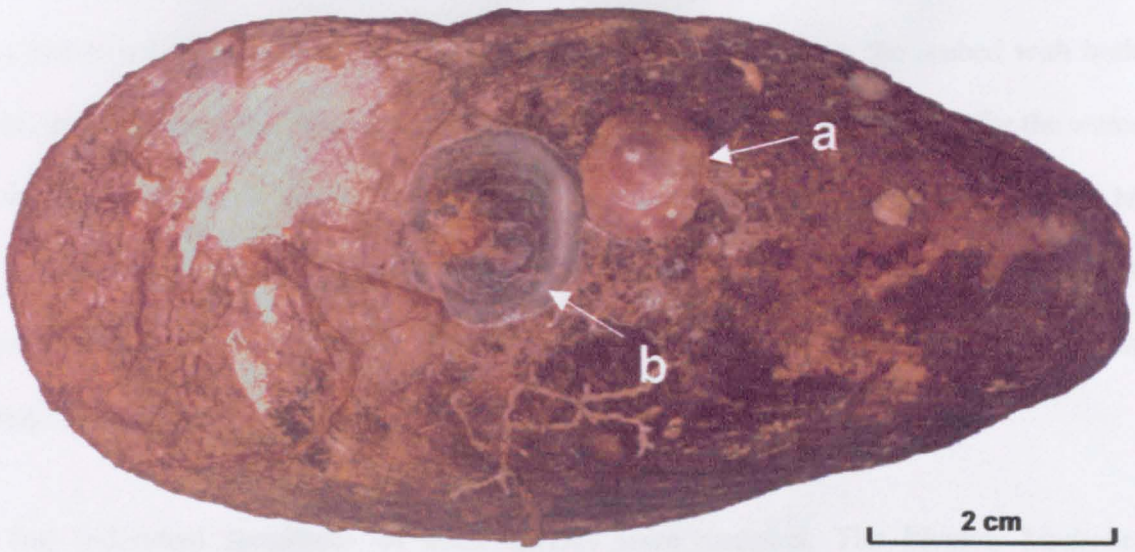

Figure 7.4: Bivalve *Modiolus modiolus* (Linnaeus) with the inarticulated craniid brachiopods *Novocrania anomala* (Müller) attached via cementation of the ventral valve.

a) is dorsal view of a complete *Novocrania anomala* (Müller) specimen. **b)** is a ventral valve of *Novocrania anomala* (Müller) cemented to the *Modiolus modiolus* (Linnaeus) shell.

(Fig 7.2), anchors itself to the mussel via a pedicle, a fleshy stalk that protrudes through the pedicle opening at the posterior end of the ventral valve. The inarticulated brachiopod *Novocrania anomala* (Müller) is from the subphylum Craniiformea (Figs 7.3 & 7.4) and attaches itself to the *Modiolus modiolus* shell by cementing its thin ventral valve directly to the mussel shell.

7.3 Materials and methods

7.3.1 Sample collection and preparation

The bivalve and brachiopod specimens were collected live by trawling the sea bed during cruises of the *RV Calanus*, a research vessel based at the Dunstaffnage Marine Laboratory, Oban, Scotland in 2002. The trawls were carried out by slowly dragging a clam dredger modified with a 15 mm mesh along the seabed. Samples were collected from the surface of the mud only.

During the same cruises, samples of seawater were collected for oxygen stable isotope analysis. These were collected from the seafloor in the sample area using a reversing bottle attached to a Lebus Hydrographic probe. This device is lowered to the seabed with both ends open to permit free flow of water through the bottle. After allowing time for the water to thoroughly flush, the sealing mechanism is triggered allowing a bottom water sample to be returned to the surface. Samples were sealed and returned to the Scottish Universities Environmental Research Centre (SUERC) laboratories for stable oxygen and carbon isotope analysis.

Ten individual specimens of each species were sampled. The bivalve *Modiolus modiolus* has two valves that mirror each other. Only one valve from each animal was analysed. To ensure there was no isotopic difference, the right valves of five specimens were used and left valves of the others. Samples were taken from the outer prismatic calcite close to the posterior (wider) end of the valve and the nacreous inner aragonite layer immediately below the sample area for the outer layer (Fig 7.5). The extracted material is a composite of several growth periods. The innermost layer of bivalve shells is often formed of dissolved and recrystallised material (Williams *et al.* 1982; Margosian *et al.* 1987), identifiable as structureless on electron micrographs (e.g. Fig. 7.5). This material was avoided during sampling. Brachiopods do not have identical valves, therefore for *Terebratulina retusa* both the dorsal and ventral valves were analysed separately. Both valves have the same general structure, namely a thin outer primary layer composed of fine granular calcite and an inner secondary layer of calcite fibres (Fig. 7.6). For *Novocrania anomala*, the ventral valves are very thin and remain cemented to the host *Modiolus modiolus* shells after the *Novocrania anomala* dorsal valves were removed (Fig. 7.4b). The dorsal valves of *Novocrania anomala* are composed of a thin outer primary layer of fine granular calcite (Fig. 7.7) and an inner secondary layer of laminar calcite sheets (Figs 7.7 & 7.8).

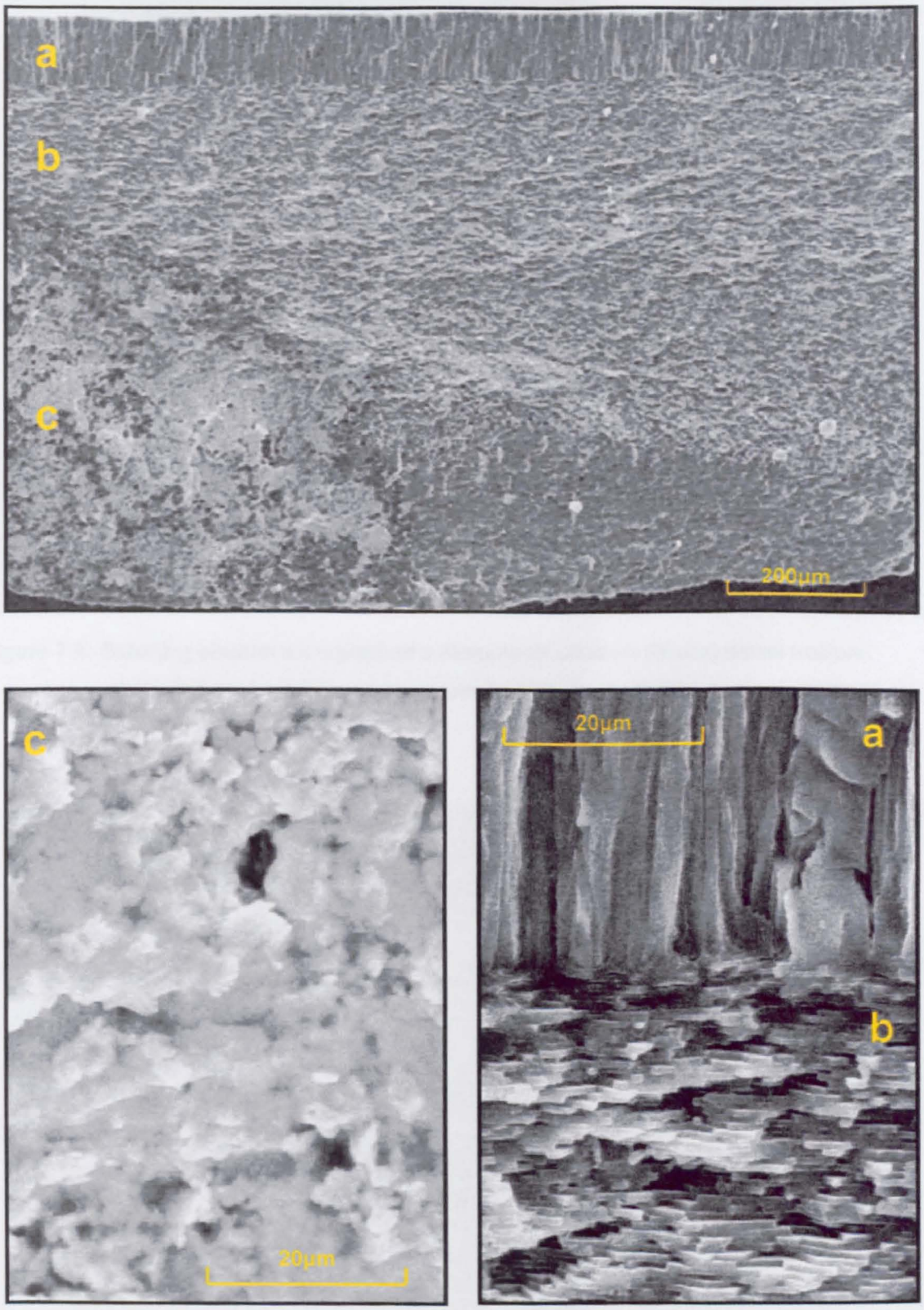

Figure 7.5: Scanning electron micrograph of *Modiolus modiolus* (Linnaeus) fracture.

Top **a)** Prismatic outer calcite layer. **b)** Nacreous inner layer of aragonite. **c)** Structureless recrystallised inner layer material. Bottom left: Close-up of structureless recrystallised material. Bottom right: close-up of prismatic and nacreous layers

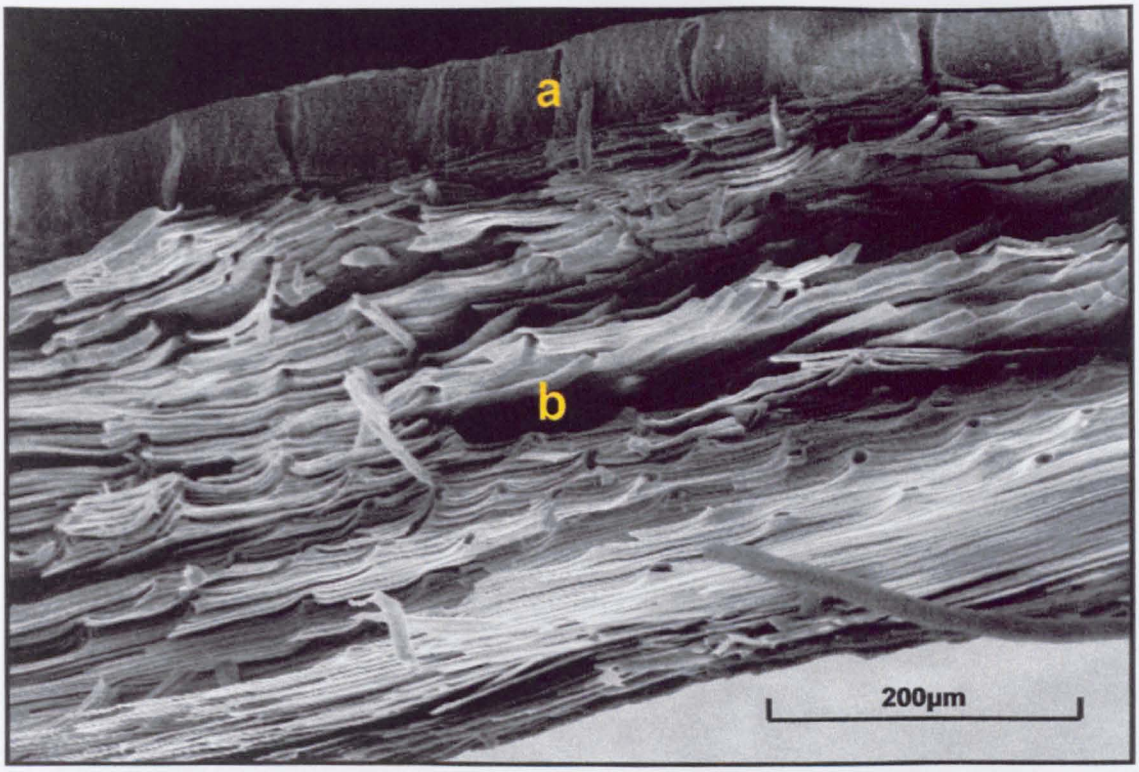

Figure 7.6: Scanning electron micrograph of a *Novocrania anomala* (Müller) dorsal fracture. **a)** Granular outer calcitic primary layer. **b)** Inner secondary layer of calcite fibres.

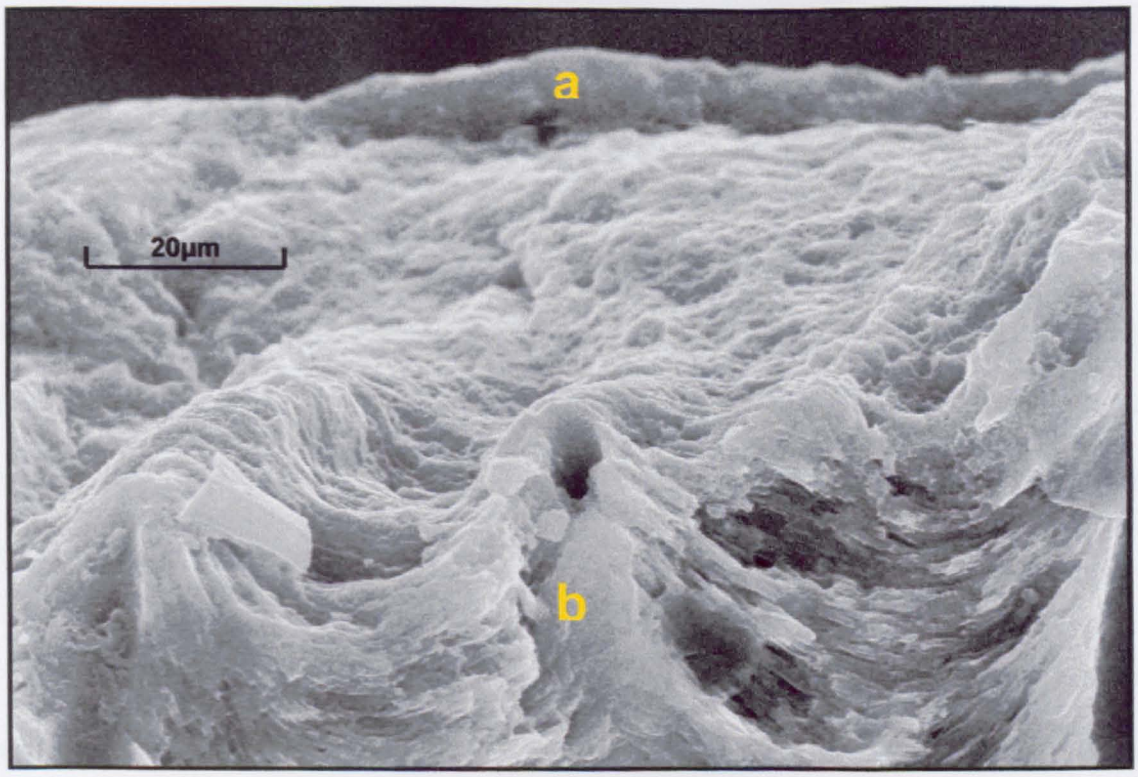

Figure 7.7: Scanning electron micrograph of a *Novocrania anomala* (Müller) dorsal fracture. **a)** Granular outer calcitic primary layer. **b)** Inner secondary layer of calcite laminar sheets.

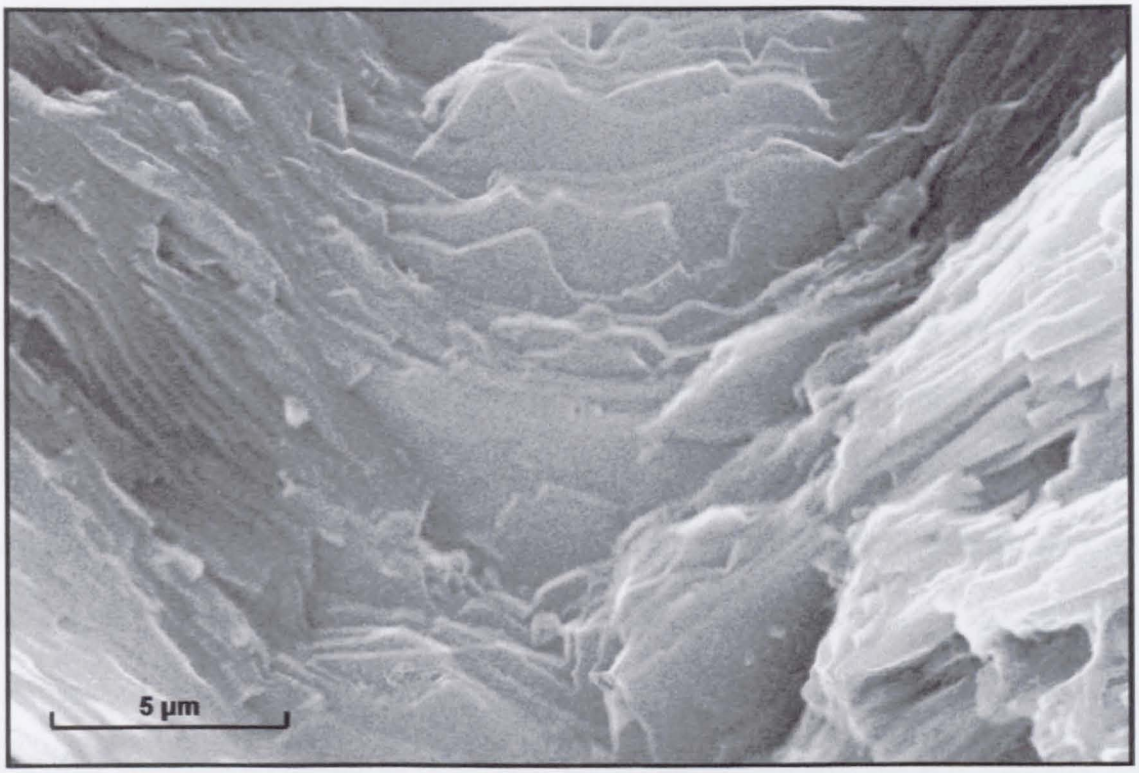

Figure 7.8 Scanning electron micrograph of a *Terebratulina retusa* (Linnaeus) dorsal fracture. The micrograph shows the laminar calcite sheets of the inner secondary layer.

7.3.2 *Stable isotope analysis*

The valves of each specimen were separated and any soft tissues removed. The shells were the treated in an ultrasonic bath with dilute commercial bleach to assist in the removal of the periostracum and any remaining organic material and foreign particles. After 30 minutes, the valves were brushed and rinsed several times with deionised water then dried. This is a variation of the method used by Rahimpour-Bonab *et al.* (1997) and recommended by Love & Woronow (1991) and Gaffey & Bronnimann (1993).

Samples of shell carbonate from the calcite and aragonite layers of *Modiolus modiolus* were taken from the wider posterior end of the shell. This is the relatively slow growing adult area of the shell unaffected by kinetic effects that can cause isotopic disequilibrium in the juvenile region (Kranz *et al.* 1987). The extracted material was taken across several

growth lines, and therefore is a composite of several growth periods. Calcite from the non-specialised secondary layer (see section 3.4) of the brachiopods was also extracted. The primary layer of the brachiopods was not sampled as it displays a strong positive correlation between $\delta^{18}O$ and $\delta^{13}C$, with many samples showing a depletion of both heavy isotopes relative to expected equilibrium with ambient seawater (see chapter 5 of this study and others e.g. Carpenter & Lohmann 1995; Auclair *et al.* 2003). This tendency is considered to be the result of kinetic fractionation effects due to relatively high growth rates in the primary layer (Rudwick 1970). Samples were extracted under a binocular microscope using a low-speed drill fitted with a 1.5 mm tapered dental burr. Care was taken to ensure that each extracted sample contained only material from the designated area. After extraction, each sample was examined under a binocular microscope to ensure that there had been no mixing of layers and any visible foreign material was removed. Any remaining organic matter or other volatile contaminant was removed by pre-treating the sample material for 4 hours in a low-temperature oxygen plasma asher.

The $^{18}O/^{16}O$ and $^{13}C/^{12}C$ ratios of the carbonate samples were determined from carbon dioxide produced by reacting 0.2-1.5 mg of sample material with 103% phosphoric acid (H_3PO_4) at 90°C, a variation of the method described by McCrea (1950). These analyses were controlled using a VG ISOCARB automated preparation system attached to a VG ISOGAS PRISM II isotope ratio mass-spectrometer at the Scottish Universities Environmental Research Centre (SUERC). The mass-spectrometer results are corrected for isotopic fractionation between calcite and CO_2 using a fractionation factor ($10^3 \ln\alpha$) of 7.904 for the reaction with 103% H_3PO_4 at 90°C. Corrections were made for isobaric molecular ions and ^{17}O using the methods described by Craig (1957) allowing for 3-collector operation. All the isotope ratios are reported using the accepted delta (δ) notation in permil (‰) relative to the Vienna Pee Dee Belemite (VPDB) international standard (Coplen 1995; Gonfiantini *et al.* 1995).

Incorporating internal laboratory marble standards within each batch of analyses allowed precision to be monitored; standard material was calibrated to the International Atomic Energy Agency's (IAEA) intercomparison material IAEA-CO-1. Reproducibility of the standard material for each isotope ratio was better than 0.1 ‰ at 1σ. Analysis of each sample was replicated up to 3 times. The precise number of replicates depended on the quantity of sample material extracted. Variability was usually < 0.2 ‰ at 1σ. Occasional samples with higher variability were probably due to either lack of homogeneity, slight contamination between shell layers or traces of foreign carbonate infiltrating the shell structure.

The bottom-seawater samples from the Firth of Lorne were analysed to determine the oxygen isotope composition of the ambient seawater. Analyses were carried out by CO_2 – equilibration using an AP2003 mass spectrometer, coupled to a fully-automated 'Gas Preparation Interface Module' (APGP) with integral water trap, GC and reference gas injector. Results are reported as $\delta^{18}O$ in relation to Vienna Standard Mean Ocean Water (VSMOW) (Coplen 1995; Gonfiantini *et al.* 1995). Precision and accuracy are around 0.2‰ at 1σ.

Isotopic temperatures were calculated from the $\delta^{18}O$ values of the calcite samples using a palaeotemperature equation based on the relationship between seawater temperature and the isotopic composition of biogenic carbonate proposed by Epstein et al. (1953). An updated version of this equation recommended by Anderson & Arthur (1983) (Equation 7.1) was used in this study:

$$T\,(^{\circ}C) = 16.0 - 4.14\,(\delta^{18}O_{calcite} - \delta^{18}O_{seawater}) + 0.13\,(\delta^{18}O_{calcite} - \delta^{18}O_{seawater})^2 \qquad [7.1]$$

Research has produced compelling evidence that oxygen isotope fractionation between aragonite and water differs from that between calcite and water. Epstein *et al.* (1953)

suggest that aragonite was depleted in ^{18}O relative to calcite. This was supported by Horibe & Oba (1972) Others have reported that aragonite is enriched in ^{18}O relative to calcite (Tarutani *et al.* 1969; Grossman & Ku 1986; Barrera *et al.* 1994; Kim & O'Neil 1997; Thorrold *et al.* 1997). The work by Grossman & Ku (1986) established the commonly used equation [7.2] for the oxygen isotope fractionation between biogenic aragonite in mollusc shells and water:

$$T\,(^{\circ}C) = 21.8 - 4.69 * (\delta^{18}O_{aragonite} - \delta^{18}O_{seawater}) \quad [7.2]$$

Grossman & Ku's (1986) relationship has a slope similar to the inorganic curve of O'Neil *et al.* (1969). Grossman & Ku's (1986) equation has been used in studies of modern bivalves from Antarctic waters (Marshall *et al.* 1996) and tropical waters (Lécuyer *et al.* in press). Böhm *et al.* (2000), using additional data, reduced the error of the original Grossman and Ku (1986) equation proposing:

$$T\,(^{\circ}C) = (19.7 \pm 0.6) - (4.34 \pm 0.24) * (\delta^{18}O_{aragonite} - \delta^{18}O_{seawater}) \quad [7.3]$$

The original Grossman and Ku (1986) equation and the revision by Böhm *et al.* (2000) are compared in this study when calculating isotopic temperatures from the $\delta^{18}O$ values of the aragonite samples from *Modiolus modiolus* from the temperate waters of the Firth of Lorne.

Using actual measured seawater temperatures, these equations were also used to calculate the carbonate $\delta^{18}O$ values expected under equilibrium conditions (Fig. 7.9).

7.4 Results and discussion

7.4.1 Seawater oxygen isotope composition

The results for the seawater oxygen isotope analyses from the Firth of Lorne are presented in Table 7.1. The samples were collected during the winter of January 2002 and the summer collection of June 2002. The $\delta^{18}O$ values range from –0.09‰ to 0.22‰ with a mean of 0.06‰ ± 0.09‰ at 1σ.

Table 7.1: Oxygen isotope composition of seawater samples collected from Firth of Lorne.

Date	Sample	Depth (metres)	$\delta^{18}O$‰ (VSMOW)
17-Jan-02	FoLW01	201	0.15
17-Jan-02	FoLW02	201	0.03
17-Jan-02	FoLW03	201	0.08
17-Jan-02	FoLW04	201	0.08
17-Jan-02	FoLW05	201	0.22
17-Jan-02	FoLW06	201	0.02
17-Jan-02	FoLW07	201	0.09
17-Jan-02	FoLW08	201	0.15
17-Jan-02	FoLW09	201	0.22
17-Jan-02	FoLW10	201	0.07
27-Jun-02	FoLS01	207	-0.08
27-Jun-02	FoLS02	207	-0.05
27-Jun-02	FoLS03	207	-0.03
27-Jun-02	FoLS04	207	0.05
27-Jun-02	FoLS05	207	-0.09
27-Jun-02	FoLS06	207	0.14
27-Jun-02	FoLS07	207	-0.03
27-Jun-02	FoLS08	207	0.12
27-Jun-02	FoLS09	207	0.02
27-Jun-02	FoLS10	207	0.00
			Mean = 0.06 ± 0.09‰

7.4.2 Oxygen and carbon isotopic composition

The crossplot Fig.7.9, shows that $\delta^{18}O$ and $\delta^{13}C$ values obtained from the different carbonates analysed are varying and wide ranging, both between species and within

individuals. $\delta^{13}C$ distribution is very wide with a range of 7.04‰. (-2.75‰ to 4.29‰). Variability of the carbon isotopic composition within a species is particularly notable in the non-specialised secondary layer of craniid brachiopod *Novocrania anomala*, which produces both of the extreme $\delta^{13}C$ values. Values of $\delta^{13}C$ for the other species fall into three distinct groups within the range of those yielded by *Novocrania anomala*. The non-specialised area of the secondary layer of terebratulid brachiopod *Terebratulina retusa* produced $\delta^{13}C$ values from both dorsal and ventral valves that were not statistically different (Mann Whitney, P = 0.103). The bivalve *Modiolus modiolus* yielded statistically disparate groups of $\delta^{13}C$ values for calcite and aragonite samples (Mann Whitney, P = 0.000). Mean $\delta^{13}C$ values for the aragonite layer are –0.12‰ compared to 0.54‰ for the calcite layer.

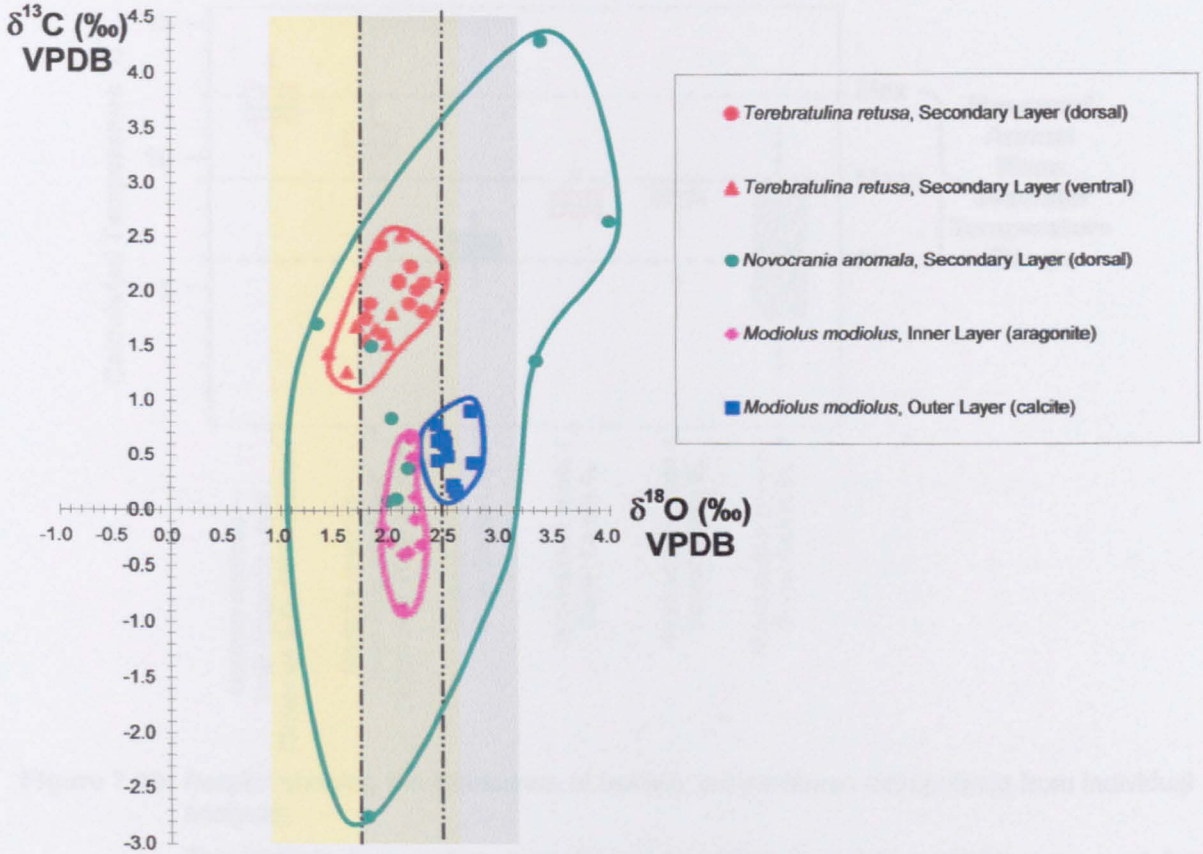

Figure 7.9: $\delta^{18}O$ – $\delta^{13}C$ crossplot showing the $\delta^{18}O$ and $\delta^{13}C$ values of the sampled carbonates. Data points are the mean for the replicates in one individual. The yellow shaded area represents the calculated range of expected equilibrium $\delta^{18}O$ values for calcite (Based on Anderson & Arthur 1983). The grey shaded area represents the calculated range of expected equilibrium $\delta^{18}O$ values for aragonite (Based on Böhm *et al.* 2000). The dashed lines represent the means of the expected $\delta^{18}O$ equilibrium values.

$\delta^{18}O$ values are less variable than $\delta^{13}C$ values ranging from, 1.33‰ to 3.99‰ a difference of 2.66‰ across all analyses. However, there is considerable variation between and within species, which could cause problems of interpretation in palaeoenvironmental studies. As was the case with carbon, the extreme values were derived from one species, *Novocrania anomala*. Seventy percent of $\delta^{18}O$ values for *Novocrania anomala* fell within the expected range calculated for oxygen isotope equilibrium between calcite and water. However, the level of fluctuation in $\delta^{18}O$ in *Novocrania anomala* is too great for unambiguous environmental interpretation. Using equation [7.1] to extrapolate isotopic temperatures from $\delta^{18}O$ values obtained from each individual, *Novocrania anomala* specimens produce a range of 1.7°C to 11°C (Fig. 7.10). Curry (1982) observed that the bottom seawater in the Firth of Lorne is

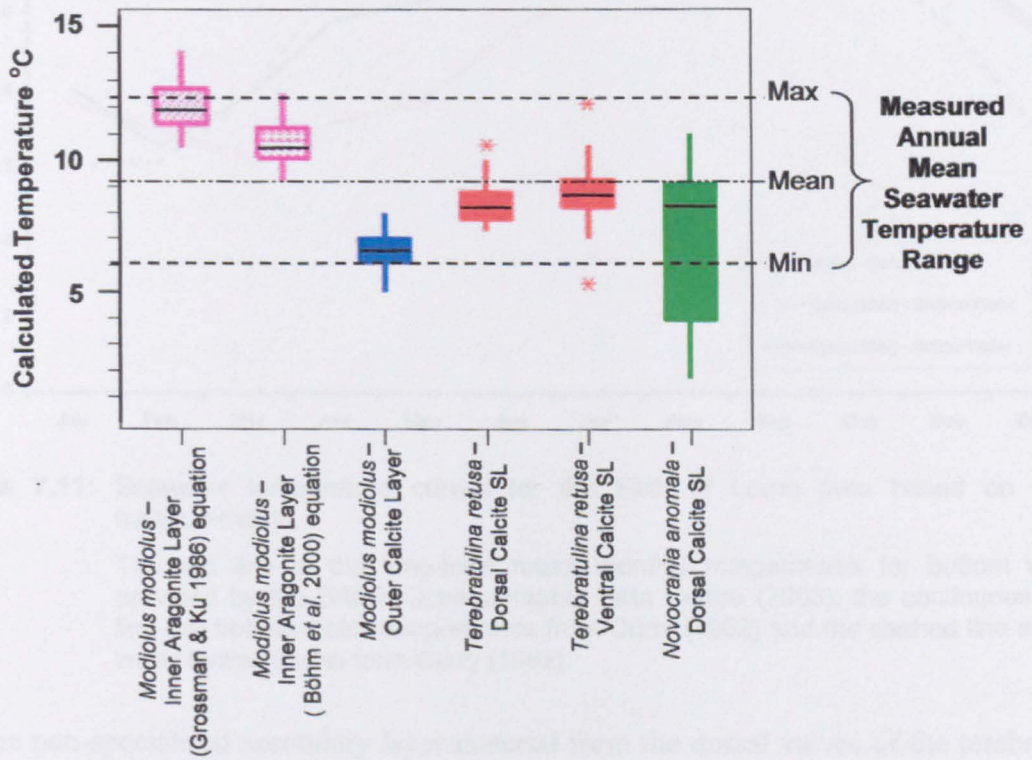

Figure 7.10: Boxplot showing the distribution of isotopic temperatures extrapolated from individual analyses.

The isotopic temperature equation of Anderson and Arthur (1983) was used for calcite and the equations of Grossman and Ku (1986) and Böhm *et al.* (2000) for aragonite. The temperature range are long-term bottom water temperatures provided by the British Oceanographic Data Centre (BODC 2003).

separated from the surface waters by a thermocline and therefore is not susceptible to the rapid fluctuations in air temperatures at the surface. The bottom water temperature is

therefore warmer in the winter and cooler in the summer than the surface waters (Fig. 7.11). The waters only become isothermal for two short periods in the spring and autumn when the thermocline breaks down. This is seen in Figure 7.11 at the points where the bottom and surface water curves of Curry (1982) cross. Although temperatures from some *Novocrania anomala* specimens reflect the temperatures in the bottom water zone, it is difficult to reconcile some of the very cold temperatures apparently recorded by other specimens.

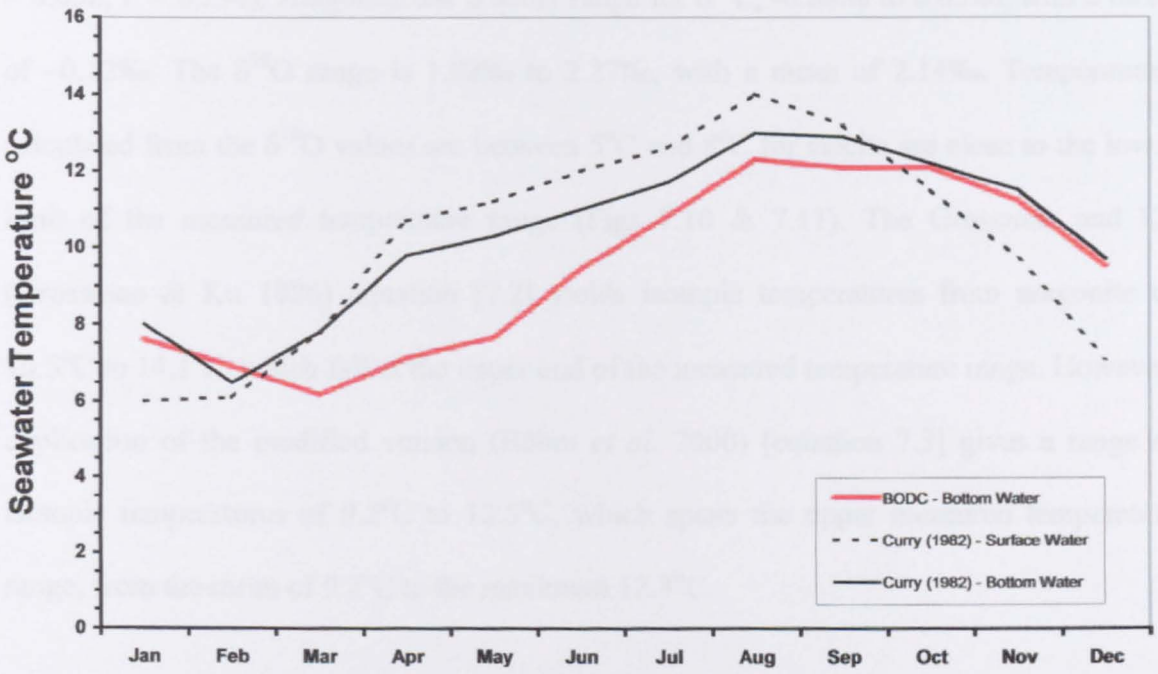

Figure 7.11: Seawater temperature curves for the Firth of Lorne area based on actual measurements.

The red line is the long-term mean monthly temperatures for bottom waters provided by the British Oceanographic Data Centre (2003); the continuous black line are bottom water temperatures from Curry (1982) and the dashed line surface water temperatures from Curry (1982).

The non-specialised secondary layer material from the dorsal valves of the terebratulid brachiopod *Terebratulina retusa* specimens produce $\delta^{18}O$ values ranging from 1.43‰ to 2.33‰. Temperatures extrapolated from these data fall between 7.3°C and 10.6°C, with a mean of 8.4°C. The ventral valves yield a range of $\delta^{18}O$ values from 1.04‰ to 2.89‰, which is not significantly different from the dorsal valve (Mann Whitney, $P = 0.08$) and equates to temperatures of 6.8°C to 12.1°C, with a mean of 8.8°C. Isotopic temperatures

calculated from both valves fall comfortably within the measured seawater temperature range of 6.2°C to 12.31°C, with a mean of 9.2°C (Figs 7.10 and 7.11).

Isotopic values from the prismatic calcite of the outer layer and the underlying nacreous aragonite layer in the bivalve *Modiolus modiolus* are different (Fig. 7.9). The calcite is enriched in both $\delta^{13}C$ and $\delta^{18}O$ relative to aragonite. The $\delta^{13}C$ values for the outer layer range from 0.17‰ to 0.91‰, with a mean of 0.54‰. For $\delta^{18}O$ the range is 2.41‰ to 2.74‰, with a mean of 2.53‰. No correlation exists between the two isotopes ($n = 30$, $R_s = 0.058$, $P = 0.294$). Aragonite has a wider range for $\delta^{13}C$, -0.88‰ to 0.65‰, with a mean of –0.12‰. The $\delta^{18}O$ range is 1.92‰ to 2.27‰, with a mean of 2.14‰. Temperatures calculated from the $\delta^{18}O$ values are between 5°C and 8°C for calcite are close to the lower limit of the measured temperature range (Figs 7.10 & 7.11). The Grossman and Ku (Grossman & Ku 1986) equation [7.2] yields isotopic temperatures from aragonite of 10.5°C to 14.1°C, which fall at the upper end of the measured temperature range. However, application of the modified version (Böhm *et al.* 2000) [equation 7.3] gives a range of isotopic temperatures of 9.2°C to 12.5°C, which spans the upper measured temperature range, from the mean of 9.2°C to the maximum 12.3°C.

The taxa studied from the Firth of Lorne have a variety of carbon and oxygen isotopic compositions. This makes unambiguous interpretation of the environmental conditions difficult. The $\delta^{13}C$ values for the species are disparate and cannot all reflect the carbon isotopic composition of HCO_3^-. The variation between species is likely to be the result of metabolic differences. If meaningful environmental data are to be obtained, a greater understanding of the physiology of the individual organisms is required.

The averages of the $\delta^{18}O$ values for each group all fall within the parameters of expected isotope equilibrium. However, the results are contrasting. The craniid brachiopod *Novocrania anomala* yields some values which produce isotopic temperature close to the

mean of measured seawater temperature, but in this study 30% of results are erratic and would confuse any palaeoinvestigation. Problems of oxygen isotope disequilibrium in modern craniid brachiopod shells have been noted in this (see chapter 5) and other studies (e.g. Carpenter & Lohmann 1995; Brand *et al.* 2003). It is possible that these effects may different biomineralisation regime that produces the laminar ultrastructure of the secondary layer (Fig 7.8). Non-specialised secondary layer material from both valves of the terebratulid brachiopod *Terebratulina retusa* produces mean $\delta^{18}O$ values close to, but higher than the average expected value for isotope equilibrium. Curry (1982) studying *Terebratulina retusa* in the Firth of Lorne observed a cessation of growth during the winter months. This would seem to conflict with the lower than mean isotopic temperatures noted here. However, the secondary layer of brachiopods is used to thicken and strengthen the structure. Therefore, a possible explanation for this effect is that *Terebratulina retusa* utilises its resources during the summer months for shell enlargement and in the winter for strengthening by secondary shell growth.

Many investigations involving modern bivalves (e.g. Mook 1971; Williams *et al.* 1982; Donner & Nord 1986; Margosian *et al.* 1987; Aharon 1991; Klein *et al.* 1996b; 1996a; Rahimpour-Bonab *et al.* 1997; Hickson *et al.* 1999; Khim *et al.* 2000; Owen *et al.* 2002; Elliot *et al.* 2003; Lécuyer *et al.* in press) found the shell material to be formed at or close to oxygen isotopic equilibrium with the surrounding seawater. The aragonite layer of the bivalve *Modiolus modiolus* employed in this study is in isotopic equilibrium when the expected isotopic equilibrium parameters are calculated using the equation of Böhm *et al.* (2000) [7.3]. However, the isotopic temperatures extrapolated are warmer than average. This could mean that the aragonite layer is only precipitated during the summer months. However, the calcite layer is more problematic. Donner and Nord (1986) and Margosian *et al.* (1987) studying *Modiolus modiolus* specimens from Norway observed that the calcite layer of this bivalve grows continually throughout the year. The $\delta^{18}O$ values from the

calcite of the *Modiolus modiolus* specimens taken from the Firth of Lorne are tightly grouped and calculated temperatures accord with only the very coldest temperatures. The sample material represented a homogenous mix of several years of growth, therefore it is not possible that only winter growth was measured. The results are consistent and obtained over several analytical batches, and therefore are unlikely to be the result of contamination or analytical error. One possible interpretation is that *Modiolus modiolus*, at this location, precipitates calcite and aragonite during different seasons. The average of the isotopic temperatures of both calcite and aragonite layers is 8.7°C close to the measured mean annual mean seawater temperature of 9.2°C. Considering the findings of Donner and Nord (1986) and Margosian *et al.* (1987) it may be that *Modiolus modiolus* adopts different growth regimes in different environments. Only a detailed study of growth patterns for the species in the Firth of Lorne will indicate if this is the case.

7.5 Conclusions

The carbon isotopic compositions of all the studied taxa in the Firth of Lorne are disparate. This is likely to be due to metabolic or dietary differences rather than reflecting variability of ^{13}C in HCO_3^-. A greater understanding of the physiology of these species is needed in order to obtain meaningful environmental information.

The oxygen isotope composition of brachiopods are widely considered to be a useful tool for palaeoenvironmental reconstruction. This study demonstrates that the secondary layer of the articulated brachiopod *Terebratulina retusa* is a good indicator of ambient temperature. However, *Novocrania anomala* also demonstrates that not all secondary layer material from brachiopods is suitable. These two brachiopods have different biomineralisation regimes. *Terebratulina retusa* has a fibrous secondary layer, whilst *Novocrania anomala* has a laminar one. Factors that determine the ultrastructure may influence the isotopic composition and is worthy of further investigation. However, it may

be possible to obtain meaningful data from *Novocrania anomala* by analysing numerous individuals and disregarding outlying values.

The calcitic and aragonitic layers of *Modiolus modiolus* from the Firth of Lorne have varying $\delta^{18}O$ values. However, amalgamating the data produces a mean isotopic temperature close to the measured mean annual seawater temperature. The differences between the two layers may be due to seasonal differences in growth.

Chapter 8

Summary

8 Summary

8.1 Summary of results

8.1.1 Shell Structure

Scanning electron microscope (SEM) examination reveals a range of different ultrastructures in modern brachiopod shells. Most terebratulids: i.e. *Calloria inconspicua* (Sowerby), *Laqueus rubellus* (Sowerby), *Neothyris lenticularis* (Deshayes), *Terebratulina retusa* (Linnaeus), *Terebratella sanguinea* (Leach) and *Terebratalia transversa* (Sowerby) have two endopunctate calcite layers in both valves. Outermost is a fine grained primary layer, underlain by an inner secondary layer composed of calcite fibres. The specialised components of the shell are formed from the secondary material. The rhynchonellid *Notosaria nigricans* (Sowerby) has a similar structure, but is impunctate. This type of ultrastructure is described as the 'standard model' for articulated brachiopods (Williams 1968b).

The terebratulid genus *Liothyrella* has a different structure. In *Liothyrella*, the secondary layer is succeeded by an inner prismatic tertiary layer, from which the specialised components are formed (MacKinnon & Williams 1974). This structure was observed in *Liothyrella neozelanica* (Thomson) from New Zealand. However, in the related Antarctic brachiopod *Liothyrella uva* (Broderip) the tertiary layer was often absent or incomplete. One possible interpretation of this is that it is the result of environmental stress.

Thecidellina barretti (Davidson) is a small anomalous articulated brachiopod around 3 to 4 mm in length (Williams 1968a). It has no layered shell structure and is composed solely of acicular primary layer calcite (Williams 1973).

The inarticulated subphylum Craniiformea, was represented by *Novocrania anomala* (Müller) and *Neoancistrocrania norfolki* (Laurin). The dorsal valve of *Novocrania anomala* has a two-layered punctate structure. The thin outer primary layer is composed of fine acicular calcite. Underlying this is an inner secondary layer of calcite sheets, which form laminae and grow by screw dislocation to form spiral structures (Williams & Wright 1970). *Neoancistrocrania norfolki* has valves with different ultrastructures. The dorsal valve is very similar to that of *Novocrania anomala*. However, the ventral valve is structurally different. A thin primary layer overlies a relatively thick secondary layer with two discernable growth phases. The upper secondary layer, adjacent to the primary layer, has an open construction formed of laminar hooped chambers. The innermost, or lower secondary layer has similar chambers, but the orientation is changed and the chambers are infilled by calcite accretion. This is interpreted as a reduction in the growth rate in the mature organism (A. Williams, personal communication, 18th November 2002).

8.1.2 Oxygen isotope analysis

Primary layer $\delta^{18}O$ values from most brachiopod species, are generally lower than those from the secondary layer components. In all species, other than the rhynchonellid *Notosaria nigricans*, $\delta^{18}O$ values from the primary layer are positively correlated with $\delta^{13}C$, possibly due to a kinetic isotope effect, which may be linked to relatively high rates of shell precipitation (Carpenter & Lohmann 1995; Auclair *et al.* 2003).

The different secondary layer components of the articulated terebratulid and rhynchonellid brachiopods , almost always yield $\delta^{18}O$ values that fall within the expected range for oxygen isotopic equilibrium. Of these components it was the non-specialised secondary layer material that most consistently produced values near to the equilibrium range. Isotopic temperatures extrapolated from $\delta^{18}O$ values are close to the measured annual average ambient seawater temperatures at the respective locations. *Liothyrella*

neozelanica with a tertiary succession also produced $\delta^{18}O$ values consistent with equilibrium precipitation and yielded calculated isotopic temperatures close to the measured mean for ambient seawater. However, this was not the case in the Antarctic brachiopod from the same genus, *Liothyrella uva*. This species had a high degree of $\delta^{18}O$ variation in the tertiary layer components. The oxygen isotopic composition was not consistent with equilibrium precipitation, and only the cardinal process and the loop samples did not have a positive correlation between $\delta^{18}O$ and $\delta^{13}C$.

The thecideidine brachiopod *Thecidellina barretti* is an articulate species that precipitates a single shell layer of acicular primary calcite (Williams 1973). Stable isotope analyses yielded only one out of ten specimens with $\delta^{18}O$ values that fell within the expected range for oxygen isotope equilibrium. This value was at the upper end of the range and the calculated isotopic temperature from this specimen is only indicative of the coolest temperature experienced during the life of the organism. All the other *Thecidellina barretti* specimens were enriched in ^{18}O relative to the oxygen equilibrium range, which would imply seawater temperatures lower than measured values.

Representatives of the Craniiformea produced very variable $\delta^{18}O$ values from the laminar secondary layer calcite. For *Novocrania anomala* many secondary layer $\delta^{18}O$ values fall within the expected range for oxygen isotope equilibrium. However, the non-specialised component yielded inconsistent results, three out of ten specimens had oxygen isotopic compositions that were too heavy to be compatible with equilibrium precipitation. None of the $\delta^{18}O$ determinations from *Neoancistrocrania norfolki* were consistent with equilibrium precipitation, and all were higher than the expected range. The implication is that *Neoancistrocrania norfolki* precipitates its shell out of oxygen isotopic equilibrium.

One specimen of each species was crushed whole. Samples of the 'bulk' shell material produced $\delta^{18}O$ values that generally fell within the expected range for precipitation in

oxygen isotopic equilibrium. However, the inclusion of the $\delta^{18}O$ depleted primary layer material yielded results, which were lower than the expected mean $\delta^{18}O$ value. The implications are that calculated isotopic temperatures from most species are at the higher end of the measured temperature range. Bulk analysis of the terebratulids *Laqueus rubellus* and *Terebratulina retusa*, the rhynchonellid *Notosaria nigricans* and craniid *Novocrania anomala* all produced $\delta^{18}O$ values close to the expected mean value for oxygen isotopic equilibrium precipitation.

8.1.3 Carbon isotope analysis

The carbon isotope composition is highly variable in all of the brachiopods studied. Analyses of samples from the components of the secondary shell layer of the articulated species shows a pattern of depletion in $\delta^{13}C$ relative to non-specialised secondary material that does not correlate with $\delta^{18}O$ values, with the lowest $\delta^{13}C$ values recorded in the posterior-most components. The general trend is for decreasing $\delta^{13}C$ values from the non-specialised component to loop, muscle scars and cardinal process in the dorsal valves; and non-specialised, teeth muscle scars and the pedicle foramen in the ventral valves. The ^{13}C fractionation is independent of $\delta^{18}O$ and is repeated in most of the articulated species, regardless of geographical location. This is possibly a vital effect produced by metabolic prioritisation.

8.1.4 Firth of Lorne

In a sub-study the craniid *Novocrania anomala*, the terebratulid *Terebratulina retusa* and the bivalve *Modiolus modiolus* co-existing at location 1, Firth of Lorne, Scotland were compared. Only the non-specialised component of *Terebratulina retusa* yielded $\delta^{18}O$ values close to the mean for oxygen isotopic equilibrium precipitation. Considerable inter-specimen variation was observed in the non-specialised component of *Novocrania anomala*. The *Modiolus modiolus* shell is composed of two polymorphs of $CaCO_3$:

aragonite and calcite. Samples from both polymorphs produced $\delta^{18}O$ values consistent with oxygen equilibrium precipitation. However, the values for aragonite implied only summer precipitation and calculated isotopic temperatures for calcite were consistent with only the coldest measured seawater temperatures. This may be due to seasonal growth patterns in the *Modiolus modiolus* shell, notwithstanding that the environmental signal is ambiguous. Whole shell analysis of both brachiopod species gave meaningful isotopic temperatures, which were close to average seawater temperatures in the Firth of Lorne.

8.2 Conclusions

The shell structures and ecologies of extant brachiopods are diverse. This study has shown that some components of the shells of brachiopods do have oxygen isotopic compositions consistent with equilibrium precipitation. However, $\delta^{18}O$ values deemed to be in stable isotopic equilibrium with ambient seawater are not meaningful proxies in themselves. If $\delta^{18}O$ values from fossil brachiopods, taken from different stratigraphic horizons are to be interpreted accurately, it is important to know what the relationship to seawater temperature is and if it is consistent. This study has shown that some modern brachiopod genera can provide estimates of seawater temperature close to the measured mean, and can be recommended as environmental proxies. A summary of those species that are recommended and those that should be avoided is given in Figure 8.1.

The secondary layer, in particular the non-specialised component of those articulated species that have the 'standard model' of shell ultrastructure (section 4.2), yielded the most meaningful $\delta^{18}O$ values i.e.: in the species *Calloria inconspicua*, *Laqueus rubellus*, *Neothyris lenticularis*, *Terebratulina retusa*, *Terebratella sanguinea* and *Terebratalia transversa*. The secondary layer carbonate of all these species can confidently be recommended for use as a proxy indicator of seawater temperature.

Those brachiopod species that have an inner prismatic primary layer gave mixed results. The oxygen isotope composition of *Liothyrella neozelanica* from the temperate waters around New Zealand provided a good record of ambient seawater temperature. However, *Liothyrella uva* from Antarctica produced very variable $\delta^{18}O$ values. This could be an ecological response as a result of survival in extreme environmental conditions. Further evidence from SEM analysis of the *Liothyrella uva* shell, suggests that it does not grow in the uniform manner expected from the *Liothyrella* genus. Caution should be taken with interpretation of oxygen isotope data from polar environments.

The Craniida and Thecideidina species yield $\delta^{18}O$ values that are either variable or inconsistent with oxygen equilibrium composition. Interpretation of stable isotope analyses may be problematic. Use of these groups of brachiopods in environmental reconstruction is not recommended (see Fig 8.1).

The primary layer of most brachiopod shells displays a strong correlation between $\delta^{18}O$ and $\delta^{13}C$ values with both heavy isotopes depleted relative to the secondary or tertiary layers. Most of these values are outside the expected range for oxygen isotopic equilibrium. Use of primary layer material should be avoided. Addition of primary layer material in whole shell samples may confuse interpretation of results in some species. Use of bulk material is therefore not recommended.

The possibility that a relationship exists between brachiopod shell structure and ^{18}O equilibrium precipitation with ambient seawater has been highlighted by this study. It is evident that not all brachiopod groups are meaningful proxies of seawater temperature. This should be taken into account in future studies using fossil brachiopods. It is recommended that until there is a greater understanding of oxygen isotopic incorporation and biomineralisation that only fossils with similar structures to those shown in green on Figure 8.1 are used.

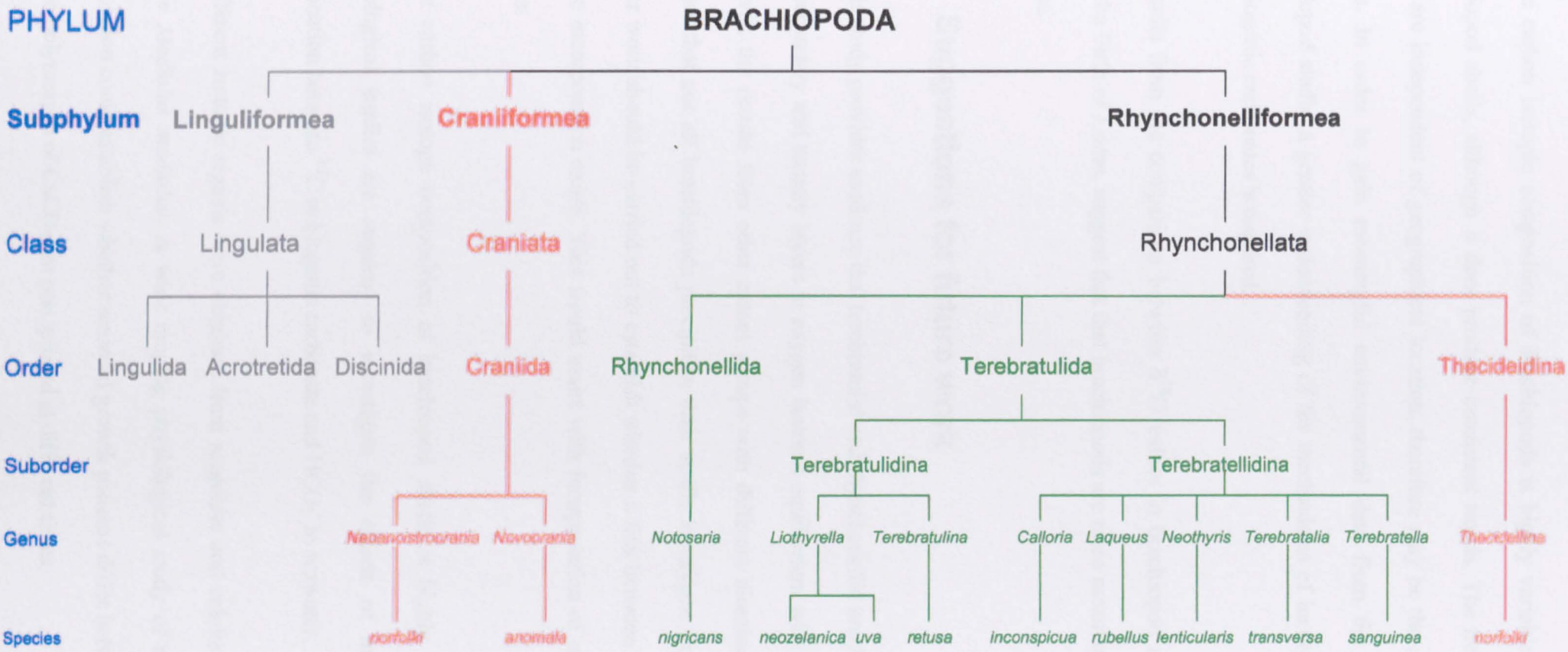

Figure 8.1: Cladogram detailing extant brachiopods studied and showing their status as proxies of seawater temperature. Those species in green are suitable, those in red are not suitable. The subphylum Linguliformea was not studied.

The carbon isotopic composition of brachiopods is highly variable within individual brachiopod shells, although it does produce consistent trends. The trends shown in this study are independent of geographical location, therefore may be the result of metabolic effects. In order to gain meaningful environmental data from the $^{13}C/^{12}C$ ratios of brachiopod shells, a greater understanding of the mechanisms of incorporation of carbon into biogenic carbonates is required.

Results from the comparison between $\delta^{18}O$ values in brachiopod and mollusc shells from the Firth of Lorne, suggest that that brachiopods are more meaningful environmental proxies.

8.3 Suggestions for future work

This study provides evidence that terebratulid and rhynchonellid brachiopods precipitate their secondary and tertiary layers in oxygen isotopic equilibrium with ambient seawater. However, the results from other extant groups with different biomineralisation regimes suggests that not all brachiopods precipitate their shells in oxygen isotopic equilibrium. Further work should be carried out to establish whether a link between shell structure and isotope incorporation exists. This would assist with interpretation of results from extinct species.

The carbon isotope composition of brachiopod shells is highly variable. Detailed physiological studies are required to investigate the effects of metabolism on the fractionation between ^{13}C in biogenic carbonate and HCO_3^- in seawater.

Different isotopic signals were obtained from aragonite and calcite samples from the bivalve *Modiolus modiolus*. A wide ranging physiological study of molluscs of mixed composition could establish whether seasonal growth patterns differ between species and if the two polymorphs of $CaCO_3$ are precipitated at different times.

Appendix A

Chronological list of samples

Chronological list of samples

Sample Number	Species	Location	Valve Number	Conjoined Valve	Valve Type	Area Sampled
0001	*Neothyris lenticularis*	Otago Shelf	NI/01	NI/08	dorsal	non-specialised secondary layer
0002	*Neothyris lenticularis*	Otago Shelf	NI/01	NI/08	dorsal	non-specialised secondary layer
0003	*Neothyris lenticularis*	Otago Shelf	NI/01	NI/08	dorsal	muscle scars
0004	*Neothyris lenticularis*	Otago Shelf	NI/01	NI/08	dorsal	muscle scars
0005	*Neothyris lenticularis*	Otago Shelf	NI/01	NI/08	dorsal	cardinal process
0006	*Neothyris lenticularis*	Otago Shelf	NI/01	NI/08	dorsal	cardinal process
0007	*Neothyris lenticularis*	Otago Shelf	NI/01	NI/08	dorsal	primary layer
0008	*Neothyris lenticularis*	Otago Shelf	NI/01	NI/08	dorsal	primary layer
0009	*Neothyris lenticularis*	Otago Shelf	NI/02	NI/09	dorsal	non-specialised secondary layer
0010	*Neothyris lenticularis*	Otago Shelf	NI/02	NI/09	dorsal	non-specialised secondary layer
0011	*Neothyris lenticularis*	Otago Shelf	NI/02	NI/09	dorsal	muscle scars
0012	*Neothyris lenticularis*	Otago Shelf	NI/02	NI/09	dorsal	muscle scars
0013	*Neothyris lenticularis*	Otago Shelf	NI/02	NI/09	dorsal	cardinal process
0014	*Neothyris lenticularis*	Otago Shelf	NI/02	NI/09	dorsal	cardinal process
0015	*Neothyris lenticularis*	Otago Shelf	NI/02	NI/09	dorsal	primary layer
0016	*Neothyris lenticularis*	Otago Shelf	NI/02	NI/09	dorsal	primary layer
0017	*Neothyris lenticularis*	Otago Shelf	NI/03	*	ventral	non-specialised secondary layer
0018	*Neothyris lenticularis*	Otago Shelf	NI/03	*	ventral	non-specialised secondary layer

(Continued on next page)

Sample Number	Species	Location	Valve Number	Conjoined Valve	Valve Type	Area Sampled
0019	*Neothyris lenticularis*	Otago Shelf	NI/03	*	ventral	teeth
0020	*Neothyris lenticularis*	Otago Shelf	NI/03	*	ventral	teeth
0021	*Neothyris lenticularis*	Otago Shelf	NI/03	*	ventral	pedicle foramen
0022	*Neothyris lenticularis*	Otago Shelf	NI/03	*	ventral	pedicle foramen
0023	*Neothyris lenticularis*	Otago Shelf	NI/03	*	ventral	muscle scars
0024	*Neothyris lenticularis*	Otago Shelf	NI/03	*	ventral	muscle scars
0025	*Neothyris lenticularis*	Otago Shelf	NI/03	*	ventral	primary layer
0026	*Neothyris lenticularis*	Otago Shelf	NI/03	*	ventral	primary layer
0027	*Neothyris lenticularis*	Otago Shelf	NI/04	NI/05	ventral	non-specialised secondary layer
0028	*Neothyris lenticularis*	Otago Shelf	NI/04	NI/05	ventral	non-specialised secondary layer
0029	*Neothyris lenticularis*	Otago Shelf	NI/04	NI/05	ventral	teeth
0030	*Neothyris lenticularis*	Otago Shelf	NI/04	NI/05	ventral	teeth
0031	*Neothyris lenticularis*	Otago Shelf	NI/04	NI/05	ventral	pedicle foramen
0032	*Neothyris lenticularis*	Otago Shelf	NI/04	NI/05	ventral	pedicle foramen
0033	*Neothyris lenticularis*	Otago Shelf	NI/04	NI/05	ventral	muscle scars
0034	*Neothyris lenticularis*	Otago Shelf	NI/04	NI/05	ventral	muscle scars
0035	*Neothyris lenticularis*	Otago Shelf	NI/04	NI/05	ventral	primary layer
0036	*Neothyris lenticularis*	Otago Shelf	NI/04	NI/05	ventral	primary layer
0037	*Terebratulina retusa*	Firth of Lorne	Tr/01	*	dorsal	loop
0038	*Terebratulina retusa*	Firth of Lorne	Tr/01	*	dorsal	non-specialised secondary layer
0039	*Terebratulina retusa*	Firth of Lorne	Tr/01	*	dorsal	non-specialised secondary layer
0040	*Terebratulina retusa*	Firth of Lorne	Tr/01	*	dorsal	muscle scars

(Continued on next page)

Sample Number	Species	Location	Valve Number	Conjoined Valve	Valve Type	Area Sampled
0041	*Terebratulina retusa*	Firth of Lorne	Tr/01	*	dorsal	internal edge
0042	*Terebratulina retusa*	Firth of Lorne	Tr/01	*	dorsal	cardinal process
0043	*Terebratulina retusa*	Firth of Lorne	Tr/01	*	dorsal	primary layer
0044	*Terebratulina retusa*	Firth of Lorne	Tr/02	Tr/03	dorsal	loop
0045	*Terebratulina retusa*	Firth of Lorne	Tr/02	Tr/03	dorsal	non-specialised secondary layer
0046	*Terebratulina retusa*	Firth of Lorne	Tr/02	Tr/03	dorsal	non-specialised secondary layer
0047	*Terebratulina retusa*	Firth of Lorne	Tr/02	Tr/03	dorsal	cardinal process
0048	*Terebratulina retusa*	Firth of Lorne	Tr/02	Tr/03	dorsal	muscle scars
0049	*Terebratulina retusa*	Firth of Lorne	Tr/02	Tr/03	dorsal	internal edge
0050	*Terebratulina retusa*	Firth of Lorne	Tr/02	Tr/03	dorsal	primary layer
0051	*Terebratulina retusa*	Firth of Lorne	Tr/03	Tr/02	ventral	non-specialised secondary layer
0052	*Terebratulina retusa*	Firth of Lorne	Tr/03	Tr/02	ventral	non-specialised secondary layer
0053	*Terebratulina retusa*	Firth of Lorne	Tr/03	Tr/02	ventral	teeth
0054	*Terebratulina retusa*	Firth of Lorne	Tr/03	Tr/02	ventral	pedicle opening
0055	*Terebratulina retusa*	Firth of Lorne	Tr/03	Tr/02	ventral	muscle scars
0056	*Terebratulina retusa*	Firth of Lorne	Tr/03	Tr/02	ventral	internal edge
0057	*Terebratulina retusa*	Firth of Lorne	Tr/03	Tr/02	ventral	primary layer
0058	*Terebratulina retusa*	Firth of Lorne	Tr/04	Tr/05	dorsal	loop
0059	*Terebratulina retusa*	Firth of Lorne	Tr/04	Tr/05	dorsal	non-specialised secondary layer
0060	*Terebratulina retusa*	Firth of Lorne	Tr/04	Tr/05	dorsal	non-specialised secondary layer
0061	*Terebratulina retusa*	Firth of Lorne	Tr/04	Tr/05	dorsal	cardinal process
0062	*Terebratulina retusa*	Firth of Lorne	Tr/04	Tr/05	dorsal	muscle scars

(Continued on next page)

Sample Number	Species	Location	Valve Number	Conjoined Valve	Valve Type	Area Sampled
0063	*Terebratulina retusa*	Firth of Lorne	Tr/04	Tr/05	dorsal	internal edge
0064	*Terebratulina retusa*	Firth of Lorne	Tr/04	Tr/05	dorsal	primary layer
0065	*Terebratulina retusa*	Firth of Lorne	Tr/05	Tr/04	ventral	non-specialised secondary layer
0066	*Terebratulina retusa*	Firth of Lorne	Tr/05	Tr/04	ventral	non-specialised secondary layer
0067	*Terebratulina retusa*	Firth of Lorne	Tr/05	Tr/04	ventral	teeth
0068	*Terebratulina retusa*	Firth of Lorne	Tr/05	Tr/04	ventral	pedicle foramen
0069	*Terebratulina retusa*	Firth of Lorne	Tr/05	Tr/04	ventral	muscle scars
0070	*Terebratulina retusa*	Firth of Lorne	Tr/05	Tr/04	ventral	internal edge
0071	*Terebratulina retusa*	Firth of Lorne	Tr/05	Tr/04	ventral	primary layer
0072	*Calloria inconspicua*	Otago Shelf	Ci/01	*	dorsal	non-specialised secondary layer
0073	*Calloria inconspicua*	Otago Shelf	Ci/01	*	dorsal	cardinal process
0074	*Calloria inconspicua*	Otago Shelf	Ci/01	*	dorsal	muscle scars
0075	*Calloria inconspicua*	Otago Shelf	Ci/01	*	dorsal	internal edge
0076	*Calloria inconspicua*	Otago Shelf	Ci/01	*	dorsal	primary layer
0077	*Calloria inconspicua*	Otago Shelf	Ci/02	*	dorsal	non-specialised secondary layer
0078	*Calloria inconspicua*	Otago Shelf	Ci/02	*	dorsal	cardinal process
0079	*Calloria inconspicua*	Otago Shelf	Ci/02	*	dorsal	muscle scars
0080	*Calloria inconspicua*	Otago Shelf	Ci/02	*	dorsal	internal edge
0081	*Calloria inconspicua*	Otago Shelf	Ci/02	*	dorsal	primary layer
0082	*Calloria inconspicua*	Otago Shelf	Ci/03	*	ventral	non-specialised secondary layer
0083	*Calloria inconspicua*	Otago Shelf	Ci/03	*	ventral	teeth
0084	*Calloria inconspicua*	Otago Shelf	Ci/03	*	ventral	pedicle foramen

(Continued on next page)

Sample Number	Species	Location	Valve Number	Conjoined Valve	Valve Type	Area Sampled
0085	*Calloria inconspicua*	Otago Shelf	Ci/03	*	ventral	muscle scars
0086	*Calloria inconspicua*	Otago Shelf	Ci/03	*	ventral	internal edge
0087	*Calloria inconspicua*	Otago Shelf	Ci/03	*	ventral	primary layer
0088	*Calloria inconspicua*	Otago Shelf	Ci/04	*	ventral	non-specialised secondary layer
0089	*Calloria inconspicua*	Otago Shelf	Ci/04	*	ventral	teeth
0090	*Calloria inconspicua*	Otago Shelf	Ci/04	*	ventral	pedicle foramen
0091	*Calloria inconspicua*	Otago Shelf	Ci/04	*	ventral	muscle scars
0092	*Calloria inconspicua*	Otago Shelf	Ci/04	*	ventral	internal edge
0093	*Calloria inconspicua*	Otago Shelf	Ci/04	*	ventral	primary layer
0094	*Notosaria nigricans*	Otago Shelf	Nn/01	*	dorsal	non-specialised secondary layer
0095	*Notosaria nigricans*	Otago Shelf	Nn/01	*	dorsal	cardinal process
0096	*Notosaria nigricans*	Otago Shelf	Nn/01	*	dorsal	muscle scars
0097	*Notosaria nigricans*	Otago Shelf	Nn/01	*	dorsal	internal edge
0098	*Notosaria nigricans*	Otago Shelf	Nn/01	*	dorsal	primary layer
0099	*Notosaria nigricans*	Otago Shelf	Nn/02	*	dorsal	non-specialised secondary layer
0100	*Notosaria nigricans*	Otago Shelf	Nn/02	*	dorsal	cardinal process
0101	*Notosaria nigricans*	Otago Shelf	Nn/02	*	dorsal	muscle scars
0102	*Notosaria nigricans*	Otago Shelf	Nn/02	*	dorsal	internal edge
0103	*Notosaria nigricans*	Otago Shelf	Nn/02	*	dorsal	primary layer
0104	*Notosaria nigricans*	Otago Shelf	Nn/03	*	ventral	non-specialised secondary layer
0105	*Notosaria nigricans*	Otago Shelf	Nn/03	*	ventral	teeth
0106	*Notosaria nigricans*	Otago Shelf	Nn/03	*	ventral	pedicle foramen

(Continued on next page)

Sample Number	Species	Location	Valve Number	Conjoined Valve	Valve Type	Area Sampled
0107	*Notosaria nigricans*	Otago Shelf	Nn/03	*	ventral	muscle scars
0108	*Notosaria nigricans*	Otago Shelf	Nn/03	*	ventral	internal edge
0109	*Notosaria nigricans*	Otago Shelf	Nn/03	*	ventral	primary layer
0110	*Notosaria nigricans*	Otago Shelf	Nn/04	*	ventral	non-specialised secondary layer
0111	*Notosaria nigricans*	Otago Shelf	Nn/04	*	ventral	teeth
0112	*Notosaria nigricans*	Otago Shelf	Nn/04	*	ventral	pedicle foramen
0113	*Notosaria nigricans*	Otago Shelf	Nn/04	*	ventral	muscle scars
0114	*Notosaria nigricans*	Otago Shelf	Nn/04	*	ventral	internal edge
0115	*Notosaria nigricans*	Otago Shelf	Nn/04	*	ventral	primary layer
0116	*Novocrania anomala*	Otago Shelf	Na/01	*	dorsal	non-specialised secondary layer
0117	*Novocrania anomala*	Otago Shelf	Na/01	*	dorsal	muscle scars
0118	*Novocrania anomala*	Otago Shelf	Na/01	*	dorsal	internal edge
0119	*Novocrania anomala*	Otago Shelf	Na/01	*	dorsal	primary layer
0120	*Novocrania anomala*	Otago Shelf	Na/02	*	dorsal	non-specialised secondary layer
0121	*Novocrania anomala*	Otago Shelf	Na/02	*	dorsal	muscle scars
0122	*Novocrania anomala*	Otago Shelf	Na/02	*	dorsal	internal edge
0123	*Novocrania anomala*	Otago Shelf	Na/02	*	dorsal	primary layer
0124	*Neothyris lenticularis*	Otago Shelf	Nl/05	Nl/04	dorsal	non-specialised secondary layer
0125	*Neothyris lenticularis*	Otago Shelf	Nl/05	Nl/04	dorsal	muscle scars
0126	*Neothyris lenticularis*	Otago Shelf	Nl/05	Nl/04	dorsal	cardinal process
0127	*Neothyris lenticularis*	Otago Shelf	Nl/05	Nl/04	dorsal	primary layer
0128	*Neothyris lenticularis*	Otago Shelf	Nl/06	Nl/10	ventral	non-specialised secondary layer

(Continued on next page)

Sample Number	Species	Location	Valve Number	Conjoined Valve	Valve Type	Area Sampled
0129	*Neothyris lenticularis*	Otago Shelf	NI/06	NI/10	ventral	teeth
0130	*Neothyris lenticularis*	Otago Shelf	NI/06	NI/10	ventral	pedicle foramen
0131	*Neothyris lenticularis*	Otago Shelf	NI/06	NI/10	ventral	muscle scars
0132	*Neothyris lenticularis*	Otago Shelf	NI/06	NI/10	ventral	primary layer
0133	*Neothyris lenticularis*	Otago Shelf	NI/07	*	dorsal	non-specialised secondary layer
0134	*Neothyris lenticularis*	Otago Shelf	NI/07	*	dorsal	muscle scars
0135	*Neothyris lenticularis*	Otago Shelf	NI/07	*	dorsal	cardinal process
0136	*Neothyris lenticularis*	Otago Shelf	NI/07	*	dorsal	primary layer
0137	*Neothyris lenticularis*	Otago Shelf	NI/08	NI/01	ventral	non-specialised secondary layer
0138	*Neothyris lenticularis*	Otago Shelf	NI/08	NI/01	ventral	teeth
0139	*Neothyris lenticularis*	Otago Shelf	NI/08	NI/01	ventral	pedicle foramen
0140	*Neothyris lenticularis*	Otago Shelf	NI/08	NI/01	ventral	muscle scars
0141	*Neothyris lenticularis*	Otago Shelf	NI/08	NI/01	ventral	primary layer
0142	*Terebratulina retusa*	Firth of Lorne	Tr/06	Tr/07	dorsal	loop
0143	*Terebratulina retusa*	Firth of Lorne	Tr/06	Tr/07	dorsal	secondary layer
0144	*Terebratulina retusa*	Firth of Lorne	Tr/06	Tr/07	dorsal	cardinal process
0145	*Terebratulina retusa*	Firth of Lorne	Tr/06	Tr/07	dorsal	muscle scars
0146	*Terebratulina retusa*	Firth of Lorne	Tr/06	Tr/07	dorsal	primary layer
0147	*Terebratulina retusa*	Firth of Lorne	Tr/07	Tr/06	ventral	non-specialised secondary layer
0148	*Terebratulina retusa*	Firth of Lorne	Tr/07	Tr/06	ventral	teeth
0149	*Terebratulina retusa*	Firth of Lorne	Tr/07	Tr/06	ventral	pedicle foramen
0150	*Terebratulina retusa*	Firth of Lorne	Tr/07	Tr/06	ventral	muscle scars

(Continued on next page)

Sample Number	Species	Location	Valve Number	Conjoined Valve	Valve Type	Area Sampled
0151	*Terebratulina retusa*	Firth of Lorne	Tr/07	Tr/06	ventral	primary layer
0152	*Terebratulina retusa*	Firth of Lorne	Tr/08	Tr/09	dorsal	loop
0153	*Terebratulina retusa*	Firth of Lorne	Tr/08	Tr/09	dorsal	non-specialised secondary layer
0154	*Terebratulina retusa*	Firth of Lorne	Tr/08	Tr/09	dorsal	cardinal process
0155	*Terebratulina retusa*	Firth of Lorne	Tr/08	Tr/09	dorsal	muscle scars
0156	*Terebratulina retusa*	Firth of Lorne	Tr/08	Tr/09	dorsal	primary layer
0157	*Terebratulina retusa*	Firth of Lorne	Tr/09	Tr/08	ventral	non-specialised secondary layer
0158	*Terebratulina retusa*	Firth of Lorne	Tr/09	Tr/08	ventral	teeth
0159	*Terebratulina retusa*	Firth of Lorne	Tr/09	Tr/08	ventral	pedicle foramen
0160	*Terebratulina retusa*	Firth of Lorne	Tr/09	Tr/08	ventral	muscle scars
0161	*Terebratulina retusa*	Firth of Lorne	Tr/09	Tr/08	ventral	primary layer
0162	*Calloria inconspicua*	Otago Shelf	Ci/05	Ci/06	dorsal	loop
0163	*Calloria inconspicua*	Otago Shelf	Ci/05	Ci/06	dorsal	non-specialised secondary layer
0164	*Calloria inconspicua*	Otago Shelf	Ci/05	Ci/06	dorsal	cardinal process
0165	*Calloria inconspicua*	Otago Shelf	Ci/05	Ci/06	dorsal	muscle scars
0166	*Calloria inconspicua*	Otago Shelf	Ci/05	Ci/06	dorsal	primary layer
0167	*Calloria inconspicua*	Otago Shelf	Ci/06	Ci/05	ventral	non-specialised secondary layer
0168	*Calloria inconspicua*	Otago Shelf	Ci/06	Ci/05	ventral	teeth
0169	*Calloria inconspicua*	Otago Shelf	Ci/06	Ci/05	ventral	pedicle foramen
0170	*Calloria inconspicua*	Otago Shelf	Ci/06	Ci/05	ventral	muscle scars
0171	*Calloria inconspicua*	Otago Shelf	Ci/06	Ci/05	ventral	primary layer
0172	*Calloria inconspicua*	Otago Shelf	Ci/07	Ci/08	dorsal	loop

(Continued on next page)

Sample Number	Species	Location	Valve Number	Conjoined Valve	Valve Type	Area Sampled
0173	*Calloria inconspicua*	Otago Shelf	Ci/07	Ci/08	dorsal	non-specialised secondary layer
0174	*Calloria inconspicua*	Otago Shelf	Ci/07	Ci/08	dorsal	cardinal process
0175	*Calloria inconspicua*	Otago Shelf	Ci/07	Ci/08	dorsal	muscle scars
0176	*Calloria inconspicua*	Otago Shelf	Ci/07	Ci/08	dorsal	primary layer
0177	*Calloria inconspicua*	Otago Shelf	Ci/08	Ci/07	ventral	non-specialised secondary layer
0178	*Calloria inconspicua*	Otago Shelf	Ci/08	Ci/07	ventral	teeth
0179	*Calloria inconspicua*	Otago Shelf	Ci/08	Ci/07	ventral	pedicle foramen
0180	*Calloria inconspicua*	Otago Shelf	Ci/08	Ci/07	ventral	muscle scars
0181	*Calloria inconspicua*	Otago Shelf	Ci/08	Ci/07	ventral	primary layer
0182	*Notosaria nigricans*	Otago Shelf	Nn/05	Nn/06	dorsal	loop
0183	*Notosaria nigricans*	Otago Shelf	Nn/05	Nn/06	dorsal	non-specialised secondary layer
0184	*Notosaria nigricans*	Otago Shelf	Nn/05	Nn/06	dorsal	cardinal process
0185	*Notosaria nigricans*	Otago Shelf	Nn/05	Nn/06	dorsal	muscle scars
0186	*Notosaria nigricans*	Otago Shelf	Nn/05	Nn/06	dorsal	primary layer
0187	*Notosaria nigricans*	Otago Shelf	Nn/06	Nn/05	ventral	non-specialised secondary layer
0188	*Notosaria nigricans*	Otago Shelf	Nn/06	Nn/05	ventral	teeth
0189	*Notosaria nigricans*	Otago Shelf	Nn/06	Nn/05	ventral	pedicle foramen
0190	*Notosaria nigricans*	Otago Shelf	Nn/06	Nn/05	ventral	muscle scars
0191	*Notosaria nigricans*	Otago Shelf	Nn/06	Nn/05	ventral	primary layer
0192	*Notosaria nigricans*	Otago Shelf	Nn/07	Nn/08	dorsal	loop
0193	*Notosaria nigricans*	Otago Shelf	Nn/07	Nn/08	dorsal	non-specialised secondary layer
0194	*Notosaria nigricans*	Otago Shelf	Nn/07	Nn/08	dorsal	cardinal process

(Continued on next page)

Sample Number	Species	Location	Valve Number	Conjoined Valve	Valve Type	Area Sampled
0195	*Notosaria nigricans*	Otago Shelf	Nn/07	Nn/08	dorsal	muscle scars
0196	*Notosaria nigricans*	Otago Shelf	Nn/07	Nn/08	dorsal	primary layer
0197	*Notosaria nigricans*	Otago Shelf	Nn/08	Nn/07	ventral	non-specialised secondary layer
0198	*Notosaria nigricans*	Otago Shelf	Nn/08	Nn/07	ventral	teeth
0199	*Notosaria nigricans*	Otago Shelf	Nn/08	Nn/07	ventral	pedicle foramen
0200	*Notosaria nigricans*	Otago Shelf	Nn/08	Nn/07	ventral	muscle scars
0201	*Notosaria nigricans*	Otago Shelf	Nn/08	Nn/07	ventral	primary layer
0202	*Novocrania anomala*	Otago Shelf	Na/03	*	dorsal	non-specialised secondary layer
0203	*Novocrania anomala*	Otago Shelf	Na/03	*	dorsal	muscle scars
0204	*Novocrania anomala*	Otago Shelf	Na/03	*	dorsal	primary layer
0205	*Novocrania anomala*	Otago Shelf	Na/04	*	dorsal	non-specialised secondary layer
0206	*Novocrania anomala*	Otago Shelf	Na/04	*	dorsal	muscle scars
0207	*Novocrania anomala*	Otago Shelf	Na/04	*	dorsal	muscle scars
0208	*Laqueus rubellus*	Sagami Bay	Lr/01	Lr/02	dorsal	loop
0209	*Laqueus rubellus*	Sagami Bay	Lr/01	Lr/02	dorsal	non-specialised secondary layer
0210	*Laqueus rubellus*	Sagami Bay	Lr/01	Lr/02	dorsal	cardinal process
0211	*Laqueus rubellus*	Sagami Bay	Lr/01	Lr/02	dorsal	muscle scars
0212	*Laqueus rubellus*	Sagami Bay	Lr/01	Lr/02	dorsal	primary layer
0213	*Laqueus rubellus*	Sagami Bay	Lr/02	Lr/01	ventral	non-specialised secondary layer
0214	*Laqueus rubellus*	Sagami Bay	Lr/02	Lr/01	ventral	teeth
0215	*Laqueus rubellus*	Sagami Bay	Lr/02	Lr/01	ventral	pedicle foramen
0216	*Laqueus rubellus*	Sagami Bay	Lr/02	Lr/01	ventral	muscle scars

(Continued on next page)

Sample Number	Species	Location	Valve Number	Conjoined Valve	Valve Type	Area Sampled
0217	*Laqueus rubellus*	Sagami Bay	Lr/02	Lr/01	ventral	primary layer
0218	*Laqueus rubellus*	Sagami Bay	Lr/03	Lr/04	dorsal	loop
0219	*Laqueus rubellus*	Sagami Bay	Lr/03	Lr/04	dorsal	non-specialised secondary layer
0220	*Laqueus rubellus*	Sagami Bay	Lr/03	Lr/04	dorsal	cardinal process
0221	*Laqueus rubellus*	Sagami Bay	Lr/03	Lr/04	dorsal	muscle scars
0222	*Laqueus rubellus*	Sagami Bay	Lr/03	Lr/04	dorsal	primary layer
0223	*Laqueus rubellus*	Sagami Bay	Lr/04	Lr/03	ventral	non-specialised secondary layer
0224	*Laqueus rubellus*	Sagami Bay	Lr/04	Lr/03	ventral	teeth
0225	*Laqueus rubellus*	Sagami Bay	Lr/04	Lr/03	ventral	pedicle foramen
0226	*Laqueus rubellus*	Sagami Bay	Lr/04	Lr/03	ventral	muscle scars
0227	*Laqueus rubellus*	Sagami Bay	Lr/04	Lr/03	ventral	primary layer
0228	*Terebratalia transversa*	Friday Harbor	Tt/01	Tt/02	dorsal	loop
0229	*Terebratalia transversa*	Friday Harbor	Tt/01	Tt/02	dorsal	non-specialised secondary layer
0230	*Terebratalia transversa*	Friday Harbor	Tt/01	Tt/02	dorsal	cardinal process
0231	*Terebratalia transversa*	Friday Harbor	Tt/01	Tt/02	dorsal	muscle scars
0232	*Terebratalia transversa*	Friday Harbor	Tt/01	Tt/02	dorsal	primary layer
0233	*Terebratalia transversa*	Friday Harbor	Tt/02	Tt/01	ventral	non-specialised secondary layer
0234	*Terebratalia transversa*	Friday Harbor	Tt/02	Tt/01	ventral	teeth
0235	*Terebratalia transversa*	Friday Harbor	Tt/02	Tt/01	ventral	pedicle foramen
0236	*Terebratalia transversa*	Friday Harbor	Tt/02	Tt/01	ventral	muscle scars
0237	*Terebratalia transversa*	Friday Harbor	Tt/02	Tt/01	ventral	primary layer
0238	*Terebratalia transversa*	Friday Harbor	Tt/03	Tt/04	dorsal	loop

(Continued on next page)

Sample Number	Species	Location	Valve Number	Conjoined Valve	Valve Type	Area Sampled
0239	*Terebratalia transversa*	Friday Harbor	Tt/03	Tt/04	dorsal	non-specialised secondary layer
0240	*Terebratalia transversa*	Friday Harbor	Tt/03	Tt/04	dorsal	cardinal process
0241	*Terebratalia transversa*	Friday Harbor	Tt/03	Tt/04	dorsal	muscle scars
0242	*Terebratalia transversa*	Friday Harbor	Tt/03	Tt/04	dorsal	primary layer
0243	*Terebratalia transversa*	Friday Harbor	Tt/04	Tt/03	ventral	non-specialised secondary layer
0244	*Terebratalia transversa*	Friday Harbor	Tt/04	Tt/03	ventral	teeth
0245	*Terebratalia transversa*	Friday Harbor	Tt/04	Tt/03	ventral	pedicle foramen
0246	*Terebratalia transversa*	Friday Harbor	Tt/04	Tt/03	ventral	muscle scars
0247	*Terebratalia transversa*	Friday Harbor	Tt/04	Tt/03	ventral	primary layer
0248	*Terebratella sanguinea*	Otago Shelf	Ts/01	Ts/02	dorsal	loop
0249	*Terebratella sanguinea*	Otago Shelf	Ts/01	Ts/02	dorsal	non-specialised secondary layer
0250	*Terebratella sanguinea*	Otago Shelf	Ts/01	Ts/02	dorsal	cardinal process
0251	*Terebratella sanguinea*	Otago Shelf	Ts/01	Ts/02	dorsal	muscle scars
0252	*Terebratella sanguinea*	Otago Shelf	Ts/01	Ts/02	dorsal	primary layer
0253	*Terebratella sanguinea*	Otago Shelf	Ts/02	Ts/01	ventral	non-specialised secondary layer
0254	*Terebratella sanguinea*	Otago Shelf	Ts/02	Ts/01	ventral	teeth
0255	*Terebratella sanguinea*	Otago Shelf	Ts/02	Ts/01	ventral	pedicle foramen
0256	*Terebratella sanguinea*	Otago Shelf	Ts/02	Ts/01	ventral	muscle scars
0257	*Terebratella sanguinea*	Otago Shelf	Ts/02	Ts/01	ventral	primary layer
0258	*Terebratella sanguinea*	Otago Shelf	Ts/03	Ts/04	dorsal	loop
0259	*Terebratella sanguinea*	Otago Shelf	Ts/03	Ts/04	dorsal	non-specialised secondary layer
0260	*Terebratella sanguinea*	Otago Shelf	Ts/03	Ts/04	dorsal	cardinal process

(Continued on next page)

Sample Number	Species	Location	Valve Number	Conjoined Valve	Valve Type	Area Sampled
0261	*Terebratella sanguinea*	Otago Shelf	Ts/03	Ts/04	dorsal	muscle scars
0262	*Terebratella sanguinea*	Otago Shelf	Ts/03	Ts/04	dorsal	primary layer
0263	*Terebratella sanguinea*	Otago Shelf	Ts/04	Ts/03	ventral	non-specialised secondary layer
0264	*Terebratella sanguinea*	Otago Shelf	Ts/04	Ts/03	ventral	teeth
0265	*Terebratella sanguinea*	Otago Shelf	Ts/04	Ts/03	ventral	pedicle foramen
0266	*Terebratella sanguinea*	Otago Shelf	Ts/04	Ts/03	ventral	muscle scars
2067	*Terebratella sanguinea*	Otago Shelf	Ts/04	Ts/03	ventral	primary layer
0268	*Neothyris lenticularis*	Otago Shelf	Nl/09	Nl/02	ventral	loop
0269	*Neothyris lenticularis*	Otago Shelf	Nl/09	Nl/02	ventral	non-specialised secondary layer
0270	*Neothyris lenticularis*	Otago Shelf	Nl/09	Nl/02	ventral	cardinal process
0271	*Neothyris lenticularis*	Otago Shelf	Nl/09	Nl/02	ventral	muscle scars
0272	*Neothyris lenticularis*	Otago Shelf	Nl/09	Nl/02	ventral	primary layer
0273	*Neothyris lenticularis*	Otago Shelf	Nl/10	Nl/06	ventral	non-specialised secondary layer
0274	*Neothyris lenticularis*	Otago Shelf	Nl/10	Nl/06	ventral	teeth
0275	*Neothyris lenticularis*	Otago Shelf	Nl/10	Nl/06	ventral	pedicle foramen
0276	*Neothyris lenticularis*	Otago Shelf	Nl/10	Nl/06	ventral	muscle scars
0277	*Neothyris lenticularis*	Otago Shelf	Nl/10	Nl/06	ventral	primary layer
0278	*Neothyris lenticularis*	Otago Shelf	Nl/11	Nl/12	dorsal	loop
0279	*Neothyris lenticularis*	Otago Shelf	Nl/11	Nl/12	dorsal	non-specialised secondary layer
0280	*Neothyris lenticularis*	Otago Shelf	Nl/11	Nl/12	dorsal	cardinal process
0281	*Neothyris lenticularis*	Otago Shelf	Nl/11	Nl/12	dorsal	muscle scars
0282	*Neothyris lenticularis*	Otago Shelf	Nl/11	Nl/12	dorsal	primary layer

(Continued on next page)

Sample Number	Species	Location	Valve Number	Conjoined Valve	Valve Type	Area Sampled
0283	*Neothyris lenticularis*	Otago Shelf	NI/12	NI/11	ventral	non-specialised secondary layer
0284	*Neothyris lenticularis*	Otago Shelf	NI/12	NI/11	ventral	teeth
0285	*Neothyris lenticularis*	Otago Shelf	NI/12	NI/11	ventral	pedicle foramen
0286	*Neothyris lenticularis*	Otago Shelf	NI/12	NI/11	ventral	muscle scars
0287	*Neothyris lenticularis*	Otago Shelf	NI/12	NI/11	ventral	primary layer
0288	*Neothyris lenticularis*	Otago Shelf	NI/05	NI/04	dorsal	Loop
0289	*Neothyris lenticularis*	Otago Shelf	NI/06	NI/10	dorsal	Loop
0290	*Neothyris lenticularis*	Otago Shelf	NI/01	NI/08	dorsal	Loop
0291	*Neothyris lenticularis*	Otago Shelf	NI/08	NI/01	dorsal	Loop
0292	*Terebratulina retusa*	Firth of Lorne	Tr/10	Tr/11	dorsal	loop
0293	*Terebratulina retusa*	Firth of Lorne	Tr/10	Tr/11	dorsal	non-specialised secondary layer
0294	*Terebratulina retusa*	Firth of Lorne	Tr/10	Tr/11	dorsal	cardinal process
0295	*Terebratulina retusa*	Firth of Lorne	Tr/10	Tr/11	dorsal	muscle scars
0296	*Terebratulina retusa*	Firth of Lorne	Tr/10	Tr/11	dorsal	primary layer
0297	*Terebratulina retusa*	Firth of Lorne	Tr/11	Tr/10	ventral	non-specialised secondary layer
0298	*Terebratulina retusa*	Firth of Lorne	Tr/11	Tr/10	ventral	teeth
0299	*Terebratulina retusa*	Firth of Lorne	Tr/11	Tr/10	ventral	pedicle foramen
0300	*Terebratulina retusa*	Firth of Lorne	Tr/11	Tr/10	ventral	muscle scars
0301	*Terebratulina retusa*	Firth of Lorne	Tr/11	Tr/10	ventral	primary layer
0302	*Terebratulina retusa*	Firth of Lorne	Tr/12	Tr/13	dorsal	loop
0303	*Terebratulina retusa*	Firth of Lorne	Tr/12	Tr/13	dorsal	non-specialised secondary layer
0304	*Terebratulina retusa*	Firth of Lorne	Tr/12	Tr/13	dorsal	cardinal process

(Continued on next page)

Sample Number	Species	Location	Valve Number	Conjoined Valve	Valve Type	Area Sampled
0305	*Terebratulina retusa*	Firth of Lorne	Tr/12	Tr/13	dorsal	muscle scars
0306	*Terebratulina retusa*	Firth of Lorne	Tr/12	Tr/13	dorsal	primary layer
0307	*Terebratulina retusa*	Firth of Lorne	Tr/13	Tr/12	ventral	non-specialised secondary layer
0308	*Terebratulina retusa*	Firth of Lorne	Tr/13	Tr/12	ventral	teeth
0309	*Terebratulina retusa*	Firth of Lorne	Tr/13	Tr/12	ventral	pedicle foramen
0310	*Terebratulina retusa*	Firth of Lorne	Tr/13	Tr/12	ventral	muscle scars
0311	*Terebratulina retusa*	Firth of Lorne	Tr/13	Tr/12	ventral	primary layer
0312	*Calloria inconspicua*	Otago Shelf	Ci/09	Ci/10	dorsal	loop
0313	*Calloria inconspicua*	Otago Shelf	Ci/09	Ci/10	dorsal	non-specialised secondary layer
0314	*Calloria inconspicua*	Otago Shelf	Ci/09	Ci/10	dorsal	cardinal process
0315	*Calloria inconspicua*	Otago Shelf	Ci/09	Ci/10	dorsal	muscle scars
0316	*Calloria inconspicua*	Otago Shelf	Ci/09	Ci/10	dorsal	primary layer
0317	*Calloria inconspicua*	Otago Shelf	Ci/10	Ci/09	ventral	non-specialised secondary layer
0318	*Calloria inconspicua*	Otago Shelf	Ci/10	Ci/09	ventral	teeth
0319	*Calloria inconspicua*	Otago Shelf	Ci/10	Ci/09	ventral	pedicle foramen
0320	*Calloria inconspicua*	Otago Shelf	Ci/10	Ci/09	ventral	muscle scars
0321	*Calloria inconspicua*	Otago Shelf	Ci/10	Ci/09	ventral	primary layer
0322	*Calloria inconspicua*	Otago Shelf	Ci/11	Ci/12	dorsal	loop
0323	*Calloria inconspicua*	Otago Shelf	Ci/11	Ci/12	dorsal	non-specialised secondary layer
0324	*Calloria inconspicua*	Otago Shelf	Ci/11	Ci/12	dorsal	cardinal process
0325	*Calloria inconspicua*	Otago Shelf	Ci/11	Ci/12	dorsal	muscle scars
0326	*Calloria inconspicua*	Otago Shelf	Ci/11	Ci/12	dorsal	primary layer

(Continued on next page)

Sample Number	Species	Location	Valve Number	Conjoined Valve	Valve Type	Area Sampled
0327	*Calloria inconspicua*	Otago Shelf	Ci/12	Ci/11	ventral	non-specialised secondary layer
0328	*Calloria inconspicua*	Otago Shelf	Ci/12	Ci/11	ventral	teeth
0329	*Calloria inconspicua*	Otago Shelf	Ci/12	Ci/11	ventral	pedicle foramen
0330	*Calloria inconspicua*	Otago Shelf	Ci/12	Ci/11	ventral	muscle scars
0331	*Calloria inconspicua*	Otago Shelf	Ci/12	Ci/11	ventral	primary layer
0332	*Notosaria nigricans*	Otago Shelf	Nn/09	Nn/10	dorsal	loop
0333	*Notosaria nigricans*	Otago Shelf	Nn/09	Nn/10	dorsal	non-specialised secondary layer
0334	*Notosaria nigricans*	Otago Shelf	Nn/09	Nn/10	dorsal	cardinal process
0335	*Notosaria nigricans*	Otago Shelf	Nn/09	Nn/10	dorsal	muscle scars
0336	*Notosaria nigricans*	Otago Shelf	Nn/09	Nn/10	dorsal	primary layer
0337	*Notosaria nigricans*	Otago Shelf	Nn/10	Nn/09	ventral	non-specialised secondary layer
0338	*Notosaria nigricans*	Otago Shelf	Nn/10	Nn/09	ventral	teeth
0339	*Notosaria nigricans*	Otago Shelf	Nn/10	Nn/09	ventral	pedicle foramen
0340	*Notosaria nigricans*	Otago Shelf	Nn/10	Nn/09	ventral	muscle scars
0341	*Notosaria nigricans*	Otago Shelf	Nn/10	Nn/09	ventral	primary layer
0342	*Notosaria nigricans*	Otago Shelf	Nn/11	Nn/12	dorsal	loop
0343	*Notosaria nigricans*	Otago Shelf	Nn/11	Nn/12	dorsal	non-specialised secondary layer
0344	*Notosaria nigricans*	Otago Shelf	Nn/11	Nn/12	dorsal	cardinal process
0345	*Notosaria nigricans*	Otago Shelf	Nn/11	Nn/12	dorsal	muscle scars
0346	*Notosaria nigricans*	Otago Shelf	Nn/11	Nn/12	dorsal	primary layer
0347	*Notosaria nigricans*	Otago Shelf	Nn/12	Nn/11	ventral	non-specialised secondary layer
0348	*Notosaria nigricans*	Otago Shelf	Nn/12	Nn/11	ventral	teeth

(Continued on next page)

Sample Number	Species	Location	Valve Number	Conjoined Valve	Valve Type	Area Sampled
0349	*Notosaria nigricans*	Otago Shelf	Nn/12	Nn/11	ventral	pedicle foramen
0350	*Notosaria nigricans*	Otago Shelf	Nn/12	Nn/11	ventral	muscle scars
0351	*Notosaria nigricans*	Otago Shelf	Nn/12	Nn/11	ventral	primary layer
0352	*Novocrania anomala*	Firth of Lorne	Na/05	*	dorsal	non-specialised secondary layer
0353	*Novocrania anomala*	Firth of Lorne	Na/05	*	dorsal	muscle scars
0354	*Novocrania anomala*	Firth of Lorne	Na/05	*	dorsal	primary layer
0355	*Novocrania anomala*	Firth of Lorne	Na/06	*	dorsal	non-specialised secondary layer
0356	*Novocrania anomala*	Firth of Lorne	Na/06	*	dorsal	muscle scars
0357	*Novocrania anomala*	Firth of Lorne	Na/06	*	dorsal	primary layer
0358	*Laqueus rubellus*	Sagami Bay	Lr/05	Lr/06	dorsal	loop
0359	*Laqueus rubellus*	Sagami Bay	Lr/05	Lr/06	dorsal	non-specialised secondary layer
0360	*Laqueus rubellus*	Sagami Bay	Lr/05	Lr/06	dorsal	cardinal process
0361	*Laqueus rubellus*	Sagami Bay	Lr/05	Lr/06	dorsal	muscle scars
0362	*Laqueus rubellus*	Sagami Bay	Lr/05	Lr/06	dorsal	primary layer
0363	*Laqueus rubellus*	Sagami Bay	Lr/06	Lr/05	ventral	non-specialised secondary layer
0364	*Laqueus rubellus*	Sagami Bay	Lr/06	Lr/05	ventral	teeth
0365	*Laqueus rubellus*	Sagami Bay	Lr/06	Lr/05	ventral	pedicle foramen
0366	*Laqueus rubellus*	Sagami Bay	Lr/06	Lr/05	ventral	muscle scars
0367	*Laqueus rubellus*	Sagami Bay	Lr/06	Lr/05	ventral	primary layer
0368	*Laqueus rubellus*	Sagami Bay	Lr/07	Lr/08	dorsal	loop
0369	*Laqueus rubellus*	Sagami Bay	Lr/07	Lr/08	dorsal	non-specialised secondary layer
0370	*Laqueus rubellus*	Sagami Bay	Lr/07	Lr/08	dorsal	cardinal process

(Continued on next page)

Sample Number	Species	Location	Valve Number	Conjoined Valve	Valve Type	Area Sampled
0371	*Laqueus rubellus*	Sagami Bay	Lr/07	Lr/08	dorsal	muscle scars
0372	*Laqueus rubellus*	Sagami Bay	Lr/07	Lr/08	dorsal	primary layer
0373	*Laqueus rubellus*	Sagami Bay	Lr/08	Lr/07	ventral	non-specialised secondary layer
0374	*Laqueus rubellus*	Sagami Bay	Lr/08	Lr/07	ventral	teeth
0375	*Laqueus rubellus*	Sagami Bay	Lr/08	Lr/07	ventral	pedicle foramen
0376	*Laqueus rubellus*	Sagami Bay	Lr/08	Lr/07	ventral	muscle scars
0377	*Laqueus rubellus*	Sagami Bay	Lr/08	Lr/07	ventral	primary layer
0378	*Terebratalia transversa*	Friday Harbor	Tt/05	Tt/06	dorsal	loop
0379	*Terebratalia transversa*	Friday Harbor	Tt/05	Tt/06	dorsal	non-specialised secondary layer
0380	*Terebratalia transversa*	Friday Harbor	Tt/05	Tt/06	dorsal	cardinal process
0381	*Terebratalia transversa*	Friday Harbor	Tt/05	Tt/06	dorsal	muscle scars
0382	*Terebratalia transversa*	Friday Harbor	Tt/05	Tt/06	dorsal	primary layer
0383	*Terebratalia transversa*	Friday Harbor	Tt/06	Tt/05	ventral	non-specialised secondary layer
0384	*Terebratalia transversa*	Friday Harbor	Tt/06	Tt/05	ventral	teeth
0385	*Terebratalia transversa*	Friday Harbor	Tt/06	Tt/05	ventral	pedicle foramen
0386	*Terebratalia transversa*	Friday Harbor	Tt/06	Tt/05	ventral	muscle scars
0387	*Terebratalia transversa*	Friday Harbor	Tt/06	Tt/05	ventral	primary layer
0388	*Terebratalia transversa*	Friday Harbor	Tt/07	Tt/08	dorsal	loop
0389	*Terebratalia transversa*	Friday Harbor	Tt/07	Tt/08	dorsal	non-specialised secondary layer
0390	*Terebratalia transversa*	Friday Harbor	Tt/07	Tt/08	dorsal	cardinal process
0391	*Terebratalia transversa*	Friday Harbor	Tt/07	Tt/08	dorsal	muscle scars
0392	*Terebratalia transversa*	Friday Harbor	Tt/07	Tt/08	dorsal	primary layer

(Continued on next page)

Sample Number	Species	Location	Valve Number	Conjoined Valve	Valve Type	Area Sampled
0393	*Terebratalia transversa*	Friday Harbor	Tt/08	Tt/07	ventral	non-specialised secondary layer
0394	*Terebratalia transversa*	Friday Harbor	Tt/08	Tt/07	ventral	teeth
0395	*Terebratalia transversa*	Friday Harbor	Tt/08	Tt/07	ventral	pedicle foramen
0396	*Terebratalia transversa*	Friday Harbor	Tt/08	Tt/07	ventral	muscle scars
0397	*Terebratalia transversa*	Friday Harbor	Tt/08	Tt/07	ventral	primary layer
0398	*Terebratella sanguinea*	Otago Shelf	Ts/05	Ts/06	dorsal	loop
0399	*Terebratella sanguinea*	Otago Shelf	Ts/05	Ts/06	dorsal	non-specialised secondary layer
0400	*Terebratella sanguinea*	Otago Shelf	Ts/05	Ts/06	dorsal	cardinal process
0401	*Terebratella sanguinea*	Otago Shelf	Ts/05	Ts/06	dorsal	muscle scars
0402	*Terebratella sanguinea*	Otago Shelf	Ts/05	Ts/06	dorsal	primary layer
0403	*Terebratella sanguinea*	Otago Shelf	Ts/06	Ts/05	ventral	non-specialised secondary layer
0404	*Terebratella sanguinea*	Otago Shelf	Ts/06	Ts/05	ventral	teeth
0405	*Terebratella sanguinea*	Otago Shelf	Ts/06	Ts/05	ventral	pedicle foramen
0406	*Terebratella sanguinea*	Otago Shelf	Ts/06	Ts/05	ventral	muscle scars
0407	*Terebratella sanguinea*	Otago Shelf	Ts/06	Ts/05	ventral	primary layer
0408	*Terebratella sanguinea*	Otago Shelf	Ts/07	Ts/08	dorsal	loop
0409	*Terebratella sanguinea*	Otago Shelf	Ts/07	Ts/08	dorsal	non-specialised secondary layer
0410	*Terebratella sanguinea*	Otago Shelf	Ts/07	Ts/08	dorsal	cardinal process
0411	*Terebratella sanguinea*	Otago Shelf	Ts/07	Ts/08	dorsal	muscle scars
0412	*Terebratella sanguinea*	Otago Shelf	Ts/07	Ts/08	dorsal	primary layer
0413	*Terebratella sanguinea*	Otago Shelf	Ts/08	Ts/07	ventral	non-specialised secondary layer
0414	*Terebratella sanguinea*	Otago Shelf	Ts/08	Ts/07	ventral	teeth

(Continued on next page)

Sample Number	Species	Location	Valve Number	Conjoined Valve	Valve Type	Area Sampled
0415	*Terebratella sanguinea*	Otago Shelf	Ts/08	Ts/07	ventral	pedicle foramen
0416	*Terebratella sanguinea*	Otago Shelf	Ts/08	Ts/07	ventral	muscle scars
0417	*Terebratella sanguinea*	Otago Shelf	Ts/08	Ts/07	ventral	primary layer
0418	*Liothyrella neozelanica*	Otago Shelf	Ln/01	Ln/02	dorsal	loop
0419	*Liothyrella neozelanica*	Otago Shelf	Ln/01	Ln/02	dorsal	non specialised tertiary layer
0420	*Liothyrella neozelanica*	Otago Shelf	Ln/01	Ln/02	dorsal	cardinal process
0421	*Liothyrella neozelanica*	Otago Shelf	Ln/01	Ln/02	dorsal	muscle scars
0422	*Liothyrella neozelanica*	Otago Shelf	Ln/01	Ln/02	dorsal	primary layer
0423	*Liothyrella neozelanica*	Otago Shelf	Ln/02	Ln/01	ventral	non specialised tertiary layer
0424	*Liothyrella neozelanica*	Otago Shelf	Ln/02	Ln/01	ventral	teeth
0425	*Liothyrella neozelanica*	Otago Shelf	Ln/02	Ln/01	ventral	pedicle foramen
0426	*Liothyrella neozelanica*	Otago Shelf	Ln/02	Ln/01	ventral	muscle scars
0427	*Liothyrella neozelanica*	Otago Shelf	Ln/02	Ln/01	ventral	primary layer
0428	*Liothyrella neozelanica*	Otago Shelf	Ln/03	Ln/04	dorsal	loop
0429	*Liothyrella neozelanica*	Otago Shelf	Ln/03	Ln/04	dorsal	non specialised tertiary layer
0430	*Liothyrella neozelanica*	Otago Shelf	Ln/03	Ln/04	dorsal	cardinal process
0431	*Liothyrella neozelanica*	Otago Shelf	Ln/03	Ln/04	dorsal	muscle scars
0432	*Liothyrella neozelanica*	Otago Shelf	Ln/03	Ln/04	dorsal	primary layer
0433	*Liothyrella neozelanica*	Otago Shelf	Ln/04	Ln/03	ventral	non specialised tertiary layer
0434	*Liothyrella neozelanica*	Otago Shelf	Ln/04	Ln/03	ventral	teeth
0435	*Liothyrella neozelanica*	Otago Shelf	Ln/04	Ln/03	ventral	pedicle foramen
0436	*Liothyrella neozelanica*	Otago Shelf	Ln/04	Ln/03	ventral	muscle scars

(Continued on next page)

Sample Number	Species	Location	Valve Number	Conjoined Valve	Valve Type	Area Sampled
0437	*Liothyrella neozelanica*	Otago Shelf	Ln/04	Ln/03	ventral	primary layer
0438	*Liothyrella neozelanica*	Otago Shelf	Ln/05	Ln/06	dorsal	loop
0439	*Liothyrella neozelanica*	Otago Shelf	Ln/05	Ln/06	dorsal	non specialised tertiary layer
0440	*Liothyrella neozelanica*	Otago Shelf	Ln/05	Ln/06	dorsal	cardinal process
0441	*Liothyrella neozelanica*	Otago Shelf	Ln/05	Ln/06	dorsal	muscle scars
0442	*Liothyrella neozelanica*	Otago Shelf	Ln/05	Ln/06	dorsal	primary layer
0443	*Liothyrella neozelanica*	Otago Shelf	Ln/06	Ln/05	ventral	non specialised tertiary layer
0444	*Liothyrella neozelanica*	Otago Shelf	Ln/06	Ln/05	ventral	teeth
0445	*Liothyrella neozelanica*	Otago Shelf	Ln/06	Ln/05	ventral	pedicle foramen
0446	*Liothyrella neozelanica*	Otago Shelf	Ln/06	Ln/05	ventral	muscle scars
0447	*Liothyrella neozelanica*	Otago Shelf	Ln/06	Ln/05	ventral	primary layer
0448	*Liothyrella neozelanica*	Otago Shelf	Ln/07	Ln/08	dorsal	loop
0449	*Liothyrella neozelanica*	Otago Shelf	Ln/07	Ln/08	dorsal	non specialised tertiary layer
0450	*Liothyrella neozelanica*	Otago Shelf	Ln/07	Ln/08	dorsal	cardinal process
0451	*Liothyrella neozelanica*	Otago Shelf	Ln/07	Ln/08	dorsal	muscle scars
0452	*Liothyrella neozelanica*	Otago Shelf	Ln/07	Ln/08	dorsal	primary layer
0453	*Liothyrella neozelanica*	Otago Shelf	Ln/08	Ln/07	ventral	non specialised tertiary layer
0454	*Liothyrella neozelanica*	Otago Shelf	Ln/08	Ln/07	ventral	teeth
0455	*Liothyrella neozelanica*	Otago Shelf	Ln/08	Ln/07	ventral	pedicle foramen
0456	*Liothyrella neozelanica*	Otago Shelf	Ln/08	Ln/07	ventral	muscle scars
0457	*Liothyrella neozelanica*	Otago Shelf	Ln/08	Ln/07	ventral	primary layer
0458	*Neothyris lenticularis*	Otago Shelf	Nl/13	Nl/14	dorsal	loop

(Continued on next page)

Sample Number	Species	Location	Valve Number	Conjoined Valve	Valve Type	Area Sampled
0459	*Neothyris lenticularis*	Otago Shelf	NI/13	NI/14	dorsal	non-specialised secondary layer
0460	*Neothyris lenticularis*	Otago Shelf	NI/13	NI/14	dorsal	cardinal process
0461	*Neothyris lenticularis*	Otago Shelf	NI/13	NI/14	dorsal	muscle scars
0462	*Neothyris lenticularis*	Otago Shelf	NI/13	NI/14	dorsal	primary layer
0463	*Neothyris lenticularis*	Otago Shelf	NI/14	NI/13	ventral	non-specialised secondary layer
0464	*Neothyris lenticularis*	Otago Shelf	NI/14	NI/13	ventral	teeth
0465	*Neothyris lenticularis*	Otago Shelf	NI/14	NI/13	ventral	pedicle foramen
0466	*Neothyris lenticularis*	Otago Shelf	NI/14	NI/13	ventral	muscle scars
0467	*Neothyris lenticularis*	Otago Shelf	NI/14	NI/13	ventral	primary layer
0468	*Terebratulina retusa*	Firth of Lorne	Tr/14	Tr/15	dorsal	loop
0469	*Terebratulina retusa*	Firth of Lorne	Tr/14	Tr/15	dorsal	non-specialised secondary layer
0470	*Terebratulina retusa*	Firth of Lorne	Tr/14	Tr/15	dorsal	cardinal process
0471	*Terebratulina retusa*	Firth of Lorne	Tr/14	Tr/15	dorsal	muscle scars
0472	*Terebratulina retusa*	Firth of Lorne	Tr/14	Tr/15	dorsal	primary layer
0473	*Terebratulina retusa*	Firth of Lorne	Tr/15	Tr/14	ventral	non-specialised secondary layer
0474	*Terebratulina retusa*	Firth of Lorne	Tr/15	Tr/14	ventral	teeth
0475	*Terebratulina retusa*	Firth of Lorne	Tr/15	Tr/14	ventral	pedicle foramen
0476	*Terebratulina retusa*	Firth of Lorne	Tr/15	Tr/14	ventral	muscle scars
0477	*Terebratulina retusa*	Firth of Lorne	Tr/15	Tr/14	ventral	primary layer
0478	*Calloria inconspicua*	Otago Shelf	Ci/13	Ci/14	dorsal	loop
0479	*Calloria inconspicua*	Otago Shelf	Ci/13	Ci/14	dorsal	non-specialised secondary layer
0480	*Calloria inconspicua*	Otago Shelf	Ci/13	Ci/14	dorsal	cardinal process

(Continued on next page)

Sample Number	Species	Location	Valve Number	Conjoined Valve	Valve Type	Area Sampled
0481	*Calloria inconspicua*	Otago Shelf	Ci/13	Ci/14	dorsal	muscle scars
0482	*Calloria inconspicua*	Otago Shelf	Ci/13	Ci/14	dorsal	primary layer
0483	*Calloria inconspicua*	Otago Shelf	Ci/14	Ci/13	ventral	non-specialised secondary layer
0484	*Calloria inconspicua*	Otago Shelf	Ci/14	Ci/13	ventral	teeth
0485	*Calloria inconspicua*	Otago Shelf	Ci/14	Ci/13	ventral	pedicle foramen
0486	*Calloria inconspicua*	Otago Shelf	Ci/14	Ci/13	ventral	muscle scars
0487	*Calloria inconspicua*	Otago Shelf	Ci/14	Ci/13	ventral	primary layer
0488	*Calloria inconspicua*	Otago Shelf	Ci/15	Ci/16	dorsal	loop
0489	*Calloria inconspicua*	Otago Shelf	Ci/15	Ci/16	dorsal	non-specialised secondary layer
0490	*Calloria inconspicua*	Otago Shelf	Ci/15	Ci/16	dorsal	cardinal process
0491	*Calloria inconspicua*	Otago Shelf	Ci/15	Ci/16	dorsal	muscle scars
0492	*Calloria inconspicua*	Otago Shelf	Ci/15	Ci/16	dorsal	primary layer
0493	*Calloria inconspicua*	Otago Shelf	Ci/16	Ci/15	ventral	non-specialised secondary layer
0494	*Calloria inconspicua*	Otago Shelf	Ci/16	Ci/15	ventral	teeth
0495	*Calloria inconspicua*	Otago Shelf	Ci/16	Ci/15	ventral	pedicle foramen
0496	*Calloria inconspicua*	Otago Shelf	Ci/16	Ci/15	ventral	muscle scars
0497	*Calloria inconspicua*	Otago Shelf	Ci/16	Ci/15	ventral	primary layer
0498	*Notosaria nigricans*	Otago Shelf	Nn/13	Nn/14	dorsal	loop
0499	*Notosaria nigricans*	Otago Shelf	Nn/13	Nn/14	dorsal	non-specialised secondary layer
0500	*Notosaria nigricans*	Otago Shelf	Nn/13	Nn/14	dorsal	cardinal process
0501	*Notosaria nigricans*	Otago Shelf	Nn/13	Nn/14	dorsal	muscle scars
0502	*Notosaria nigricans*	Otago Shelf	Nn/13	Nn/14	dorsal	primary layer

(Continued on next page)

Sample Number	Species	Location	Valve Number	Conjoined Valve	Valve Type	Area Sampled
0503	*Notosaria nigricans*	Otago Shelf	Nn/14	Nn/13	ventral	non-specialised secondary layer
0504	*Notosaria nigricans*	Otago Shelf	Nn/14	Nn/13	ventral	teeth
0505	*Notosaria nigricans*	Otago Shelf	Nn/14	Nn/13	ventral	pedicle foramen
0506	*Notosaria nigricans*	Otago Shelf	Nn/14	Nn/13	ventral	muscle scars
0507	*Notosaria nigricans*	Otago Shelf	Nn/14	Nn/13	ventral	primary layer
0508	*Notosaria nigricans*	Otago Shelf	Nn/15	Nn/16	dorsal	loop
0509	*Notosaria nigricans*	Otago Shelf	Nn/15	Nn/16	dorsal	non-specialised secondary layer
0510	*Notosaria nigricans*	Otago Shelf	Nn/15	Nn/16	dorsal	cardinal process
0511	*Notosaria nigricans*	Otago Shelf	Nn/15	Nn/16	dorsal	muscle scars
0512	*Notosaria nigricans*	Otago Shelf	Nn/15	Nn/16	dorsal	primary layer
0513	*Notosaria nigricans*	Otago Shelf	Nn/16	Nn/15	ventral	non-specialised secondary layer
0514	*Notosaria nigricans*	Otago Shelf	Nn/16	Nn/15	ventral	teeth
0515	*Notosaria nigricans*	Otago Shelf	Nn/16	Nn/15	ventral	pedicle foramen
0516	*Notosaria nigricans*	Otago Shelf	Nn/16	Nn/15	ventral	muscle scars
0517	*Notosaria nigricans*	Otago Shelf	Nn/16	Nn/15	ventral	primary layer
0518	*Laqueus rubellus*	Sagami Bay	Lr/09	Lr/10	dorsal	loop
0519	*Laqueus rubellus*	Sagami Bay	Lr/09	Lr/10	dorsal	non-specialised secondary layer
0520	*Laqueus rubellus*	Sagami Bay	Lr/09	Lr/10	dorsal	cardinal process
0521	*Laqueus rubellus*	Sagami Bay	Lr/09	Lr/10	dorsal	muscle scars
0522	*Laqueus rubellus*	Sagami Bay	Lr/09	Lr/10	dorsal	primary layer
0523	*Laqueus rubellus*	Sagami Bay	Lr/10	Lr/09	ventral	non-specialised secondary layer
0524	*Laqueus rubellus*	Sagami Bay	Lr/10	Lr/09	ventral	teeth

(Continued on next page)

Sample Number	Species	Location	Valve Number	Conjoined Valve	Valve Type	Area Sampled
0525	*Laqueus rubellus*	Sagami Bay	Lr/10	Lr/09	ventral	pedicle foramen
0526	*Laqueus rubellus*	Sagami Bay	Lr/10	Lr/09	ventral	muscle scars
0527	*Laqueus rubellus*	Sagami Bay	Lr/10	Lr/09	ventral	primary layer
0528	*Laqueus rubellus*	Sagami Bay	Lr/11	Lr/12	dorsal	loop
0529	*Laqueus rubellus*	Sagami Bay	Lr/11	Lr/12	dorsal	non-specialised secondary layer
0530	*Laqueus rubellus*	Sagami Bay	Lr/11	Lr/12	dorsal	cardinal process
0531	*Laqueus rubellus*	Sagami Bay	Lr/11	Lr/12	dorsal	muscle scars
0532	*Laqueus rubellus*	Sagami Bay	Lr/11	Lr/12	dorsal	primary layer
0533	*Laqueus rubellus*	Sagami Bay	Lr/12	Lr/11	ventral	non-specialised secondary layer
0534	*Laqueus rubellus*	Sagami Bay	Lr/12	Lr/11	ventral	teeth
0535	*Laqueus rubellus*	Sagami Bay	Lr/12	Lr/11	ventral	pedicle foramen
0536	*Laqueus rubellus*	Sagami Bay	Lr/12	Lr/11	ventral	muscle scars
0537	*Laqueus rubellus*	Sagami Bay	Lr/12	Lr/11	ventral	primary layer
0538	*Terebratalia transversa*	Friday Harbor	Tt/09	Tt/10	dorsal	loop
0539	*Terebratalia transversa*	Friday Harbor	Tt/09	Tt/10	dorsal	non-specialised secondary layer
0540	*Terebratalia transversa*	Friday Harbor	Tt/09	Tt/10	dorsal	cardinal process
0541	*Terebratalia transversa*	Friday Harbor	Tt/09	Tt/10	dorsal	muscle scars
0542	*Terebratalia transversa*	Friday Harbor	Tt/09	Tt/10	dorsal	primary layer
0543	*Terebratalia transversa*	Friday Harbor	Tt/10	Tt/09	ventral	non-specialised secondary layer
0544	*Terebratalia transversa*	Friday Harbor	Tt/10	Tt/09	ventral	teeth
0545	*Terebratalia transversa*	Friday Harbor	Tt/10	Tt/09	ventral	pedicle foramen
0546	*Terebratalia transversa*	Friday Harbor	Tt/10	Tt/09	ventral	muscle scars

(Continued on next page)

Sample Number	Species	Location	Valve Number	Conjoined Valve	Valve Type	Area Sampled
0547	*Terebratalia transversa*	Friday Harbor	Tt/10	Tt/09	ventral	primary layer
0548	*Terebratalia transversa*	Friday Harbor	Tt/11	Tt/12	dorsal	loop
0549	*Terebratalia transversa*	Friday Harbor	Tt/11	Tt/12	dorsal	non-specialised secondary layer
0550	*Terebratalia transversa*	Friday Harbor	Tt/11	Tt/12	dorsal	cardinal process
0551	*Terebratalia transversa*	Friday Harbor	Tt/11	Tt/12	dorsal	muscle scars
0552	*Terebratalia transversa*	Friday Harbor	Tt/11	Tt/12	dorsal	primary layer
0553	*Terebratalia transversa*	Friday Harbor	Tt/12	Tt/11	ventral	non-specialised secondary layer
0554	*Terebratalia transversa*	Friday Harbor	Tt/12	Tt/11	ventral	teeth
0555	*Terebratalia transversa*	Friday Harbor	Tt/12	Tt/11	ventral	pedicle foramen
0556	*Terebratalia transversa*	Friday Harbor	Tt/12	Tt/11	ventral	muscle scars
0557	*Terebratalia transversa*	Friday Harbor	Tt/12	Tt/11	ventral	primary layer
0558	*Terebratella sanguinea*	Otago Shelf	Ts/09	Ts/10	dorsal	loop
0559	*Terebratella sanguinea*	Otago Shelf	Ts/09	Ts/10	dorsal	non-specialised secondary layer
0560	*Terebratella sanguinea*	Otago Shelf	Ts/09	Ts/10	dorsal	cardinal process
0561	*Terebratella sanguinea*	Otago Shelf	Ts/09	Ts/10	dorsal	muscle scars
0562	*Terebratella sanguinea*	Otago Shelf	Ts/09	Ts/10	dorsal	primary layer
0563	*Terebratella sanguinea*	Otago Shelf	Ts/10	Ts/09	ventral	non-specialised secondary layer
0564	*Terebratella sanguinea*	Otago Shelf	Ts/10	Ts/09	ventral	teeth
0565	*Terebratella sanguinea*	Otago Shelf	Ts/10	Ts/09	ventral	pedicle foramen
0566	*Terebratella sanguinea*	Otago Shelf	Ts/10	Ts/09	ventral	muscle scars
0567	*Terebratella sanguinea*	Otago Shelf	Ts/10	Ts/09	ventral	primary layer
0568	*Terebratella sanguinea*	Otago Shelf	Ts/11	Ts/12	dorsal	loop

(Continued on next page)

Sample Number	Species	Location	Valve Number	Conjoined Valve	Valve Type	Area Sampled
0569	*Terebratella sanguinea*	Otago Shelf	Ts/11	Ts/12	dorsal	non-specialised secondary layer
0570	*Terebratella sanguinea*	Otago Shelf	Ts/11	Ts/12	dorsal	cardinal process
0571	*Terebratella sanguinea*	Otago Shelf	Ts/11	Ts/12	dorsal	muscle scars
0572	*Terebratella sanguinea*	Otago Shelf	Ts/11	Ts/12	dorsal	primary layer
0573	*Terebratella sanguinea*	Otago Shelf	Ts/12	Ts/11	ventral	non-specialised secondary layer
0574	*Terebratella sanguinea*	Otago Shelf	Ts/12	Ts/11	ventral	teeth
0575	*Terebratella sanguinea*	Otago Shelf	Ts/12	Ts/11	ventral	pedicle foramen
0576	*Terebratella sanguinea*	Otago Shelf	Ts/12	Ts/11	ventral	muscle scars
0577	*Terebratella sanguinea*	Otago Shelf	Ts/12	Ts/11	ventral	primary layer
5078	*Liothyrella neozelanica*	Otago Shelf	Ln/09	Ln/10	dorsal	loop
0579	*Liothyrella neozelanica*	Otago Shelf	Ln/09	Ln/10	dorsal	non specialised tertiary layer
0580	*Liothyrella neozelanica*	Otago Shelf	Ln/09	Ln/10	dorsal	cardinal process
0581	*Liothyrella neozelanica*	Otago Shelf	Ln/09	Ln/10	dorsal	muscle scars
0582	*Liothyrella neozelanica*	Otago Shelf	Ln/09	Ln/10	dorsal	primary layer
0583	*Liothyrella neozelanica*	Otago Shelf	Ln/10	Ln/09	ventral	non specialised tertiary layer
0584	*Liothyrella neozelanica*	Otago Shelf	Ln/10	Ln/09	ventral	teeth
0585	*Liothyrella neozelanica*	Otago Shelf	Ln/10	Ln/09	ventral	pedicle foramen
0586	*Liothyrella neozelanica*	Otago Shelf	Ln/10	Ln/09	ventral	muscle scars
0587	*Liothyrella neozelanica*	Otago Shelf	Ln/10	Ln/09	ventral	primary layer
0588	*Liothyrella neozelanica*	Otago Shelf	Ln/11	Ln/12	dorsal	loop
0589	*Liothyrella neozelanica*	Otago Shelf	Ln/11	Ln/12	dorsal	non specialised tertiary layer
0590	*Liothyrella neozelanica*	Otago Shelf	Ln/11	Ln/12	dorsal	cardinal process

(Continued on next page)

Sample Number	Species	Location	Valve Number	Conjoined Valve	Valve Type	Area Sampled
0591	*Liothyrella neozelanica*	Otago Shelf	Ln/11	Ln/12	dorsal	muscle scars
0592	*Liothyrella neozelanica*	Otago Shelf	Ln/11	Ln/12	dorsal	primary layer
0593	*Liothyrella neozelanica*	Otago Shelf	Ln/12	Ln/11	ventral	non specialised tertiary layer
0594	*Liothyrella neozelanica*	Otago Shelf	Ln/12	Ln/11	ventral	teeth
0595	*Liothyrella neozelanica*	Otago Shelf	Ln/12	Ln/11	ventral	pedicle foramen
0596	*Liothyrella neozelanica*	Otago Shelf	Ln/12	Ln/11	ventral	muscle scars
0597	*Liothyrella neozelanica*	Otago Shelf	Ln/12	Ln/11	ventral	primary layer
0598	*Neothyris lenticularis*	Otago Shelf	Nl/15	Nl/16	dorsal	loop
0599	*Neothyris lenticularis*	Otago Shelf	Nl/15	Nl/16	dorsal	non-specialised secondary layer
0600	*Neothyris lenticularis*	Otago Shelf	Nl/15	Nl/16	dorsal	cardinal process
0601	*Neothyris lenticularis*	Otago Shelf	Nl/15	Nl/16	dorsal	muscle scars
0602	*Neothyris lenticularis*	Otago Shelf	Nl/15	Nl/16	dorsal	primary layer
0603	*Neothyris lenticularis*	Otago Shelf	Nl/16	Nl/15	ventral	non-specialised secondary layer
0604	*Neothyris lenticularis*	Otago Shelf	Nl/16	Nl/15	ventral	teeth
0605	*Neothyris lenticularis*	Otago Shelf	Nl/16	Nl/15	ventral	pedicle foramen
0606	*Neothyris lenticularis*	Otago Shelf	Nl/16	Nl/15	ventral	muscle scars
0607	*Neothyris lenticularis*	Otago Shelf	Nl/16	Nl/15	ventral	primary layer
0608	*Neothyris lenticularis*	Otago Shelf	Nl/17	Nl/18	dorsal	loop
0609	*Neothyris lenticularis*	Otago Shelf	Nl/17	Nl/18	dorsal	non-specialised secondary layer
0610	*Neothyris lenticularis*	Otago Shelf	Nl/17	Nl/18	dorsal	cardinal process
0611	*Neothyris lenticularis*	Otago Shelf	Nl/17	Nl/18	dorsal	muscle scars
0612	*Neothyris lenticularis*	Otago Shelf	Nl/17	Nl/18	dorsal	primary layer

(Continued on next page)

Sample Number	Species	Location	Valve Number	Conjoined Valve	Valve Type	Area Sampled
0613	*Neothyris lenticularis*	Otago Shelf	NI/18	NI/17	ventral	non-specialised secondary layer
0614	*Neothyris lenticularis*	Otago Shelf	NI/18	NI/17	ventral	teeth
0615	*Neothyris lenticularis*	Otago Shelf	NI/18	NI/17	ventral	pedicle foramen
0616	*Neothyris lenticularis*	Otago Shelf	NI/18	NI/17	ventral	muscle scars
0617	*Neothyris lenticularis*	Otago Shelf	NI/18	NI/17	ventral	primary layer
0618	*Terebratulina retusa*	Firth of Lorne	Tr/16	Tr/17	dorsal	loop
0619	*Terebratulina retusa*	Firth of Lorne	Tr/16	Tr/17	dorsal	non-specialised secondary layer
0620	*Terebratulina retusa*	Firth of Lorne	Tr/16	Tr/17	dorsal	cardinal process
0621	*Terebratulina retusa*	Firth of Lorne	Tr/16	Tr/17	dorsal	muscle scars
0622	*Terebratulina retusa*	Firth of Lorne	Tr/16	Tr/17	dorsal	primary layer
0623	*Terebratulina retusa*	Firth of Lorne	Tr/17	Tr/16	ventral	non-specialised secondary layer
0624	*Terebratulina retusa*	Firth of Lorne	Tr/17	Tr/16	ventral	teeth
0625	*Terebratulina retusa*	Firth of Lorne	Tr/17	Tr/16	ventral	pedicle foramen
0626	*Terebratulina retusa*	Firth of Lorne	Tr/17	Tr/16	ventral	muscle scars
0627	*Terebratulina retusa*	Firth of Lorne	Tr/17	Tr/16	ventral	primary layer
0628	*Terebratulina retusa*	Firth of Lorne	Tr/18	Tr/18	dorsal	loop
0629	*Terebratulina retusa*	Firth of Lorne	Tr/18	Tr/18	dorsal	non-specialised secondary layer
0630	*Terebratulina retusa*	Firth of Lorne	Tr/18	Tr/18	dorsal	cardinal process
0631	*Terebratulina retusa*	Firth of Lorne	Tr/18	Tr/18	dorsal	muscle scars
0632	*Terebratulina retusa*	Firth of Lorne	Tr/18	Tr/18	dorsal	primary layer
0633	*Terebratulina retusa*	Firth of Lorne	Tr/18	Tr/18	ventral	non-specialised secondary layer
0634	*Terebratulina retusa*	Firth of Lorne	Tr/18	Tr/18	ventral	teeth

(Continued on next page)

Sample Number	Species	Location	Valve Number	Conjoined Valve	Valve Type	Area Sampled
0635	*Terebratulina retusa*	Firth of Lorne	Tr/18	Tr/18	ventral	pedicle foramen
0636	*Terebratulina retusa*	Firth of Lorne	Tr/18	Tr/18	ventral	muscle scars
0637	*Terebratulina retusa*	Firth of Lorne	Tr/18	Tr/18	ventral	primary layer
0638	*Calloria inconspicua*	Otago Shelf	Ci/17	Ci/18	dorsal	loop
0639	*Calloria inconspicua*	Otago Shelf	Ci/17	Ci/18	dorsal	non-specialised secondary layer
0640	*Calloria inconspicua*	Otago Shelf	Ci/17	Ci/18	dorsal	cardinal process
0641	*Calloria inconspicua*	Otago Shelf	Ci/17	Ci/18	dorsal	muscle scars
0642	*Calloria inconspicua*	Otago Shelf	Ci/17	Ci/18	dorsal	primary layer
0643	*Calloria inconspicua*	Otago Shelf	Ci/18	Ci/17	ventral	non-specialised secondary layer
0644	*Calloria inconspicua*	Otago Shelf	Ci/18	Ci/17	ventral	teeth
0645	*Calloria inconspicua*	Otago Shelf	Ci/18	Ci/17	ventral	pedicle foramen
0646	*Calloria inconspicua*	Otago Shelf	Ci/18	Ci/17	ventral	muscle scars
0647	*Calloria inconspicua*	Otago Shelf	Ci/18	Ci/17	ventral	primary layer
0648	*Calloria inconspicua*	Otago Shelf	Ci/19	Ci/20	dorsal	loop
0649	*Calloria inconspicua*	Otago Shelf	Ci/19	Ci/20	dorsal	non-specialised secondary layer
0650	*Calloria inconspicua*	Otago Shelf	Ci/19	Ci/20	dorsal	cardinal process
0651	*Calloria inconspicua*	Otago Shelf	Ci/19	Ci/20	dorsal	muscle scars
0652	*Calloria inconspicua*	Otago Shelf	Ci/19	Ci/20	dorsal	primary layer
0653	*Calloria inconspicua*	Otago Shelf	Ci/20	Ci/19	ventral	non-specialised secondary layer
0654	*Calloria inconspicua*	Otago Shelf	Ci/20	Ci/19	ventral	teeth
0655	*Calloria inconspicua*	Otago Shelf	Ci/20	Ci/19	ventral	pedicle foramen
0656	*Calloria inconspicua*	Otago Shelf	Ci/20	Ci/19	ventral	muscle scars

(Continued on next page)

Sample Number	Species	Location	Valve Number	Conjoined Valve	Valve Type	Area Sampled
0657	*Calloria inconspicua*	Otago Shelf	Ci/20	Ci/19	ventral	primary layer
0658	*Notosaria nigricans*	Otago Shelf	Nn/17	Nn/18	dorsal	loop
0659	*Notosaria nigricans*	Otago Shelf	Nn/17	Nn/18	dorsal	non-specialised secondary layer
0660	*Notosaria nigricans*	Otago Shelf	Nn/17	Nn/18	dorsal	cardinal process
0661	*Notosaria nigricans*	Otago Shelf	Nn/17	Nn/18	dorsal	muscle scars
0662	*Notosaria nigricans*	Otago Shelf	Nn/17	Nn/18	dorsal	primary layer
0663	*Notosaria nigricans*	Otago Shelf	Nn/18	Nn/17	ventral	non-specialised secondary layer
0664	*Notosaria nigricans*	Otago Shelf	Nn/18	Nn/17	ventral	teeth
0665	*Notosaria nigricans*	Otago Shelf	Nn/18	Nn/17	ventral	pedicle foramen
0666	*Notosaria nigricans*	Otago Shelf	Nn/18	Nn/17	ventral	muscle scars
0667	*Notosaria nigricans*	Otago Shelf	Nn/18	Nn/17	ventral	primary layer
0668	*Notosaria nigricans*	Otago Shelf	Nn/19	Nn/20	dorsal	loop
0669	*Notosaria nigricans*	Otago Shelf	Nn/19	Nn/20	dorsal	non-specialised secondary layer
0670	*Notosaria nigricans*	Otago Shelf	Nn/19	Nn/20	dorsal	cardinal process
0671	*Notosaria nigricans*	Otago Shelf	Nn/19	Nn/20	dorsal	muscle scars
0672	*Notosaria nigricans*	Otago Shelf	Nn/19	Nn/20	dorsal	primary layer
0673	*Notosaria nigricans*	Otago Shelf	Nn/20	Nn/19	ventral	non-specialised secondary layer
0674	*Notosaria nigricans*	Otago Shelf	Nn/20	Nn/19	ventral	teeth
0675	*Notosaria nigricans*	Otago Shelf	Nn/20	Nn/19	ventral	pedicle foramen
0676	*Notosaria nigricans*	Otago Shelf	Nn/20	Nn/19	ventral	muscle scars
0677	*Notosaria nigricans*	Otago Shelf	Nn/20	Nn/19	ventral	primary layer
0678	*Terebratalia transversa*	Friday Harbor	Tt/13	Tt/14	dorsal	loop

(Continued on next page)

Sample Number	Species	Location	Valve Number	Conjoined Valve	Valve Type	Area Sampled
0679	*Terebratalia transversa*	Friday Harbor	Tt/13	Tt/14	dorsal	non-specialised secondary layer
0680	*Terebratalia transversa*	Friday Harbor	Tt/13	Tt/14	dorsal	cardinal process
0681	*Terebratalia transversa*	Friday Harbor	Tt/13	Tt/14	dorsal	muscle scars
0682	*Terebratalia transversa*	Friday Harbor	Tt/13	Tt/14	dorsal	primary layer
0683	*Terebratalia transversa*	Friday Harbor	Tt/14	Tt/13	ventral	non-specialised secondary layer
0684	*Terebratalia transversa*	Friday Harbor	Tt/14	Tt/13	ventral	teeth
0685	*Terebratalia transversa*	Friday Harbor	Tt/14	Tt/13	ventral	pedicle foramen
0686	*Terebratalia transversa*	Friday Harbor	Tt/14	Tt/13	ventral	muscle scars
0687	*Terebratalia transversa*	Friday Harbor	Tt/14	Tt/13	ventral	primary layer
0688	*Terebratalia transversa*	Friday Harbor	Tt/15	Tt/16	dorsal	loop
0689	*Terebratalia transversa*	Friday Harbor	Tt/15	Tt/16	dorsal	non-specialised secondary layer
0690	*Terebratalia transversa*	Friday Harbor	Tt/15	Tt/16	dorsal	cardinal process
0691	*Terebratalia transversa*	Friday Harbor	Tt/15	Tt/16	dorsal	muscle scars
0692	*Terebratalia transversa*	Friday Harbor	Tt/15	Tt/16	dorsal	primary layer
0693	*Terebratalia transversa*	Friday Harbor	Tt/16	Tt/15	ventral	non-specialised secondary layer
0694	*Terebratalia transversa*	Friday Harbor	Tt/16	Tt/15	ventral	teeth
0695	*Terebratalia transversa*	Friday Harbor	Tt/16	Tt/15	ventral	pedicle foramen
0696	*Terebratalia transversa*	Friday Harbor	Tt/16	Tt/15	ventral	muscle scars
0697	*Terebratalia transversa*	Friday Harbor	Tt/16	Tt/15	ventral	primary layer
0698	*Terebratella sanguinea*	Otago Shelf	Ts/13	Ts/14	dorsal	loop
0699	*Terebratella sanguinea*	Otago Shelf	Ts/13	Ts/14	dorsal	non-specialised secondary layer
0700	*Terebratella sanguinea*	Otago Shelf	Ts/13	Ts/14	dorsal	cardinal process

(Continued on next page)

Sample Number	Species	Location	Valve Number	Conjoined Valve	Valve Type	Area Sampled
0701	*Terebratella sanguinea*	Otago Shelf	Ts/13	Ts/14	dorsal	muscle scars
0702	*Terebratella sanguinea*	Otago Shelf	Ts/13	Ts/14	dorsal	primary layer
0703	*Terebratella sanguinea*	Otago Shelf	Ts/14	Ts/13	ventral	non-specialised secondary layer
0704	*Terebratella sanguinea*	Otago Shelf	Ts/14	Ts/13	ventral	teeth
0705	*Terebratella sanguinea*	Otago Shelf	Ts/14	Ts/13	ventral	pedicle foramen
0706	*Terebratella sanguinea*	Otago Shelf	Ts/14	Ts/13	ventral	muscle scars
0707	*Terebratella sanguinea*	Otago Shelf	Ts/14	Ts/13	ventral	primary layer
0708	*Terebratella sanguinea*	Otago Shelf	Ts/15	Ts/16	dorsal	loop
0709	*Terebratella sanguinea*	Otago Shelf	Ts/15	Ts/16	dorsal	non-specialised secondary layer
0710	*Terebratella sanguinea*	Otago Shelf	Ts/15	Ts/16	dorsal	cardinal process
0711	*Terebratella sanguinea*	Otago Shelf	Ts/15	Ts/16	dorsal	muscle scars
0712	*Terebratella sanguinea*	Otago Shelf	Ts/15	Ts/16	dorsal	primary layer
0713	*Terebratella sanguinea*	Otago Shelf	Ts/16	Ts/15	ventral	non-specialised secondary layer
0714	*Terebratella sanguinea*	Otago Shelf	Ts/16	Ts/15	ventral	teeth
0715	*Terebratella sanguinea*	Otago Shelf	Ts/16	Ts/15	ventral	pedicle foramen
0716	*Terebratella sanguinea*	Otago Shelf	Ts/16	Ts/15	ventral	muscle scars
0717	*Terebratella sanguinea*	Otago Shelf	Ts/16	Ts/15	ventral	primary layer
0718	*Liothyrella neozelanica*	Otago Shelf	Ln/13	Ln/14	dorsal	loop
0719	*Liothyrella neozelanica*	Otago Shelf	Ln/13	Ln/14	dorsal	non specialised tertiary layer
0720	*Liothyrella neozelanica*	Otago Shelf	Ln/13	Ln/14	dorsal	cardinal process
0721	*Liothyrella neozelanica*	Otago Shelf	Ln/13	Ln/14	dorsal	muscle scars
0722	*Liothyrella neozelanica*	Otago Shelf	Ln/13	Ln/14	dorsal	primary layer

(Continued on next page)

Sample Number	Species	Location	Valve Number	Conjoined Valve	Valve Type	Area Sampled
0723	*Liothyrella neozelanica*	Otago Shelf	Ln/14	Ln/13	ventral	non specialised tertiary layer
0724	*Liothyrella neozelanica*	Otago Shelf	Ln/14	Ln/13	ventral	teeth
0725	*Liothyrella neozelanica*	Otago Shelf	Ln/14	Ln/13	ventral	pedicle foramen
0726	*Liothyrella neozelanica*	Otago Shelf	Ln/14	Ln/13	ventral	muscle scars
0727	*Liothyrella neozelanica*	Otago Shelf	Ln/14	Ln/13	ventral	primary layer
0728	*Liothyrella neozelanica*	Otago Shelf	Ln/15	Ln/16	dorsal	loop
0729	*Liothyrella neozelanica*	Otago Shelf	Ln/15	Ln/16	dorsal	non specialised tertiary layer
0730	*Liothyrella neozelanica*	Otago Shelf	Ln/15	Ln/16	dorsal	cardinal process
0731	*Liothyrella neozelanica*	Otago Shelf	Ln/15	Ln/16	dorsal	muscle scars
0732	*Liothyrella neozelanica*	Otago Shelf	Ln/15	Ln/16	dorsal	primary layer
0733	*Liothyrella neozelanica*	Otago Shelf	Ln/16	Ln/15	ventral	non specialised tertiary layer
0734	*Liothyrella neozelanica*	Otago Shelf	Ln/16	Ln/15	ventral	teeth
0735	*Liothyrella neozelanica*	Otago Shelf	Ln/16	Ln/15	ventral	pedicle foramen
0736	*Liothyrella neozelanica*	Otago Shelf	Ln/16	Ln/15	ventral	muscle scars
0737	*Liothyrella neozelanica*	Otago Shelf	Ln/16	Ln/15	ventral	primary layer
0738	*Liothyrella uva*	Signy Island	Lu/01	Lu/02	dorsal	loop
0739	*Liothyrella uva*	Signy Island	Lu/01	Lu/02	dorsal	non specialised tertiary layer
0740	*Liothyrella uva*	Signy Island	Lu/01	Lu/02	dorsal	cardinal process
0741	*Liothyrella uva*	Signy Island	Lu/01	Lu/02	dorsal	muscle scars
0742	*Liothyrella uva*	Signy Island	Lu/01	Lu/02	dorsal	primary layer
0743	*Liothyrella uva*	Signy Island	Lu/02	Lu/01	ventral	non specialised tertiary layer
0744	*Liothyrella uva*	Signy Island	Lu/02	Lu/01	ventral	teeth

(Continued on next page)

Sample Number	Species	Location	Valve Number	Conjoined Valve	Valve Type	Area Sampled
0745	*Liothyrella uva*	Signy Island	Lu/02	Lu/01	ventral	pedicle foramen
0746	*Liothyrella uva*	Signy Island	Lu/02	Lu/01	ventral	muscle scars
0747	*Liothyrella uva*	Signy Island	Lu/02	Lu/01	ventral	primary layer
0748	*Liothyrella uva*	Signy Island	Lu/03	Lu/04	dorsal	loop
0749	*Liothyrella uva*	Signy Island	Lu/03	Lu/04	dorsal	non specialised tertiary layer
0750	*Liothyrella uva*	Signy Island	Lu/03	Lu/04	dorsal	cardinal process
0751	*Liothyrella uva*	Signy Island	Lu/03	Lu/04	dorsal	muscle scars
0752	*Liothyrella uva*	Signy Island	Lu/03	Lu/04	dorsal	primary layer
0753	*Liothyrella uva*	Signy Island	Lu/04	Lu/03	ventral	non specialised tertiary layer
0754	*Liothyrella uva*	Signy Island	Lu/04	Lu/03	ventral	teeth
0755	*Liothyrella uva*	Signy Island	Lu/04	Lu/03	ventral	pedicle foramen
0756	*Liothyrella uva*	Signy Island	Lu/04	Lu/03	ventral	muscle scars
0757	*Liothyrella uva*	Signy Island	Lu/04	Lu/03	ventral	primary layer
0758	*Laqueus rubellus*	Sagami Bay	Lr/13	Lr/14	dorsal	loop
0759	*Laqueus rubellus*	Sagami Bay	Lr/13	Lr/14	dorsal	non-specialised secondary layer
0760	*Laqueus rubellus*	Sagami Bay	Lr/13	Lr/14	dorsal	cardinal process
0761	*Laqueus rubellus*	Sagami Bay	Lr/13	Lr/14	dorsal	muscle scars
0762	*Laqueus rubellus*	Sagami Bay	Lr/13	Lr/14	dorsal	primary layer
0763	*Laqueus rubellus*	Sagami Bay	Lr/14	Lr/13	ventral	non-specialised secondary layer
0764	*Laqueus rubellus*	Sagami Bay	Lr/14	Lr/13	ventral	teeth
0765	*Laqueus rubellus*	Sagami Bay	Lr/14	Lr/13	ventral	pedicle foramen
0766	*Laqueus rubellus*	Sagami Bay	Lr/14	Lr/13	ventral	muscle scars

(Continued on next page)

Sample Number	Species	Location	Valve Number	Conjoined Valve	Valve Type	Area Sampled
0767	*Laqueus rubellus*	Sagami Bay	Lr/14	Lr/13	ventral	primary layer
0768	*Laqueus rubellus*	Otsuchi Bay	Lr/15	Lr/16	dorsal	loop
0769	*Laqueus rubellus*	Otsuchi Bay	Lr/15	Lr/16	dorsal	non-specialised secondary layer
0770	*Laqueus rubellus*	Otsuchi Bay	Lr/15	Lr/16	dorsal	cardinal process
0771	*Laqueus rubellus*	Otsuchi Bay	Lr/15	Lr/16	dorsal	muscle scars
0772	*Laqueus rubellus*	Otsuchi Bay	Lr/15	Lr/16	dorsal	primary layer
0773	*Laqueus rubellus*	Otsuchi Bay	Lr/16	Lr/15	ventral	non-specialised secondary layer
0774	*Laqueus rubellus*	Otsuchi Bay	Lr/16	Lr/15	ventral	teeth
0775	*Laqueus rubellus*	Otsuchi Bay	Lr/16	Lr/15	ventral	pedicle foramen
0776	*Laqueus rubellus*	Otsuchi Bay	Lr/16	Lr/15	ventral	muscle scars
0777	*Laqueus rubellus*	Otsuchi Bay	Lr/16	Lr/15	ventral	primary layer
0778	*Laqueus rubellus*	Otsuchi Bay	Lr/17	Lr/18	dorsal	loop
0779	*Laqueus rubellus*	Otsuchi Bay	Lr/17	Lr/18	dorsal	non-specialised secondary layer
0780	*Laqueus rubellus*	Otsuchi Bay	Lr/17	Lr/18	dorsal	cardinal process
0781	*Laqueus rubellus*	Otsuchi Bay	Lr/17	Lr/18	dorsal	muscle scars
0782	*Laqueus rubellus*	Otsuchi Bay	Lr/17	Lr/18	dorsal	primary layer
0783	*Laqueus rubellus*	Otsuchi Bay	Lr/18	Lr/17	ventral	non-specialised secondary layer
0784	*Laqueus rubellus*	Otsuchi Bay	Lr/18	Lr/17	ventral	teeth
0785	*Laqueus rubellus*	Otsuchi Bay	Lr/18	Lr/17	ventral	pedicle foramen
0786	*Laqueus rubellus*	Otsuchi Bay	Lr/18	Lr/17	ventral	muscle scars
0787	*Laqueus rubellus*	Otsuchi Bay	Lr/18	Lr/17	ventral	primary layer
0788	*Laqueus rubellus*	Sagami Bay	Lr/19	Lr/20	dorsal	loop

(Continued on next page)

Sample Number	Species	Location	Valve Number	Conjoined Valve	Valve Type	Area Sampled
0789	*Laqueus rubellus*	Sagami Bay	Lr/19	Lr/20	dorsal	non-specialised secondary layer
0790	*Laqueus rubellus*	Sagami Bay	Lr/19	Lr/20	dorsal	cardinal process
0791	*Laqueus rubellus*	Sagami Bay	Lr/19	Lr/20	dorsal	muscle scars
0792	*Laqueus rubellus*	Sagami Bay	Lr/19	Lr/20	dorsal	primary layer
0793	*Laqueus rubellus*	Sagami Bay	Lr/20	Lr/19	ventral	non-specialised secondary layer
0794	*Laqueus rubellus*	Sagami Bay	Lr/20	Lr/19	ventral	teeth
0795	*Laqueus rubellus*	Sagami Bay	Lr/20	Lr/19	ventral	pedicle foramen
0796	*Laqueus rubellus*	Sagami Bay	Lr/20	Lr/19	ventral	muscle scars
0797	*Laqueus rubellus*	Sagami Bay	Lr/20	Lr/19	ventral	primary layer
0798	*Liothyrella uva*	Signy Island	Lu/05	Lu/06	dorsal	loop
0799	*Liothyrella uva*	Signy Island	Lu/05	Lu/06	dorsal	non specialised tertiary layer
0800	*Liothyrella uva*	Signy Island	Lu/05	Lu/06	dorsal	cardinal process
0801	*Liothyrella uva*	Signy Island	Lu/05	Lu/06	dorsal	muscle scars
0802	*Liothyrella uva*	Signy Island	Lu/05	Lu/06	dorsal	primary layer
0803	*Liothyrella uva*	Signy Island	Lu/06	Lu/05	ventral	non specialised tertiary layer
0804	*Liothyrella uva*	Signy Island	Lu/06	Lu/05	ventral	teeth
0805	*Liothyrella uva*	Signy Island	Lu/06	Lu/05	ventral	pedicle foramen
0806	*Liothyrella uva*	Signy Island	Lu/06	Lu/05	ventral	muscle scars
0807	*Liothyrella uva*	Signy Island	Lu/06	Lu/05	ventral	primary layer
0808	*Liothyrella uva*	Signy Island	Lu/07	Lu/08	dorsal	loop
0809	*Liothyrella uva*	Signy Island	Lu/07	Lu/08	dorsal	non specialised tertiary layer
0810	*Liothyrella uva*	Signy Island	Lu/07	Lu/08	dorsal	cardinal process

(Continued on next page)

Sample Number	Species	Location	Valve Number	Conjoined Valve	Valve Type	Area Sampled
0811	*Liothyrella uva*	Signy Island	Lu/07	Lu/08	dorsal	muscle scars
0812	*Liothyrella uva*	Signy Island	Lu/07	Lu/08	dorsal	primary layer
0813	*Liothyrella uva*	Signy Island	Lu/08	Lu/07	ventral	non specialised tertiary layer
0814	*Liothyrella uva*	Signy Island	Lu/08	Lu/07	ventral	teeth
0815	*Liothyrella uva*	Signy Island	Lu/08	Lu/07	ventral	pedicle foramen
0816	*Liothyrella uva*	Signy Island	Lu/08	Lu/07	ventral	muscle scars
0817	*Liothyrella uva*	Signy Island	Lu/08	Lu/07	ventral	primary layer
0818	*Liothyrella uva*	Signy Island	Lu/09	Lu/10	dorsal	loop
0819	*Liothyrella uva*	Signy Island	Lu/09	Lu/10	dorsal	non specialised tertiary layer
0820	*Liothyrella uva*	Signy Island	Lu/09	Lu/10	dorsal	cardinal process
0821	*Liothyrella uva*	Signy Island	Lu/09	Lu/10	dorsal	muscle scars
0822	*Liothyrella uva*	Signy Island	Lu/09	Lu/10	dorsal	primary layer
0823	*Liothyrella uva*	Signy Island	Lu/10	Lu/09	ventral	non specialised tertiary layer
0824	*Liothyrella uva*	Signy Island	Lu/10	Lu/09	ventral	teeth
0825	*Liothyrella uva*	Signy Island	Lu/10	Lu/09	ventral	pedicle foramen
0826	*Liothyrella uva*	Signy Island	Lu/10	Lu/09	ventral	muscle scars
0827	*Liothyrella uva*	Signy Island	Lu/10	Lu/09	ventral	primary layer
0828	*Liothyrella uva*	Signy Island	Lu/11	Lu/12	dorsal	loop
0829	*Liothyrella uva*	Signy Island	Lu/11	Lu/12	dorsal	non specialised tertiary layer
0830	*Liothyrella uva*	Signy Island	Lu/11	Lu/12	dorsal	cardinal process
0831	*Liothyrella uva*	Signy Island	Lu/11	Lu/12	dorsal	muscle scars
0832	*Liothyrella uva*	Signy Island	Lu/11	Lu/12	dorsal	primary layer

(Continued on next page)

Sample Number	Species	Location	Valve Number	Conjoined Valve	Valve Type	Area Sampled
0833	*Liothyrella uva*	Signy Island	Lu/12	Lu/11	ventral	non specialised tertiary layer
0834	*Liothyrella uva*	Signy Island	Lu/12	Lu/11	ventral	teeth
0835	*Liothyrella uva*	Signy Island	Lu/12	Lu/11	ventral	pedicle foramen
0836	*Liothyrella uva*	Signy Island	Lu/12	Lu/11	ventral	muscle scars
0837	*Liothyrella uva*	Signy Island	Lu/12	Lu/11	ventral	primary layer
0838	*Laqueus rubellus*	Sagami Bay	Lr/21	Lr/22	dorsal	loop
0839	*Laqueus rubellus*	Sagami Bay	Lr/21	Lr/22	dorsal	non-specialised secondary layer
0840	*Laqueus rubellus*	Sagami Bay	Lr/21	Lr/22	dorsal	cardinal process
0841	*Laqueus rubellus*	Sagami Bay	Lr/21	Lr/22	dorsal	muscle scars
0842	*Laqueus rubellus*	Sagami Bay	Lr/21	Lr/22	dorsal	primary layer
0843	*Laqueus rubellus*	Sagami Bay	Lr/22	Lr/21	ventral	non-specialised secondary layer
0844	*Laqueus rubellus*	Sagami Bay	Lr/22	Lr/21	ventral	teeth
0845	*Laqueus rubellus*	Sagami Bay	Lr/22	Lr/21	ventral	pedicle foramen
0846	*Laqueus rubellus*	Sagami Bay	Lr/22	Lr/21	ventral	muscle scars
0847	*Laqueus rubellus*	Sagami Bay	Lr/22	Lr/21	ventral	primary layer
0848	*Laqueus rubellus*	Sagami Bay	Lr/23	Lr/24	dorsal	loop
0849	*Laqueus rubellus*	Sagami Bay	Lr/23	Lr/24	dorsal	non-specialised secondary layer
0850	*Laqueus rubellus*	Sagami Bay	Lr/23	Lr/24	dorsal	cardinal process
0851	*Laqueus rubellus*	Sagami Bay	Lr/23	Lr/24	dorsal	muscle scars
0852	*Laqueus rubellus*	Sagami Bay	Lr/23	Lr/24	dorsal	primary layer
0853	*Laqueus rubellus*	Sagami Bay	Lr/24	Lr/23	ventral	non-specialised secondary layer
0854	*Laqueus rubellus*	Sagami Bay	Lr/24	Lr/23	ventral	teeth

(Continued on next page)

Sample Number	Species	Location	Valve Number	Conjoined Valve	Valve Type	Area Sampled
0855	*Laqueus rubellus*	Sagami Bay	Lr/24	Lr/23	ventral	pedicle foramen
0856	*Laqueus rubellus*	Sagami Bay	Lr/24	Lr/23	ventral	muscle scars
0857	*Laqueus rubellus*	Sagami Bay	Lr/24	Lr/23	ventral	primary layer
0858	*Liothyrella uva*	Signy Island	Lu/13	Lu/14	dorsal	loop
0859	*Liothyrella uva*	Signy Island	Lu/13	Lu/14	dorsal	non specialised tertiary layer
0860	*Liothyrella uva*	Signy Island	Lu/13	Lu/14	dorsal	cardinal process
0861	*Liothyrella uva*	Signy Island	Lu/13	Lu/14	dorsal	muscle scars
0862	*Liothyrella uva*	Signy Island	Lu/13	Lu/14	dorsal	primary layer
0863	*Liothyrella uva*	Signy Island	Lu/14	Lu/13	ventral	non specialised tertiary layer
0864	*Liothyrella uva*	Signy Island	Lu/14	Lu/13	ventral	teeth
0865	*Liothyrella uva*	Signy Island	Lu/14	Lu/13	ventral	pedicle foramen
0866	*Liothyrella uva*	Signy Island	Lu/14	Lu/13	ventral	muscle scars
0867	*Liothyrella uva*	Signy Island	Lu/14	Lu/13	ventral	primary layer
0868	*Liothyrella uva*	Signy Island	Lu/15	Lu/16	dorsal	loop
0869	*Liothyrella uva*	Signy Island	Lu/15	Lu/16	dorsal	non specialised tertiary layer
0870	*Liothyrella uva*	Signy Island	Lu/15	Lu/16	dorsal	cardinal process
0871	*Liothyrella uva*	Signy Island	Lu/15	Lu/16	dorsal	muscle scars
0872	*Liothyrella uva*	Signy Island	Lu/15	Lu/16	dorsal	primary layer
0873	*Liothyrella uva*	Signy Island	Lu/16	Lu/15	ventral	non specialised tertiary layer
0874	*Liothyrella uva*	Signy Island	Lu/16	Lu/15	ventral	teeth
0875	*Liothyrella uva*	Signy Island	Lu/16	Lu/15	ventral	pedicle foramen
0876	*Liothyrella uva*	Signy Island	Lu/16	Lu/15	ventral	muscle scars

(Continued on next page)

Sample Number	Species	Location	Valve Number	Conjoined Valve	Valve Type	Area Sampled
0877	*Liothyrella uva*	Signy Island	Lu/16	Lu/15	ventral	primary layer
0878	*Neothyris lenticularis*	Otago Shelf	Nl/19	Nl/20	dorsal	loop
0879	*Neothyris lenticularis*	Otago Shelf	Nl/19	Nl/20	dorsal	non-specialised secondary layer
0880	*Neothyris lenticularis*	Otago Shelf	Nl/19	Nl/20	dorsal	cardinal process
0881	*Neothyris lenticularis*	Otago Shelf	Nl/19	Nl/20	dorsal	muscle scars
0882	*Neothyris lenticularis*	Otago Shelf	Nl/19	Nl/20	dorsal	primary layer
0883	*Neothyris lenticularis*	Otago Shelf	Nl/20	Nl/19	ventral	non-specialised secondary layer
0884	*Neothyris lenticularis*	Otago Shelf	Nl/20	Nl/19	ventral	teeth
0885	*Neothyris lenticularis*	Otago Shelf	Nl/20	Nl/19	ventral	pedicle foramen
0886	*Neothyris lenticularis*	Otago Shelf	Nl/20	Nl/19	ventral	muscle scars
0887	*Neothyris lenticularis*	Otago Shelf	Nl/20	Nl/19	ventral	primary layer
0888	*Neothyris lenticularis*	Otago Shelf	Nl/21	Nl/22	dorsal	loop
0889	*Neothyris lenticularis*	Otago Shelf	Nl/21	Nl/22	dorsal	non-specialised secondary layer
0890	*Neothyris lenticularis*	Otago Shelf	Nl/21	Nl/22	dorsal	cardinal process
0891	*Neothyris lenticularis*	Otago Shelf	Nl/21	Nl/22	dorsal	muscle scars
0892	*Neothyris lenticularis*	Otago Shelf	Nl/21	Nl/22	dorsal	primary layer
0893	*Neothyris lenticularis*	Otago Shelf	Nl/22	Nl/21	ventral	non-specialised secondary layer
0894	*Neothyris lenticularis*	Otago Shelf	Nl/22	Nl/21	ventral	teeth
0895	*Neothyris lenticularis*	Otago Shelf	Nl/22	Nl/21	ventral	pedicle foramen
0896	*Neothyris lenticularis*	Otago Shelf	Nl/22	Nl/21	ventral	muscle scars
0897	*Neothyris lenticularis*	Otago Shelf	Nl/22	Nl/21	ventral	primary layer
0898	*Terebratulina retusa*	Firth of Lorne	Tr/20	Tr/21	dorsal	loop

(Continued on next page)

Sample Number	Species	Location	Valve Number	Conjoined Valve	Valve Type	Area Sampled
0899	*Terebratulina retusa*	Firth of Lorne	Tr/20	Tr/21	dorsal	non-specialised secondary layer
0900	*Terebratulina retusa*	Firth of Lorne	Tr/20	Tr/21	dorsal	cardinal process
0901	*Terebratulina retusa*	Firth of Lorne	Tr/20	Tr/21	dorsal	muscle scars
0902	*Terebratulina retusa*	Firth of Lorne	Tr/20	Tr/21	dorsal	primary layer
0903	*Terebratulina retusa*	Firth of Lorne	Tr/21	Tr/20	ventral	non-specialised secondary layer
0904	*Terebratulina retusa*	Firth of Lorne	Tr/21	Tr/20	ventral	teeth
0905	*Terebratulina retusa*	Firth of Lorne	Tr/21	Tr/20	ventral	pedicle foramen
0906	*Terebratulina retusa*	Firth of Lorne	Tr/21	Tr/20	ventral	muscle scars
0907	*Terebratulina retusa*	Firth of Lorne	Tr/21	Tr/20	ventral	primary layer
0908	*Terebratulina retusa*	Firth of Lorne	Tr/22	Tr/23	dorsal	loop
0909	*Terebratulina retusa*	Firth of Lorne	Tr/22	Tr/23	dorsal	non-specialised secondary layer
0910	*Terebratulina retusa*	Firth of Lorne	Tr/22	Tr/23	dorsal	cardinal process
0911	*Terebratulina retusa*	Firth of Lorne	Tr/22	Tr/23	dorsal	muscle scars
0912	*Terebratulina retusa*	Firth of Lorne	Tr/22	Tr/23	dorsal	primary layer
0913	*Terebratulina retusa*	Firth of Lorne	Tr/23	Tr/22	ventral	non-specialised secondary layer
0914	*Terebratulina retusa*	Firth of Lorne	Tr/23	Tr/22	ventral	teeth
0915	*Terebratulina retusa*	Firth of Lorne	Tr/23	Tr/22	ventral	pedicle foramen
0916	*Terebratulina retusa*	Firth of Lorne	Tr/23	Tr/22	ventral	muscle scars
0917	*Terebratulina retusa*	Firth of Lorne	Tr/23	Tr/22	ventral	primary layer
0918	*Calloria inconspicua*	Otago Shelf	Ci/21	Ci/22	dorsal	loop
0919	*Calloria inconspicua*	Otago Shelf	Ci/21	Ci/22	dorsal	non-specialised secondary layer
0920	*Calloria inconspicua*	Otago Shelf	Ci/21	Ci/22	dorsal	cardinal process

(Continued on next page)

Sample Number	Species	Location	Valve Number	Conjoined Valve	Valve Type	Area Sampled
0921	*Calloria inconspicua*	Otago Shelf	Ci/21	Ci/22	dorsal	muscle scars
0922	*Calloria inconspicua*	Otago Shelf	Ci/21	Ci/22	dorsal	primary layer
0923	*Calloria inconspicua*	Otago Shelf	Ci/22	Ci/21	ventral	non-specialised secondary layer
0924	*Calloria inconspicua*	Otago Shelf	Ci/22	Ci/21	ventral	teeth
0925	*Calloria inconspicua*	Otago Shelf	Ci/22	Ci/21	ventral	pedicle foramen
0926	*Calloria inconspicua*	Otago Shelf	Ci/22	Ci/21	ventral	muscle scars
0927	*Calloria inconspicua*	Otago Shelf	Ci/22	Ci/21	ventral	primary layer
0928	*Calloria inconspicua*	Otago Shelf	Ci/23	Ci/24	dorsal	loop
0929	*Calloria inconspicua*	Otago Shelf	Ci/23	Ci/24	dorsal	non-specialised secondary layer
0930	*Calloria inconspicua*	Otago Shelf	Ci/23	Ci/24	dorsal	cardinal process
0931	*Calloria inconspicua*	Otago Shelf	Ci/23	Ci/24	dorsal	muscle scars
0932	*Calloria inconspicua*	Otago Shelf	Ci/23	Ci/24	dorsal	primary layer
0933	*Calloria inconspicua*	Otago Shelf	Ci/24	Ci/23	ventral	non-specialised secondary layer
0934	*Calloria inconspicua*	Otago Shelf	Ci/24	Ci/23	ventral	teeth
0935	*Calloria inconspicua*	Otago Shelf	Ci/24	Ci/23	ventral	pedicle foramen
0936	*Calloria inconspicua*	Otago Shelf	Ci/24	Ci/23	ventral	muscle scars
0937	*Calloria inconspicua*	Otago Shelf	Ci/24	Ci/23	ventral	primary layer
0938	*Notosaria nigricans*	Otago Shelf	Nn/21	Nn/22	dorsal	loop
0939	*Notosaria nigricans*	Otago Shelf	Nn/21	Nn/22	dorsal	non-specialised secondary layer
0940	*Notosaria nigricans*	Otago Shelf	Nn/21	Nn/22	dorsal	cardinal process
0941	*Notosaria nigricans*	Otago Shelf	Nn/21	Nn/22	dorsal	muscle scars
0942	*Notosaria nigricans*	Otago Shelf	Nn/21	Nn/22	dorsal	primary layer

(Continued on next page)

Sample Number	Species	Location	Valve Number	Conjoined Valve	Valve Type	Area Sampled
0943	*Notosaria nigricans*	Otago Shelf	Nn/22	Nn/21	ventral	non-specialised secondary layer
0944	*Notosaria nigricans*	Otago Shelf	Nn/22	Nn/21	ventral	teeth
0945	*Notosaria nigricans*	Otago Shelf	Nn/22	Nn/21	ventral	pedicle foramen
0946	*Notosaria nigricans*	Otago Shelf	Nn/22	Nn/21	ventral	muscle scars
0947	*Notosaria nigricans*	Otago Shelf	Nn/22	Nn/21	ventral	primary layer
0948	*Notosaria nigricans*	Otago Shelf	Nn/23	Nn/24	dorsal	loop
0949	*Notosaria nigricans*	Otago Shelf	Nn/23	Nn/24	dorsal	non-specialised secondary layer
0950	*Notosaria nigricans*	Otago Shelf	Nn/23	Nn/24	dorsal	cardinal process
0951	*Notosaria nigricans*	Otago Shelf	Nn/23	Nn/24	dorsal	muscle scars
0952	*Notosaria nigricans*	Otago Shelf	Nn/23	Nn/24	dorsal	primary layer
0953	*Notosaria nigricans*	Otago Shelf	Nn/24	Nn/23	ventral	non-specialised secondary layer
0954	*Notosaria nigricans*	Otago Shelf	Nn/24	Nn/23	ventral	teeth
0955	*Notosaria nigricans*	Otago Shelf	Nn/24	Nn/23	ventral	pedicle foramen
0956	*Notosaria nigricans*	Otago Shelf	Nn/24	Nn/23	ventral	muscle scars
0957	*Notosaria nigricans*	Otago Shelf	Nn/24	Nn/23	ventral	primary layer
0958	*Terebratalia transversa*	Friday Harbor	Tt/17	Tt/18	dorsal	loop
0959	*Terebratalia transversa*	Friday Harbor	Tt/17	Tt/18	dorsal	non-specialised secondary layer
0960	*Terebratalia transversa*	Friday Harbor	Tt/17	Tt/18	dorsal	cardinal process
0961	*Terebratalia transversa*	Friday Harbor	Tt/17	Tt/18	dorsal	muscle scars
0962	*Terebratalia transversa*	Friday Harbor	Tt/17	Tt/18	dorsal	primary layer
0963	*Terebratalia transversa*	Friday Harbor	Tt/18	Tt/17	ventral	non-specialised secondary layer
0964	*Terebratalia transversa*	Friday Harbor	Tt/18	Tt/17	ventral	teeth

(Continued on next page)

Sample Number	Species	Location	Valve Number	Conjoined Valve	Valve Type	Area Sampled
0965	*Terebratalia transversa*	Friday Harbor	Tt/18	Tt/17	ventral	pedicle foramen
0966	*Terebratalia transversa*	Friday Harbor	Tt/18	Tt/17	ventral	muscle scars
0967	*Terebratalia transversa*	Friday Harbor	Tt/18	Tt/17	ventral	primary layer
0968	*Terebratalia transversa*	Friday Harbor	Tt/19	Tt/20	dorsal	loop
0969	*Terebratalia transversa*	Friday Harbor	Tt/19	Tt/20	dorsal	non-specialised secondary layer
0970	*Terebratalia transversa*	Friday Harbor	Tt/19	Tt/20	dorsal	cardinal process
0971	*Terebratalia transversa*	Friday Harbor	Tt/19	Tt/20	dorsal	muscle scars
0972	*Terebratalia transversa*	Friday Harbor	Tt/19	Tt/20	dorsal	primary layer
0973	*Terebratalia transversa*	Friday Harbor	Tt/20	Tt/19	ventral	non-specialised secondary layer
0974	*Terebratalia transversa*	Friday Harbor	Tt/20	Tt/19	ventral	teeth
0975	*Terebratalia transversa*	Friday Harbor	Tt/20	Tt/19	ventral	pedicle foramen
0976	*Terebratalia transversa*	Friday Harbor	Tt/20	Tt/19	ventral	muscle scars
0977	*Terebratalia transversa*	Friday Harbor	Tt/20	Tt/19	ventral	primary layer
0978	*Terebratella sanguinea*	Otago Shelf	Ts/17	Ts/18	dorsal	loop
0979	*Terebratella sanguinea*	Otago Shelf	Ts/17	Ts/18	dorsal	non-specialised secondary layer
0980	*Terebratella sanguinea*	Otago Shelf	Ts/17	Ts/18	dorsal	cardinal process
0981	*Terebratella sanguinea*	Otago Shelf	Ts/17	Ts/18	dorsal	muscle scars
0982	*Terebratella sanguinea*	Otago Shelf	Ts/17	Ts/18	dorsal	primary layer
0983	*Terebratella sanguinea*	Otago Shelf	Ts/18	Ts/17	ventral	non-specialised secondary layer
0984	*Terebratella sanguinea*	Otago Shelf	Ts/18	Ts/17	ventral	teeth
0985	*Terebratella sanguinea*	Otago Shelf	Ts/18	Ts/17	ventral	pedicle foramen
0986	*Terebratella sanguinea*	Otago Shelf	Ts/18	Ts/17	ventral	muscle scars

(Continued on next page)

Sample Number	Species	Location	Valve Number	Conjoined Valve	Valve Type	Area Sampled
0987	*Terebratella sanguinea*	Otago Shelf	Ts/18	Ts/17	ventral	primary layer
0988	*Terebratella sanguinea*	Otago Shelf	Ts/19	Ts/20	dorsal	loop
0989	*Terebratella sanguinea*	Otago Shelf	Ts/19	Ts/20	dorsal	non-specialised secondary layer
0990	*Terebratella sanguinea*	Otago Shelf	Ts/19	Ts/20	dorsal	cardinal process
0991	*Terebratella sanguinea*	Otago Shelf	Ts/19	Ts/20	dorsal	muscle scars
0992	*Terebratella sanguinea*	Otago Shelf	Ts/19	Ts/20	dorsal	primary layer
0993	*Terebratella sanguinea*	Otago Shelf	Ts/20	Ts/19	ventral	non-specialised secondary layer
0994	*Terebratella sanguinea*	Otago Shelf	Ts/20	Ts/19	ventral	teeth
0995	*Terebratella sanguinea*	Otago Shelf	Ts/20	Ts/19	ventral	pedicle foramen
0996	*Terebratella sanguinea*	Otago Shelf	Ts/20	Ts/19	ventral	muscle scars
0997	*Terebratella sanguinea*	Otago Shelf	Ts/20	Ts/19	ventral	primary layer
0998	*Liothyrella neozelanica*	Otago Shelf	Ln/17	Ln/18	dorsal	loop
0999	*Liothyrella neozelanica*	Otago Shelf	Ln/17	Ln/18	dorsal	non specialised tertiary layer
1000	*Liothyrella neozelanica*	Otago Shelf	Ln/17	Ln/18	dorsal	cardinal process
1001	*Liothyrella neozelanica*	Otago Shelf	Ln/17	Ln/18	dorsal	muscle scars
1002	*Liothyrella neozelanica*	Otago Shelf	Ln/17	Ln/18	dorsal	primary layer
1003	*Liothyrella neozelanica*	Otago Shelf	Ln/18	Ln/17	ventral	non specialised tertiary layer
1004	*Liothyrella neozelanica*	Otago Shelf	Ln/18	Ln/17	ventral	teeth
1005	*Liothyrella neozelanica*	Otago Shelf	Ln/18	Ln/17	ventral	pedicle foramen
1006	*Liothyrella neozelanica*	Otago Shelf	Ln/18	Ln/17	ventral	muscle scars
1007	*Liothyrella neozelanica*	Otago Shelf	Ln/18	Ln/17	ventral	primary layer
1008	*Liothyrella neozelanica*	Otago Shelf	Ln/19	Ln/20	dorsal	loop

(Continued on next page)

Sample Number	Species	Location	Valve Number	Conjoined Valve	Valve Type	Area Sampled
1009	*Liothyrella neozelanica*	Otago Shelf	Ln/19	Ln/20	dorsal	non specialised tertiary layer
1010	*Liothyrella neozelanica*	Otago Shelf	Ln/19	Ln/20	dorsal	cardinal process
1011	*Liothyrella neozelanica*	Otago Shelf	Ln/19	Ln/20	dorsal	muscle scars
1012	*Liothyrella neozelanica*	Otago Shelf	Ln/19	Ln/20	dorsal	primary layer
1013	*Liothyrella neozelanica*	Otago Shelf	Ln/20	Ln/19	ventral	non specialised tertiary layer
1014	*Liothyrella neozelanica*	Otago Shelf	Ln/20	Ln/19	ventral	teeth
1015	*Liothyrella neozelanica*	Otago Shelf	Ln/20	Ln/19	ventral	pedicle foramen
1016	*Liothyrella neozelanica*	Otago Shelf	Ln/20	Ln/19	ventral	muscle scars
1017	*Liothyrella neozelanica*	Otago Shelf	Ln/20	Ln/19	ventral	primary layer
1018	*Novocrania anomala*	Otago Shelf	Na/07	*	dorsal	non-specialised secondary layer
1019	*Novocrania anomala*	Otago Shelf	Na/07	*	dorsal	muscle scars
1020	*Novocrania anomala*	Otago Shelf	Na/07	*	dorsal	primary layer
1021	*Novocrania anomala*	Otago Shelf	Na/08	*	dorsal	non-specialised secondary layer
1022	*Novocrania anomala*	Otago Shelf	Na/08	*	dorsal	muscle scars
1023	*Novocrania anomala*	Otago Shelf	Na/08	*	dorsal	primary layer
1024	*Novocrania anomala*	Otago Shelf	Na/09	*	dorsal	non-specialised secondary layer
1025	*Novocrania anomala*	Otago Shelf	Na/09	*	dorsal	muscle scars
1026	*Novocrania anomala*	Otago Shelf	Na/09	*	dorsal	primary layer
1027	*Novocrania anomala*	Otago Shelf	Na/10	*	dorsal	non-specialised secondary layer
1028	*Novocrania anomala*	Otago Shelf	Na/10	*	dorsal	muscle scars
1029	*Novocrania anomala*	Otago Shelf	Na/10	*	dorsal	primary layer
1030	*Novocrania anomala*	Otago Shelf	Na/11	*	dorsal	non-specialised secondary layer

(Continued on next page)

Sample Number	Species	Location	Valve Number	Conjoined Valve	Valve Type	Area Sampled
1031	*Novocrania anomala*	Otago Shelf	Na/11	*	dorsal	muscle scars
1032	*Novocrania anomala*	Otago Shelf	Na/11	*	dorsal	primary layer
1033	*Novocrania anomala*	Otago Shelf	Na/12	*	dorsal	non-specialised secondary layer
1034	*Novocrania anomala*	Otago Shelf	Na/12	*	dorsal	muscle scars
1035	*Novocrania anomala*	Otago Shelf	Na/12	*	dorsal	primary layer
1036	*Liothyrella uva*	Signy Island	Lu/17	Lu/18	dorsal	loop
1037	*Liothyrella uva*	Signy Island	Lu/17	Lu/18	dorsal	non specialised tertiary layer
1038	*Liothyrella uva*	Signy Island	Lu/17	Lu/18	dorsal	cardinal process
1039	*Liothyrella uva*	Signy Island	Lu/17	Lu/18	dorsal	muscle scars
1040	*Liothyrella uva*	Signy Island	Lu/17	Lu/18	dorsal	primary layer
1041	*Liothyrella uva*	Signy Island	Lu/18	Lu/17	ventral	non specialised tertiary layer
1042	*Liothyrella uva*	Signy Island	Lu/18	Lu/17	ventral	teeth
1043	*Liothyrella uva*	Signy Island	Lu/18	Lu/17	ventral	pedicle foramen
1044	*Liothyrella uva*	Signy Island	Lu/18	Lu/17	ventral	muscle scars
1045	*Liothyrella uva*	Signy Island	Lu/18	Lu/17	ventral	primary layer
1046	*Liothyrella uva*	Signy Island	Lu/19	Lu/20	dorsal	loop
1047	*Liothyrella uva*	Signy Island	Lu/19	Lu/20	dorsal	non specialised tertiary layer
1048	*Liothyrella uva*	Signy Island	Lu/19	Lu/20	dorsal	cardinal process
1049	*Liothyrella uva*	Signy Island	Lu/19	Lu/20	dorsal	muscle scars
1050	*Liothyrella uva*	Signy Island	Lu/19	Lu/20	dorsal	primary layer
1051	*Liothyrella uva*	Signy Island	Lu/20	Lu/19	ventral	non specialised tertiary layer
1052	*Liothyrella uva*	Signy Island	Lu/20	Lu/19	ventral	teeth

(Continued on next page)

Sample Number	Species	Location	Valve Number	Conjoined Valve	Valve Type	Area Sampled
1053	*Liothyrella uva*	Signy Island	Lu/20	Lu/19	ventral	pedicle foramen
1054	*Liothyrella uva*	Signy Island	Lu/20	Lu/19	ventral	muscle scars
1055	*Liothyrella uva*	Signy Island	Lu/20	Lu/19	ventral	primary layer
1056	*Modiolus modiolus*	Firth of Lorne	Mm/01	*	*	aragonite
1057	*Modiolus modiolus*	Firth of Lorne	Mm/01	*	*	calcite
1058	*Modiolus modiolus*	Firth of Lorne	Mm/02	*	*	aragonite
1059	*Modiolus modiolus*	Firth of Lorne	Mm/02	*	*	calcite
1060	*Modiolus modiolus*	Firth of Lorne	Mm/03	*	*	aragonite
1061	*Modiolus modiolus*	Firth of Lorne	Mm/03	*	*	calcite
1062	*Modiolus modiolus*	Firth of Lorne	Mm/04	*	*	aragonite
1063	*Modiolus modiolus*	Firth of Lorne	Mm/04	*	*	calcite
1064	*Modiolus modiolus*	Firth of Lorne	Mm/05	*	*	aragonite
1065	*Modiolus modiolus*	Firth of Lorne	Mm/05	*	*	calcite
1066	*Modiolus modiolus*	Firth of Lorne	Mm/06	*	*	aragonite
1067	*Modiolus modiolus*	Firth of Lorne	Mm/06	*	*	calcite
1068	*Modiolus modiolus*	Firth of Lorne	Mm/07	*	*	aragonite
1069	*Modiolus modiolus*	Firth of Lorne	Mm/07	*	*	calcite
1070	*Modiolus modiolus*	Firth of Lorne	Mm/08	*	*	aragonite
1071	*Modiolus modiolus*	Firth of Lorne	Mm/08	*	*	calcite
1072	*Modiolus modiolus*	Firth of Lorne	Mm/09	*	*	aragonite
1073	*Modiolus modiolus*	Firth of Lorne	Mm/09	*	*	calcite
1074	*Modiolus modiolus*	Firth of Lorne	Mm/10	*	*	aragonite

(Continued on next page)

Sample Number	Species	Location	Valve Number	Conjoined Valve	Valve Type	Area Sampled
1075	*Modiolus modiolus*	Firth of Lorne	Mm/10	*	*	calcite
1076	*Laqueus rubellus*	Otago Shelf	Lr/bulk	*	*	whole shell
1077	*Liothyrella uva*	Signy Island	Lu/bulk	*	*	whole shell
1078	*Calloria inconspicua*	Otago Shelf	Ci/bulk	*	*	whole shell
1079	*Terebratalia transversa*	Friday Harbor	Tt/bulk	*	*	whole shell
1080	*Neothyris lenticularis*	Otago Shelf	Nl/bulk	*	*	whole shell
1081	*Terebratulina retusa*	Firth of Lorne	Tr/bulk	*	*	whole shell
1082	*Terebratella sanguinea*	Otago Shelf	Ts/bulk	*	*	whole shell
1083	*Notosaria nigricans*	Otago Shelf	Nn/bulk	*	*	whole shell
1084	*Novocrania anomala*	Firth of Lorne	Na/bulk	*	*	whole shell
1085	*Thecidellina*	Rio Bueno	Th/01	*	*	whole shell
1086	*Thecidellina*	Rio Bueno	Th/02	*	*	whole shell
1087	*Thecidellina*	Rio Bueno	Th/03	*	*	whole shell
1088	*Thecidellina*	Rio Bueno	Th/04	*	*	whole shell
1089	*Thecidellina*	Rio Bueno	Th/05	*	*	whole shell
1090	*Thecidellina*	Rio Bueno	Th/06	*	*	whole shell
1091	*Thecidellina*	Rio Bueno	Th/07	*	*	whole shell
1092	*Thecidellina*	Rio Bueno	Th/08	*	*	whole shell
1093	*Thecidellina*	Rio Bueno	Th/09	*	*	whole shell
1094	*Thecidellina*	Rio Bueno	Th/10	*	*	whole shell
1095	*Thecidellina*	Rio Bueno	Th/11	*	*	whole shell
1096	*Patella caerulea*	Efthalou	Pc/01	*	*	aragonite

(Continued on next page)

Sample Number	Species	Location	Valve Number	Conjoined Valve	Valve Type	Area Sampled
1097	*Patella caerulea*	Efthalou	Pc/02	*	*	calcite
1098	*Patella caerulea*	Efthalou	Pc/02	*	*	aragonite
1099	*Patella caerulea*	Efthalou	Pc/02	*	*	calcite
1100	*Patella caerulea*	Efthalou	Pc/03	*	*	aragonite
1101	*Patella caerulea*	Efthalou	Pc/03	*	*	calcite
1102	*Patella caerulea*	Efthalou	Pc/04	*	*	aragonite
1103	*Patella caerulea*	Efthalou	Pc/04	*	*	calcite
1104	*Patella caerulea*	Efthalou	Pc/05	*	*	aragonite
1105	*Patella caerulea*	Efthalou	Pc/05	*	*	calcite
1106	*Patella caerulea*	Efthalou	Pc/06	*	*	aragonite
1107	*Patella caerulea*	Efthalou	Pc/06	*	*	calcite
1108	*Patella caerulea*	Efthalou	Pc/07	*	*	aragonite
1109	*Patella caerulea*	Efthalou	Pc/07	*	*	calcite
1110	*Patella caerulea*	Efthalou	Pc/08	*	*	aragonite
1111	*Patella caerulea*	Efthalou	Pc/08	*	*	calcite
1112	*Patella caerulea*	Efthalou	Pc/09	*	*	aragonite
1113	*Patella caerulea*	Efthalou	Pc/09	*	*	calcite
1114	*Patella caerulea*	Efthalou	Pc/10	*	*	aragonite
1115	*Patella caerulea*	Efthalou	Pc/10	*	*	calcite
1116	*Neoancistrocrania norfolki*	Norfolk Ridge	Nnf/01	*	dorsal	crura
1117	*Neoancistrocrania norfolki*	Norfolk Ridge	Nnf/01	*	dorsal	muscle scars
1118	*Neoancistrocrania norfolki*	Norfolk Ridge	Nnf/01	*	dorsal	non-specialised secondary layer

(Continued on next page)

Sample Number	Species	Location	Valve Number	Conjoined Valve	Valve Type	Area Sampled
1119	*Neoancistrocrania norfolki*	Norfolk Ridge	Nnf/01	*	dorsal	primary layer
1120	*Neoancistrocrania norfolki*	Norfolk Ridge	Nnf/02	*	ventral	Depressed muscle scars
1121	*Neoancistrocrania norfolki*	Norfolk Ridge	Nnf/02	*	ventral	Lower non-specialised secondary layer
1122	*Neoancistrocrania norfolki*	Norfolk Ridge	Nnf/02	*	ventral	primary layer
1123	*Neoancistrocrania norfolki*	Norfolk Ridge	Nnf/02	*	ventral	Upper non-specialised secondary layer
1124	*Neoancistrocrania norfolki*	Norfolk Ridge	Nnf/02	*	ventral	Raised muscle scars
1125	*Neoancistrocrania norfolki*	Norfolk Ridge	Nnf/03	*	dorsal	crura
1126	*Neoancistrocrania norfolki*	Norfolk Ridge	Nnf/03	*	dorsal	muscle scars
1127	*Neoancistrocrania norfolki*	Norfolk Ridge	Nnf/03	*	dorsal	non-specialised secondary layer
1128	*Neoancistrocrania norfolki*	Norfolk Ridge	Nnf/03	*	dorsal	primary layer
1129	*Neoancistrocrania norfolki*	Norfolk Ridge	Nnf/04	*	ventral	Depressed muscle scars
1130	*Neoancistrocrania norfolki*	Norfolk Ridge	Nnf/04	*	ventral	Lower non-specialised secondary layer
1131	*Neoancistrocrania norfolki*	Norfolk Ridge	Nnf/04	*	ventral	primary layer
1132	*Neoancistrocrania norfolki*	Norfolk Ridge	Nnf/04	*	ventral	Upper non-specialised secondary layer
1133	*Neoancistrocrania norfolki*	Norfolk Ridge	Nnf/04	*	ventral	Raised muscle scars
1134	*Neoancistrocrania norfolki*	Norfolk Ridge	Nnf/05	*	dorsal	crura
1135	*Neoancistrocrania norfolki*	Norfolk Ridge	Nnf/05	*	dorsal	muscle scars
1136	*Neoancistrocrania norfolki*	Norfolk Ridge	Nnf/05	*	dorsal	non-specialised secondary layer
1137	*Neoancistrocrania norfolki*	Norfolk Ridge	Nnf/05	*	dorsal	primary layer
1138	*Neoancistrocrania norfolki*	Norfolk Ridge	Nnf/06	*	ventral	Depressed muscle scars
1139	*Neoancistrocrania norfolki*	Norfolk Ridge	Nnf/06	*	ventral	Lower non-specialised secondary layer
1140	*Neoancistrocrania norfolki*	Norfolk Ridge	Nnf/06	*	ventral	primary layer

(Continued on next page)

Sample Number	Species	Location	Valve Number	Conjoined Valve	Valve Type	Area Sampled
1141	*Neoancistrocrania norfolki*	Norfolk Ridge	Nnf/06	*	ventral	Upper non-specialised secondary layer
1142	*Neoancistrocrania norfolki*	Norfolk Ridge	Nnf/06	*	ventral	Raised muscle scars
1143	*Neoancistrocrania norfolki*	Norfolk Ridge	Nnf/07	*	dorsal	crura
1144	*Neoancistrocrania norfolki*	Norfolk Ridge	Nnf/07	*	dorsal	muscle scars
1145	*Neoancistrocrania norfolki*	Norfolk Ridge	Nnf/07	*	dorsal	non-specialised secondary layer
1146	*Neoancistrocrania norfolki*	Norfolk Ridge	Nnf/07	*	dorsal	primary layer
1147	*Neoancistrocrania norfolki*	Norfolk Ridge	Nnf/08	*	ventral	Depressed muscle scars
1148	*Neoancistrocrania norfolki*	Norfolk Ridge	Nnf/08	*	ventral	Lower non-specialised secondary layer
1149	*Neoancistrocrania norfolki*	Norfolk Ridge	Nnf/08	*	ventral	primary layer
1150	*Neoancistrocrania norfolki*	Norfolk Ridge	Nnf/08	*	ventral	Upper non-specialised secondary layer
1151	*Neoancistrocrania norfolki*	Norfolk Ridge	Nnf/08	*	ventral	Raised muscle scars
1152	*Neoancistrocrania norfolki*	Norfolk Ridge	Nnf/09	*	dorsal	crura
1153	*Neoancistrocrania norfolki*	Norfolk Ridge	Nnf/09	*	dorsal	muscle scars
1154	*Neoancistrocrania norfolki*	Norfolk Ridge	Nnf/09	*	dorsal	non-specialised secondary layer
1155	*Neoancistrocrania norfolki*	Norfolk Ridge	Nnf/09	*	dorsal	primary layer
1156	*Neoancistrocrania norfolki*	Norfolk Ridge	Nnf/10	*	ventral	Depressed muscle scars
1157	*Neoancistrocrania norfolki*	Norfolk Ridge	Nnf/10	*	ventral	Lower non-specialised secondary layer
1158	*Neoancistrocrania norfolki*	Norfolk Ridge	Nnf/10	*	ventral	primary layer
1159	*Neoancistrocrania norfolki*	Norfolk Ridge	Nnf/10	*	ventral	Upper non-specialised secondary layer
1160	*Neoancistrocrania norfolki*	Norfolk Ridge	Nnf/10	*	ventral	Raised muscle scars

Appendix B

$\delta^{18}O$ and $\delta^{13}C$ values

no pre-treatment

versus

plasma ashing

$\delta^{18}O$ and $\delta^{13}C$ values - no pre-treatment versus plasma ashing

Species	Sample number	No Treatment		Plasma Ashed	
		$\delta^{13}C$ ‰ VPDB	$\delta^{18}O$ ‰ VPDB	$\delta^{13}C$ ‰ VPDB	$\delta^{18}O$ ‰ VPDB
Novocrania anomala	0116	1.376	2.248	1.232	2.140
	0120	1.446	2.319	1.360	2.181
Terebratulina retusa	0044	1.871	1.982	1.524	2.043
	0045	1.858	1.974	1.973	2.106
	0046	1.920	2.112	1.999	2.154
	0047	1.538	1.898	1.450	1.883
	0048	1.266	1.924	1.111	1.784
	0051	1.622	1.863	1.561	1.782
	0053	1.898	1.715	1.784	1.795
	0054	1.503	1.819	1386	1.753
	0055	0.743	1.758	0.830	1.194
	0057	0.315	1.203	0.922	1.665
Calloria inconspicua	0072	2.228	1.480	2.154	1.654
	0073	1.961	1.728	1.781	1.625
	0074	2.323	1.970	2.168	1.862
	0075	2.067	1.509	2.000	1.457
	0076	0.295	0.442	0.365	0.642

(Continued on next page)

$\delta^{18}O$ and $\delta^{13}C$ values - no pre-treatment verses plasma ashing

Species	Sample number	No Treatment		Plasma Ashed	
		$\delta^{13}C$ ‰ VPDB	$\delta^{18}O$ ‰ VPDB	$\delta^{13}C$ ‰ VPDB	$\delta^{18}O$ ‰ VPDB
	0077	2.187	1.559	2.167	1.612
	0082	1.855	1.344	1.884	1.194
	0083	2.332	1.477	2.240	1.336
	0084	1.491	1.196	1.356	1.137
	0085	1.885	1.425	1.810	1.313
	0086	2.062	1.308	2.010	1.214
	0087	0.154	-0.184	0.087	-0.162
Neothyris lenticularis	0001	2.218	1.713	2.228	1.486
	0002	2.540	1.925	2.598	2.049
	0003	2.196	1.825	2.245	1.642
	0004	2.177	1.762	2.145	1.680
	0005	1.356	2.068	1.354	1.884
	0006	1.359	2.026	1.080	1.949
	0007	2.253	1.484	2.186	1.315
	0008	2.169	1.445	2.139	1.544
	0009	2.546	1.953	2.447	1.684
	0010	2.405	1.787	2.324	1.697
	0011	2.375	1.962	2.340	1.766
	0012	2.604	1.876	2.585	1.876
	0013	2.145	1.463	2.071	1.380
	0014	2.176	1.581	2.135	1.586

(Continued on next page)

$\delta^{18}O$ and $\delta^{13}C$ values - no pre-treatment verses plasma ashing

Species	Sample number	No Treatment		Plasma Ashed	
		$\delta^{13}C$ ‰ VPDB	$\delta^{18}O$ ‰ VPDB	$\delta^{13}C$ ‰ VPDB	$\delta^{18}O$ ‰ VPDB
	0015	2.340	1.394	2.303	1.237
	0016	2.216	1.341	2.206	1.325
	0017	2.699	1.777	2.594	1.708
	0018	2.605	2.022	2.518	1.902
	0019	2.560	2.026	2.439	1.704
	0020	2.468	1.786	2.020	2.075
	0021	2.555	1.869	2.108	1.495
	0022	2.195	1.661	2.215	1.748
	0023	2.564	1.583	2.478	1.479
	0024	2.641	1.594	2.638	1.639
	0025	2.496	1.605	2.476	1.249
	0026	2.654	1.963	2.655	1.694
	0027	2.817	2.119	2.863	2.236
	0028	2.940	2.274	2.933	2.316
	0029	2.466	2.115	2.491	1.935
	0030	2.355	2.058	2.302	2.039
	0031	2.154	1.718	2.172	1.774
	0032	2.392	1.692	2.262	1.737
	0033	2.394	1.501	2.520	1.753
	0034	2.494	1.734	2.613	1.899
	0036	1.699	0.934	1.705	0.983

Continued on next page

$\delta^{18}O$ and $\delta^{13}C$ values - no pre-treatment verses plasma ashing

Species	Sample number	No Treatment		Plasma Ashed	
		$\delta^{13}C$ ‰ VPDB	$\delta^{18}O$ ‰ VPDB	$\delta^{13}C$ ‰ VPDB	$\delta^{18}O$ ‰ VPDB
Notosaria nigricans	0099	2.599	1.654	2.304	1.638
	0100	1.326	1.598	1.283	1.656
	0101	1.504	1.930	1.600	1.643
	0102	2.300	1.924	2.478	1.762
	0103	1.449	0.956	1.658	0.903
	0104	2.089	1.747	2.129	1.782
	0105	2.599	2.071	2.307	1.879
	0107	0.922	1.711	0.895	1.676
	0108	2.342	1.778	2.337	1.785
	0109	2.132	1.435	1.918	1.265

Appendix C

$\delta^{18}O$ and $\delta^{13}C$ values

from

brachiopod shell

analysis

δ18O and δ13C values from brachiopod shell analysis

Species	Location	Specimen	Sample no.	Valve	Layer	Area	δ13C VPDB				δ18O VPDB			
							1	2	3	Mean	1	2	3	Mean
Novocrania anomala	1. Firth of Lorne,	1	0202	D	SL	Non-specialised	1.37	*	*	1.37	3.32	*	*	3.32
	Scotland		0203	D	SL	Muscle Scars	1.13	*	*	1.13	1.68	*	*	1.68
			0204	D	PL	Primary Layer	0.65	*	*	0.65	1.50	*	*	1.50
		2	0205	D	SL	Secondary Layer	0.84	*	*	0.84	2.00	*	*	2.00
			0206	D	SL	Muscle Scars	0.91	*	*	0.91	2.48	*	*	2.48
			0207	D	PL	Non-specialised	0.49	*	*	0.49	1.71	*	*	1.71
		3	0353	D	SL	Non-specialised	4.31	4.27	*	4.29	3.36	3.12	*	3.36
			0352	D	SL	Muscle Scars	1.07	*	*	1.07	2.00	*	*	2.00
			0354	D	PL	Non-specialised	0.14	*	*	0.14	0.99	*	*	0.99
		4	0355	D	SL	Non-specialised	1.50	*	*	1.50	1.82	*	*	1.82
			0356	D	SL	Muscle Scars	0.79	*	*	0.79	1.59	*	*	1.59
			0357	D	PL	Non-specialised	0.06	0.02	*	0.04	0.80	1.34	*	1.07
		5	1018	D	SL	Non-specialised	2.65	*	*	2.65	3.99	*	*	3.99
			1019	D	SL	Muscle Scars	1.05	*	*	1.05	2.00	*	*	2.00
			1020	D	PL	Non-specialised	0.12	*	*	0.12	1.23	*	*	1.23
		6	1021	D	SL	Secondary Layer	-2.75	*		-2.75	1.78	*	*	1.78
			1022	D	SL	Muscle Scars	1.15	*	*	1.15	1.62	*	*	1.62

(Continued on next page)

Species	Location	Specimen	Sample no.	Valve	Layer	Area	$\delta^{13}C$ VPDB				$\delta^{18}O$ VPDB			
							1	2	3	Mean	1	2	3	Mean
			1023	D	PL	Non-specialised	0.28	*	*	0.28	0.98	*	*	0.98
		7	1024	D	SL	Non-specialised	0.38	*	*	0.38	2.15	*	*	2.15
			1025	D	SL	Muscle Scars	1.10	0.97		1.03	2.15	1.44		1.79
			1026	D	PL	Non-specialised	1.19	*	*	1.19	0.99	*	*	0.99
		8	1027	D	SL	Non-specialised	1.71	*	*	1.71	1.33	*	*	1.33
			1028	D	SL	Muscle Scars	1.12	1.08	*	1.10	1.88	1.44	*	1.66
			1029	D	PL	Non-specialised	0.20	*	*	0.20	1.34	*	*	1.34
		9	1030	D	SL	Non-specialised	0.08	*	*	0.08	1.97	*	*	1.97
			1031	D	SL	Muscle Scars	0.84	*	*	0.84	1.82	*	*	1.82
			1032	D	PL	Non-specialised	0.28	*	*	0.28	1.42	*	*	1.42
		10	1033	D	SL	Non-specialised	0.10	*	*	0.10	2.05	*	*	2.05
			1034	D	SL	Muscle Scars	0.83	*	*	0.83	1.93	*	*	1.93
			1035	D	PL	Non-specialised	0.03	*	*	0.03	0.93	*	*	0.93
Terebratulina retusa	1. Firth of Lorne,	1	0044	D	SL	Loop	1.52	*	*	1.52	2.04	*	*	2.04
	Scotland		0046	D	SL	Non-specialised	2.00	2.04	*	2.02	2.15	2.33	*	2.24
			0048	D	SL	Muscle Scars	1.11	*	*	1.11	1.78	*	*	1.78
			0047	D	SL	Cardinal Process	1.45	1.32	*	1.38	1.83	1.46	*	1.64
			0050	D	PL	Non-specialised	1.71	1.72	*	1.71	1.91	1.74	*	1.83
			0051	V	SL	Non-specialised	1.56	*	*	1.56	1.78	*	*	1.78
			0053	V	SL	Teeth	1.78	1.85	*	1.82	1.80	1.95	*	1.87
			0054	V	SL	Pedicle Foramen	1.39	*	*	1.39	1.75	*	*	1.75
			0055	V	SL	Muscle Scars	0.83	*	*	0.83	1.19	*	*	1.19

(Continued on next page)

Species	Location	Specimen	Sample no.	Valve	Layer	Area	$\delta^{13}C$ VPDB				$\delta^{18}O$ VPDB			
							1	2	3	Mean	1	2	3	Mean
			0057	V	PL	Non-specialised	0.92	*	*	0.92	1.67	*	*	1.67
		2	0142	D	SL	Loop	2.23	*	*	2.23	2.21	*	*	2.21
			0143	D	SL	Non-specialised	2.09	2.12	*	2.10	2.11	2.04	*	2.07
			0144	D	SL	Muscle Scars	1.17	*	*	1.17	1.97	*	*	1.97
			0145	D	SL	Cardinal Process	1.54	*	*	1.54	1.80	*	*	1.80
			0146	D	PL	Non-specialised	0.83	*	*	0.83	1.31	*	*	1.31
			0147	V	SL	Non-specialised	0.75	1.78	*	1.27	1.63	1.56	*	1.60
			0148	V	SL	Teeth	1.91	*	*	1.91	2.23	*	*	2.23
			0149	V	SL	Pedicle Foramen	1.61	*	*	1.61	1.77	*	*	1.77
			0150	V	SL	Muscle Scars	0.36	*	*	0.36	1.79	*	*	1.79
			0151	V	PL	Non-specialised	1.57	*	*	1.57	1.80	*	*	1.80
		3	0152	D	SL	Loop	0.73	*	*	0.73	1.75	*	*	1.75
			0153	D	SL	Non-specialised	2.08	*	*	2.08	2.30	*	*	2.30
			0154	D	SL	Muscle Scars	1.58	*	*	1.58	1.50	*	*	1.50
			0155	D	SL	Cardinal Process	1.17	*	*	1.17	1.43	*	*	1.43
			0156	D	PL	Non-specialised	0.18	*	*	0.18	1.23	*	*	1.23
			0157	V	SL	Non-specialised	1.52	1.72	*	1.62	1.91	1.96	*	1.94
			0158	V	SL	Teeth	1.29	*	*	1.29	1.98	*	*	1.98
			0159	V	SL	Pedicle Foramen	-0.21	1.79	*	0.79	1.86	2.25	*	2.06
			0160	V	SL	Muscle Scars	1.56	*	*	1.56	1.71	*	*	1.71
			0161	V	PL	Non-specialised	0.30	*	*	0.30	1.73	*	*	1.73
		4	0292	D	SL	Loop	2.47	*	*	2.47	2.67	*	*	2.67

(Continued on next page)

Species	Location	Specimen	Sample no.	Valve	Layer	Area	$\delta^{13}C$ VPDB				$\delta^{18}O$ VPDB			
							1	2	3	Mean	1	2	3	Mean
			0293	D	SL	Non-specialised	2.43	*	*	**2.43**	1.90	*	*	**1.90**
			0294	D	SL	Muscle Scars	0.09	*	*	**0.09**	1.31	*	*	**1.31**
			0295	D	SL	Cardinal Process	1.05	*	*	**1.05**	1.94	*	*	**1.94**
			0296	D	PL	Non-specialised	1.24	*	*	**1.24**	2.14	*	*	**2.14**
			0297	V	SL	Non-specialised	2.58	2.38	2.61	**2.52**	2.23	2.10	2.00	**2.11**
			0298	V	SL	Teeth	1.46	1.25	*	**1.36**	1.53	1.91	*	**1.72**
			0299	V	SL	Pedicle Foramen	0.89	*	*	**0.89**	1.38	*	*	**1.38**
			0300	V	SL	Muscle Scars	1.16	1.67	*	**1.41**	1.61	2.41	*	**2.01**
			0301	V	PL	Non-specialised	0.01	*	*	**0.01**	1.61	*	*	**1.61**
		5	0302	D	SL	Loop	2.17	1.61	*	**1.89**	1.99	1.78	*	**1.88**
			0303	D	SL	Non-specialised	2.32	2.13	*	**2.23**	2.19	2.17	*	**2.18**
			0304	D	SL	Muscle Scars	1.36	*	*	**1.36**	2.04	*	*	**2.04**
			0305	D	SL	Cardinal Process	0.91	*	*	**0.91**	1.58	*	*	**1.58**
			0306	D	PL	Non-specialised	1.28	*	*	**1.28**	2.17	*	*	**2.17**
			0307	V	SL	Non-specialised	1.64	1.81	1.52	**1.66**	1.85	1.93	1.82	**1.87**
			0308	V	SL	Teeth	1.59	*	*	**1.59**	1.48	*	*	**1.48**
			0309	V	SL	Pedicle Foramen	0.29	*	*	**0.29**	2.01	*	*	**2.01**
			0310	V	SL	Muscle Scars	1.24	*	*	**1.24**	2.14	*	*	**2.14**
			0311	V	PL	Non-specialised	0.50	*	*	**0.50**	1.33	*	*	**1.33**
		6	0468	D	SL	Loop	0.64	1.42	2.07	**1.38**	0.61	2.05	3.04	**1.90**
			0469	D	SL	Non-specialised	2.33	1.82	*	**2.08**	2.24	1.91	*	**2.07**
			0470	D	SL	Muscle Scars	1.96	1.34	*	**1.65**	2.45	1.93	*	**2.19**

(Continued on next page)

Species	Location	Specimen	Sample no.	Valve	Layer	Area	$\delta^{13}C$ VPDB				$\delta^{18}O$ VPDB			
							1	2	3	Mean	1	2	3	Mean
			0471	D	SL	Cardinal Process	1.12	*	*	1.12	1.93	*	*	1.93
			0472	D	PL	Non-specialised	1.62	*	*	1.62	2.63	*	*	2.63
			0473	V	SL	Non-specialised	2.29	1.92	2.21	2.14	2.40	2.07	2.89	2.45
			0474	V	SL	Teeth	1.93	1.53	1.48	1.65	2.58	1.93	2.11	2.21
			0475	V	SL	Pedicle Foramen	0.71	0.51	*	0.61	2.11	2.28	*	2.20
			0476	V	SL	Muscle Scars	1.87	1.50	*	1.69	2.72	1.69	*	2.20
			0477	V	PL	Non-specialised	1.42	0.88	*	1.15	2.91	2.20	*	2.55
		7	0618	D	SL	Loop	1.99	*	*	1.99	1.53	*	*	1.53
			0619	D	SL	Non-specialised	1.82	*	*	1.82	2.30	*	*	2.30
			0620	D	SL	Muscle Scars	1.36	*	*	1.36	2.00	*	*	2.00
			0621	D	SL	Cardinal Process	1.05	*	*	1.05	2.03	*	*	2.03
			0622	D	PL	Non-specialised	0.41	*	*	0.41	1.06	*	*	1.06
			0623	V	SL	Non-specialised	1.62	1.50	1.44	1.52	2.03	2.00	1.92	1.98
			0624	V	SL	Teeth	1.27	*	*	1.27	1.78	*	*	1.78
			0625	V	SL	Pedicle Foramen	0.68	*	*	0.68	1.67	*	*	1.67
			0626	V	SL	Muscle Scars	1.52	*	*	1.52	1.87	*	*	1.87
			0627	V	PL	Non-specialised	0.52	*	*	0.52	1.14	*	*	1.14
		8	0628	D	SL	Loop	2.24	*	*	2.24	2.42	*	*	2.42
			0629	D	SL	Non-specialised	1.89	*	*	1.89	2.17	*	*	2.17
			0630	D	SL	Muscle Scars	0.89	*	*	0.89	1.65	*	*	1.65
			0631	D	SL	Cardinal Process	1.00	*	*	1.00	1.54	*	*	1.54
			0632	D	PL	Non-specialised	0.40	*	*	0.40	1.09	*	*	1.09

(Continued on next page)

Species	Location	Specimen	Sample no.	Valve	Layer	Area	δ13C VPDB				δ18O VPDB			
							1	2	3	Mean	1	2	3	Mean
			0633	V	SL	Non-specialised	1.89	1.70	*	1.80	2.17	1.85	*2.01	
			0634	V	SL	Teeth	1.42	*	*	1.42	1.66	*	*	1.66
			0635	V	SL	Pedicle Foramen	0.17	*	*	0.17	1.73	*	*	1.73
			0636	V	SL	Muscle Scars	1.10	*	*	1.10	1.59	*	*	1.59
			0637	V	PL	Non-specialised	-0.13	*	*	-0.13	0.87	*	*	0.87
		9	0898	D	SL	Loop	1.94	1.85		1.89	1.90	1.97		1.93
			0899	D	SL	Non-specialised	2.01	1.99	1.68	1.89	2.05	1.94	1.43	1.81
			0900	D	SL	Muscle Scars	0.83	*	*	0.83	1.59	*	*	1.59
			0901	D	SL	Cardinal Process	0.67	*	*	0.67	1.80	*	*	1.80
			0902	D	PL	Non-specialised	0.90	*	*	0.90	1.59	*	*	1.59
			0903	V	SL	Non-specialised	1.64	1.78	1.66	1.69	1.74	1.93	1.41	1.69
			0904	V	SL	Teeth	1.47	1.51	*	1.49	1.61	1.60	*	1.61
			0905	V	SL	Pedicle Foramen	0.46	*	*	0.46	1.71	*	*	1.71
			0906	V	SL	Muscle Scars	1.35	*	*	1.35	1.90	*	*	1.90
			0907	V	PL	Non-specialised	0.38	*	*	0.38	1.55	*	*	1.55
		10	0908	D	SL	Loop	2.04	*	*	2.04	2.35	*	*	2.35
			0909	D	SL	Non-specialised	1.70	1.75	1.84	1.76	1.80	1.58	1.93	1.77
			0910	D	SL	Muscle Scars	1.13	*	*	1.13	1.80	*	*	1.80
			0911	D	SL	Cardinal Process	0.76	*	*	0.76	2.12	*	*	2.12
			0912	D	PL	Non-specialised	0.84	*	*	0.84	1.32	*	*	1.32
			0913	V	SL	Non-specialised	1.52	1.36	*	1.44	1.81	1.04	*	1.43
			0914	V	SL	Teeth	1.85	1.72	*	1.79	2.15	1.69	*	1.92

(Continued on next page)

Species	Location	Specimen	Sample no.	Valve	Layer	Area	$\delta^{13}C$ VPDB				$\delta^{18}O$ VPDB			
							1	2	3	Mean	1	2	3	Mean
			0915	V	SL	Pedicle Foramen	0.26	*	*	**0.26**	1.89	*	*	**1.89**
			0916	V	SL	Muscle Scars	1.51	*	*	**1.51**	2.45	*	*	**2.45**
			0917	V	PL	Non-specialised	0.43	0.22	*	**0.32**	1.59	1.10	*	**1.34**
Terebratalia transversa	2. Puget Sound,	1	0228	D	SL	Loop	-1.08	-1.12	-2.11	**-1.44**	-0.43	-0.47	-0.66	**-0.52**
	Friday Harbor,		0229	D	SL	Non-specialised	0.85	1.00	0.62	**0.82**	0.24	0.27	0.18	**0.23**
	Washington,		0230	D	SL	Muscle Scars	0.04	0.06	*	**0.05**	0.22	0.22	*	**0.22**
	USA.		0231	D	SL	Cardinal Process	-0.17	-0.11	*	**-0.14**	0.09	0.35	*	**0.22**
			0232	D	PL	Non-specialised	-3.71	-1.96	*	**-2.83**	-2.23	0.14	*	**-1.04**
			0233	V	SL	Non-specialised	0.74	0.71	0.70	**0.72**	0.49	0.32	0.27	**0.36**
			0234	V	SL	Teeth	-1.27	-0.69	-0.73	**-0.90**	-1.25	-0.17	-0.13	**-0.51**
			0235	V	SL	Pedicle Foramen	-1.34	-1.35	-1.40	**-1.36**	-0.46	-0.43	-0.40	**-0.43**
			0236	V	SL	Muscle Scars	0.64	0.66	*	**0.65**	0.19	0.66	*	**0.43**
			0237	V	PL	Non-specialised	-3.80	-3.58	*	**-3.69**	-2.30	-1.94	*	**-2.12**
		2	0238	D	SL	Loop	-1.22	-1.90	-1.74	**-1.62**	-0.32	-0.55	-0.50	**-0.46**
			0239	D	SL	Non-specialised	0.63	0.60	0.74	**0.66**	0.26	0.19	0.20	**0.22**
			0240	D	SL	Muscle Scars	-0.16	-0.13	-0.13	**-0.14**	-0.02	0.43	0.40	**0.27**
			0241	D	SL	Cardinal Process	-0.24	-0.20	-0.21	**-0.22**	0.21	0.34	0.28	**0.28**
			0242	D	PL	Non-specialised	-3.39	-2.97	-3.24	**-3.20**	-1.89	-1.55	-2.00	**-1.81**
			0243	V	SL	Non-specialised	0.51	0.58	0.72	**0.60**	-0.17	0.08	0.07	**-0.01**
			0244	V	SL	Teeth	-1.15	-0.71	*	**-0.93**	-0.58	-0.42	*	**-0.50**
			0245	V	SL	Pedicle Foramen	-0.51	-0.66	*	**-0.59**	-0.06	-0.04	*	**-0.05**
			0246	V	SL	Muscle Scars	0.48	0.51	0.48	**0.49**	0.05	0.12	0.12	**0.10**

(Continued on next page)

Species	Location	Specimen	Sample no.	Valve	Layer	Area	$\delta^{13}C$ VPDB				$\delta^{18}O$ VPDB			
							1	2	3	Mean	1	2	3	Mean
			0247	V	PL	Non-specialised	-3.77	-3.69	-3.36	**-3.61**	-2.46	-2.36	-2.16	**-2.33**
		3	0378	D	SL	Loop	0.59	*	*	**0.59**	0.25	*	*	**0.25**
			0379	D	SL	Non-specialised	0.59	0.79	0.33	**0.57**	-0.11	0.07	0.38	**0.11**
			0380	D	SL	Muscle Scars	-0.15	-0.10	-0.24	**-0.16**	0.00	0.12	0.09	**0.07**
			0381	D	SL	Cardinal Process	-0.26	0.10	*	**-0.08**	-0.38	0.41	*	**0.02**
			0382	D	PL	Non-specialised	-3.62	-3.69	-3.56	**-3.62**	-2.29	-2.27	-1.99	**-2.18**
			0383	V	SL	Non-specialised	0.62	0.78	0.81	**0.74**	-0.21	0.00	0.34	**0.04**
			0384	V	SL	Teeth	-0.06	-0.02	*	**-0.06**	-0.21	-0.04	*	**-0.13**
			0385	V	SL	Pedicle Foramen	-0.73	*	*	**-0.73**	-0.41	*	*	**-0.41**
			0386	V	SL	Muscle Scars	0.14	0.35	*	**0.25**	-0.18	0.20	*	**0.01**
			0387	V	PL	Non-specialised	-3.63	-3.09	*	**-3.36**	-2.39	-1.91	*	**-2.15**
		4	0388	D	SL	Loop	0.22	0.56	*	**0.39**	-0.01	0.05	*	**0.02**
			0389	D	SL	Non-specialised	0.73	0.67	0.71	**0.71**	0.25	0.02	0.17	**0.15**
			0390	D	SL	Muscle Scars	-0.17	0.01	-0.05	**-0.07**	-0.24	0.11	0.22	**0.03**
			0391	D	SL	Cardinal Process	0.00	0.02	0.07	**0.03**	0.08	-0.05	0.37	**0.14**
			0392	D	PL	Non-specialised	-2.66	-2.53	-2.74	**-2.64**	-1.79	-1.53	-1.59	**-1.64**
			0393	V	SL	Non-specialised	0.63	0.73	0.72	**0.69**	-0.21	0.06	-0.09	**-0.08**
			0394	V	SL	Teeth	0.13	-0.03	*	**0.05**	-0.30	-0.18	*	**-0.24**
			0395	V	SL	Pedicle Foramen	-0.20	-0.17	-0.22	**-0.20**	-0.20	0.03	0.04	**-0.04**
			0396	V	SL	Muscle Scars	0.07	0.21	*	**0.14**	-0.17	0.11	*	**-0.03**
			0397	V	PL	Non-specialised	-2.71	-2.80	-2.90	**-2.80**	-1.71	-1.73	-1.61	**-1.68**
		5	0538	D	SL	Loop	0.68	*	*	**0.68**	0.48	*	*	**0.48**

(Continued on next page)

Species	Location	Specimen	Sample no.	Valve	Layer	Area	$\delta^{13}C$ VPDB				$\delta^{18}O$ VPDB			
							1	2	3	Mean	1	2	3	Mean
			0539	D	SL	Non-specialised	0.88	0.70	0.67	**0.75**	0.27	0.36	0.45	**0.36**
			0540	D	SL	Muscle Scars	0.33	0.21	0.01	**0.18**	0.37	0.18	0.38	**0.31**
			0541	D	SL	Cardinal Process	-0.31	-0.35	-0.57	**-0.41**	-0.13	0.02	-0.02	**-0.04**
			0542	D	PL	Non-specialised	-2.94	-2.90	-2.97	**-2.94**	-1.69	-1.38	-1.43	**-1.50**
			0543	V	SL	Non-specialised	0.73	0.44	0.53	**0.57**	0.17	0.15	0.21	**0.18**
			0544	V	SL	Teeth	0.18	0.01	-0.08	**0.04**	-0.15	-0.21	-0.17	**-0.18**
			0545	V	SL	Pedicle Foramen	-0.67	-0.66	-0.76	**-0.70**	0.11	0.13	0.14	**0.13**
			0546	V	SL	Muscle Scars	0.11	-0.57	0.23	**-0.08**	-0.14	-0.03	-0.25	**-0.14**
			0547	V	PL	Non-specialised	-2.92	-3.07	-2.77	**-2.92**	-1.65	-1.96	-1.79	**-1.80**
		6	0548	D	SL	Loop	0.18	-0.12	*	**0.03**	0.24	-0.14	*	**0.05**
			0549	D	SL	Non-specialised	0.46	0.41	0.58	**0.48**	-0.19	-0.29	0.31	**-0.05**
			0550	D	SL	Muscle Scars	0.10	-0.13	0.11	**0.03**	0.16	-0.30	0.31	**0.06**
			0551	D	SL	Cardinal Process	-0.29	-0.20	*	**-0.25**	0.12	-0.02	*	**0.05**
			0552	D	PL	Non-specialised	-2.25	-2.69	-2.82	**-2.59**	-1.42	-1.31	-1.88	**-1.54**
			0553	V	SL	Non-specialised	0.62	0.49	0.50	**0.54**	0.15	0.20	-0.20	**0.05**
			0554	V	SL	Teeth	0.74	0.50	0.36	**0.53**	0.37	0.39	-0.16	**0.20**
			0555	V	SL	Pedicle Foramen	-0.47	-0.57	-0.69	**-0.57**	0.15	0.15	-0.19	**0.04**
			0556	V	SL	Muscle Scars	0.24	0.13	-0.09	**0.09**	0.35	0.13	-0.28	**0.07**
			0557	V	PL	Non-specialised	-3.42	-3.47	-3.64	**-3.51**	-1.73	-1.66	-2.30	**-1.90**
		7	0678	D	SL	Loop	1.66	1.70	*	**1.68**	1.31	1.34	*	**1.32**
			0679	D	SL	Non-specialised	0.57	0.66	0.51	**0.58**	0.09	0.01	-0.20	**-0.03**
			0680	D	SL	Muscle Scars	-0.29	-0.39	*	**-0.34**	0.10	0.16	*	**0.13**

(Continued on next page)

Species	Location	Specimen	Sample no.	Valve	Layer	Area	$\delta^{13}C$ VPDB				$\delta^{18}O$ VPDB			
							1	2	3	Mean	1	2	3	Mean
			0681	D	SL	Cardinal Process	-0.66	*	*	**-0.66**	0.30	*	*	**0.30**
			0682	D	PL	Non-specialised	-4.24	-3.68	*	**-3.96**	-2.25	-1.72	*	**-1.98**
			0683	V	SL	Non-specialised	0.49	0.43	0.47	**0.46**	-0.18	-0.09	-0.20	**-0.15**
			0684	V	SL	Teeth	-0.34	-1.66	*	**-1.00**	-0.14	-0.79	*	**-0.46**
			0685	V	SL	Pedicle Foramen	-1.48	*	*	**-1.48**	-0.52		*	**-0.52**
			0686	V	SL	Muscle Scars	0.11	0.05	*	**0.08**	0.03	0.04	*	**0.03**
			0687	V	PL	Non-specialised	-4.63	-3.36	*	**-4.00**	-2.51	-1.63	*	**-2.07**
		8	0688	D	SL	Loop	0.54	*	*	**0.54**	0.19	*	*	**0.19**
			0689	D	SL	Non-specialised	0.66	0.69	0.57	**0.64**	0.17	0.14	-0.01	**0.10**
			0690	D	SL	Muscle Scars	0.36	0.66	0.26	**0.49**	0.25	0.21	0.18	**0.21**
			0691	D	SL	Cardinal Process	0.11	-0.07	-0.11	**-0.02**	0.34	-0.21	0.09	**0.08**
			0692	D	PL	Non-specialised	-3.25	-3.35	-3.18	**-3.26**	-1.66	-1.81	-1.67	**-1.72**
			0693	V	SL	Non-specialised	0.80	0.44	0.84	**0.70**	0.31	0.08	0.64	**0.34**
			0694	V	SL	Teeth	0.20	0.03	0.06	**0.10**	0.25	0.05	-0.56	**-0.09**
			0695	V	SL	Pedicle Foramen	-0.42	-0.44	-0.34	**-0.40**	-0.07	-0.23	0.00	**-0.10**
			0696	V	SL	Muscle Scars	0.62	0.57	0.64	**0.61**	0.24	0.08	0.33	**0.22**
			0697	V	PL	Non-specialised	-2.76	-2.75	-2.85	**-2.79**	-1.38	-1.21	-1.46	**-1.35**
		9	0958	D	SL	Loop	-0.59	-0.58	-0.90	**-0.69**	0.11	-0.43	-0.35	**-0.22**
			0959	D	SL	Non-specialised	0.33	0.56	0.59	**0.49**	0.11	-0.38	0.72	**0.15**
			0960	D	SL	Muscle Scars	-0.25	*	*	**-0.25**	0.61	*	*	**0.61**
			0961	D	SL	Cardinal Process	-0.79	-0.78	*	**-0.78**	0.34	0.31	*	**0.32**
			0962	D	PL	Non-specialised	-4.16	*	*	**-4.16**	-2.01	*	*	**-2.01**

(Continued on next page)

Species	Location	Specimen	Sample no.	Valve	Layer	Area	$\delta^{13}C$ VPDB				$\delta^{18}O$ VPDB			
							1	2	3	Mean	1	2	3	Mean
			0963	V	SL	Non-specialised	0.46	0.51	0.42	**0.46**	0.28	0.21	-0.02	**0.16**
			0964	V	SL	Teeth	-1.39	-1.17	-1.61	**-1.39**	-0.23	-1.02	-0.81	**-0.69**
			0965	V	SL	Pedicle Foramen	-1.11	-1.01	*	**-1.06**	-0.04	-0.54	*	**-0.29**
			0966	V	SL	Muscle Scars	0.01	*	*	**0.01**	0.02	*	*	**0.02**
			0967	V	PL	Non-specialised	-4.26	-4.20	*	**-4.23**	-1.65	-2.20	*	**-1.93**
		10	0968	D	SL	Loop	-1.24	*	*	**-1.24**	0.10	*	*	**0.10**
			0969	D	SL	Non-specialised	0.65	0.58	0.13	**0.46**	0.18	-0.16	-0.05	**-0.01**
			0970	D	SL	Muscle Scars	0.08	0.06	*	**0.07**	0.34	0.32	*	**0.33**
			0971	D	SL	Cardinal Process	-0.52	*	*	**-0.52**	-0.30	*	*	**-0.30**
			0972	D	PL	Non-specialised	-3.79	*	*	**-3.79**	-2.08	*	*	**-2.08**
			0973	V	SL	Non-specialised	0.40	0.67	0.46	**0.51**	-0.15	0.58	-0.21	**0.07**
			0974	V	SL	Teeth	-1.38	-1.61	*	**-1.49**	-0.46	-0.54	*	**-0.50**
			0975	V	SL	Pedicle Foramen	-1.78	*	*	**-1.78**	-0.73	*	*	**-0.73**
			0976	V	SL	Muscle Scars	0.46	0.43	*	**0.44**	0.40	0.00	*	**0.20**
			0977	V	PL	Non-specialised	-4.38	*	*	**-4.38**	-2.70	*	*	**-2.70**
Laqueus rubellus	3. Otsuchi Bay,	1	0768	D	SL	Loop	1.55	*	*	**1.55**	1.31	*	*	**1.31**
	Japan.		0769	D	SL	Non-specialised	1.12	*	*	**1.12**	1.38	*	*	**1.38**
			0770	D	SL	Muscle Scars	0.64	0.21	*	**0.42**	1.52	0.93	*	**1.23**
			0771	D	SL	Cardinal Process	0.49	0.38		**0.43**	1.02	1.02		**1.02**
			0772	D	PL	Non-specialised	-3.31	*	*	**-3.31**	-1.21	*	*	**-1.21**
			0773	V	SL	Non-specialised	1.10	1.27	*	**1.18**	1.22	1.02	*	**1.12**
			0774	V	SL	Teeth	1.09	1.16	1.03	**1.09**	1.18	1.09	0.83	**1.03**

(Continued on next page)

Species	Location	Specimen	Sample no.	Valve	Layer	Area	$\delta^{13}C$ VPDB				$\delta^{18}O$ VPDB			
							1	2	3	Mean	1	2	3	Mean
			0775	V	SL	Pedicle Foramen	0.01	*	*	0.01	0.70	*	*	0.70
			0776	V	SL	Muscle Scars	0.67	*	*	0.67	0.94	*	*	0.94
			0777	V	PL	Non-specialised	-2.06	*	*	-2.06	-0.59	*	*	-0.59
		2	0778	D	SL	Loop	1.62	*	*	1.62	0.90	*	*	0.90
			0779	D	SL	Non-specialised	2.14	2.07	*	2.10	1.21	1.07	*	1.14
			0780	D	SL	Muscle Scars	1.56	*	*	1.56	1.12	*	*	1.12
			0781	D	SL	Cardinal Process	1.16	*	*	1.16	0.93	*	*	0.93
			0782	D	PL	Non-specialised	-0.75	*	*	-0.75	-0.72	*	*	-0.72
			0783	V	SL	Non-specialised	2.16	*	*	2.16	1.40	*	*	1.40
			0784	V	SL	Teeth	1.67	1.57	*	1.62	0.72	0.53	*	0.62
			0785	V	SL	Pedicle Foramen	1.21	*	*	1.21	0.74	*	*	0.74
			0786	V	SL	Muscle Scars	1.49	*	*	1.49	1.18	*	*	1.18
			0787	V	PL	Non-specialised	-0.29	*	*	-0.29	0.06	*	*	0.06
Lequeus rubellus	4. Sagami Bay,	1	0208	D	SL	Loop	1.27	1.49	1.49	1.42	0.67	0.83	1.30	0.93
	Japan.		0209	D	SL	Non-specialised	1.44	1.41	1.39	1.41	0.37	0.79	1.21	0.79
			0210	D	SL	Muscle Scars	1.02	0.98	*	1.00	0.48	0.65	*	0.56
			0211	D	SL	Cardinal Process	0.55	0.79	*	0.67	0.41	0.79	*	0.60
			0212	D	PL	Non-specialised	0.17	*	*	0.17	0.12	*	*	0.12
			0213	V	SL	Non-specialised	1.38	*	*	1.38	0.90	*	*	0.90
			0214	V	SL	Teeth	0.79	0.78	0.88	0.82	0.39	0.18	0.59	0.39
			0215	V	SL	Pedicle Foramen	0.15	*	*	0.15	0.11	*	*	0.11
			0216	V	SL	Muscle Scars	1.11	1.30	*	1.20	0.36	0.80	*	0.58

(Continued on next page)

Species	Location	Specimen	Sample no.	Valve	Layer	Area	$\delta^{13}C$ VPDB				$\delta^{18}O$ VPDB			
							1	2	3	Mean	1	2	3	Mean
			0217	V	PL	Non-specialised	0.39	0.72	0.63	**0.58**	0.10	0.17	0.76	**0.34**
		2	0218	D	SL	Loop	0.68	0.56	0.90	**0.71**	0.45	0.44	0.82	**0.57**
			0219	D	SL	Non-specialised	1.57	1.51	*	**1.54**	0.71	0.63	*	**0.67**
			0220	D	SL	Muscle Scars	1.93	1.76	1.61	**1.76**	1.53	1.02	1.13	**1.23**
			0221	D	SL	Cardinal Process	0.89	0.77	*	**0.83**	0.61	0.67	*	**0.64**
			0222	D	PL	Non-specialised	0.88	0.77	0.38	**0.68**	0.30	0.26	0.33	**0.30**
			0223	V	SL	Non-specialised	1.49	1.44	*	**1.47**	0.57	0.54	*	**0.55**
			0224	V	SL	Teeth	1.13	1.09	1.13	**1.12**	0.52	0.48	0.85	**0.62**
			0225	V	SL	Pedicle Foramen	1.08	*	*	**1.08**	0.34	*	*	**0.34**
			0226	V	SL	Muscle Scars	0.20	*	*	**0.20**	0.57	*	*	**0.57**
			0227	V	PL	Non-specialised	1.12	0.94	0.49	**0.85**	0.53	0.35	0.37	**0.42**
		3	0358	D	SL	Loop	1.47	*	*	**1.47**	1.10	*	*	**1.10**
			0359	D	SL	Non-specialised	1.38	1.35	1.53	**1.42**	0.57	0.82	0.86	**0.75**
			0360	D	SL	Muscle Scars	1.26	1.15	1.37	**1.26**	0.66	0.75	0.96	**0.79**
			0361	D	SL	Cardinal Process	0.88	0.71	1.30	**0.96**	0.45	0.37	1.43	**0.75**
			0362	D	PL	Non-specialised	-0.42	0.26	-0.11	**-0.08**	-0.15	0.32	0.21	**0.13**
			0363	V	SL	Non-specialised	1.38	1.33	1.45	**1.38**	0.38	0.52	0.66	**0.52**
			0364	V	SL	Teeth	0.86	0.73	0.98	**0.86**	0.40	0.39	0.44	**0.41**
			0365	V	SL	Pedicle Foramen	0.45	0.63	*	**0.54**	0.19	0.51	*	**0.35**
			0366	V	SL	Muscle Scars	1.33	1.30	1.42	**1.35**	0.47	0.47	0.71	**0.55**
			0367	V	PL	Non-specialised	-1.07	-1.3	-0.46	**-0.93**	-0.46	-0.50	0.41	**-0.19**
		4	0368	D	SL	Loop	1.69	*	*	**1.69**	0.75	*	*	**0.75**

(Continued on next page)

Species	Location	Specimen	Sample no.	Valve	Layer	Area	$\delta^{13}C$ VPDB				$\delta^{18}O$ VPDB			
							1	2	3	Mean	1	2	3	Mean
			0369	D	SL	Non-specialised	1.63	1.60	*	**1.61**	0.74	0.65	*	**0.69**
			0370	D	SL	Muscle Scars	1.30	1.27	1.31	**1.30**	0.60	0.49	0.70	**0.60**
			0371	D	SL	Cardinal Process	1.02	1.06	1.45	**1.18**	0.38	0.59	0.89	**0.62**
			0372	D	PL	Non-specialised	-0.52	-0.26	*	**-0.39**	0.00	0.11	*	**0.05**
			0373	V	SL	Non-specialised	1.53	1.56	*	**1.54**	0.96	0.60	*	**0.78**
			0374	V	SL	Teeth	1.74	1.37	1.55	**1.55**	0.69	0.44	0.76	**0.63**
			0375	V	SL	Pedicle Foramen	0.81	*	*	**0.81**	0.68	*	*	**0.68**
			0376	V	SL	Muscle Scars	1.74	*	*	**1.74**	0.81	*	*	**0.81**
			0377	V	PL	Non-specialised	-1.60	-1.4	*	**-1.51**	-0.93	-0.7	*	**-0.83**
		5	0518	D	SL	Loop	2.26	*	*	**2.26**	2.55	*	*	**2.55**
			0519	D	SL	Non-specialised	1.42	1.56	*	**1.49**	0.74	0.70	*	**0.72**
			0520	D	SL	Muscle Scars	0.88	0.95	0.85	**0.89**	0.50	0.78	1.26	**0.85**
			0521	D	SL	Cardinal Process	1.22	0.76	*	**0.99**	1.71	0.84	*	**1.28**
			0522	D	PL	Non-specialised	1.55	-0.62	-0.55	**0.13**	1.57	-0.07	-0.12	**0.46**
			0523	V	SL	Non-specialised	1.47	1.42	1.49	**1.46**	0.44	0.46	0.40	**0.43**
			0524	V	SL	Teeth	1.09	1.06	0.94	**1.03**	0.10	0.38	0.25	**0.24**
			0525	V	SL	Pedicle Foramen	0.28	0.21	*	**0.24**	-0.12	0.16	*	**0.02**
			0526	V	SL	Muscle Scars	1.13	1.36	1.26	**1.25**	0.19	0.42	0.67	**0.43**
			0527	V	PL	Non-specialised	-0.49	0.73	0.27	**0.17**	-0.47	0.25	-0.08	**-0.10**
		6	0528	D	SL	Loop	1.52	*	*	**1.52**	0.75	*	*	**0.75**
			0529	D	SL	Non-specialised	1.46	1.61	1.68	**1.58**	0.31	0.80	0.95	**0.69**
			0530	D	SL	Muscle Scars	1.41	1.02	*	**1.21**	0.11	0.96	*	**0.54**

(Continued on next page)

Species	Location	Specimen	Sample no.	Valve	Layer	Area	$\delta^{13}C$ VPDB				$\delta^{18}O$ VPDB			
							1	2	3	Mean	1	2	3	Mean
			0531	D	SL	Cardinal Process	0.57	1.00	0.49	**0.69**	0.20	0.61	0.53	**0.44**
			0532	D	PL	Non-specialised	-1.94	*	*	**-1.94**	-1.74	*	*	**-1.74**
			0533	V	SL	Non-specialised	1.32	1.65	1.63	**1.54**	0.29	0.85	1.11	**0.75**
			0534	V	SL	Teeth	1.19	0.78	0.93	**0.97**	0.85	0.59	0.29	**0.57**
			0535	V	SL	Pedicle Foramen	0.62	0.67	*	**0.64**	1.54	0.30	*	**0.92**
			0536	V	SL	Muscle Scars	1.50	1.23	1.17	**1.30**	0.85	0.68	0.83	**0.79**
			0537	V	PL	Non-specialised	-1.55	-1.16	*	**-1.35**	-0.85	-0.25	*	**-0.55**
		7	0758	D	SL	Loop	0.98	1.33	*	**1.16**	0.36	0.98	*	**0.67**
			0759	D	SL	Non-specialised	1.18	0.99	*	**1.09**	0.68	0.37	*	**0.53**
			0760	D	SL	Muscle Scars	0.59	0.41	0.55	**0.52**	0.64	0.72	0.71	**0.69**
			0761	D	SL	Cardinal Process	0.18	*	*	**0.18**	0.48	*	*	**0.48**
			0762	D	PL	Non-specialised	-2.56	-2.36	-2.41	**-2.44**	-1.15	0.90	-1.27	**-0.51**
			0763	V	SL	Non-specialised	1.24	*	*	**1.24**	0.73	*	*	**0.73**
			0764	V	SL	Teeth	1.07	0.57	0.65	**0.76**	0.53	0.22	0.29	**0.34**
			0765	V	SL	Pedicle Foramen	0.20	*	*	**0.20**	0.51	*	*	**0.51**
			0766	V	SL	Muscle Scars	0.74	0.19	*	**0.47**	1.02	0.44	*	**0.73**
			0767	V	PL	Non-specialised	-3.16	*	*	**-3.16**	-1.28	*	*	**-1.28**
		8	0768	D	SL	Loop	1.09	*	*	**1.09**	0.83	*	*	**0.83**
			0769	D	SL	Non-specialised	1.33	*	*	**1.33**	0.86	*	*	**0.86**
			0770	D	SL	Muscle Scars	0.66	*	*	**0.66**	0.72	*	*	**0.72**
			0771	D	SL	Cardinal Process	0.05	*	*	**0.05**	0.51	*	*	**0.51**
			0772	D	PL	Non-specialised	-4.29	*	*	**-4.29**	-2.30	*	*	**-2.30**

(Continued on next page)

Species	Location	Specimen	Sample no.	Valve	Layer	Area	$\delta^{13}C$ VPDB				$\delta^{18}O$ VPDB			
							1	2	3	Mean	1	2	3	Mean
			0773	V	SL	Non-specialised	0.81	0.87	*	0.84	0.69	0.65	*	0.67
			0774	V	SL	Teeth	-0.32	-0.52	-0.57	-0.47	-0.12	-0.33	-0.48	-0.31
			0775	V	SL	Pedicle Foramen	-0.46	*	*	-0.46	0.09	*	*	0.09
			0776	V	SL	Muscle Scars	0.04	*	*	0.04	0.42	*	*	0.42
			0777	V	PL	Non-specialised	-4.34	*	*	-4.34	-2.03	*	*	-2.03
		9	0838	D	SL	Loop	1.03	*	*	1.03	1.12	*	*	1.12
			0839	D	SL	Non-specialised	1.16	*	*	1.16	0.83	*	*	0.83
			0840	D	SL	Muscle Scars	1.18	*	*	1.18	1.04	*	*	1.04
			0841	D	SL	Cardinal Process	0.78	*	*	0.78	0.64	*	*	0.64
			0842	D	PL	Non-specialised	-3.13	*	*	-3.13	-1.67	*	*	-1.67
			0843	V	SL	Non-specialised	0.89	*	*	0.89	0.76	*	*	0.76
			0844	V	SL	Teeth	-0.24	-0.41	*	-0.32	0.28	-0.16	*	0.06
			0845	V	SL	Pedicle Foramen	0.25	*	*	0.25	0.57	*	*	0.57
			0846	V	SL	Muscle Scars	1.07	*	*	1.07	0.64	*	*	0.64
			0847	V	PL	Non-specialised	-4.69	*	*	-4.69	-2.36	*	*	-2.36
		10	0848	D	SL	Loop	1.07	*	*	1.07	1.05	*	*	1.05
			0849	D	SL	Non-specialised	0.78	*	*	0.78	0.82	*	*	0.82
			0850	D	SL	Muscle Scars	0.30	*	*	0.30	0.58	*	*	0.58
			0851	D	SL	Cardinal Process	0.68	*	*	0.68	1.30	*	*	1.30
			0852	D	PL	Non-specialised	-4.13	*	*	-4.13	-1.68	*	*	-1.68
			0853	V	SL	Non-specialised	0.48	*	*	0.48	0.49	*	*	0.49
			0854	V	SL	Teeth	-0.80	*	*	-0.80	0.00	*	*	0.00

(Continued on next page)

Species	Location	Specimen	Sample no.	Valve	Layer	Area	$\delta^{13}C$ VPDB				$\delta^{18}O$ VPDB			
							1	2	3	Mean	1	2	3	Mean
			0855	V	SL	Pedicle Foramen	0.24	*	*	**0.24**	1.33	*	*	**1.33**
			0856	V	SL	Muscle Scars	0.82	*	*	**0.82**	1.44	*	*	**1.44**
			0857	V	PL	Non-specialised	-3.76	*	*	**-3.76**	-1.52	*	*	**-1.52**
Thecidellina barretti	5. Rio Buneo,	1	1086	n/a	n/a	Whole Shell	1.80	1.86	*	**1.83**	-1.02	-0.93	*	**-0.93**
	Jamaica	2	1087	n/a	n/a	Whole Shell	1.84	*	*	**1.84**	-0.96	*	*	*
		3	1088	n/a	n/a	Whole Shell	2.11	2.00	2.20	**2.10**	-1.10	-1.15	-1.00	**-1.07**
		4	1089	n/a	n/a	Whole Shell	2.07	2.00	2.04	**2.04**	-1.17	-1.11	-1.05	**-1.08**
		5	1090	n/a	n/a	Whole Shell	2.22	2.12	2.10	**2.14**	-1.22	-1.32	-1.34	**-1.29**
		6	1091	n/a	n/a	Whole Shell	1.88	1.85	1.80	**1.85**	-1.16	-1.10	-1.01	**-1.09**
		7	1092	n/a	n/a	Whole Shell	2.15	2.16	*	**2.16**	-1.03	-0.94	*	**-0.99**
		8	1093	n/a	n/a	Whole Shell	2.06	1.98	2.14	**2.06**	-0.96	-1.17	-0.86	**-1.00**
		9	1094	n/a	n/a	Whole Shell	2.27	2.54	2.36	**2.39**	-1.19	-1.12	-1.06	**-1.12**
		10	1095	n/a	n/a	Whole Shell	2.02	2.16	1.95	**2.04**	-1.07	-1.10	-1.15	**-1.11**
Neoancistrocrania norfolki	6. Norfolk Seamount,	1	1116	D	SL	Crura	2.49	2.24	*	**2.36**	1.30	1.14	*	**1.22**
	Southern Pacific Ocean		1117	D	SL	Muscle Scars	2.43	2.90	*	**2.66**	1.66	2.09	*	**1.87**
			1118	D	SL	Non-specialised	2.54	2.14	2.23	**2.30**	1.39	0.90	1.26	**1.18**
			1119	D	PL	Non-specialised	2.57	2.42	*	**2.49**	1.78	1.46	*	**1.62**
		2	1120	V	SL	Muscle Scars	1.97	1.97	*	**1.97**	1.70	1.69	*	**1.70**
			1121	V	SL	Upper S.L.	1.61	1.09	1.04	**1.24**	2.51	1.44	1.51	**1.82**
			1122	V	PL	Primary Layer	3.15	2.10	*	**2.63**	3.38	1.62	*	**2.50**
			1123	V	SL	Lower S.L.	2.17	2.32	2.10	**2.20**	1.15	1.45	1.10	**1.23**
			1124	V	SL	Raised Muscle Scars	2.76	2.12	1.95	**2.28**	2.61	1.67	1.30	**1.86**

(Continued on next page)

Species	Location	Specimen	Sample no.	Valve	Layer	Area	$\delta^{13}C$ VPDB				$\delta^{18}O$ VPDB			
							1	2	3	Mean	1	2	3	Mean
		3	1125	D	SL	Crura	2.66	2.27	2.05	2.33	2.14	1.50	1.04	1.56
			1126	D	SL	Muscle Scars	2.14	2.19	*	2.16	1.76	1.97	*	1.87
			1127	D	SL	Non-specialised	2.13	1.80	*	1.97	1.63	0.99	*	1.31
			1128	D	PL	Non-specialised	2.71	2.11	*	2.41	2.11	1.26	*	1.68
		4	1129	V	SL	Muscle Scars	2.08	1.73	*	1.91	1.40	1.05	*	1.23
			1130	V	SL	Upper S.L.	1.91	1.54	1.64	1.70	1.59	1.10	0.92	1.20
			1131	V	PL	Primary Layer	2.16	*	*	2.16	1.07	*	*	1.07
			1132	V	SL	Lower S.L.	2.48	*	*	2.48	1.49	*	*	1.49
			1133	V	SL	Raised Muscle Scars	1.81	2.02	*	1.92	1.55	0.61	*	1.08
		5	1134	D	SL	Crura	2.34	2.66	2.35	2.45	1.63	2.06	2.08	1.92
			1135	D	SL	Muscle Scars	1.84	*	*	1.84	1.26	*	*	1.26
			1136	D	SL	Non-specialised	2.39	*	*	2.39	1.63	*	*	1.63
			1137	D	PL	Non-specialised	2.46	*	*	2.46	1.88	*	*	1.88
		6	1138	V	SL	Muscle Scars	1.72	2.15	*	1.94	0.87	1.57	*	1.22
			1139	V	SL	Upper S.L.	1.80	3.16	*	2.48	1.49	3.80	*	2.65
			1140	V	PL	Primary Layer	1.81	*	*	1.81	1.05	*	*	1.05
			1141	V	SL	Lower S.L.	2.29	2.03	*	2.16	1.14	1.00	*	1.07
			1142	V	SL	Raised Muscle Scars	2.21	*	*	2.21	1.32	*	*	1.32
		7	1143	D	SL	Crura	2.79	2.94	*	2.87	1.50	2.40	*	1.95
			1144	D	SL	Muscle Scars	2.23	*	*	2.23	1.04	*	*	1.04
			1145	D	SL	Non-specialised	2.21	*	*	2.21	1.10	*	*	1.10
			1146	D	PL	Non-specialised	2.98	*	*	2.98	2.73	*	*	2.73

(Continued on next page)

Species	Location	Specimen	Sample no.	Valve	Layer	Area	$\delta^{13}C$ VPDB				$\delta^{18}O$ VPDB			
							1	2	3	Mean	1	2	3	Mean
		8	1147	V	SL	Muscle Scars	1.70	*	*	1.70	1.42	*	*	1.42
			1148	V	SL	Upper S.L.	1.80	1.36	*	1.58	2.02	1.36	*	1.69
			1149	V	PL	Primary Layer	2.82	2.15	2.24	2.40	2.34	1.22	1.23	1.59
			1150	V	SL	Lower S.L.	2.68	2.30	2.40	2.46	1.61	1.10	1.12	1.27
			1151	V	SL	Raised Muscle Scars	1.77	1.42	1.27	1.48	1.64	0.96	0.95	1.18
		9	1152	D	SL	Crura	2.39	1.95	*	2.17	1.75	1.05	*	1.40
			1153	D	SL	Muscle Scars	1.70	1.22	*	1.46	1.51	1.13	*	1.32
			1154	D	SL	Non-specialised	2.35	1.65	*	2.00	2.08	0.87	*	1.48
			1155	D	PL	Non-specialised	2.81	2.12	*	2.47	2.19	0.93	*	1.56
		10	1156	V	SL	Muscle Scars	1.92	1.44	*	1.68	1.87	0.94	*	1.40
			1157	V	SL	Upper S.L.	2.03	1.79	*	1.91	1.41	1.20	*	1.31
			1158	V	PL	Primary Layer	23.00	2.19	*	12.59	3.39	1.00	*	2.20
			1159	V	SL	Lower S.L.	2.70	1.85	*	2.28	2.24	0.86	*	1.55
			1160	V	SL	Raised Muscle Scars	1.85	1.65	*	1.75	1.50	1.01	*	1.26
Calloria inconspicua	7. Otago Shelf,	1	0162	D	SL	Loop	1.98	1.67	*	1.82	1.49	2.04	*	1.76
	South Island,		0163	D	SL	Non-specialised	1.82	1.92	1.91	1.88	1.34	1.21	1.37	1.31
	New Zealand.		0164	D	SL	Muscle Scars	0.90	1.91	*	1.41	1.63	1.35	*	1.49
			0165	D	SL	Cardinal Process	0.83	0.81	0.95	0.86	1.29	0.77	1.46	1.17
			0166	D	PL	Non-specialised	-0.11	-0.29	-0.34	-0.25	0.58	0.41	0.81	0.60
			0167	V	SL	Non-specialised	1.79	1.75	1.81	1.78	1.28	1.26	1.16	1.23
			0168	V	SL	Teeth	1.85	1.91	*	1.88	1.47	1.43	*	1.45
			0169	V	SL	Pedicle Foramen	0.89	0.86	0.75	0.83	1.23	1.17	0.86	1.09

(Continued on next page)

Species	Location	Specimen	Sample no.	Valve	Layer	Area	$\delta^{13}C$ VPDB				$\delta^{18}O$ VPDB			
							1	2	3	Mean	1	2	3	Mean
			0170	V	SL	Muscle Scars	1.45	1.39	*	1.42	1.46	1.39	*	1.43
			0171	V	PL	Non-specialised	-0.97	-0.83	*	-0.90	0.19	0.10	*	0.14
		2	0172	D	SL	Loop	1.83	1.84	*	1.83	1.05	1.20	*	1.12
			0173	D	SL	Non-specialised	1.90	1.95	1.92	1.93	1.14	1.25	1.25	1.21
			0174	D	SL	Muscle Scars	1.33	1.56	*	1.44	0.97	1.50	*	1.23
			0175	D	SL	Cardinal Process	0.86	0.61	*	0.73	0.97	0.63	*	0.80
			0176	D	PL	Non-specialised	-2.08	-1.89	*	-1.98	-0.48	-0.44	*	-0.46
			0177	V	SL	Non-specialised	1.66	2.25	1.81	1.91	0.99	2.00	1.05	1.35
			0178	V	SL	Teeth	1.59	1.89	*	1.74	1.10	1.71	*	1.40
			0179	V	SL	Pedicle Foramen	0.98	1.14	*	1.06	1.08	1.15	*	1.12
			0180	V	SL	Muscle Scars	1.22	1.39	*	1.31	1.07	2.09	*	1.58
			0181	V	PL	Non-specialised	-0.75	-1.69	*	-1.22	-0.43	-0.40	*	-0.42
		3	0312	D	SL	Loop	1.83	1.67	*	1.75	1.35	1.62	*	1.48
			0313	D	SL	Non-specialised	2.06	2.18	*	2.12	1.54	1.44	*	1.49
			0314	D	SL	Muscle Scars	1.31	1.39	*	1.35	1.26	1.07	*	1.16
			0315	D	SL	Cardinal Process	1.10	1.06	*	1.08	1.54	1.19	*	1.37
			0316	D	PL	Non-specialised	-1.93	-1.6	-1.84	-1.78	-0.91	0.13	-0.5	-0.42
			0317	V	SL	Non-specialised	1.90	2.02	1.97	1.96	1.17	1.48	1.36	1.34
			0318	V	SL	Teeth	1.97	2.04	*	2.01	1.60	1.44	*	1.52
			0319	V	SL	Pedicle Foramen	0.85	1.11	*	0.98	1.10	1.38	*	1.24
			0320	V	SL	Muscle Scars	1.83	1.99	*	1.91	1.37	1.54	*	1.46
			0321	V	PL	Non-specialised	-0.11	-0.28	-0.43	-0.27	0.12	0.02	0.18	0.11

(Continued on next page)

Species	Location	Specimen	Sample no.	Valve	Layer	Area	$\delta^{13}C$ VPDB				$\delta^{18}O$ VPDB			
							1	2	3	Mean	1	2	3	Mean
		4	0322	D	SL	Loop	2.05	*	*	2.05	2.04	*	*	2.04
			0323	D	SL	Non-specialised	1.78	1.86	1.56	1.73	0.98	1.33	1.00	1.10
			0324	D	SL	Muscle Scars	1.34	1.38	1.32	1.35	1.22	1.11	1.44	1.26
			0325	D	SL	Cardinal Process	1.14	1.24	1.08	1.15	1.20	1.10	1.41	1.24
			0326	D	PL	Non-specialised	-0.61	-0.5	-1.02	-0.72	0.12	-0.1	-0.3	-0.09
			0327	V	SL	Non-specialised	1.81	1.83	1.51	1.72	1.32	1.32	1.00	1.21
			0328	V	SL	Teeth	1.63	1.77	*	1.70	1.08	1.45	*	1.27
			0329	V	SL	Pedicle Foramen	1.02	1.33	*	1.17	0.93	1.49	*	1.21
			0330	V	SL	Muscle Scars	1.69	1.68	1.60	1.66	1.18	0.83	1.23	1.08
			0331	V	PL	Non-specialised	-0.66	-0.9	-0.81	-0.78	-0.06	-0.9	0.08	-0.29
		5	0478	D	SL	Loop	1.69	1.61	1.68	1.69	1.51	1.51	1.50	1.51
			0479	D	SL	Non-specialised	2.14	2.04	1.84	2.01	1.75	2.15	1.03	1.64
			0480	D	SL	Muscle Scars	1.54	1.28	1.25	1.36	1.64	1.46	1.29	1.46
			0481	D	SL	Cardinal Process	1.46	0.79	*	1.13	2.28	1.36	*	1.82
			0482	D	PL	Non-specialised	-1.75	*	*	-1.75	-0.07	*	*	-0.07
			0483	V	SL	Non-specialised	1.75	1.70	1.75	1.72	1.29	1.00	0.80	1.14
			0484	V	SL	Teeth	1.82	1.46	*	1.64	1.45	1.42	*	1.44
			0485	V	SL	Pedicle Foramen	0.94	1.70	*	1.32	1.42	1.04	*	1.23
			0486	V	SL	Muscle Scars	1.92	1.85	*	1.88	1.44	1.47	*	1.46
			0487	V	PL	Non-specialised	-1.62	-2.08	-2.19	-1.96	-0.25	-0.3	-0.57	-0.36
		6	0488	D	SL	Loop	1.68	*	*	1.68	1.47	*	*	1.47
			0489	D	SL	Non-specialised	1.85	1.84	1.96	1.88	1.27	1.31	1.09	1.22

(Continued on next page)

Species	Location	Specimen	Sample no.	Valve	Layer	Area	$\delta^{13}C$ VPDB				$\delta^{18}O$ VPDB			
							1	2	3	Mean	1	2	3	Mean
			0490	D	SL	Muscle Scars	0.8	0.7	*	0.74	1.54	1.49	*	1.52
			0491	D	SL	Cardinal Process	0.71	0.83	0.74	0.76	1.69	1.77	1.74	1.73
			0492	D	PL	Non-specialised	-1.70	-2.20	*	-1.95	-0.05	-0.39	*	-0.22
			0493	V	SL	Non-specialised	1.75	1.68	1.87	1.77	1.45	1.47	1.23	1.38
			0494	V	SL	Teeth	1.79	1.78	*	1.79	1.73	1.66	*	1.70
			0495	V	SL	Pedicle Foramen	0.73	0.81	*	0.77	1.44	1.33	*	1.38
			0496	V	SL	Muscle Scars	1.61	1.69	*	1.65	1.51	1.31	*	1.41
			0497	V	PL	Non-specialised	-2.15	-2.14	*	-2.15	-0.40	-0.58	*	-0.49
		7	0638	D	SL	Loop	1.65	*	*	1.65	1.28	*	*	1.28
			0639	D	SL	Non-specialised	2.07	1.87	1.85	1.93	1.52	1.35	1.40	1.42
			0640	D	SL	Muscle Scars	1.47	1.33	1.35	1.38	1.16	1.18	1.33	1.22
			0641	D	SL	Cardinal Process	0.75	0.68	*	0.71	1.30	1.44	*	1.37
			0642	D	PL	Non-specialised	-0.65	-3.33	-1.05	-1.67	0.15	-1.95	0.11	-0.56
			0643	V	SL	Non-specialised	1.94	2.06	1.80	1.93	1.42	1.57	1.18	1.39
			0644	V	SL	Teeth	2.14	2.13	*	2.14	1.87	1.88	*	1.87
			0645	V	SL	Pedicle Foramen	0.83	0.72	*	0.78	1.12	1.18	*	1.15
			0646	V	SL	Muscle Scars	1.76	1.84	*	1.80	1.26	1.63	*	1.44
			0647	V	PL	Non-specialised	-2.17	*	*	-2.17	-0.67	*	*	-0.67
		8	0648	D	SL	Loop	1.53	*	*	1.53	1.57	*	*	1.57
			0649	D	SL	Non-specialised	1.85	2.01	1.84	1.90	1.37	1.61	1.36	1.45
			0650	D	SL	Muscle Scars	1.05	0.99	1.20	1.08	1.34	1.30	1.21	1.28
			0651	D	SL	Cardinal Process	0.84	0.48	*	0.66	1.15	1.14	*	1.14

(Continued on next page)

Species	Location	Specimen	Sample no.	Valve	Layer	Area	$\delta^{13}C$ VPDB				$\delta^{18}O$ VPDB			
							1	2	3	Mean	1	2	3	Mean
			0852	D	PL	Non-specialised	-2.17	-2.58	-2.39	**-2.38**	-0.54	-0.32	-0.81	**-0.56**
			0853	V	SL	Non-specialised	1.47	1.30	1.33	**1.37**	1.44	1.52	1.22	**1.40**
			0854	V	SL	Teeth	1.52	1.23	1.37	**1.37**	1.32	1.57	1.25	**1.38**
			0855	V	SL	Pedicle Foramen	0.67	*	*	**0.67**	1.23	*	*	**1.23**
			0856	V	SL	Muscle Scars	1.26	0.94	1.13	**1.11**	1.53	1.42	1.16	**1.37**
			0857	V	PL	Non-specialised	-2.45	-2.90	-1.98	**-2.44**	-0.27	-0.61	-0.24	**-0.37**
		9	0918	D	SL	Loop	1.74	1.70	*	**1.72**	1.44	1.45		**1.44**
			0919	D	SL	Non-specialised	1.89	1.91	1.92	**1.91**	1.32	1.35	1.32	**1.33**
			0920	D	SL	Muscle Scars	1.31	1.46	1.15	**1.31**	1.37	1.50	1.50	**1.46**
			0921	D	SL	Cardinal Process	0.99	0.97	*	**0.98**	1.50	1.57	*	**1.53**
			0922	D	PL	Non-specialised	-1.10	-1.69	*	**-1.39**	0.39	0.34	*	**0.37**
			0923	V	SL	Non-specialised	1.50	1.59	1.73	**1.61**	1.65	1.62	1.61	**1.62**
			0924	V	SL	Teeth	1.64	1.60	1.63	**1.63**	1.73	1.70	1.57	**1.67**
			0925	V	SL	Pedicle Foramen	0.58	0.60	*	**0.59**	1.83	1.55	*	**1.69**
			0926	V	SL	Muscle Scars	1.20	1.23	*	**1.21**	1.98	1.87	*	**1.93**
			0927	V	PL	Non-specialised	-1.26	-1.35	*	**-1.31**	0.27	-0.29	*	**-0.01**
		10	0928	D	SL	Loop	1.68	1.57	*	**1.63**	1.41	1.58	*	**1.49**
			0929	D	SL	Non-specialised	2.01	2.06	1.96	**2.01**	1.48	1.61	1.31	**1.47**
			0930	D	SL	Muscle Scars	1.45	1.45	*	**1.45**	1.43	1.53	*	**1.48**
			0931	D	SL	Cardinal Process	1.10	1.11	*	**1.10**	1.53	1.56	*	**1.54**
			0932	D	PL	Non-specialised	-0.57	-0.48	*	**-0.53**	0.42	0.41	*	**0.42**
			0933	V	SL	Non-specialised	1.88	1.89	1.94	**1.90**	1.69	1.60	1.29	**1.53**

(Continued on next page)

Species	Location	Specimen	Sample no.	Valve	Layer	Area	$\delta^{13}C$ VPDB				$\delta^{18}O$ VPDB			
							1	2	3	Mean	1	2	3	Mean
			0934	V	SL	Teeth	1.76	1.74	1.69	1.73	1.65	1.29	1.36	1.43
			0935	V	SL	Pedicle Foramen	1.27	1.37	*	1.32	1.48	1.57	*	1.52
			0936	V	SL	Muscle Scars	1.69	1.70	*	1.70	1.28	1.30	*	1.29
			0937	V	PL	Non-specialised	-0.47	-0.32	*	-0.39	0.20	0.41	*	0.30
Liothyrella neozelanica	7. Otago Shelf,	1	0418	D	TL	Loop	2.40	2.42	2.05	2.29	1.09	1.30	1.19	1.19
	South Island,		0419	D	TL	Non-specialised	3.31	3.28	3.19	3.26	1.22	1.33	1.22	1.26
	New Zealand.		0420	D	TL	Muscle Scars	0.71	0.90	0.88	0.83	0.64	1.06	1.00	0.90
			0421	D	TL	Cardinal Process	0.97	0.93	0.99	0.96	0.93	1.35	1.19	1.16
			0422	D	PL	Non-specialised	-0.65	-0.61	-0.24	-0.50	-0.54	-0.14	0.03	-0.22
			0423	V	TL	Non-specialised	3.15	3.03	3.09	3.09	1.18	1.32	1.35	1.28
			0424	V	TL	Teeth	2.59	2.56	2.43	2.53	0.81	1.21	1.17	1.06
			0425	V	TL	Pedicle Foramen	1.25	1.26	1.23	1.24	0.95	1.23	1.06	1.08
			0426	V	TL	Muscle Scars	1.59	1.53	1.58	1.57	1.02	1.24	1.20	1.15
			0427	V	PL	Non-specialised	-1.28	-1.27	-0.98	-1.18	-0.58	-0.26	-0.24	-0.36
		2	0428	D	TL	Loop	2.26	2.16	2.27	2.23	1.04	1.21	1.25	1.17
			0429	D	TL	Non-specialised	2.85	2.96	2.96	2.92	1.10	1.19	1.08	1.12
			0430	D	TL	Muscle Scars	1.93	1.90	2.20	2.01	1.00	0.95	1.07	1.01
			0431	D	TL	Cardinal Process	1.02	1.02	*	1.02	1.01	1.25	*	1.13
			0432	D	PL	Non-specialised	0.63	1.92	*	1.28	0.05	1.11	*	0.58
			0433	V	TL	Non-specialised	3.03	0.92	3.17	2.37	0.67	0.54	1.24	0.82
			0434	V	TL	Teeth	2.00	2.55	3.22	2.59	1.12	1.47	1.31	1.30
			0435	V	TL	Pedicle Foramen	1.04	1.10	1.00	1.05	1.33	1.12	1.02	1.16

(Continued on next page)

Species	Location	Specimen	Sample no.	Valve	Layer	Area	$\delta^{13}C$ VPDB				$\delta^{18}O$ VPDB			
							1	2	3	Mean	1	2	3	Mean
			0436	V	TL	Muscle Scars	2.40	2.02	2.00	**2.14**	1.37	1.28	1.20	**1.28**
			0437	V	PL	Non-specialised	3.23	0.22	0.28	**1.24**	1.49	0.53	0.22	**0.75**
		3	0438	D	TL	Loop	2.59	*	*	**2.59**	1.42	*	*	**1.42**
			0439	D	TL	Non-specialised	3.51	3.35	3.37	**3.41**	1.50	1.42	1.29	**1.40**
			0440	D	TL	Muscle Scars	2.08	1.91	1.89	**1.96**	1.54	1.25	1.24	**1.35**
			0441	D	TL	Cardinal Process	1.24	1.18	1.15	**1.19**	1.43	1.36	1.17	**1.32**
			0442	D	PL	Non-specialised	1.07	0.96	1.05	**1.03**	0.36	0.30	0.32	**0.33**
			0443	V	TL	Non-specialised	3.47	3.42	3.44	**3.45**	1.67	1.25	1.34	**1.42**
			0444	V	TL	Teeth	2.50	2.21	2.35	**2.35**	1.33	1.07	1.05	**1.15**
			0445	V	TL	Pedicle Foramen	1.64	1.11	1.61	**1.45**	1.40	1.18	1.24	**1.27**
			0446	V	TL	Muscle Scars	1.79	1.71	1.77	**1.75**	1.28	1.22	1.34	**1.28**
			0447	V	PL	Non-specialised	1.00	0.86	0.88	**0.92**	0.54	0.17	0.13	**0.28**
		4	0448	D	TL	Loop	2.57	2.42	*	**2.50**	1.41	1.41	*	**1.41**
			0449	D	TL	Non-specialised	2.95	2.94	2.91	**2.93**	1.34	1.40	1.30	**1.35**
			0450	D	TL	Muscle Scars	1.16	*	*	**1.16**	1.26	*	*	**1.26**
			0451	D	TL	Cardinal Process	0.53	0.33	0.47	**0.44**	1.12	1.01	1.24	**1.13**
			0452	D	PL	Non-specialised	0.05	0.07	*	**0.06**	0.27	0.25	*	**0.26**
			0453	V	TL	Non-specialised	3.03	2.99	3.05	**3.02**	1.54	1.46	1.45	**1.48**
			0454	V	TL	Teeth	1.95	2.04	*	**1.99**	1.06	1.19	*	**1.12**
			0455	V	TL	Pedicle Foramen	0.54	0.41	0.55	**0.50**	1.24	1.04	1.22	**1.17**
			0456	V	TL	Muscle Scars	1.77	1.89	1.89	**1.85**	1.24	1.08	1.22	**1.18**
			0457	V	PL	Non-specialised	-0.82	-0.73	-0.13	**-0.56**	0.00	-0.13	0.62	**0.16**

(Continued on next page)

Species	Location	Specimen	Sample no.	Valve	Layer	Area	$\delta^{13}C$ VPDB				$\delta^{18}O$ VPDB			
							1	2	3	Mean	1	2	3	Mean
		5	0578	D	TL	Loop	2.53	2.37	*	**2.45**	1.43	1.41	*	**1.42**
			0579	D	TL	Non-specialised	3.11	3.17	*	**3.14**	1.32	1.18	*	**1.25**
			0580	D	TL	Muscle Scars	0.39	0.58	*	**0.48**	1.08	1.07	*	**1.07**
			0581	D	TL	Cardinal Process	0.59	1.11	*	**0.85**	1.22	0.66	*	**0.94**
			0582	D	PL	Non-specialised	0.23	*	*	**0.23**	0.25	*	*	**0.25**
			0583	V	TL	Non-specialised	3.05	3.13	2.93	**3.04**	1.25	1.16	1.37	**1.26**
			0584	V	TL	Teeth	2.39	2.46	2.14	**2.33**	1.19	1.00	0.83	**1.01**
			0585	V	TL	Pedicle Foramen	0.27	0.29	0.63	**0.40**	1.09	1.09	1.13	**1.10**
			0586	V	TL	Muscle Scars	1.41	1.58	1.45	**1.48**	1.11	1.11	1.19	**1.14**
			0587	V	PL	Non-specialised	-0.05	0.23	-0.09	**0.03**	0.29	0.12	-0.15	**0.09**
		6	0588	D	TL	Loop	1.53	*	*	**1.53**	1.42	*	*	**1.42**
			0589	D	TL	Non-specialised	3.34	3.30	3.36	**3.33**	1.29	1.17	1.37	**1.28**
			0590	D	TL	Muscle Scars	0.11	0.27	0.09	**0.16**	1.09	0.91	0.87	**0.96**
			0591	D	TL	Cardinal Process	0.15	*	*	**0.15**	1.11	*	*	**1.11**
			0592	D	PL	Non-specialised	0.93	*	*	**0.93**	0.26	*	*	**0.26**
			0593	V	TL	Non-specialised	2.98	3.06	3.04	**3.03**	1.29	1.48	1.15	**1.31**
			0594	V	TL	Teeth	2.34	2.34	2.23	**2.30**	1.20	1.42	1.35	**1.32**
			0595	V	TL	Pedicle Foramen	-0.02	0.27	*	**0.13**	0.76	1.82	*	**1.29**
			0596	V	TL	Muscle Scars	0.24	-0.01	0.33	**0.19**	1.11	1.02	1.17	**1.10**
			0597	V	PL	Non-specialised	0.59	0.38	0.59	**0.52**	0.97	0.12	0.50	**0.53**
		7	0718	D	TL	Loop	2.61	2.38	*	**2.49**	1.17	1.21	*	**1.19**
			0719	D	TL	Non-specialised	3.30	3.32	3.51	**3.38**	1.17	1.23	1.69	**1.36**

(Continued on next page)

Species	Location	Specimen	Sample no.	Valve	Layer	Area	$\delta^{13}C$ VPDB				$\delta^{18}O$ VPDB			
							1	2	3	Mean	1	2	3	Mean
			0720	D	TL	Muscle Scars	0.56	1.18	*	**0.88**	0.88	1.69	*	**1.28**
			0721	D	TL	Cardinal Process	1.24	1.34	*	**1.29**	0.71	0.87	*	**0.79**
			0722	D	PL	Non-specialised	1.70	1.82	1.86	**1.79**	0.50	0.64	1.02	**0.72**
			0723	V	TL	Non-specialised	3.30	3.37	3.46	**3.38**	1.10	1.26	1.53	**1.30**
			0724	V	TL	Teeth	2.33	2.24	2.91	**2.49**	0.95	1.09	1.49	**1.18**
			0725	V	TL	Pedicle Foramen	1.27	1.37	*	**1.32**	0.94	1.08	*	**1.01**
			0726	V	TL	Muscle Scars	2.84	2.87	2.40	**2.70**	1.04	1.26	1.15	**1.15**
			0727	V	PL	Non-specialised	0.78	0.94	1.09	**0.94**	-0.01	0.27	0.67	**0.31**
		8	0728	D	TL	Loop	2.64	2.50	1.64	**2.26**	1.02	1.24	0.98	**1.08**
			0729	D	TL	Non-specialised	3.83	3.72	2.92	**3.49**	1.29	1.22	1.49	**1.33**
			0730	D	TL	Muscle Scars	1.28	1.33	1.26	**1.29**	1.06	1.24	1.21	**1.17**
			0731	D	TL	Cardinal Process	1.31	1.31	*	**1.31**	1.02	1.30	*	**1.16**
			0732	D	PL	Non-specialised	1.36	1.47	1.55	**1.46**	0.40	0.64	0.73	**0.59**
			0733	V	TL	Non-specialised	3.51	3.48	3.46	**3.48**	1.24	1.27	1.20	**1.24**
			0734	V	TL	Teeth	2.45	2.46	2.42	**2.44**	0.95	1.16	1.21	**1.10**
			0735	V	TL	Pedicle Foramen	1.39	*	*	**1.39**	0.82	*	*	**0.82**
			0736	V	TL	Muscle Scars	2.26	2.20	2.22	**2.23**	1.31	1.17	1.23	**1.23**
			0737	V	PL	Non-specialised	1.42	1.35	*	**1.39**	0.72	0.62	*	**0.67**
		9	0998	D	TL	Loop	2.31	2.39	*	**2.35**	1.40	1.09	*	**1.24**
			0999	D	TL	Non-specialised	2.65	2.98	2.68	**2.77**	1.19	1.37	1.05	**1.20**
			1000	D	TL	Muscle Scars	1.99	0.67	0.20	**0.95**	1.27	1.10	0.59	**0.99**
			1001	D	TL	Cardinal Process	1.55	0.99	0.90	**1.15**	1.32	0.48	0.81	**0.87**

(Continued on next page)

Species	Location	Specimen	Sample no.	Valve	Layer	Area	$\delta^{13}C$ VPDB				$\delta^{18}O$ VPDB			
							1	2	3	Mean	1	2	3	Mean
			1002	D	PL	Non-specialised	1.16	*	*	1.16	1.07	*	*	1.07
			1003	V	TL	Non-specialised	3.04	2.97	2.55	2.85	1.62	0.90	0.70	1.07
			1004	V	TL	Teeth	2.97	2.25	1.99	2.40	1.67	0.80	0.67	1.05
			1005	V	TL	Pedicle Foramen	0.55	0.77	*	0.66	1.28	0.82	*	1.05
			1006	V	TL	Muscle Scars	0.54	*	*	0.54	1.33	*	*	1.33
			1007	V	PL	Non-specialised	0.26	*	*	0.26	1.01	*	*	1.01
		10	1008	D	TL	Loop	2.36	2.46	*	2.41	-0.64	1.73	*	0.55
			1009	D	TL	Non-specialised	2.38	2.26	2.36	2.33	0.48	1.03	1.04	0.85
			1010	D	TL	Muscle Scars	2.58	2.39	2.31	2.43	1.49	1.26	0.98	1.24
			1011	D	TL	Cardinal Process	1.06	1.04	*	1.05	1.55	1.37	*	1.46
			1012	D	PL	Non-specialised	0.46	*	*	0.46	0.90	*	*	0.90
			1013	V	TL	Non-specialised	1.98	2.92	2.72	2.54	1.19	1.04	0.66	0.97
			1014	V	TL	Teeth	2.19	2.17	*	2.18	1.42	1.10	*	1.26
			1015	V	TL	Pedicle Foramen	0.91	*	*	0.91	1.32	*	*	1.32
			1016	V	TL	Muscle Scars	1.19	*	*	1.19	1.33	*	*	1.33
			1017	V	PL	Non-specialised	-0.84	*	*	-0.84	0.06	*	*	0.06
Neothyris lenticularis	7. Otago Shelf,	1	0288	D	SL	Loop	2.02	*	*	2.02	2.03	*	*	2.03
	South Island,		0124	D	SL	Non-specialised	2.73	2.57	2.89	2.73	2.01	1.76	2.44	2.07
	New Zealand.		0125	D	SL	Muscle Scars	1.65	1.51	1.80	1.65	2.10	1.60	2.11	1.93
			0126	D	SL	Cardinal Process	1.86	1.77	1.70	1.78	2.13	1.91	1.77	1.94
			0127	D	PL	Non-specialised	2.28	2.20	2.13	2.20	1.54	1.51	1.17	1.41
			0027	V	SL	Non-specialised	2.86	2.86	2.81	2.84	2.24	2.16	2.00	2.13

(Continued on next page)

Species	Location	Specimen	Sample no.	Valve	Layer	Area	$\delta^{13}C$ VPDB				$\delta^{18}O$ VPDB			
							1	2	3	Mean	1	2	3	Mean
			0029	V	SL	Teeth	2.49	2.43	2.53	2.48	1.94	1.88	1.80	1.87
			0032	V	SL	Pedicle Foramen	2.26	2.33	2.27	2.29	1.74	1.73	1.57	1.68
			0033	V	SL	Muscle Scars	2.52	2.47	2.42	2.47	1.75	1.70	1.77	1.74
			0035	V	PL	Non-specialised	1.44	1.49	1.48	1.47	0.95	0.89	0.79	0.88
		2	0290	D	SL	Loop	1.82	1.78	1.93	1.84	1.99	1.80	2.01	1.93
			0002	D	SL	Non-specialised	2.60	2.67	2.46	2.58	2.05	1.89	1.88	1.94
			0003	D	SL	Muscle Scars	2.25	2.24	2.36	2.28	1.64	1.68	1.89	1.74
			0005	D	SL	Cardinal Process	1.35	1.36	1.35	1.35	1.88	1.97	1.76	1.87
			0008	D	PL	Non-specialised	2.14	2.13	2.10	2.12	1.54	1.57	1.51	1.54
			0137	V	SL	Non-specialised	2.71	2.82	2.62	2.72	1.96	1.91	2.12	1.99
			0138	V	SL	Teeth	2.67	2.65	2.70	2.67	1.90	1.94	2.02	1.95
			0139	V	SL	Pedicle Foramen	1.87	1.99	1.96	1.94	1.71	1.78	1.87	1.79
			0140	V	SL	Muscle Scars	2.45	2.55	2.41	2.47	1.60	2.28	1.71	1.86
			0141	V	PL	Non-specialised	1.10	1.37	1.19	1.22	0.74	1.04	0.95	0.91
		3	0291	D	SL	Loop	2.30	2.23	2.43	2.32	2.05	1.85	2.06	1.99
			0009	D	SL	Non-specialised	2.45	2.45	2.52	2.47	1.68	1.65	1.66	1.66
			0014	D	SL	Muscle Scars	2.14	2.27	2.28	2.23	1.59	1.81	1.50	1.63
			0011	D	SL	Cardinal Process	2.34	2.42	2.40	2.38	1.77	1.88	1.80	1.82
			0015	D	PL	Non-specialised	2.30	2.36	2.51	2.39	1.24	1.34	1.46	1.35
			0268	V	SL	Non-specialised	2.89	2.82	2.69	2.80	1.98	1.63	1.96	1.86
			0269	V	SL	Teeth	2.71	2.75	2.66	2.71	2.04	1.87	1.68	1.86
			0270	V	SL	Pedicle Foramen	2.29	2.35	2.28	2.30	1.77	1.81	1.81	1.80

(Continued on next page)

Species	Location	Specimen	Sample no.	Valve	Layer	Area	$\delta^{13}C$ VPDB				$\delta^{18}O$ VPDB			
							1	2	3	Mean	1	2	3	Mean
			0271	V	SL	Muscle Scars	2.56	2.56	2.55	2.56	1.91	1.86	2.32	2.03
			0272	V	PL	Non-specialised	1.88	1.80	1.88	1.85	1.07	0.96	1.14	1.06
		4	0269	D	SL	Loop	2.57	2.07	2.29	2.31	2.03	1.74	2.08	1.95
			0128	D	SL	Non-specialised	1.57	2.64	2.59	2.27	1.88	1.85	1.73	1.82
			0129	D	SL	Muscle Scars	1.52	1.55	1.51	1.53	1.99	1.79	1.64	1.81
			0130	D	SL	Cardinal Process	2.69	1.44	1.40	1.84	2.04	1.94	1.83	1.87
			0131	D	PL	Non-specialised	-0.42	-0.50	-0.46	-0.46	0.23	-0.10	0.12	0.09
			0273	V	SL	Non-specialised	2.78	2.80	2.87	2.75	2.02	2.07	1.94	2.01
			0274	V	SL	Teeth	2.80	2.93	2.79	2.84	2.01	2.06	1.76	1.94
			0275	V	SL	Pedicle Foramen	2.18	2.15	*	2.17	1.84	1.68	*	1.76
			0276	V	SL	Muscle Scars	2.45	2.40	2.38	2.41	1.93	1.80	1.72	1.81
			0277	V	PL	Non-specialised	-1.08	-0.85	-1.46	-1.13	-0.07	0.22	-0.6	-0.15
		5	0278	D	SL	Loop	2.77	2.64	2.16	2.53	2.02	1.94	2.05	2.00
			0279	D	SL	Non-specialised	2.84	2.87	2.78	2.83	2.00	2.15	1.90	2.02
			0280	D	SL	Muscle Scars	1.86	1.85	1.86	1.86	1.78	1.71	1.76	1.75
			0281	D	SL	Cardinal Process	1.31	1.23	1.30	1.28	1.85	1.93	1.72	1.83
			0282	D	PL	Non-specialised	-1.70	-1.70	-1.61	-1.67	-0.23	-0.30	-0.39	-0.31
			0283	V	SL	Non-specialised	2.73	2.66	2.69	2.69	2.09	1.86	1.80	1.92
			0284	V	SL	Teeth	2.60	2.54	2.63	2.59	1.90	1.66	1.85	1.80
			0285	V	SL	Pedicle Foramen	1.64	1.49	1.52	1.55	1.68	1.23	1.06	1.32
			0286	V	SL	Muscle Scars	2.23	2.17	2.30	2.23	1.71	1.71	1.64	1.68
			0287	V	PL	Non-specialised	-2.27	-2.06	-2.17	-2.17	-0.60	-0.44	-0.75	-0.59

(Continued on next page)

Species	Location	Specimen	Sample no.	Valve	Layer	Area	$\delta^{13}C$ VPDB				$\delta^{18}O$ VPDB			
							1	2	3	Mean	1	2	3	Mean
		6	0458	D	SL	Loop	1.70	1.55	1.70	1.65	1.67	1.23	1.48	1.46
			0459	D	SL	Non-specialised	1.94	2.05	2.03	2.01	1.05	1.41	1.32	1.26
			0460	D	SL	Muscle Scars	1.22	1.31	1.28	1.27	1.31	1.40	1.44	1.38
			0461	D	SL	Cardinal Process	0.96	1.01	1.21	1.06	1.35	1.39	1.82	1.52
			0462	D	PL	Non-specialised	-1.89	-1.94	-1.90	-1.91	1.03	-1.03	-1.00	-0.33
			0463	V	SL	Non-specialised	1.71	1.82	1.84	1.79	0.92	1.01	1.37	1.10
			0464	V	SL	Teeth	0.87	0.90	0.99	0.92	0.80	0.82	1.31	0.97
			0465	V	SL	Pedicle Foramen	1.06	1.33	1.49	1.29	1.00	1.38	1.87	1.42
			0466	V	SL	Muscle Scars	1.66	1.69	1.80	1.71	1.49	1.33	1.56	1.46
			0467	V	PL	Non-specialised	-1.99	-1.87	-1.85	-1.90	-0.96	-0.91	-0.43	-0.77
		7	0598	D	SL	Loop	1.66	1.56	1.72	1.64	1.40	1.19	1.05	1.21
			0599	D	SL	Non-specialised	2.17	1.93	2.08	2.06	1.53	1.42	1.27	1.41
			0600	D	SL	Muscle Scars	1.45	1.39	0.82	1.22	1.36	1.41	0.84	1.21
			0601	D	SL	Cardinal Process	0.66	0.34	0.28	0.43	1.56	1.46	0.92	1.32
			0602	D	PL	Non-specialised	-2.36	-2.17	-1.84	-2.12	-0.88	-0.91	-0.17	-0.65
			0603	V	SL	Non-specialised	2.33	2.08	1.97	2.13	1.37	1.29	0.87	1.17
			0604	V	SL	Teeth	2.04	1.70	0.88	1.54	1.14	0.97	1.15	1.09
			0605	V	SL	Pedicle Foramen	1.06	0.75	0.77	0.86	1.10	0.88	0.72	0.90
			0606	V	SL	Muscle Scars	1.69	1.13	1.18	1.33	2.15	1.36	1.38	1.63
			0607	V	PL	Non-specialised	-2.67	-2.97	-2.79	-2.81	-1.01	-1.28	-1.10	-1.13
		8	0608	D	SL	Loop	1.67	1.37	1.58	1.54	1.74	1.42	1.72	1.63
			0609	D	SL	Non-specialised	1.51	1.28	1.36	1.39	1.30	1.06	1.06	1.14

(Continued on next page)

Species	Location	Specimen	Sample no.	Valve	Layer	Area	$\delta^{13}C$ VPDB				$\delta^{18}O$ VPDB			
							1	2	3	Mean	1	2	3	Mean
			0610	D	SL	Muscle Scars	0.85	0.60	0.86	0.77	1.42	1.29	1.18	1.30
			0611	D	SL	Cardinal Process	0.75	0.48	0.62	0.61	1.63	1.09	1.40	1.37
			0612	D	PL	Non-specialised	-2.57	-2.77	-2.60	-2.65	-1.13	-1.30	-1.30	-1.25
			0613	V	SL	Non-specialised	1.67	1.60	1.63	1.63	1.21	1.10	1.28	1.20
			0614	V	SL	Teeth	2.54	2.46	2.41	2.47	1.49	1.04	1.29	1.27
			0615	V	SL	Pedicle Foramen	1.45	1.26	*	1.35	1.24	0.95	*	1.10
			0616	V	SL	Muscle Scars	1.32	1.26	1.32	1.30	1.47	1.29	1.42	1.39
			0617	V	PL	Non-specialised	-2.86	-3.21	-3.17	-3.08	-1.13	-1.44	-1.48	-1.35
		9	0878	D	SL	Loop	1.85	1.50	1.92	1.75	1.66	1.72	2.21	1.86
			0879	D	SL	Non-specialised	2.00	1.85	1.99	1.95	1.64	1.51	1.62	1.59
			0880	D	SL	Muscle Scars	1.52	1.29	1.24	1.35	1.49	1.21	1.39	1.36
			0881	D	SL	Cardinal Process	1.27	0.95	1.16	1.13	1.87	1.34	1.95	1.72
			0882	D	PL	Non-specialised	-1.36	*	*	-1.36	-0.11	*	*	-0.11
			0883	V	SL	Non-specialised	2.00	1.82		1.91	1.49	1.43		1.46
			0884	V	SL	Teeth	1.44	1.25	1.17	1.28	1.14	0.84	1.02	1.00
			0885	V	SL	Pedicle Foramen	1.17	*	*	1.17	1.29	*	*	1.29
			0886	V	SL	Muscle Scars	1.85	1.62	1.48	1.65	1.72	1.38	1.07	1.39
			0887	V	PL	Non-specialised	-1.54	*	*	-1.54	-0.22	*	*	-0.22
		10	0888	D	SL	Loop	1.80	1.80	1.59	1.73	1.86	1.78	1.76	1.80
			0889	D	SL	Non-specialised	2.33	2.32	2.31	2.32	2.15	1.44	1.54	1.71
			0890	D	SL	Muscle Scars	1.44	1.46	1.14	1.35	1.82	1.52	1.24	1.53
			0891	D	SL	Cardinal Process	1.18	0.93	0.82	0.98	1.92	1.43	1.17	1.51

(Continued on next page)

Species	Location	Specimen	Sample no.	Valve	Layer	Area	$\delta^{13}C$ VPDB				$\delta^{18}O$ VPDB			
							1	2	3	Mean	1	2	3	Mean
			0892	D	PL	Non-specialised	-2.85	-2.61	-2.39	-2.62	-0.38	-0.42	-0.29	-0.37
			0893	V	SL	Non-specialised	2.22	1.62	1.59	1.81	1.82	1.20	0.90	1.31
			0894	V	SL	Teeth	1.97	1.67	1.71	1.78	1.75	1.20	0.95	1.30
			0895	V	SL	Pedicle Foramen	1.41	1.03	1.06	1.17	1.79	1.30	1.24	1.44
			0896	V	SL	Muscle Scars	1.95	1.69	1.47	1.70	1.87	1.38	1.18	1.48
			0897	V	PL	Non-specialised	-0.89	-2.76	-2.11	-1.92	1.26	-0.61	-0.29	0.12
Notosaria nigricans	7. Otago Shelf,	1	0182	D	SL	Loop	1.70	1.68	*	1.69	1.93	2.10	*	2.01
	South Island,		0183	D	SL	Non-specialised	2.71	2.76	2.66	2.72	1.76	2.07	1.83	1.89
	New Zealand.		0184	D	SL	Muscle Scars	1.79	1.73	*	1.76	1.73	1.69	*	1.71
			0185	D	SL	Cardinal Process	0.87	*	*	0.87	1.55	*	*	1.55
			0186	D	PL	Non-specialised	1.62	1.70	1.63	1.65	1.24	1.39	1.26	1.30
			0187	V	SL	Non-specialised	2.25	2.22	2.23	2.23	1.57	1.54	1.48	1.53
			0188	V	SL	Teeth	2.34	2.34	2.54	2.41	1.94	2.00	1.95	1.96
			0189	V	SL	Pedicle Foramen	0.71	0.76	*	0.74	1.64	1.58	*	1.61
			0190	V	SL	Muscle Scars	1.15	1.23	1.04	1.14	1.63	1.82	1.76	1.74
			0191	V	PL	Non-specialised	2.20	2.31	2.23	2.25	1.37	1.81	1.61	1.60
		2	0192	D	SL	Loop	2.14	*	*	2.14	1.97	*	*	1.97
			0193	D	SL	Non-specialised	2.54	2.49	*	2.51	1.66	1.72	*	1.69
			0194	D	SL	Muscle Scars	0.37	*	*	0.37	1.77	*	*	1.77
			0195	D	SL	Cardinal Process	0.93	*	*	0.93	1.60	*	*	1.60
			0196	D	PL	Non-specialised	2.15	2.18	2.13	2.16	1.51	1.42	1.58	1.50
			0197	V	SL	Non-specialised	2.59	2.56	2.55	2.57	1.79	1.77	1.88	1.81

(Continued on next page)

Species	Location	Specimen	Sample no.	Valve	Layer	Area	$\delta^{13}C$ VPDB				$\delta^{18}O$ VPDB			
							1	2	3	Mean	1	2	3	Mean
			0198	V	SL	Teeth	2.04	1.81	*	1.93	1.73	1.63	*	1.68
			0199	V	SL	Pedicle Foramen	0.70	*	*	0.70	1.39	*	*	1.39
			0200	V	SL	Muscle Scars	1.35	*	*	1.35	1.51	*	*	1.51
			0201	V	PL	Non-specialised	1.20	1.43	*	1.32	0.97	0.95	*	0.96
		3	0332	D	SL	Loop	1.43	*	*	1.43	1.79	*	*	1.79
			0333	D	SL	Non-specialised	2.47	2.69	2.29	2.48	1.15	1.79	1.04	1.33
			0334	D	SL	Muscle Scars	0.57	*	*	0.57	1.07	*	*	1.07
			0335	D	SL	Cardinal Process	0.91	*	*	0.91	1.38	*	*	1.38
			0336	D	PL	Non-specialised	1.21	1.51	1.13	1.28	0.63	1.05	0.62	0.77
			0337	V	SL	Non-specialised	2.32	2.52	2.19	2.34	1.14	1.49	1.11	1.25
			0338	V	SL	Teeth	1.84	2.03	1.80	1.89	1.45	1.48	1.45	1.46
			0339	V	SL	Pedicle Foramen	0.99	0.97	*	0.98	1.02	0.73	*	0.87
			0340	V	SL	Muscle Scars	0.86	0.66	0.87	0.80	1.29	0.43	0.55	0.76
			0341	V	PL	Non-specialised	1.61	1.57	*	1.59	1.09	0.59	*	0.84
		4	0342	D	SL	Loop	1.53	*	*	1.53	1.36	*	*	1.36
			0343	D	SL	Non-specialised	2.10	2.13	1.90	2.04	1.49	1.46	1.31	1.42
			0344	D	SL	Muscle Scars	0.34	0.46	*	0.40	1.53	1.37	*	1.45
			0345	D	SL	Cardinal Process	0.70	0.51	*	0.61	1.20	0.29	*	0.74
			0346	D	PL	Non-specialised	1.72	1.78	1.51	1.67	1.01	1.02	0.92	0.98
			0347	V	SL	Non-specialised	1.90	1.71	*	1.80	1.35	1.18	*	1.27
			0348	V	SL	Teeth	1.72	1.54	1.76	1.67	1.51	1.34	1.56	1.47
			0349	V	SL	Pedicle Foramen	0.43	0.35	0.95	0.57	1.07	1.18	1.83	1.36

(Continued on next page)

Species	Location	Specimen	Sample no.	Valve	Layer	Area	$\delta^{13}C$ VPDB				$\delta^{18}O$ VPDB			
							1	2	3	Mean	1	2	3	Mean
			0350	V	SL	Muscle Scars	0.72	0.68	0.71	0.71	1.14	1.29	1.22	1.22
			0351	V	PL	Non-specialised	1.73	1.60	1.75	1.69	1.01	1.16	1.16	1.11
		5	0498	D	SL	Loop	1.71	*	*	1.71	2.09	*	*	2.09
			0499	D	SL	Non-specialised	2.17	2.14	*	2.16	1.76	1.64	*	1.70
			0500	D	SL	Muscle Scars	1.44	1.54	*	1.49	2.09	1.93	*	2.01
			0501	D	SL	Cardinal Process	1.04	*	*	1.04	1.85	*	*	1.85
			0502	D	PL	Non-specialised	1.78	1.84	*	1.81	1.46	1.40	*	1.43
			0503	V	SL	Non-specialised	2.09	2.30	1.92	2.10	1.77	2.05	1.69	1.84
			0504	V	SL	Teeth	1.90	2.00	1.85	1.92	1.96	1.82	1.54	1.77
			0505	V	SL	Pedicle Foramen	0.81	0.88	*	0.85	1.66	1.58	*	1.62
			0506	V	SL	Muscle Scars	0.85	0.81	*	0.83	1.79	1.31	*	1.55
			0507	V	PL	Non-specialised	1.83	1.65	1.76	1.75	1.19	1.03	1.03	1.08
		6	0508	D	SL	Loop	1.55	*	*	1.55	1.76	*	*	1.76
			0509	D	SL	Non-specialised	2.14	2.29	2.13	2.19	1.26	1.49	1.40	1.38
			0510	D	SL	Muscle Scars	0.57	0.51	*	0.54	1.27	1.49	*	1.38
			0511	D	SL	Cardinal Process	0.83	*	*	0.83	1.81	*	*	1.81
			0512	D	PL	Non-specialised	1.82	1.52	1.89	1.74	0.95	0.88	0.99	0.94
			0513	V	SL	Non-specialised	2.10	1.33	1.95	1.79	1.18	1.51	1.87	1.52
			0514	V	SL	Teeth	2.20	0.84	1.97	1.67	1.55	1.78	1.92	1.75
			0515	V	SL	Pedicle Foramen	1.28	1.30	*	1.29	1.27	0.90	*	1.09
			0516	V	SL	Muscle Scars	0.76	0.73	0.72	0.73	1.12	1.17	1.13	1.14
			0517	V	PL	Non-specialised	1.57	1.62	*	1.59	1.07	1.05	*	1.06

(Continued on next page)

Species	Location	Specimen	Sample no.	Valve	Layer	Area	$\delta^{13}C$ VPDB				$\delta^{18}O$ VPDB			
							1	2	3	Mean	1	2	3	Mean
		7	0658	D	SL	Loop	1.88	*	*	1.88	2.21	*	*	2.21
			0659	D	SL	Non-specialised	2.17	1.82	2.02	2.00	1.57	1.67	1.33	1.52
			0660	D	SL	Muscle Scars	1.08	*	*	1.08	1.75	*	*	1.75
			0661	D	SL	Cardinal Process	0.40	*	*	0.40	1.53	*	*	1.53
			0662	D	PL	Non-specialised	0.61	0.24	0.60	0.48	0.71	0.79	0.77	0.76
			0663	V	SL	Non-specialised	2.39	2.19	2.32	2.30	1.57	1.70	1.54	1.60
			0664	V	SL	Teeth	1.84	1.58	*	1.71	1.81	2.06	*	1.93
			0665	V	SL	Pedicle Foramen	1.78	0.55	*	1.17	1.81	1.71	*	1.76
			0666	V	SL	Muscle Scars	1.02	0.98	*	1.00	1.67	1.82	*	1.74
			0667	V	PL	Non-specialised	1.15	0.37	0.49	0.67	1.42	0.96	0.73	1.04
		8	0668	D	SL	Loop	0.64	*	*	0.64	0.73	*	*	0.73
			0669	D	SL	Non-specialised	1.93	2.21	2.28	2.14	2.18	1.95	1.60	1.91
			0670	D	SL	Muscle Scars	2.31	*	*	2.31	1.66	*	*	1.66
			0671	D	SL	Cardinal Process	0.67	0.52	*	0.59	1.62	1.87	*	1.74
			0672	D	PL	Non-specialised	0.69	1.55	1.56	1.27	1.72	1.53	1.16	1.47
			0673	V	SL	Non-specialised	1.78	2.19	2.25	2.07	1.24	1.96	1.50	1.57
			0674	V	SL	Teeth	1.49	1.42	1.93	1.61	1.15	1.17	1.66	1.42
			0675	V	SL	Pedicle Foramen	0.76	0.79	*	0.78	1.75	1.87	*	1.81
			0676	V	SL	Muscle Scars	1.01	1.09	*	1.05	1.58	1.89	*	1.74
			0677	V	PL	Non-specialised	0.54	1.60	1.56	1.24	1.64	1.77	1.23	1.55
		9	0938	D	SL	Loop	1.41	*	*	1.41	2.18	*	*	2.18
			0939	D	SL	Non-specialised	2.06	2.10	2.09	2.08	1.68	1.61	1.53	1.61

(Continued on next page)

Species	Location	Specimen	Sample no.	Valve	Layer	Area	$\delta^{13}C$ VPDB				$\delta^{18}O$ VPDB			
							1	2	3	Mean	1	2	3	Mean
			0940	D	SL	Muscle Scars	0.21	0.27	*	0.24	1.44	1.49	*	1.46
			0941	D	SL	Cardinal Process	0.43	0.46	*	0.45	1.78	1.53	*	1.66
			0942	D	PL	Non-specialised	1.81	1.97	1.83	1.87	1.44	1.29	1.17	1.30
			0943	V	SL	Non-specialised	2.12	2.26	2.10	2.16	1.80	1.72	1.47	1.66
			0944	V	SL	Teeth	1.90	1.97	1.77	1.88	2.26	1.90	1.61	1.92
			0945	V	SL	Pedicle Foramen	1.03	1.18	*	1.10	1.66	1.78	*	1.72
			0946	V	SL	Muscle Scars	0.94	0.70	*	0.82	1.49	1.72	*	1.60
			0947	V	PL	Non-specialised	1.69	1.80	1.80	1.77	1.25	1.26	1.31	1.27
		10	0948	D	SL	Loop	1.70	1.94	*	1.82	2.09	2.44	*	2.27
			0949	D	SL	Non-specialised	2.22	2.15	*	2.18	1.36	0.98	*	1.17
			0950	D	SL	Muscle Scars	1.26	1.30	*	1.28	1.52	1.67	*	1.59
			0951	D	SL	Cardinal Process	1.09	1.15	*	1.12	1.56	1.46	*	1.51
			0952	D	PL	Non-specialised	1.94	1.80	*	1.87	1.43	1.66	*	1.54
			0953	V	SL	Non-specialised	2.06	2.28	*	2.17	0.81	1.21	*	1.01
			0954	V	SL	Teeth	2.20	1.96	1.73	1.96	1.94	1.71	1.34	1.66
			0955	V	SL	Pedicle Foramen	0.77	0.68	*	0.73	1.80	1.75	*	1.78
			0956	V	SL	Muscle Scars	0.95	1.10	*	1.03	1.63	1.69	*	1.66
			0957	V	PL	Non-specialised	1.95	1.92	1.85	1.91	1.58	1.25	1.00	1.28
Terebratella sanguinea	7. Otago Shelf,	1	0248	D	SL	Loop	1.62	*	*	1.62	1.28	*	*	1.28
	South Island,		0249	D	SL	Non-specialised	1.46	1.46	1.46	1.46	1.33	1.39	1.45	1.39
	New Zealand.		0250	D	SL	Muscle Scars	1.77	1.82	1.80	1.80	1.20	1.54	1.37	1.37
			0251	D	SL	Cardinal Process	0.45	0.67	1.03	0.71	1.08	1.32	1.85	1.41

(Continued on next page)

Species	Location	Specimen	Sample no.	Valve	Layer	Area	$\delta^{13}C$ VPDB				$\delta^{18}O$ VPDB			
							1	2	3	Mean	1	2	3	Mean
			0252	D	PL	Non-specialised	-0.28	-0.19	-2.37	-0.94	0.06	0.34	-0.14	0.09
			0253	V	SL	Non-specialised	1.81	1.83	1.89	1.84	1.37	1.24	1.26	1.29
			0254	V	SL	Teeth	1.82	1.74	*	1.78	1.27	1.32	*	1.29
			0255	V	SL	Pedicle Foramen	1.16	1.34	1.81	1.44	1.08	1.31	1.35	1.25
			0256	V	SL	Muscle Scars	1.44	1.60	1.48	1.51	1.23	1.60	1.40	1.41
			0257	V	PL	Non-specialised	-1.21	-1.27	-1.23	-1.24	-0.16	-0.33	-0.27	-0.25
		2	0258	D	SL	Loop	2.12	*	*	2.12	1.35	*	*	1.35
			0259	D	SL	Non-specialised	1.50	1.38	1.56	1.48	0.81	0.82	1.04	0.89
			0260	D	SL	Muscle Scars	1.38	1.32	1.36	1.35	0.68	0.62	0.66	0.65
			0261	D	SL	Cardinal Process	0.29	0.26	*	0.28	0.46	0.32	*	0.39
			0262	D	PL	Non-specialised	-1.05	-0.89	-0.94	-0.96	-0.91	-0.56	-0.74	-0.74
			0263	V	SL	Non-specialised	1.26	1.03	1.16	1.15	1.17	0.87	1.08	1.04
			0264	V	SL	Teeth	2.01	1.90	1.72	1.88	1.43	1.23	1.37	1.34
			0265	V	SL	Pedicle Foramen	0.81	0.65	*	0.73	0.87	0.51	*	0.69
			0266	V	SL	Muscle Scars	1.40	1.31	1.55	1.42	0.88	0.64	0.58	0.70
			0267	V	PL	Non-specialised	-0.47	-0.37	-0.54	-0.46	-0.17	-0.33	-0.4	-0.30
		3	0398	D	SL	Loop	1.93	*	*	1.93	0.98	*	*	0.98
			0399	D	SL	Non-specialised	2.04	2.04	2.29	2.12	0.81	1.00	1.24	1.02
			0400	D	SL	Muscle Scars	1.99	2.18	2.13	2.10	0.97	1.22	1.05	1.08
			0401	D	SL	Cardinal Process	1.08	1.23	1.18	1.16	0.60	1.07	1.08	0.92
			0402	D	PL	Non-specialised	0.56	0.24	0.28	0.36	0.65	0.14	0.27	0.35
			0403	V	SL	Non-specialised	2.08	2.03	2.03	2.04	1.50	1.30	1.19	1.33

(Continued on next page)

Species	Location	Specimen	Sample no.	Valve	Layer	Area	$\delta^{13}C$ VPDB				$\delta^{18}O$ VPDB			
							1	2	3	Mean	1	2	3	Mean
			0404	V	SL	Teeth	2.05	2.00	1.93	1.99	1.16	1.28	1.24	1.23
			0405	V	SL	Pedicle Foramen	1.45	1.40	0.99	1.28	1.40	1.23	1.26	1.30
			0406	V	SL	Muscle Scars	1.97	1.97	1.87	1.94	1.03	1.31	1.38	1.24
			0407	V	PL	Non-specialised	-0.53	-0.81	-0.38	-0.58	-0.25	-0.64	-0.10	-0.33
		4	0408	D	SL	Loop	1.51	*	*	1.51	1.57	*	*	1.57
			0409	D	SL	Non-specialised	1.75	1.69	1.70	1.71	1.17	1.26	1.18	1.20
			0410	D	SL	Muscle Scars	1.26	1.17	1.11	1.18	1.27	1.15	0.92	1.11
			0411	D	SL	Cardinal Process	0.72	0.66	*	0.69	1.04	1.12	*	1.08
			0412	D	PL	Non-specialised	-1.12	-1.44	-1.46	-1.34	-0.82	-0.79	-0.85	-0.82
			0413	V	SL	Non-specialised	1.31	1.31	1.20	1.27	0.99	1.18	0.96	1.04
			0414	V	SL	Teeth	1.59	1.41	1.28	1.43	1.14	1.09	1.09	1.11
			0415	V	SL	Pedicle Foramen	1.02	1.25	0.96	1.08	0.73	1.76	1.29	1.26
			0416	V	SL	Muscle Scars	0.55	0.52	0.51	0.53	0.67	1.24	1.14	1.02
			0417	V	PL	Non-specialised	-1.47	-1.21	-1.30	-1.33	-0.65	-0.50	-0.40	-0.52
		5	0558	D	SL	Loop	1.51	1.29	1.65	1.48	1.25	1.01	1.39	1.21
			0559	D	SL	Non-specialised	1.67	1.66	1.53	1.62	1.14	1.12	0.47	0.91
			0560	D	SL	Muscle Scars	1.38	1.18	1.44	1.33	1.18	1.00	1.33	1.17
			0561	D	SL	Cardinal Process	1.05	0.89	1.32	1.09	1.09	1.05	0.94	1.03
			0562	D	PL	Non-specialised	0.07	-0.11	-0.21	-0.08	0.17	-0.08	-0.59	-0.17
			0563	V	SL	Non-specialised	1.85	1.73	1.71	1.76	1.32	1.20	0.99	1.17
			0564	V	SL	Teeth	1.80	1.67	1.84	1.77	1.28	1.29	1.20	1.26
			0565	V	SL	Pedicle Foramen	1.48	1.46	*	1.47	1.16	1.22	*	1.19

(Continued on next page)

Species	Location	Specimen	Sample no.	Valve	Layer	Area	$\delta^{13}C$ VPDB				$\delta^{18}O$ VPDB			
							1	2	3	Mean	1	2	3	Mean
			0566	V	SL	Muscle Scars	0.91	0.99	1.08	**0.99**	0.89	1.19	1.20	**1.09**
			0567	V	PL	Non-specialised	-0.42	-0.55	-0.25	**-0.41**	-0.53	-0.23	0.11	**-0.22**
		6	0568	D	SL	Loop	1.55	*	*	**1.55**	1.29	*	*	**1.29**
			0569	D	SL	Non-specialised	1.73	1.75	1.81	**1.76**	1.10	1.21	1.41	**1.24**
			0570	D	SL	Muscle Scars	1.75	1.81	0.81	**1.46**	1.01	0.84	1.13	**0.99**
			0571	D	SL	Cardinal Process	0.74	0.84	1.07	**0.88**	0.90	0.86	0.73	**0.83**
			0572	D	PL	Non-specialised	-1.03	-1.41	-1.44	**-1.29**	-0.51	-1.08	-1.16	**-0.92**
			0573	V	SL	Non-specialised	1.50	1.43	1.60	**1.51**	1.15	1.08	1.02	**1.09**
			0574	V	SL	Teeth	1.39	0.88	1.50	**1.26**	0.95	0.74	0.74	**0.81**
			0575	V	SL	Pedicle Foramen	0.84	0.80	0.72	**0.78**	1.01	0.96	0.97	**0.98**
			0576	V	SL	Muscle Scars	1.21	1.24	1.22	**1.22**	1.11	1.13	1.08	**1.11**
			0577	V	PL	Non-specialised	-1.62	-1.47	-1.97	**-1.69**	-0.84	-0.71	-1.53	**-1.03**
		7	0698	D	SL	Loop	1.61	1.46	1.92	**1.66**	1.01	0.77	1.21	**1.00**
			0699	D	SL	Non-specialised	2.39	2.31	2.57	**2.42**	1.23	0.67	1.16	**1.02**
			0700	D	SL	Muscle Scars	1.87	2.07	2.32	**2.09**	0.90	1.05	1.55	**1.16**
			0701	D	SL	Cardinal Process	0.94	1.23	1.44	**1.21**	0.38	0.93	1.23	**0.85**
			0702	D	PL	Non-specialised	-1.43	-1.26	-1.35	**-1.35**	-0.91	-0.67	-0.72	**-0.76**
			0703	V	SL	Non-specialised	2.36	2.38	2.59	**2.44**	0.52	0.68	1.02	**0.74**
			0704	V	SL	Teeth	1.85	1.81	1.99	**1.88**	0.78	0.94	0.95	**0.89**
			0705	V	SL	Pedicle Foramen	1.43	1.50	*	**1.46**	0.93	1.08	*	**1.01**
			0706	V	SL	Muscle Scars	2.05	2.12	2.26	**2.14**	0.98	1.10	1.28	**1.12**
			0707	V	PL	Non-specialised	-1.37	-0.65	-0.98	**-1.00**	-0.78	-0.38	-0.40	**-0.52**

(Continued on next page)

Species	Location	Specimen	Sample no.	Valve	Layer	Area	$\delta^{13}C$ VPDB				$\delta^{18}O$ VPDB			
							1	2	3	Mean	1	2	3	Mean
		8	0708	D	SL	Loop	1.73	*	*	1.73	1.18	*	*	1.18
			0709	D	SL	Non-specialised	2.17	2.22	2.33	2.24	0.80	0.69	1.12	0.87
			0710	D	SL	Muscle Scars	1.36	1.43	*	1.39	0.96	1.88	*	1.42
			0711	D	SL	Cardinal Process	1.38	1.44	*	1.41	1.03	1.22	*	1.13
			0712	D	PL	Non-specialised	-1.64	-1.43	-1.29	-1.45	-0.75	-0.49	-0.54	-0.59
			0713	V	SL	Non-specialised	2.16	2.23	2.21	2.20	0.88	0.87	1.10	0.95
			0714	V	SL	Teeth	1.94	1.75	1.90	1.86	1.02	0.99	1.03	1.01
			0715	V	SL	Pedicle Foramen	1.64	1.55	*	1.59	0.86	1.11	*	0.98
			0716	V	SL	Muscle Scars	1.81	1.73	*	1.77	0.91	1.27	*	1.09
			0717	V	PL	Non-specialised	-1.94	-1.90	1.72	-0.71	-0.93	-0.90	1.07	-0.25
		9	0978	D	SL	Loop	1.66	1.54	1.64	1.61	-0.29	1.55	1.19	0.82
			0979	D	SL	Non-specialised	1.53	1.51	*	1.52	1.03	0.85	*	0.94
			0980	D	SL	Muscle Scars	0.95	1.05	*	1.00	1.17	0.82	*	0.99
			0981	D	SL	Cardinal Process	0.88	0.76	*	0.82	1.23	1.16	*	1.20
			0982	D	PL	Non-specialised	-1.89	-1.69	-1.69	-1.76	-0.89	-0.49	-0.70	-0.69
			0983	V	SL	Non-specialised	1.28	1.19	1.07	1.18	1.18	1.10	0.69	0.99
			0984	V	SL	Teeth	0.93	0.63	0.67	0.74	1.18	0.77	0.76	0.90
			0985	V	SL	Pedicle Foramen	0.93	0.81	*	0.87	1.25	0.97	*	1.11
			0986	V	SL	Muscle Scars	0.96	0.71	*	0.83	1.40	0.77	*	1.08
			0987	V	PL	Non-specialised	-2.46	-2.44	-2.60	-2.50	-0.70	-0.67	-1.24	-0.87
		10	0988	D	SL	Loop	1.48	1.45	*	1.47	1.11	1.13	*	1.12
			0989	D	SL	Non-specialised	2.28	1.98	1.90	2.05	1.33	1.11	0.88	1.11

(Continued on next page)

Species	Location	Specimen	Sample no.	Valve	Layer	Area	$\delta^{13}C$ VPDB				$\delta^{18}O$ VPDB			
							1	2	3	Mean	1	2	3	Mean
			0990	D	SL	Muscle Scars	2.16	2.14	2.01	**2.10**	0.81	1.31	0.83	**0.98**
			0991	D	SL	Cardinal Process	0.17	1.18	*	**0.67**	0.64	1.14	*	**0.89**
			0992	D	PL	Non-specialised	0.04	0.52	0.05	**0.20**	0.41	0.43	0.39	**0.41**
			0993	V	SL	Non-specialised	2.00	2.25	1.89	**2.05**	1.21	0.44	0.66	**0.77**
			0994	V	SL	Teeth	2.22	1.99	2.11	**2.11**	1.60	1.50	0.99	**1.36**
			0995	V	SL	Pedicle Foramen	1.49	1.58	1.34	**1.47**	1.27	1.38	0.67	**1.11**
			0996	V	SL	Muscle Scars	1.10	0.91	*	**1.01**	1.22	0.85	*	**1.03**
			0997	V	PL	Non-specialised	-0.50	-0.38	-0.08	**-0.32**	0.07	-0.05	0.40	**0.14**
Liothyrella uva	Signy Island	1	0738	D	TL	Loop	1.26	*	*	**1.26**	2.80	*	*	**2.80**
	Antarctica		0739	D	TL	Non-specialised	-0.72	*	*	**-0.72**	2.67	*	*	**2.67**
			0740	D	TL	Muscle Scars	-0.93	*	*	**-0.93**	2.92	*	*	**2.92**
			0741	D	TL	Cardinal Process	-0.10	0.82	*	**0.36**	3.02	3.63	*	**3.33**
			0742	D	PL	Non-specialised	-3.95	*	*	**-3.95**	0.68	*	*	**0.68**
			0743	V	TL	Non-specialised	-0.25	*	*	**-0.25**	2.82	*	*	**2.82**
			0744	V	TL	Teeth	0.89	1.05	*	**0.97**	2.93	3.30	*	**3.11**
			0745	V	TL	Pedicle Foramen	-1.48	*	*	**-1.48**	2.54	*	*	**2.54**
			0746	V	TL	Muscle Scars	0.84	*	*	**0.84**	2.54	*	*	**2.54**
			0747	V	PL	Non-specialised	-3.75	*	*	**-3.75**	0.86	*	*	**0.86**
		2	0748	D	TL	Loop	0.78	*	*	**0.78**	3.26	*	*	**3.26**
			0749	D	TL	Non-specialised	-1.46	*	*	**-1.46**	2.29	*	*	**2.29**
			0750	D	TL	Muscle Scars	-1.99	*	*	**-1.99**	2.55	*	*	**2.55**
			0751	D	TL	Cardinal Process	0.19	*	*	**0.19**	3.42	*	*	**3.42**

(Continued on next page)

Species	Location	Specimen	Sample no.	Valve	Layer	Area	$\delta^{13}C$ VPDB				$\delta^{18}O$ VPDB			
							1	2	3	Mean	1	2	3	Mean
			0752	D	PL	Non-specialised	-4.26	*	*	-4.26	0.26		*	0.26
			0753	V	TL	Non-specialised	-0.79	-0.81		-0.80	2.46	2.46		2.46
			0754	V	TL	Teeth	0.65	0.68	0.87	0.80	3.22	2.96	3.16	3.11
			0755	V	TL	Pedicle Foramen	-0.61	*	*	-0.61	3.05	*	*	3.05
			0756	V	TL	Muscle Scars	-0.85	-1.04	-0.48	-0.79	2.45	2.69	2.55	2.56
			0757	V	PL	Non-specialised	-4.95	-5.23	-4.73	-4.97	0.59	0.45	0.40	0.48
		3	0798	D	TL	Loop	1.38	1.04	0.94	1.12	3.70	3.26	3.03	3.33
			0799	D	TL	Non-specialised	-0.45	-0.55	-0.79	-0.60	2.65	2.65	1.81	2.37
			0800	D	TL	Muscle Scars	-1.07	-1.33	-1.33	-1.25	3.50	3.40	2.67	3.19
			0801	D	TL	Cardinal Process	0.55	0.37	0.25	0.39	3.70	3.69	3.18	3.52
			0802	D	PL	Non-specialised	-3.55	-3.10	*	-3.32	1.46	0.70	*	1.08
			0803	V	TL	Non-specialised	-2.13	-2.34	-2.37	-2.28	1.97	1.55	1.05	1.52
			0804	V	TL	Teeth	-0.72	0.45	0.42	0.05	3.23	2.97	2.48	2.89
			0805	V	TL	Pedicle Foramen	-0.93	-1.04	-1.12	-1.03	3.14	3.22	2.73	3.03
			0806	V	TL	Muscle Scars	-1.80	-1.80	*	-1.80	2.70	2.78	*	2.74
			0807	V	PL	Non-specialised	-4.04	-4.22	-4.24	-4.16	0.97	0.61	0.43	0.67
		4	0808	D	TL	Loop	1.23	*	*	1.23	3.52	*	*	3.52
			0809	D	TL	Non-specialised	1.56	*	*	1.56	3.68	*	*	3.68
			0810	D	TL	Muscle Scars	0.25	*	*	0.25	3.63	*	*	3.63
			0811	D	TL	Cardinal Process	0.71	*	*	0.71	3.61	*	*	3.61
			0812	D	PL	Non-specialised	-3.21	*	*	-3.21	1.36	*	*	1.36
			0813	V	TL	Non-specialised	1.05	0.81	*	0.93	2.98	2.17	*	2.57

(Continued on next page)

Species	Location	Specimen	Sample no.	Valve	Layer	Area	$\delta^{13}C$ VPDB				$\delta^{18}O$ VPDB			
							1	2	3	Mean	1	2	3	Mean
			0814	V	TL	Teeth	0.64	*	*	0.64	3.31	*	*	3.31
			0815	V	TL	Pedicle Foramen	-0.56	-0.51	*	-0.53	3.46	3.07	*	3.27
			0816	V	TL	Muscle Scars	1.13	*	*	1.13	3.51	*	*	3.51
			0817	V	PL	Non-specialised	-4.28	*	*	-4.28	0.42	*	*	0.42
		5	0818	D	TL	Loop	0.96	1.21	1.28	1.15	3.19	3.12	3.04	3.12
			0819	D	TL	Non-specialised	0.84	0.32	0.51	0.56	3.10	2.04	2.49	2.54
			0820	D	TL	Muscle Scars	-0.35	*	*	-0.35	3.20	*	*	3.20
			0821	D	TL	Cardinal Process	0.70	*	*	0.70	3.65	*	*	3.65
			0822	D	PL	Non-specialised	-1.93	*	*	-1.93	2.05	*	*	2.05
			0823	V	TL	Non-specialised	0.72	0.11	0.07	0.30	2.62	2.12	2.29	2.34
			0824	V	TL	Teeth	1.66	1.24	0.72	1.21	3.76	3.24	2.54	3.18
			0825	V	TL	Pedicle Foramen	-1.00	*	*	-1.00	3.19	*	*	3.19
			0826	V	TL	Muscle Scars	-0.53	*	*	-0.53	3.34	*	*	3.34
			0827	V	PL	Non-specialised	-2.79	*	*	-2.79	1.80	*	*	1.80
		6	0828	D	TL	Loop	1.03	1.27	1.06	1.12	3.55	2.76	3.21	3.17
			0829	D	TL	Non-specialised	0.10	*	*	0.10	2.43	*	*	2.43
			0830	D	TL	Muscle Scars	0.26	*	*	0.26	3.75	*	*	3.75
			0831	D	TL	Cardinal Process	0.71	*	*	0.71	3.67	*	*	3.67
			0832	D	PL	Non-specialised	-3.60	*	*	-3.60	1.15	*	*	1.15
			0833	V	TL	Non-specialised	-0.16	*	*	-0.16	2.84	*	*	2.84
			0834	V	TL	Teeth	0.46	0.36	0.14	0.32	2.88	2.22	1.90	2.33
			0835	V	TL	Pedicle Foramen	-0.85	-1.32	*	-1.09	3.11	2.05	*	2.58

(Continued on next page)

Species	Location	Specimen	Sample no.	Valve	Layer	Area	$\delta^{13}C$ VPDB				$\delta^{18}O$ VPDB			
							1	2	3	Mean	1	2	3	Mean
			0836	V	TL	Muscle Scars	-0.25	*	*	-0.25	3.01	*	*	3.01
			0837	V	PL	Non-specialised	-3.99	*	*	-3.99	0.82	*	*	0.82
		7	0858	D	TL	Loop	1.40	*	*	1.40	3.36	*	*	3.36
			0859	D	TL	Non-specialised	1.55	*	*	1.55	3.58	*	*	3.58
			0860	D	TL	Muscle Scars	0.50	*		0.50	3.49	*	*	3.49
			0861	D	TL	Cardinal Process	1.29	*	*	1.29	3.97	*	*	3.97
			0862	D	PL	Non-specialised	-1.50	*	*	-1.50	2.38	*	*	2.38
			0863	V	TL	Non-specialised	1.25	1.03	*	1.14	3.33	2.81	*	3.07
			0864	V	TL	Teeth	1.21	*	*	1.21	3.38	*	*	3.38
			0865	V	TL	Pedicle Foramen	-0.67	*	*	-0.67	3.19	*	*	3.19
			0866	V	TL	Muscle Scars	1.22	*	*	1.22	3.12	*	*	3.12
			0867	V	PL	Non-specialised	-2.73	*	*	-2.73	1.53	*	*	1.53
		8	0868	D	TL	Loop	1.51	*	*	1.51	3.52	*	*	3.52
			0869	D	TL	Non-specialised	1.39	*	*	1.39	3.25	*	*	3.25
			0870	D	TL	Muscle Scars	0.43	*	*	0.43	3.51	*		3.51
			0871	D	TL	Cardinal Process	0.85	*	*	0.85	3.33	*	*	3.33
			0872	D	PL	Non-specialised	-2.47	*	*	-2.47	1.85	*	*	1.85
			0873	V	TL	Non-specialised	1.27	*	*	1.27	3.18	*	*	3.18
			0874	V	TL	Teeth	1.24	*	*	1.24	3.37	*	*	3.37
			0875	V	TL	Pedicle Foramen	0.01	*	*	0.01	3.25	*	*	3.25
			0876	V	TL	Muscle Scars	1.27	*	*	1.27	3.65	*	*	3.65
			0877	V	PL	Non-specialised	-3.83	*	*	-3.83	0.93	*	*	0.93

(Continued on next page)

Species	Location	Specimen	Sample no.	Valve	Layer	Area	$\delta^{13}C$ VPDB				$\delta^{18}O$ VPDB			
							1	2	3	Mean	1	2	3	Mean
		9	1036	D	TL	Loop	1.26	0.93	*	1.09	3.78	3.11	*	3.45
			1037	D	TL	Non-specialised	0.30	0.08	*	0.19	2.98	1.85	*	2.41
			1038	D	TL	Muscle Scars	-0.81	-0.07	*	-0.44	3.63	3.14	*	3.39
			1039	D	TL	Cardinal Process	0.53	0.20	*	0.37	3.76	2.50	*	3.13
			1040	D	PL	Non-specialised	-0.94	-0.71	*	-0.83	2.22	2.46	*	2.34
			1041	V	TL	Non-specialised	-0.83	-0.18	-0.71	-0.57	2.39	2.09	1.97	2.15
			1042	V	TL	Teeth	1.21	0.98	1.02	1.07	3.41	2.82	2.81	3.01
			1043	V	TL	Pedicle Foramen	0.63	0.57	*	0.60	3.17	2.89	*	3.03
			1044	V	TL	Muscle Scars	-0.57	-0.21	*	-0.39	2.73	2.35	*	2.54
			1045	V	PL	Non-specialised	-1.65	*	*	-1.65	1.56	*	*	1.56
		10	1046	D	TL	Loop	1.23	1.15	1.46	1.28	3.28	3.21	3.28	3.26
			1047	D	TL	Non-specialised	-0.87	-1.01	-0.62	-0.84	2.21	1.87	2.42	2.16
			1048	D	TL	Muscle Scars	-1.11	-1.31	*	-1.21	2.90	2.61	*	2.75
			1049	D	TL	Cardinal Process	0.64	0.62	*	0.63	3.14	3.48	*	3.31
			1050	D	PL	Non-specialised	-1.57	*	*	-1.57	1.66	*	*	1.66
			1051	V	TL	Non-specialised	-0.03	0.16	*	0.06	2.38	2.26	*	2.32
			1052	V	TL	Teeth	1.17	1.33	1.25	1.25	2.94	3.17	2.99	3.03
			1053	V	TL	Pedicle Foramen	-0.05	0.41	0.27	0.21	2.76	3.33	3.21	3.10
			1054	V	TL	Muscle Scars	-0.72	*	*	-0.72	2.61	*	*	2.61
			1055	V	PL	Non-specialised	-1.78	*	*	-1.78	2.07	*	*	2.07

Appendix D

$\delta^{18}O$ and $\delta^{13}C$ values

for

mollusc shell

analysis

δ18O and δ13C values from mollusc shell analysis

Species	Location	Specimen	Sample no.	Valve	Area	δ13C VPDB				δ18O VPDB			
						1	2	3	Mean	1	2	3	Mean
Modiolus modiolus	1. Firth of Lorne,	1	1056	L	Aragonite	-0.26	0.01	-0.24	**-0.16**	1.90	2.15	1.71	**1.92**
	Scotland		1057	L	Calcite	0.66	0.91	0.77	**0.78**	2.36	2.62	2.26	**2.41**
		2	1058	L	Aragonite	0.40	0.58	0.47	**0.48**	2.30	2.27	2.01	**2.19**
			1059	L	Calcite	0.54	0.80	0.68	**0.67**	2.38	2.53	2.51	**2.47**
		3	1060	L	Aragonite	0.66	0.70	0.60	**0.65**	2.34	2.18	2.00	**2.17**
-			1061	L	Calcite	0.19	0.34	0.12	**0.22**	2.70	2.51	2.47	**2.56**
		4	1062	L	Aragonite	-0.25	-0.18	-0.40	**-0.28**	2.09	2.10	1.77	**1.99**
			1063	L	Aragonite	0.43	0.46	0.41	**0.43**	2.95	2.69	2.57	**2.74**
		5	1064	L	Aragonite	-0.43	-0.31	-0.40	**-0.38**	2.35	2.19	1.96	**1.96**
			1065	L	Calcite	0.94	0.95	0.85	**0.91**	2.98	2.66	2.54	**2.72**
		6	1066	R	Aragonite	-0.31	-0.39	-0.24	**-0.31**	2.47	2.21	2.14	**2.27**
			1067	R	Calcite	0.51	0.39	0.56	**0.49**	2.67	2.46	2.41	**2.51**
		7	1068	R	Aragonite	0.17	-0.02	0.22	**0.12**	2.27	2.22	2.17	**2.22**
			1069	R	Calcite	0.54	0.38	0.44	**0.45**	2.63	2.50	2.13	**2.42**
		8	1070	R	Aragonite	-0.29	-0.45	-0.46	**-0.40**	2.36	2.26	1.72	**2.11**
			1071	R	Calcite	0.25	0.06	0.21	**0.17**	2.77	2.59	2.42	**2.59**
		9	1072	R	Aragonite	-0.79	-0.82	-1.02	**-0.88**	2.23	2.14	1.92	**2.10**

Continued on next page)

$\delta^{18}O$ and $\delta^{13}C$ values from mollusc shell analysis

Species	Location	Specimen	Sample no.	Valve	Area	$\delta^{13}C$ VPDB				$\delta^{18}O$ VPDB			
						1	2	3	Mean	1	2	3	Mean
			1073	R	Calcite	0.73	0.51	0.65	**0.63**	2.64	2.46	2.14	**2.42**
		10	1074	R	Aragonite	0.01	-0.16	-0.09	**-0.08**	2.38	2.18	2.11	**2.22**
			1075	R	Calcite	0.74	0.58	0.51	**0.61**	2.75	2.55	2.16	**2.49**

Glossary

Glossary

Adductor muscles: muscles which close the valves. They leave a pair of muscle scars in the ventral valve and two pairs in the dorsal valve.

Articulated: valves are articulated by a hinge mechanism.

Astrophic: shell with posterior margin not parallel with hinge axis.

Brachial valve: see dorsal valve.

Brachidium: (plural brachia) a calcareous support for the lophophore in some groups of articulate brachiopods. it is usually loop shaped.

Cardinalia: structures of secondary shell in prosteromedian region of the dorsal valve, associated with articulation, support of lophophore, and muscle attachment; include for example, cardinal process, socket ridges, crural bases, and their accessory plates

Cardinal process: a knobbly projection of secondary shell situated medially at the posterior end of the dorsal valve. Serves for separation or attachment of paired diductor muscles.

Commissure: line of junction between edges or margins of valves.

Crura: (singular crus) paired processes extending from the posterior end of the dorsal valve to support the lophophore.

Delthyrium: a triangular gap along the hinge line of the ventral valve, through which the pedicle emerges.

Delthyrium plates: two plates growing medially from the margins of the delthyrium, partly or completely closing it.

Diductor muscles: muscles serving to open the valves of articulated brachiopods. There are two pairs which run from the floor of the ventral valve to the cardinal process in the dorsal valve.

Dorsal valve: also known as the brachial valve, normally the smaller valve to which the brachidium is attached.

Endopunctate: the shell structure is penetrated from the inside by large regularly arranged, elongated cavities known as puncta.

Fold: major elevation of valve surface, externally convex in transverse profile and radial from umbo.

Hinge: articulation mechanism.

Hinge axis: line joining the points of articulation about which the valves rotate when they are opening or closing.

Impunctate: has no perforations or cavities within the shell structure.

Inarticulated: valves are not articulated by a hinge mechanism.

Loop: attached to the dorsal valve, secondary or tertiary shell support for the lophophore.

Lophophore: the feeding and respiratory organ with tentacles, symmetrically disposed around the mouth, and typically suspended from the anterior body wall, but may be attached to to dorsal mantle; occupies the mantle cavity.

Muscle scars: the impressions or elevations on the inside of the valves which mark the areas of attachment of the adductor, diductor and pedicle muscles.

Pedicle: the stalk by which the brachiopod is attached to the substrate.

Pedicle foramen: subcircular or circular opening in the shell through which the pedicle passes.

Pedicle opening: see pedicle foramen.

Pedicle valve: see ventral valve.

Periostracum: organic external layer of the shell secreted by the outer mantle lobe.

Plectolophous: lophophore in which each brachidium consists of a U-shaped bearing a double row of paired tentacles but terminating distally in medially placed planospire normal to commissural plane and bearing a single row of paired tentacles.

Posterior margin: posterior part of the junction between the edges of the valves; may be hinge line or posterior margin.

Primary layer: outer mineralised shell layer immediately beneath the periostracum, deposited by vesicular cells of the outer mantle lobe.

Pseudopunctate: has conical deflections of the secondary layer, which appear to be punctae on the internal surface.

Ptycholophe: lophophore with brachia folded into one or more lobes in addition to median indentation.

Secondary layer: shell deposited by a layer of the outer epithelium within the circumferential lobes of the mantle and consisting of fibres or laminae that are ensheathed in interconnecting membranes.

Septum: relatively long narrow and central elevation of secondary shell, usually bladelike.

Sockets: pits in the posterior margin of the dorsal valve for reception of the teeth.

Spicules: small irregular bodies of calcite secreted by scleroblasts within connective tissue of the mantle and lophophore.

Spirolophous: lophophore in which brachia are spirally coiled and bear a single row of paired tentacles.

Sulcus: major depression of valve surface, externally concave in transverse and radial from umbo.

Teeth: two principle articulating process on the ventral valve that articulate with the sockets on the dorsal valve.

Tertiary layer: continuous layer of prismatic shell secreted by outer epithelium underlying the secondary layer and forming the internal surface.

Umbo: apical portion of either valve around the beak.

Ventral valve : also known as the pedicle valve, the valve by which the brachiopod is attached to a substrate either by a pedicle or by cementation.

List of references

List of references

ADKINS, J. F., BOYLE, E. A., CURRY, W. B. & LUTRINGER, A. 2003. Stable isotopes in deep-sea corals and a new mechanism for "vital effects". *Geochimica et Cosmochimica Acta.* **67,** 1129-1143.

AHARON, P. 1991. Recorders of reef environment histories: stable isotopes in corals, giant clams, and calcareous algae. *Coral Reefs.* **10,** 71-90.

AL-ASSAM, I. & VEIZER, J. 1982. Chemical stabilisation of low-Mg calcite: An example of brachiopods. *Journal of Sedimentary Petrology.* **52,** 1101-1109.

ANDERSON, T. F. & ARTHUR, M. A. 1983. Stable isotopes of oxygen and carbon and their application to sedimentologic and paleoenvironmental problems. *In*: M.A. ARTHUR, T.F. ANDERSON, I.R. KAPLAN, J. VEIZER & L.S. LAND (eds.), *Stable Isotopes in Sedimentary Geology, SEPM Short Course Notes No 10.* Society of Economic Paleontologists and Mineralologists, Tulsa, Oklahoma, 1-151.

AUCLAIR, A.-C., JOACHIMSKI, M. M. & LÉCUYER, C. 2003. Deciphering kinetic, metabolic and environmental controls on stable isotope fractionations between seawater and the shell of *Terebratalia transversa* (Brachiopoda). *Chemical Geology.* **202,** 59-78.

AZMY, K. 1998. Oxygen and carbon isotopic composition of Silurian brachiopods: Implications for coeval seawater and glaciations. *Geological Society of America Bulletin.* **110,** 1499-1512.

BARBER, P. L., DOBSON, M. R. & WHITTINGTON, R. J. 1979. The geology of the Firth of Lorne, as determined by seismic and live sampling methods. *Scottish Journal of Geology.* **15,** 217-230.

BARRERA, E., TEVESZ, M. J., CARTER, J. G. & MCCALL, P. L. 1994. Oxygen and carbon isotopic composition and shell mictostructure of the bivalve *Laternula elliptica* from Antarctica. *Palaios.* **9,** 275-287.

BATES, N. R. & BRAND, U. 1991. Environmental and physiological influences on isotopic and elemental compositions of brachiopod shell carbonate. Implications for the isotopic evolution of Paleozoic oceans. *Chemical Geology*. **94,** 67-78.

BERNER, R. A. 1989. A model for atmospheric CO_2 over Phanerozoic time. *American Journal of Science*. **291,** 339-376.

BLACK, R. M. 1970. *The Elements of Palaeontology*. Cambridge University Press, Cambridge.

BODC. 2003. British Oceanographic Data Centre. http://www.bodc.ac.uk

BÖHM, F., JOACHIMSKI, M. M., DULLO, W.-C., EISENHAUER, A., LEHNERT, H., REITNER, J. & WÖRHEIDE, G. 2000. Oxygen isotope fractionation in marine aragonite of coralline sponges. *Geochimica et Cosmochimica Acta*. **64,** 1695-1703.

BRAND, U. 1989a. Biogeochemistry of Late Paleozoic North American brachiopods and secular variation of seawater composition. *Biogeochemistry*. **7,** 159-193.

BRAND, U. 1989b. Global climatic changes during the Devonian-Mississippian: Stable isotope biogeochemistry of brachiopods. *Palaeogeography, Palaeoclimatology, Palaeoecology*. **75,** 175-191.

BRAND, U., LOGAN, A., HILLER, N. & RICHARDSON, J. 2003. Geochemistry of modern brachiopods: applications and implications for oceanography and paleoceanography. *Chemical Geology*. **198,** 305-334.

BRENCHLEY, P. J., CARDEN, G. A. F. & MARSHALL, J. D. 1995. Environmental changes associated with the "first strike" of late Ordovician mass extinction. *Modern Geology*. **20,** 69-82.

BROECKER, W. S. 1989. The salinity contrast between the Atlantic and Pacific Oceans during glacial time. *Paleoceanography*. **4,** 207-212.

BUCHARDT, B. & SIMONARSON, L. A. 2003. Isotope palaeotemperatures from the Tjörnes beds in Iceland: evidence of Pliocene cooling. *Palaeogeography, Palaeoclimatology, Palaeoecology*. **189,** 71-95.

BUENING, N. 2001. Brachiopod shells: Recorders of the present and keys to the past. *In*: S.J. CARLSON & M.R. SANDY (eds.), *The Paleontological Society Papers: Brachiopods Ancient and Modern, A Tribute to G. Arthur Cooper*. Volume 7. The Paleontological Society, 117-144.

BUENING, N., CARLSON, S. J., SPERO, H. J. & LEE, D. E. 1998. Evidence for the early Oligocene formation of a proto-subtropical convergence from oxygen isotope records of New Zealand Paleogene brachiopods. *Palaeogeography, Palaeoclimatology, Palaeoecology*. **138,** 43-68.

BUENING, N. & SPERO, H. J. 1996. Oxygen- and carbon-isotope analyses of the articulate brachiopod *Laqueus californianus*: a recorder of environmental changes in the subeuphotic zone. *Marine Biology*. **127,** 105-114.

CARPENTER, S. J. & LOHMANN, K. C. 1992. Sr/Mg ratios of modern marine calcite: Empirical indicators of ocean chemistry and precipitation rate. *Geochimica et Cosmochimica Acta*. **56,** 1837-1849.

CARPENTER, S. J. & LOHMANN, K. C. 1995. $\delta^{18}O$ and $\delta^{13}C$ values of modern brachiopod shells. *Geochimica et Cosmochimica Acta*. **59,** 3749-3764.

CLARKE, A., HOLMES, L. J. & WHITE, M. G. 1988. The annual cycle of temperature, chlorophyll and major nutrients at Signy Island, South Orkney Islands, 1969-82. *British Antarctic Survey Bulletin*. **80,** 65-86.

CLARKSON, E. N. K. 1998. *Invertebrate Palaeontology and Evolution*. Blackwell Science, Oxford.

COMPSTON, W. 1960. The carbon isotopic compositions of certain marine invertebrates and coals from the Australian Permian. *Geochimica et Cosmochimica Acta*. **18,** 1-22.

COPLEN, T. B. 1995. New manuscript guidelines for the reporting of stable hydrogen, carbon and oxygen isotope-ratio data. *Geothermics*. **24,** 707-712.

CRAIG, H. 1957. Isotopic standards for carbon and oxygen and correction factors for mass-spectrometric analysis of carbon dioxide. *Geochimica et Cosmochimica Acta*. **12,** 133-149.

CRAIG, H. & GORDON, L. I. 1965. Deuterium and oxygen-18 variations in the ocean and the marine atmosphere. *In*: E. TONGIORGI (ed.), *Stable Isotopes in Oceanographic Studies and Paleotemperatures*, Spoleto 1965, 9-130.

CROWLEY, S. & TAYLOR, P. D. 2000. Stable isotope composition of modern bryozoan skeletal carbonate from the Otago Shelf, New Zealand. *New Zealand Journal of Marine and Freshwater Research*. **34,** 333-353.

CURRY, G. B. 1982. Ecology and population structure of the Recent brachiopod *Terebratulina* from Scotland. *Palaeontology*. **25,** 227-246.

CURRY, G. B. 1999. Original shell colouration in Late Pleistocene Terebratulid brachiopods from New Zealand. *Palaeontologica Electronica*. **2,** 32 pp.

CURRY, G. B. & FALLICK, A. E. 2002. Use of stable oxygen isotope determinations from brachiopods in palaeoenvironmental reconstruction. *Palaeogeography, Palaeoclimatology, Palaeoecology*. **182,** 133-143.

DESHAYES, D. P. 1839. Nouvelles espèces de mollusques provenant des côtes de la Californie, du Mexique, du Kamchatka, et de la nouvelle Zélande. *Review of the Zoological Society Curierienne*. **2,** 356-361.

DONNER, J. & NORD, A. G. 1986. Carbon and oxygen stable isotope values in shells of *Mytilus edulis* and *Modiolus modiolus* from Holocene raised beaches at the outer coast of the

Varanger peninsula, North Norway. *Palaeogeography, Palaeoclimatology, Palaeoecology.* **56,** 35-50.

DURRANCE, E. M. 1976. A gravity survey of Islay, Scotland. *Geological Magazine.* **113,** 251-261.

ELLIOT, M., DEMENOCAL, P. B., LINSLEY, B. K. & HOWE, S. S. 2003. Environmental controls on the stable isotopic composition of *Mercenaria mercenaria*: Potential application to paleoenvironmental studies. *Geochemistry Geophysics Geosystems.* **4.**

EPSTEIN, S., BUCHSBAUM, R., LOWENSTAM, H. A. & UREY, H. C. 1951. Carbonate-water isotopic temperature scale. *Bulletin of the Geological Society of America.* **62,** 417-426.

EPSTEIN, S., BUCHSBAUM, R., LOWENSTAM, H. A. & UREY, H. C. 1953. Revised carbonate-water isotopic temperature scale. *Bulletin of the Geological Society of America.* **64,** 1315-1326.

EPSTEIN, S. & MAYEDA, T. 1953. Variation of the O^{18} content of waters from natural sources. *Geochimica et Cosmochimica Acta.* **4,** 213-224.

EREZ, J. 1978. Vital effect on stable isotope compositions seen in foraminifera and coral skeletons. *Nature.* **273,** 199-202.

FAURE, G. 2001. *Principles of Isotope Geology.* John Wiley & Sons, Chichester.

FRIEDMAN, I. & O'NEIL, J. R. 1977. Compilation of stable isotope fractionation factors of geochemical interest. *In*: M. FLEISHER (ed.), *Data of Geochemistry, Chapter KK, Sixth Edition. United States Geological Survey Professional Paper 440-K.*

GAFFEY, S. J. & BRONNIMANN, C. E. 1993. Effects of bleaching on organic and mineral and mineral phases in biogenic carbonates. *Journal of Sedimentary Petrology.* **63,** 752-457.

GONFIANTINI, R., STICHLER, W. & ROZANSKI, K. 1995. Standards and intercomparison materials distributed by the International Atomic Energy Agency for stable isotope measurements. *In,* Reference and intercomparison materials for stable isotopes of light elements: International Atomic Energy Agency, TECDOC-825. 13-29

GONZALEZ, L. A. & LOHMANN, K. C. 1985. Carbon and oxygen isotopic composition of Holocene reefal carbonates. *Geology*. **13,** 811-814.

GROSSMAN, E. L. & KU, T.-L. 1986. Oxygen and carbon isotope fractionation in biogenic aragonite: temperature effects. *Chemical Geology*. **59,** 59-74.

GROSSMAN, E. L., MII, H.-S. & YANCEY, T. E. 1993. Stable isotopes in Late Pennsylvanian brachiopods from the United States: Implications for Carboniferous paleoceanography. *Geological Society of America Bulletin*. **105,** 1284-1296.

GROSSMAN, E. L., ZHANG, C. & YANCEY, T. E. 1991. Stable-isotope stratigraphy of brachiopods from Pennsylvanian shales in Texas. *Geological Society of America Bulletin*. **103,** 953-965.

HICKSON, J. A., JOHNSON, A. L. A., HEATON, T. H. E. & BALSON, P. S. 1999. The shell of the Queen Scallop *Aequipecten opercularis* (L.) as a promising tool for palaeoenvironmental reconstruction: evidence and reasons for equilibrium stable isotope incorporation. *Palaeogeography, Palaeoclimatology, Palaeoecology*. **154,** 325-337.

HOEFS, J. 1997. *Stable Isotope Geochemistry*. Springer, Berlin.

HOLGATE, N. 1969. Palaeozoic and Tertiary transcurrent movements on the Great Glen Fault. *Scottish Journal of Geology*. **5,** 97-139.

HONG, W., KEPPENS, E., NIELSEN, P. & VAN RIET, A. 1995. Oxygen and carbon isotope study of the Holocene oyster reefs and paleoenvironmental reconstruction on the northwest coast of Bohai Bay, China. *Marine Geology*. **124,** 289-302.

HORIBE, Y. & OBA, T. 1972. Temperature scales of aragonite -water and calcite-water systems. *Fossils*. **23/24,** 69-79.

JAMES, N. P., BONE, Y. & KYSER, T. K. 1997. Brachiopod $\delta^{18}O$ values do reflect ambient oceanography: Lacepede Shelf, southern Australia. *Geology*. **25,** 551-554.

JODC. 2001. Japanese Oceanographic Data Centre. http://www.jodc.jhd.go.jp

JOPE, H. M. 1965. Composition of brachiopod shell. *In*: R.C. MOORE (ed.), *Treatise on Invertebrate Paleontology. Part H. Brachiopoda.* The Geological Society of America and University of Kansas Press, Lawrence, Kansas, H159-H164.

KEITH, M. L. & WEBER, J. N. 1965. Systematic relationships between carbon and oxygen isotopes in carbonates deposited by modern corals and algae. *Science.* **150,** 498-501.

KHIM, B.-K., WOO, K. S. & JE, J.-G. 2000. Stable isotope profiles of bivalve shells: seasonal temperature variations, latitudinal temperature gradients and biological carbon cycling along the east coast of Korea. *Continental Shelf Research.* **20,** 843-861.

KIM, K. H., TANAKA, T., NAKAMURA, T., NAGAO, K., YOUN, J. S., KIM, K. R. & YUN, M. Y. 1999. Palaeoclimatic and chronostratigraphic interpretations from strontium, carbon and oxygen isotopic ratios in molluscan fossils of Quaternary Seoguipo and Shinyangri Formations, Cheju Island, Korea. *Palaeogeography, Palaeoclimatology, Palaeoecology.* **154,** 219-235.

KIM, S. T. & O'NEIL, J. R. 1997. Equilibrium and nonequilibrium effects in synthetic carbonates. *Geochimica et Cosmochimica Acta.* **61,** 3461-3475.

KLEIN, R. T., LOHMANN, K. C. & THAYER, C. W. 1996a. Bivalve skeletons record sea-surface temperature and $\delta^{18}O$ via Mg/Ca and $^{18}O/^{16}O$ ratios. *Geology.* **24,** 415-418.

KLEIN, R. T., LOHMANN, K. C. & THAYER, C. W. 1996b. Sr/Ca and $^{13}C/^{12}C$ ratios in skeletal calcite of *Mytilus trossulus:* Covariation with metabolic rate, salinity, and carbon isotopic composition of seawater. *Geochimica et Cosmochimica Acta.* **60,** 4207-4221.

KRANZ, D. E., WILLIAMS, D. F. & JONES, D. S. 1987. Ecological and palaeoenvironmental information using stable isotope profiles from living and fossil molluscs. *Palaeogeography, Palaeoclimatology, Palaeoecology.* **58,** 249-266.

KROOPNICK, P. M. 1985. The distribution of ^{13}C of ΣCO_2 in world oceans. *Deep-Sea Research.* **32,** 57-84.

KUMP, L. R. & ARTHUR, M. A. 1999. Interpreting carbon-isotope excursions: carbon and organic matter. *Chemical Geology*. **161,** 181-198.

KUMP, L. R., KASTING, J. F. & CRANE, R. G. 1999. *The Earth System*. Prentice Hall, Inc, New Jersey.

LÉCUYER, C., REYNARD, B. & MARTINEAU, F. M. in press. Stable isotope fractionation between mollusc shells and marine waters from Martinique Island. *Chemical Geology*. **2004,** in press.

LEPZELTER, C. G., ANDERSON, T. F. & SANDBERG, P. A. 1983. Stable isotope variations in modern articulate brachiopods. *American Association of Petroleum Geologists Bulletin*. **67,** 500-501.

LONG, D. G. F. 1993. Oxygen and carbon isotopes and event stratigraphy near the Ordovician-Silurian boundary, Anticosti island, Quebec. *Palaeogeography, Palaeoclimatology, Palaeoecology*. **104,** 43-59.

LOVE, K. M. & WORONOW, A. 1991. Chemical changes induced in aragonite using treatments for the destruction of organic material. *Chemical Geology*. **93,** 291-301.

LOWENSTAM, H. A. 1961. Mineralogy, O^{18}/O^{16} ratios, and strontium and magnesium contents of recent and fossil brachiopods and their bearing on the history of the oceans. *The Journal of Geology*. **69,** 241-260.

MACKINNON, D. I. & WILLIAMS, A. 1974. Shell structure of terebratulid brachiopods. *Palaeontology*. **17,** 179-202.

MARGOSIAN, A., TAN, F. C., CAI, D. & MANN, K. H. 1987. Seawater temperature records from stable isotopic profiles in the shell of *Modiolus modiolus*. *Estuarine, Coastal and Shelf Science*. **25,** 81-89.

MARSHALL, J. D., BRENCHLEY, P. J., MASON, P., WOLFF, G. A., ASTINI, R. A., HINTS, L. & MEIDLA, T. 1997. Global carbon isotopic events associated with mass extinction and

glaciation in the late Ordovician. *Palaeogeography, Palaeoclimatology, Palaeoecology.* **132,** 195-210.

MARSHALL, J. D. & MIDDLETON, P. D. 1990. Changes in marine isotopic composition and the late Ordovician glaciation. *Journal of the Geological Society, London.* **147,** 1-4.

MARSHALL, J. D., PIRRIE, D., CLARKE, A., NOLAN, C. P. & SHARMAN, J. 1996. Stable-isotopic composition of skeletal carbonates from living Antarctic marine invertebrates. *Lethaia.* **29,** 203-212.

M^{C}CONNAUGHEY, T. A. 1989a. ^{13}C and ^{18}O isotopic disequilibrium in biological carbonates: I. Patterns. *Geochimica et Cosmochimica Acta.* **53,** 151-162.

M^{C}CONNAUGHEY, T. A. 1989b. ^{13}C and ^{18}O isotopic disequilibrium in biological carbonates: II. *In vitro* simulation of kinetic isotope effects. *Geochimica et Cosmochimica Acta.* **53,** 163-171.

M^{C}CONNAUGHEY, T. A., BURDETT, J., WHELAN, J. F. & PAULL, C. K. 1997. Carbon isotopes in biological carbonates: Respiration and photosynthesis. *Geochimica et Cosmochimica Acta.* **61,** 611-622.

M^{C}CREA, J. M. 1950. On the isotopic chemistry of carbonates and a paleotemperature scale. *The Journal of Chemical Physics.* **18,** 849-857.

M^{C}KINNEY, C. R., M^{C}CREA, J. M., EPSTEIN, S., ALLEN, H. A. & UREY, H. C. 1950. Improvements in mass spectrometers for the measurements of small differences in isotope abundance ratios. *Reviews of Scientific Instruments.* **21,** 724-730.

MII, H.-S., GROSSMAN, E. L., YANCEY, T. E., CHUVASHOV, B. & ERGOROV, A. 2001. Isotopic records of brachiopod shells from the Russian Platform - evidence for the onset of mid-Carboniferous glaciation. *Chemical Geology.* **175,** 133-147.

MOOK, W. G. 1971. Paleotemperatures and chlorinities from stable carbon and oxygen isotopes in shell carbonate. *Palaeogeography, Palaeoclimatology, Palaeoecology.* **9,** 245-263.

MORRISON, J. O. & BRAND, U. 1986. Geochemistry of recent Marine invertebrates. *Geocscience Canada*. **13,** 237-253.

NIER, A. O. 1940. A mass spectrometer for routine isotope abundance measurements. *Reviews of Scientific Instruments*. **11,** 212-216.

NIER, A. O. 1947. A mass spectrometer for isotope and gas analysis. *Reviews of Scientific Instruments*. **18,** 398-411.

O'NEIL, J. R., CLAYTON, R. N. & MAYEDA, T. K. 1969. Oxygen isotope fractionation in divalent metal carbonates. *Journal of Chemical Physics*. **51,** 5547-5558.

ORTIZ, J. D., MIX, A. C., RUGH, W., WATKINS, J. M. & COLLIER, R. W. 1996. Deep-dwelling planktonic foraminifera of the northeastern Pacific Ocean reveal environmental control of oxygen and carbon isotopic disequilibria. *Geochimica et Cosmochimica Acta*. **60,** 4509-4523.

OWEN, R., KENNEDY, H. & RICHARDSON, C. 2002. Isotopic partitioning between scallop shell calcite and seawater: Effect of shell growth. *Geochimica et Cosmochimica Acta*. **66,** 1727-1737.

PECK, L. S., BROCKINGTON, S. & BREY, T. 1997. Growth and metabolism in the Antarctic brachiopod *Liothyrella uva*. *Philosophical Transactions of the Royal Society. London. B.* **352,** 851-858.

PECK, L. S. & HOLMES, L. J. 1989. Seasonal ontogenetic changes in tissue size in the the Antarctic brachiopod *Liothyrella uva* (Broderip 1833). *Journal of Experimental Marine Biology and Ecology*. **134,** 25-36.

POPP, B. N., ANDERSON, T. F. & SANDBERG, P. A. 1986a. Brachiopods as indicators of original isotopic compositions in some Paleozoic limestones. *Geological Society of America Bulletin*. **97,** 1262-1269.

POPP, B. N., ANDERSON, T. F. & SANDBERG, P. A. 1986b. Textural, elemental and isotopic variations among constituents in middle Devonian limestones, North America. *Journal of Sedimentary Petrology*. **56**, 715-727.

QING, H. & VEIZER, J. 1994. Oxygen and carbon isotopic composition of Ordovician brachiopods: Implications for coeval seawater. *Geochimica et Cosmochimica Acta*. **58**, 4429-4442.

RAHIMPOUR-BONAB, H., BONE, Y. & MOUSSAVI-HARAMI, R. 1997. Stable isotope aspects of modern molluscs, brachiopods, and marine cements from cool-water carbonates, Lacepede Shelf, South Australia. *Geochimica et Cosmochimica Acta*. **61**, 207-218.

RAO, C. P. 1996. Oxygen and carbon isotope composition of skeletons from temperate shelf carbonates, Eastern Tasmania, Australia. *Carbonates and Evaporites*. **11**, 169-181.

REYNAUD-VAGANAY, S., JUILLET-LECLERC, A., JAUBERT, J. & GATTUSO, J.-P. 2001. Effect of light on skeletal $\delta^{13}C$ and $\delta^{18}O$, and interaction with photosynthesis, respiration and calcification in two zooxanthellate scleractinian corals. *Palaeogeography, Palaeoclimatology, Palaeoecology*. **175**, 393-404.

ROMANEK, C. S., GROSSMAN, E. L. & MORSE, J. W. 1992. Carbon isotopic fractionation in synthetic aragonite and calcite: Effects of temperature and precipitation rate. *Geochimica et Cosmochimica Acta*. **56**, 419-430.

ROSENBERG, G. D., HUGHES, W. W. & TKACHUCK, R. D. 1988. Intermediary metabolism and shell growth in the brachiopod *Terebratalia transversa*. *Lethaia*. **21**, 219-230.

RUDWICK, M. J. S. 1970. *Living and Fossil Brachiopods*. Hutchinson University Library, London.

RUSH, P. F. & CHAFETZ, H. S. 1990. Fabric-retentive, non-luminescent brachiopods as indicators of original $\delta^{13}C$ and $\delta^{18}O$ composition: A test. *Journal of Sedimentary Petrology*. **60**, 968-981.

RYE, D. M. & SOMMER II, M. A. 1980. Reconstructing paleotemperatures and paleo-salinity regimes with oxygen isotopes. *In*: D.C. RHOADS & R.A. LUTZ (eds.), *Topics in Geobiology, 1 Skeletal Growth of Aquatic Organisms*. Plenum, New York, 169-202.

SAMTLEBEN, C., MUNNECKE, A., BICKERT, T. & PÄTZOLD, J. 2001. Shell succession, assemblage and species dependent effects on C/O-isotopic composition of brachiopods - examples from the Silurian of Gotland. *Chemical Geology*. **175,** 61-107.

SOWERBY, G. B. 1846. Descriptions of thirteen new species of brachiopoda. *Proceedings of the Zoological society*. **?,** 92-93.

STANLEY, G. D., JR. & SWART, P. K. 1995. Evolution of the coral-zooxanthellae symbiosis during the Triassic: a geochemical approach. *Paleobiology*. **21,** 179-199.

STANTON, R. J., JEFFERY, D. L. & AHR, W. M. 2002. Early Mississippian climate based on oxygen isotope compositions of brachiopods, Alamogordo Member of the Lake Valley Formation, south-central New Mexico. *Geological Society of America Bulletin*. **114,** 4-11.

STEUBER, T. 1999. Isotopic and chemical intra-shell variations in low-Mg calcite of rudist bivalves (Mollusca-Hippuritacea): disequilibrium fractions and late Cretaceous seasonality. *International Journal of Earth Sciences*. **88,** 551-570.

SWART, P. K. 1983. Carbon and oxygen isotope fractionation in Scleractinian corals: A review. *Earth Science Reviews*. **19,** 51-80.

TARUTANI, T., CLAYTON, R. N. & MAYEDA, T. K. 1969. The effects of polymorphism and magnesium substitution on oxygen isotope fractionation between calcium carbonate and water. *Geochimica et Cosmochimica Acta*. **33,** 987-996.

THORROLD, S. R., CAMPANA, S. E., JONES, C. M. & SWART, P. K. 1997. Factors determining $\delta^{13}C$ and $\delta^{18}O$ fractionation in aragonite otoliths of marine fish. *Geochimica et Cosmochimica Acta*. **61,** 2909-2919.

TURNER, J. V. 1992. Kinetic fractionation of carbon-13 during calcium carbonate precipitation. *Geochimica et Cosmochimica Acta.* **46,** 1183-1191.

UREY, H. C. 1947. The thermodynamic properties of isotopic substances. *Journal of Chemical Society.* 562-581.

UREY, H. C., LOWENSTAM, H. A., EPSTEIN, S. & MCKINNEY, C. R. 1951. Measurement of paleotemperatures and temperatures of the Upper Cretaceous of England, Denmark and the Southeastern United States. *Bulletin of the Geological Society of America.* **62,** 399-416.

VEIZER, J. 1983a. Chemical diagenesis of carbonates: Theory and application of trace element technique, *Stable Isotopes in Sedimentary geology, Society of Economic Paleontologists and Mineralogists Short Course No 10,* 3.1-3.100.

VEIZER, J. 1983b. Trace elements and isotopes in sedimentary carbonates. *In*: R.J. REEDER (ed.), *Carbonates: Mineralogy and Chemistry.* Volume 11, Reviews in Mineralogy. Mineralogical Society of America, Washington D.C., 265-393.

VEIZER, J., ALA, D., AZMY, K., BRUCKSCHEN, P., BUHL, D., BRUHN, F., CARDEN, G. A. F., DIENER, A., EBNETH, S., GODDERIS, Y., JASPER, T., KORTE, C., PAWELLEK, F., PODLAHA, O. G. & STRAUSS, H. 1999. $^{87}Sr/^{86}Sr$, $\delta^{13}C$ and $\delta^{18}O$ evolution of Phanerozoic seawater. *Chemical Geology.* **161,** 59-88.

VEIZER, J., FRITZ, P. & JONES, B. 1986. Geochemistry of brachiopods: Oxygen and carbon isotopic records of Paleozoic oceans. *Geochimica et Cosmochimica Acta.* **50,** 1679-1696.

WEBER, J. N. & RAUP, D. M. 1966. Fractionation of the stable isotopes of carbon and oxygen in marine organisms - The Echinoidea. Part 1. Variation of C^{13} and O^{18} content within individuals. *Geochimica et Cosmochimica Acta.* **30,** 33-70.

WEBER, J. N. & WOODHEAD, P. M. J. 1970. Carbon and oxygen isotope fractionation in the skeletal carbonate of reef building corals. *Chemical Geology.* **6,** 93-117.

WEFER, G. & BERGER, W. H. 1991. Isotope paleontology: growth and composition of extant calcareous species. *Marine Geology*. **100,** 207-248.

WENZEL, B. & JOACHIMSKI, M. M. 1996. Carbon and oxygen isotopic composition of Silurian brachiopods (Gotland/Sweden): palaeoceanographic implications. *Palaeogeography, Palaeoclimatology, Palaeoecology*. **122,** 143-166.

WENZEL, B., LÉCUYER, C. & JOACHIMSKI, M. M. 2000. Comparing oxygen isotope records of Silurian calcite and phosphate - $\delta^{18}O$ compositions of brachiopods and conodonts. *Geochimica et Cosmochimica Acta*. **64,** 1859-1872.

WILLIAMS, A. 1968a. Evolution of the shell structure of articulate brachiopods, *Special Papers in Palaeontology No 2*. The Palaeontological Association, London.

WILLIAMS, A. 1968b. A history of skeletal secretion among articulate brachiopods. *Lethaia*. **1,** 268-287.

WILLIAMS, A. 1973. The secretion and structural evolution of the shell of Thecideidine brachiopods. *Philosophical Transactions of the Royal Society, London. B*. **264,** 439-478.

WILLIAMS, A. 1997. Shell structure. *In*: R.L. KAESLER (ed.), *Treatise on Invertebrate Paleontology. Part H. Brachiopoda (Revised) 1*. The Geological Society of America and University of Kansas Press, Boulder, Colorado and Lawrence, Kansas, 267-320.

WILLIAMS, A. & BRUNTON, C. H. C. 1997. Morphological and Anatomical Terms Applied to Brachiopods, *Treatise on Invertebrate Paleontology. Part H. Brachiopoda (Revised) 1*. The Geological Society of America and University of Kansas Press, Boulder, Colorado and Lawrence, Kansas, 423-440

WILLIAMS, A., CARLSON, S. J., BRUNTON, C. H. C., HOLMER, L. E. & POPOV, L. E. 1996. A supra-ordinal classification of the Brachiopoda. *Philosophical Transactions of the Royal Society, London. B*. **351,** 1171-1193.

WILLIAMS, A., JAMES, M. A., EMIG, C. C., MACKAY, S. & RHODES, M. C. 1997. Anatomy. *In*: R.L. KAESLER (ed.), *Treatise on Invertebrate Paleontology. Part H. Brachiopoda (Revised) 1*. The Geological Society of America and University of Kansas Press, Lawrence, Kansas, 7-188.

WILLIAMS, A. & WRIGHT, A. D. 1970. Shell structure of the Craniacea and other calcareous inarticulated brachiopoda, *Special Papers in Palaeontology No 7*. The Palaeontological Association, London.

WILLIAMS, D. F., ARTHUR, M. A., JONES, D. S. & HEALY-WILLIAMS, N. 1982. Seasonality and mean annual sea surface temperatures from isotopic and sclerochronological records. *Nature*. **296**, 432-434.